

Durham E-Theses

PLS3 promoter methylation and plastin expression in colorectal cancer

BATTLE, DANIELLE, MARIE

How to cite:

BATTLE, DANIELLE, MARIE (2012) *PLS3 promoter methylation and plastin expression in colorectal cancer*, Durham theses, Durham University. Available at Durham E-Theses Online:
<http://etheses.dur.ac.uk/5583/>

Use policy



This work is licensed under a [Creative Commons Public Domain Dedication 1.0 \(CC0\)](https://creativecommons.org/licenses/by/4.0/)

Durham University

School of Biological and Biomedical Sciences

PLS3 promoter methylation and plastin
expression in colorectal cancer

Danielle Marie Battle

Thesis submitted for the degree of Doctor of Philosophy

August 2012

For my Mum

I love you and miss you

Σε αγαπω και μου λειπεις παρα πολυ

Ντανιελ

Table of Contents

List of figures.....	vii
List of tables.....	xi
Declaration.....	xii
Acknowledgements.....	xiii
List of abbreviations.....	xiv
Abstract.....	xxi
Chapter 1 – Introduction.....	1
1.1 Colorectal cancer epidemiology.....	1
1.2 Colorectal cancer risk factors.....	5
1.2.1 Age.....	5
1.2.2 Gender.....	5
1.2.3 Adult-attained height.....	6
1.2.4 Obesity.....	6
1.2.5 Red and processed meat.....	7
1.2.6 Alcohol.....	8
1.2.7 Smoking.....	8
1.2.8 Energy restriction.....	9
1.2.9 Physical activity.....	9
1.2.10 Fibre intake.....	9
1.2.11 Aspirin.....	10
1.2.12 Other dietary factors.....	10
1.3 Hereditary colorectal cancer.....	11
1.3.1 Familial adenomatous polyposis coli (FAP).....	12
1.3.2 Hereditary non-polyposis colorectal cancer (HNPCC).....	13
1.3.3 Hamartomatous polyposis syndromes.....	15
1.4 The molecular basis of colorectal cancer	16
1.4.1 Anatomy of the colorectum.....	16
1.4.2 The colonic crypt.....	18
1.4.3 The adenoma-carcinoma sequence.....	21
1.4.4 APC and the canonical Wnt signalling pathway.....	22

1.4.5 KRAS and the MAPK pathway.....	24
1.4.6 Tumour suppressor <i>TP53</i>	26
1.4.7 The chromosomal instability pathway (CIN).....	27
1.4.8 The microsatellite instability pathway (MIN).....	27
1.5 Epigenetics and colorectal cancer.....	28
1.5.1 The role of epigenetics.....	28
1.5.2 DNA methylation and CpG islands.....	29
1.5.3 Aberrant DNA methylation and colorectal cancer.....	30
1.5.3.1 DNA hypomethylation.....	31
1.5.3.2 DNA promoter hypermethylation.....	32
1.5.4 CpG island promoter methylator phenotype (CIMP).....	35
1.6 Clinicopathological staging of colorectal cancer.....	36
1.7 Screening.....	38
1.8 Treatment.....	39
1.9 Prognostic biomarkers in colorectal cancer.....	40
1.9.1 Genetic biomarkers.....	41
1.9.2 DNA methylation biomarkers.....	42
1.10 Lamins and colorectal cancer.....	44
1.10.1 Lamins and the nuclear envelope.....	44
1.10.2 Lamin structure and function.....	45
1.10.3 A-type lamins and cancer.....	48
1.11 Plastins: actin bundling proteins.....	50
1.11.1 The actin cytoskeleton: overview.....	50
1.11.2 Early biochemical studies of plastins.....	55
1.11.3 Plastin structure.....	56
1.11.4 Tissue-specific expression and localisation.....	58
1.11.5 Plastin function.....	59
1.11.6 Plastins and cancer.....	61
1.12 Thesis aims and rationale.....	63
Chapter 2 – Materials and methods.....	65
2.1 General chemicals and materials.....	65
2.2 The Netherlands Cohort Study on Diet and Cancer.....	65

2.2.1 Tissue samples.....	65
2.2.2 The CREAM database and retrospective study.....	66
2.2.3 Statistical analysis.....	66
2.3 Mammalian cell culture and transfections.....	67
2.3.1 Cell lines and subculture.....	67
2.3.2 DAC treatment.....	68
2.4 Nested methylation-specific PCR (N-MSP).....	69
2.4.1 Primer design.....	69
2.4.2 DNA isolation.....	70
2.4.3 Sodium bisulphite conversion.....	71
2.4.4 N-MSP.....	72
2.4.5 DNA gel electrophoresis.....	72
2.5 Bisulphite sequencing.....	73
2.5.1 Primer design.....	73
2.5.2 Amplification of sodium-bisulphite modified DNA and ligation into pCR®2.1 vector.....	73
2.5.3 Transformation.....	74
2.5.4 Colony PCR.....	74
2.5.5 Purification of recombinant DNA.....	75
2.5.6 DNA amplification and sequencing analysis.....	75
2.6 Quantitative real-time PCR.....	76
2.6.1 Primer design.....	76
2.6.2 Total RNA isolation.....	77
2.6.4 Quantification and purity of RNA.....	78
2.6.3 cDNA synthesis.....	78
2.6.5 qPCR primer validation.....	78
2.6.6 qPCR.....	79
2.7 Generation of plastin polyclonal antibodies.....	80
2.7.1 Animal selection.....	80
2.7.2 Peptide immunogen design.....	80
2.7.3 Conjugation and antibody production.....	81
2.8 Immunohistochemistry.....	82
2.8.1 Antigen retrieval.....	82

2.8.2 Antibody incubation and antigen visualisation.....	82
2.8.3 Counterstaining and mounting.....	83
2.8.4 Photography.....	83
2.9 One-dimensional SDS-PAGE and immunoblotting.....	83
2.9.1 Preparation of recombinant plastin proteins.....	83
2.9.2 Preparation of mouse tissue.....	84
2.9.3 Preparation of whole cell extracts.....	84
2.9.4 Bradford assay.....	85
2.9.5 SDS-PAGE.....	85
2.9.6 Coomassie blue staining.....	85
2.9.7 Western blotting.....	86
2.9.8 Peptide inhibition assay.....	86
2.10 Bioinformatics.....	87
2.10.1 DNA microarray dataset.....	87
2.10.3 Ingenuity Pathway Analysis.....	88
Chapter 3 – <i>PLS3</i> promoter methylation in colorectal cancer.....	89
3.1 Introduction.....	89
3.2 Results.....	92
3.2.1 <i>PLS3</i> promoter methylation and mRNA expression in CRC cell lines.....	92
3.2.2 <i>PLS3</i> promoter methylation in normal colonic mucosa and primary colorectal carcinomas.....	97
3.2.4 Patient analysis.....	105
3.2.4.1 <i>PLS3</i> methylation versus tumour progression and location.....	105
3.2.4.2 <i>PLS3</i> promoter methylation and patient survival.....	109
3.3 Discussion.....	112
Chapter 4 – Characterisation of polyclonal plastin antibodies.....	117
4.1 Introduction.....	117
4.2 Results.....	120
4.2.1 Sequence alignments of plastin isoforms.....	120
4.2.2 Characterisation of the polyclonal Dann antibodies.....	123
4.2.2.1 Producing recombinant plastins to test reference antibodies.....	123

4.2.2.2 Characterising the Dann1a antibody against recombinant plastins.....	126
4.2.3.3 Characterising the Dann1b, Dann2a, Dann2b, Dann3a and Dann3b antibodies against recombinant plastins.....	128
4.2.2.4 Confirming the specificity of Dann antibodies by peptide inhibition assay.....	130
4.2.2.5 Detection of plastins in mouse tissue using the Dann antibodies..	134
4.2.2.6 Detection of plastins in CRC cell lines.....	136
4.3 Discussion.....	138

Chapter 5 – Immunohistochemical analysis of plastin expression

in colorectal cancer.....	141
5.1 Introduction.....	141
5.2 Results.....	143
5.2.1 Characterisation of plastin antibodies in normal human skin and colon.....	143
5.2.2 Immunohistochemical analysis of T/L-plastin expression in CRC.....	146
5.2.3 T/L-plastin is strongly expressed at the invasive front of colorectal tumours.....	150
5.2.4 T/L-plastin expression in signet ring carcinoma.....	150
5.2.5 Patient analysis.....	156
5.2.5.1 Plastin expression versus tumour progression and location.....	156
5.2.5.2 T/L-plastin expression versus lamin A/C expression.....	157
5.2.5.3 T/L-pastin expression and patient survival analysis.....	158
5.3 Discussion.....	162

Chapter 6 – Identification and validation of candidate colorectal cancer gene network.....

6.1 Introduction.....	166
6.2 Results.....	168
6.2.1 Generation of a gene interaction network using Ingenuity Pathway Analysis.....	168
6.2.2 Confirmation of microarray data by real-time PCR.....	173

6.2.3 Confirmation of microarray data by Western blotting.....	177
6.3 Discussion.....	180
Chapter 7 – Discussion and future perspectives.....	186
7.1 Background and aims of thesis.....	186
7.2 <i>PLS3</i> promoter CpG island methylation is a mechanism for controlling T-plastin expression.....	187
7.3 Does <i>PLS3</i> promoter hypomethylation play a pivotal role in switching on T-plastin in CRC?.....	188
7.4 Is there a role for active demethylation in CRC?.....	189
7.5 <i>PLS3</i> methylation is strongly associated with sex and tumour location.....	191
7.6 T/L-plastin expression is switched on in CRC and frequently observed at the invasive front of the tumour.....	192
7.7 Identification of a candidate gene network based on the expression of GFP-lamin A in CRC cell line SW480.....	196
7.8 Conclusion.....	197
Appendix – Supplementary figures.....	199
Bibliography.....	219

List of Figures

Chapter 1

Figure 1.1: Global estimated age-standardised incidence rates for CRC: both sexes.....	3
Figure 1.2: CRC incidence rates.....	4
Figure 1.3: Age-specific mortality rates of CRC, UK, 2008.....	5
Figure 1.4: Adenomatous polyposis coli (APC) key functional domains.....	13
Figure 1.5: DNA mismatch repair system overview.....	15
Figure 1.6: Anatomic structure of colorectum.....	16
Figure 1.7: Schematic representation of gastrointestinal tract.....	18
Figure 1.8: Colonic crypt architecture.....	20
Figure 1.9: The colorectal adenoma-carcinoma sequence.....	21
Figure 1.10: Overview of the canonical Wnt signaling pathway.....	24
Figure 1.11: Overview of the Ras-Raf-MEK-ERK Pathway.....	26
Figure 1.12: CpG island DNA hypermethylation and global DNA hypomethylation in normal colonic epithelia and colorectal cancer.....	31
Figure 1.13: Overview of the structure of the nucleus.....	44
Figure 1.14: General structure of lamin polypeptide.....	45
Figure 1.15: Schematic representation of the nuclear envelope.....	47
Figure 1.16: Monomeric and filamentous actin.....	51
Figure 1.17: Actin filament networks.....	53
Figure 1.18: Schematic representations of human platin isoforms.....	58

Chapter 3

Figure 3.1: Study design of the Netherlands Cohort Study on Diet and Cancer (NLCS).....	91
Figure 3.2: <i>PLS3</i> (T-plastin) promoter structure and N-MSP primer location.....	92
Figure 3.3: <i>PLS3</i> promoter methylation in CRC cell lines.....	94
Figure 3.4: Amplification of bisulphite-modified DNA from CRC cell lines.....	94
Figure 3.5: Bisulphite sequencing of SW948 and SW620 colorectal cancer cell lines.....	95
Figure 3.6: T-plastin mRNA expression is restored after treatment with 5-aza-2'-doxycytidine.....	96
Figure 3.7: <i>PLS3</i> promoter methylation in normal colonic mucosa.....	99

Figure 3.8: <i>PLS3</i> promoter methylation in primary colorectal tumours.....	100
Figure 3.9: Amplification of bisulphite-modified DNA from human CRC tissue and cell lines.....	102
Figure 3.10: <i>PLS3</i> promoter methylation in colorectal carcinomas and corresponding normal colonic mucosa from a small independent subset.....	102
Figure 3.11: T-plastin mRNA expression in colorectal carcinomas and corresponding normal colonic mucosa from three patients.....	103
Figure 3.12: Amplification of bisulphite-modified DNA from frozen normal and tumour tissue and CRC cell lines.....	103
Figure 3.13: Bisulphite sequencing of normal colon versus tumour tissue from three CRC patients.....	104
Figure 3.14 <i>PLS3</i> promoter methylation in relation to sex and Dukes stage.....	107
Figure 3.16: <i>PLS3</i> promoter methylation in relation to tumour location.....	108
Figure 3.16: Kaplan-Meier survival analysis.....	111

Chapter 4

Figure 4.1: Schematic representations of human plastin isoforms.....	119
Figure 4.2: Alignment of human T-plastin with L-plastin and I-plastin.....	121
Figure 4.3: Alignment of human T-plastin with mouse and T-plastin.....	122
Figure 4.4: Coomassie staining of recombinant plastin proteins.....	124
Figure 4.5: Western blotting analysis of plastin GST-fusion proteins.....	125
Figure 4.6: Characterisation of Dann1a antibodies by Western blot analysis.....	127
Figure 4.7: Characterisation of Dann1b-3b antibodies by Western blot analysis.....	129
Figure 4.8: Confirmation of the specificity of Dann1a antibody by peptide inhibition assay.....	131
Figure 4.9: Confirmation of the specificity of Dann2b antibody by peptide inhibition assay.....	132
Figure 4.10: Confirmation of the specificity of Dann3b antibody by peptide inhibition assay.....	133
Figure 4.11: Confirmation of the specificity of Dann1a using mouse tissue.....	135
Figure 4.12: Confirmation of the specificity of Dann1a using CRC cell lines.....	137

Chapter 5

Figure 5.1: Study design of the Netherlands Cohort Study on Diet and Cancer (NLCS).....	142
Figure 5.2: Optimisation of Dann1a antibody in normal human skin.....	144
Figure 5.3: T /L-plastin is absent in normal colonic epithelia.....	145
Figure 5.4: Positive plastin expression in muscle and negative plastin expression of normal colonic epithelia within CRC tissue.....	147
Figure 5.5: T/L-plastin expression in CRC.....	149
Figure 5.6: T/L-plastin expression at the invasive front of a tumour (patient 1).....	152
Figure 5.7: T/L-plastin expression at the invasive front of a tumour (patient 2).....	154
Figure 5.8: T/L-plastin expression in signet cell carcinomas.....	155
Figure 5.9: T/ L-plastin expression in relation to Dukes' stage and tumour location.....	159
Figure 5.10 : T/L-plastin expression verses lamin A/C expression in NLCS tumours.....	160
Figure 5.11: T/L-plastin expression in CRC and survival.....	161

Chapter 6

Figure 6.1: Biological network linked to Cancer, Cellular movement, Cellular growth and Proliferation	171
Figure 6.2: Interactions and molecules used in Ingenuity Pathway Analysis network.....	172
Figure 6.3 Confirmation of microarray data by quantitative real-time PCR.....	174
Figure 6.4: Microarray versus quantitative real-time PCR: fold change in gene expression	176
Figure 6.5: Coomassie and immunoblotting of selected proteins identified by microarray	129
Figure 6.6: Overview of the EGF signaling pathway.....	183

Chapter 7

Figure 7.1 Figure 7.1: Upregulation of plastin at the invasive front may lead to increased formation of specialised membrane protrusions and hence metastasis.....	194
Figure 7.2 Increased expression of lamin A in SW480 cells may induce EMT through the upregulation of EGFR, down regulation of E-cadherin and upregulation of T-plastin.....	197

Appendix – Supplementary figures.....

199

Figure S1: Representative graphs generated from qPCR experiments.....	200
Figure S2: ELISA analysis for Dann antibodies.....	203

Figure S3: <i>PLS3</i> promoter sequence: location of the CpG island.....	204
Figure S4: <i>PLS3</i> promoter sequence: location of N-MSP primer sets 1 and 2.....	206
Figure S5: <i>PLS3</i> promoter sequence: location of N-MSP primer set 3.....	207
Figure S6: <i>PLS3</i> promoter sequence: location of bisulfite sequencing primers.....	208
Figure S7: Colony PCR: CRC cells.....	209
Figure S8: Bisulfite sequencing analysis of <i>PLS3</i> CpG island in SW948 CRC cell line.....	211
Figure S9: Bisulfite sequencing analysis of <i>PLS3</i> CpG island in SW620 CRC cell line.....	213
Figure S10: Bisulphite sequence alignment of methylated T-plastin, unmethylated T-plastin and consensus sequence.....	214
Figure S11: Colony PCR: patient DNA.....	215
Figure S12: Bisulfite sequencing analysis of <i>PLS3</i> CpG island in normal colonic mucosa (Patient 1).....	217
Figure S13: Bisulphite sequence alignment of methylated T-plastin, unmethylated T-plastin and consensus sequence.....	218

List of tables

Table 1: Representative genes commonly methylated and silenced in CRC.....	33
Table 2: Clinicopathological staging and 5-year survival of CRC patients.....	37
Table 3: Clinical correlations between actin-bundling proteins and cancer.....	54
Table 2.1: CRC cell lines.....	68
Table 2.2: N-MSP <i>PLS3</i> primer set.....	70
Table 2.3: Bisulphite sequencing primers.....	73
Table 2.4: Primers for qPCR analysis.....	77
Table 2.5: Peptides sequences for generation of platin polyclonal antibodies.....	81
Table 2.6: Primary antibodies for Western blotting.....	87
Table 3.1: Prevalence of <i>PLS3</i> promoter methylation in 161 CRC patient samples.....	101
Table 3.2: <i>PLS3</i> promoter methylation in relation to clinicopathological characteristics....	106
Table 5.1: Follow-up analysis.....	157
Table 6.1: List of genes identified in a cancer network by Ingenuity Pathway Analysis.....	170

Declaration

I declare that the data presented in this thesis is a result of my own work and was carried out at the School of Biological and Biomedical Sciences, Durham University, under the supervision of Professor Christopher J. Hutchison and Dr Martin D. Watson. The data presented in Chapters 3 and 5 was undertaken at the University of Maastricht, Netherlands. Any data cited from the unpublished or published work of another person(s) has been duly acknowledged. This thesis has been composed by myself. No material has been submitted previously for a higher degree. The copyright of this thesis rests with the author. No quotation from it should be published in any format, including electronic and the internet, without the author's prior written consent. All information derived from this thesis must be acknowledged appropriately.

Acknowledgements

“A dream becomes a goal when action is taken toward its achievement.”

Bo Bennett

Surviving the last few years and completing this PhD project would have been impossible without the help of many people. Firstly, I would like to thank my supervisor Professor Chris Hutchison for giving me the opportunity to study for a PhD. I would also like to express my great appreciation to Dr Martin Watson, for his valuable advice, encouragement and above all, patience. Special thanks go to my collaborators at Maastricht, for their support and guidance through my time there. In particular, Dr Manon van Engeland for her insightful contributions and Dr Kim Smits, Kim Wouters, Dr Peter Moerkerk and Dr Robert Riedl for all their constructive suggestions and generous help with the project.

I have so many people to thank in the Biological Sciences Department at Durham who have supported me all the way: my thesis committee Dr Arto Maatta, Dr Tony O’Sullivan, Professor Roy Quinlan and Dr Nick Hole, my colleagues in the lab, Dr Clare Foster, Dr Ian Gibbs Seymour, Dr Vanya Pekovic, Dr Pam Ritchie; and around the department Professor Marc Knight, Dr Heather Knight, Dr Ari Sadanandom and Professor Patrick Hussey. Special thanks to my Plan C band members: Professor Keith Lindsey, Dr Jen Topping, Dr Tim Hawkins and Dr Phil Stephens (I had a wicked time and will miss our practices and gigs!).

I would also like to thank my amazing friends who have been incredible throughout. I love you all! Nadine, Georgia, Sue (the 4!) – you ladies are awesome, thanks you so much for your support over the years. Jo – you have been a massive source of inspiration and strength, Mark – I live by your rules (!), Laura & Richard, thank you so much for taking me under your wing in Maastricht, Marten – your love and support in the beginning will always be remembered, Paul - living together was so much fun, Pete – you have always been there for me, and Adam – you are simply wonderful and I couldn’t have done it without you xxx.

Finally, to my Brother and Dad, I love you more than anything in the world. Thank you for always believing in me. I dedicate this thesis to Mum.

List of abbreviations

µg	Microgram
µl	Microlitre
1D	One-dimensional
2D	Two-dimensional
2D-DIGE	Two-dimensional difference in-gel electrophoresis
5-FU	5-fluorouracil
ABP	Actin binding protein
ABD	Actin binding domain
ACF	aberrant crypt foci
AD	Anno Domini
ADP	Adenosine Diphosphate
AICR	American Institute for Cancer Research
AJCC	American Joint Committee on Cancer
AKAP11	A kinase (PRKA) anchor protein 11
AP	Activating protein
APC	Adenomatous polposis coli
APS	Ammonium persulphate
AR	Amphiregulin
AREG	Amphiregulin
ARP	Actin related protein
ATP	Adenosine Triphosphate
BAF	Barrier to autointegration factor
BC	Before Christ
BMI	Body mass index
BMP	Bone morphogenic protein
bp	Base pair
BRAF	v-Raf murine sarcoma viral oncogene homolog B1
BRCA2	Breast cancer 2, early onset
BSA	Bovine Serum Albumin
C-	Carboxy terminal
CACNA1G	Calcium channel, voltage-dependent, T type, alpha 1G
CCS	Cronkhite-Canada Syndrome
CD	Cluster of differentiation
CDC42EP	CDC42 effector protein
CDKN	Cyclin-dependent kinase inhibitor
CDH1	Cadherin 1, type 1, E-cadherin
cDNA	Complementary DNA
CEA	Carcinoembryonic antigen
CH	Calponin homology

CHAPS	3-[(3-Cholamidopropyl)dimethylammonio]-1-propanesulphonate
CHFR	Checkpoint with forkhead and RING finger domains
CHGA	Chromogranin A
CHO	Chinese hamster ovary
CI	Confidence Interval
CIMP	CpG island methylator phenotype
CIN	Chromosomal Instability
CK	Casein kinase
CKAP2	Cytoskeleton associated protein 2
Cntl	Control
COL18A1	Collagen, type XVIII, alpha 1
COX	Cyclooxygenase
CpG	Cytosine-phosphate-guanine
CRC	Colorectal cancer
CREAM	Colorectal epidemiology and mutation
CREB	cyclic AMP response element binding protein
CS	Cowden syndrome
C _T	Cycle threshold
CXCL	Chemokine (C-X-C motif) ligand
Da	Daltons
DAB	3,3'-Diaminobenzidine
DAC	5-Aza-2' deoxycytidine
DAPK	Death associated protein kinase
ddH ₂ O	Double distilled water
DFS	Disease-free survival
DKK1	Dickkopf homolog 1
DMEM	Dulbecco's modified Eagle's medium
DMF	Dimethylformamide
DNA	Deoxyribonucleic acid
DNase	Deoxyribonuclease
DNMT	Deoxynucleotide methyltransferase
Dsh	Dishevelled
DTT	Dithiothreitol
EB1	End binding protein 1
ECACC	European Collection of Cell Cultures
ECL	Enhanced Chemiluminescence
ECM	Extracellular matrix
EDTA	Ethylenediamine tetraacetic acid
EF	EF hand
EGFP	Enhanced Green Fluorescent Protein
EGFR	Epidermal Growth Factor Receptor
EGTA	Ethylene glycol tetraacetic acid

eIF	Eukaryotic translation initiation factor
ELISA	Enzyme-linked Immunosorbent assay
ERK	Extracellular signal-regulated kinase
ELK	E twenty-six (ETS)-like transcription factor
EMT	Epithelial-mesenchymal transition
EMP	Epithelial membrane protein
ENA	Extractable nuclear antigen
EPI	Epiregulin
ER	Endoplasmic reticulum
EREG	Epiregulin
ERK	Extracellular signal-regulated kinase
ESR	Estrogen receptor
EtOH	Ethanol
ETS	Erythroblastosis virus E26 oncogene homolog
EVL	Ena/VASP-like protein
EXO	Exonuclease
FAP	Familial Adenomatous Polyposis
FBS	Foetal Bovine Serum
FN	Fibronectin
FOBt	Faecal Occult Blood test
Frz	Frizelled
GAMPO	Goat anti-mouse peroxidase
GCRMA	Guanine Cytosine Robust Multi-Array Analysis
GFP	Green Fluorescent Protein
GI	Gastrointestinal
GSK	Glycogen synthase kinase
GST	Glutathione S-transferase
GTP	Guanosine triphosphate
GWAS	Genome wide association study
HCl	Hydrochloric Acid
HDAC	Histone deacetylase
HDLG	Human Disc Large
HG U133	Human Genome U133 Genechip
HLTF	Helicase-like transcription factor
HNPCC	Hereditary Non-polyposis Colorectal Cancer
HR	Hazard Ratio
HRP	Horseradish Peroxidase
Hsp	Heat shock protein
HUVEC	Human umbilical vein endothelial cells
ICD	International classification of disease
ID	Inhibitor of DNA binding
IF	Intermediate Filament

iFOBT	Immunochemical Faecal Occult Blood test
Ig	Immunoglobulin
IGF	Insulin growth factor
IGFBP	Insulin growth factor binding protein
IHC	Immunohistochemistry
IL	Interleukin
INM	Inner Nuclear Membrane
INSIG	Insulin induced gene
IPA	Ingenuity Pathways Analysis
IPGT	Isopropyl beta-D-thiogalactoside
IVD	<i>In vitro</i> methylated
JAK/STAT	Janus Kinase/Signal Transducers and Activators of Transcription
JPS	Juvenile Polyposis syndrome
KASH	<u>K</u> larsicht/ <u>A</u> NC-1/ <u>S</u> yne <u>h</u> omology
kb	Kilobase
kDa	Kilodalton
KRAS	Kirsten rat sarcoma
L-15	Leibovitz growth medium
LAD	Lamina-associated domain
LamA	Lamin A
LAP	Lamina Associated Polypeptide
LBR	Lamin B receptor
LCC	Left-sided colon cancer
LEF	Lymphoid enhancer factor
LINC	<u>L</u> inker of <u>n</u> ucleoskeleton and <u>c</u> ytoskeleton
LOH	Loss of Heterozygosity
LOI	Loss of imprinting
M	Molar
mA	Milliampere
MAC	Modified Astler Coller system
MALDI-ToF-ToF	Matrix-assisted laser-desorption/ionization time-of-flight/time-of-flight
MAP	Mitogen-activated protein
MBD	Methyl-CpG-binding domain protein
MBS	Maleimidobenzoic acid N-hydroxysuccinimide
MCR	Mutational cluster region
MEF	Mouse embryonic fibroblasts
MEK	MAPK/ERK kinase
MGMT	Methylguanine DNA methyltransferase
mg	Milligram
MHC	Major histocompatibility complex
MIN	Microsatellite instability

MINT	Methylated in tumour locus
ml	Millilitre
MLH	MutL Homolog
mM	Millimolar
MMLV	Moloney murine leukemia virus
MMR	Mismatch Repair
MRC	Medical Research Council
mRNA	Messenger RNA
MS	Mass spectrometry
MSI	Microsatellite Instability
MSP	Methylation specific PCR
MSS	Microsatellite stability
MSX	msh homeobox
N-	Amino terminal
NCR	Netherlands Cancer Registry
NE	Nuclear Envelope
NEM	N-ethylmaleimide
NES	Nuclear export signal
NET	Nuclear envelope transmembrane protein
NEUROG	Neurogenin
NHS	National Health Service
NK	Natural killer
NL	Normal lymphocytes
NLCS	Netherlands Cohort Study on Diet and Cancer
NLRP3	NACHT, LRR and PYD domains-containing protein 3
NLS	Nuclear Localisation Signal
NMD	Nonsense mediated decay
NPC	Nuclear Pore Complex
NRP	Neuropilin
NSAID	Non-steroidal anti-inflammatory drug
NF	Nuclear factor
ONM	Outer nuclear membrane
ORF	Open reading frame
PAI-1	plasminogen activator inhibitor 1
PALGA	Pathologisch anatomisch landelijk geautomatiseerd archief
PBS	Phosphate Buffered Saline
PCR	Polymerase Chain Reaction
PHTS	PTEN hamartomatous tumour syndrome
PI3K	Phosphoinositol kinase
PJS	Peutz-Jeghers Syndrome
PMS	Postmeiotic segregation increased
PVDF	Polyvinylidifluoride

Q-PCR	Quantitative Real-Time Polymerase Chain Reaction
RCC	Right-sided colon cancer
RNA	Ribonucleic acid
RNase	Ribonuclease
ROD	Regulator of differentiation
rpm	Revolutions per minute
RT	Room temperature
RUNX	Runt-related transcription factor
SAMP	Serine alanine methionine proline
SCC	Squamous cell carcinoma
SD	Standard deviation
SDS	Sodium Dodecyl Sulphate
SDS-PAGE	Sodium Dodecyl Sulphate - Polyacrylamide Gel Electrophoresis
SE	Standard error of the mean
SERPINE	Serpin peptidase inhibitor
siRNA	Small interfering ribonucleic acid
SMAD	Mothers against decapentaplegic homologue
SNAI2	Snail homolog 2
SOCS	Suppressor of cytokine signaling
SOS	Son of sevenless
SPSS	Statistical Package for the Social Sciences
SRF	Serum response factor
SUN	<u>Sad1/UNC-84</u> homology
SWARPO	Swine anti-rabbit peroxidase
TBS	Tris buffered saline
TCF	T cell factor
TEMED	N,N,N',N'-Tetramethylethylenediamine
TGF	Transforming growth factor,
TGFβ1	Transforming growth factor, beta - induced
TIMP	Tissue inhibitor of metalloproteinase
T _m	Melting temperature
TNF	Tumour necrosis factor
TNM	Tumour-Node-Metastasis
TSS	Transcription start site
TUSC	Tumour suppressor candidate
UICC	International union against cancer
UK	United Kingdom
V	Volts
VASP	Vasodilator-stimulated phosphoprotein
VCA	Verprolin, cofilin, acidic
VEGF	Vascular endothelial growth factor
v/v	Volume/volume
WAS	Wiscott-Aldrich syndrome

w/v
WCRF

Weight/volume
World Cancer Research Fund

Abstract

Colorectal cancer (CRC) is one of the most prevalent malignancies in the Western world. It is a heterogeneous disease that begins from a benign polyp and progresses to invasive carcinoma via at least three distinct pathways. Prognosis of newly diagnosed cases mainly relies on the Dukes' classification system, yet the 5-year survival rate of patients with CRC varies from 90% to 10% with tumour progression. The pursuit of biomarkers that can accurately predict patient prognosis has intensified in recent years. In our laboratory, we have previously shown that positive lamin A/C expression is a potential risk biomarker in CRC. Subsequent downstream investigations revealed that CRC cells overexpressing lamin A were significantly more motile compared to their GFP-only counterparts. This increase in motility was, in part, due to upregulation of the actin-bundling protein T-plastin (encoded by the *PLS3* gene). The main aims of this thesis were to investigate *PLS3* promoter methylation and plastin expression in CRC, using a combination of both epigenetic and immunohistochemical approaches. *PLS3* promoter methylation was studied in CRC cell lines and a large cohort of CRC patients from the Netherlands Cohort Study on Diet and Cancer (NLCS) tissue archive. T-plastin expression was suppressed because of promoter methylation and its expression was restored upon treatment with the DNA methylation inhibitor 5-aza-2'-deoxycytidine ($p = 0.01$; $p = 0.05$). Furthermore, T-plastin was methylated in ~50% of CRC patients but methylation status did not provide any prognostic value. However, there was an association between both methylation status and sex ($p = 0.01$) and methylation status and tumour location ($p = 0.05$). The expression of plastin proteins in CRC was studied by raising polyclonal antibodies against two plastin isoforms and determining their specificity using immunoblotting and peptide inhibition assays. The most promising antibody, Dann1a, was used to analyse the expression of plastin by immunohistochemistry, using patient sections obtained from the NLCS archive. Strikingly, plastin was absent from normal colonic mucosa but was aberrantly expressed in 80% of CRC patients and was frequently observed at the invasive front of the tumour. Finally, we identified and validated a candidate gene network using Ingenuity Pathway Analysis, based on the over expression of GFP-lamin A in CRC cells. This data suggests that lamin A is a master regulator of a pathway linked to cancer and cell motility. These studies will stimulate further studies into the role of specific plastins in epithelial cancers and provide a framework for the development of novel drugable targets for treatment of CRC.

Chapter 1: Introduction

1.1 Colorectal cancer epidemiology

Cancer is a group of more than 100 diseases characterized by uncontrolled cellular growth and has probably existed since antiquity. Indeed, some of the earliest evidence of cancer in humans was found in an ancient Egyptian papyrus written between 3000-5000 BC. It describes eight cases of tumours or ulcers of the breast. The manuscript concludes 'there is no treatment' and cauterization was given as a palliative measure. The origin of the word cancer (*karkinos* which translates into carcinos/carcinoma) is credited to the Greek physician Hippocrates (460-370 BC), who is thought to be one of the first to make the distinction between benign and malignant tumours. Over 200 years later, Galen (130-200 AD) coined the word *oncos* to describe tumours (which translates to swelling in Greek). Since these initial observations made thousands of years ago, our knowledge of tumour biology has improved tremendously.

Despite decades of research and clinical practice, cancer is today the most common cause of death in the Western world (Jemal et al., 2011). According to recent global estimates, there are 12.7 million new cancer cases and 7.6 million deaths each year (Ferlay et al., 2010). Lung cancer is the most commonly diagnosed cancer (1.61 million cases) followed by breast cancer (1.38 million cases). Colorectal cancer (CRC) is the third most common malignancy with over 1.23 million cases per year. It is the third most common cause of cancer in men, and the second most common cause of cancer in women.

Perhaps unsurprisingly, there are striking geographical differences in the global distribution of CRC (Jemal et al., 2011) (Figure 1.1). Age-adjusted incidence rates vary up to 25-fold between countries with the highest rates (Australia, New Zealand, USA and Western Europe) and those with the lowest rates (Africa and Asia) (Ferlay et al., 2010; Parkin et al., 2005) (Figure 1.2 A). Within Europe, Slovakia and Denmark have the highest CRC incidence rates for men and women (91 per 100,000 and 50 per 100,000 per year, respectively). By stark comparison, Greece has the lowest rates for both men (24 per 100,000) and women (17 per 100,000) (GLOBOCAN, 2008) (Figure 1.2 B). Moreover, cancer incidence has risen dramatically over the past 40 years in Japan, Singapore and Eastern European countries; all

of which have significantly increased their gross domestic product (GDP) (Parkin et al., 2005). This can be attributed, in part, to aging populations and adoption of cancer-associated lifestyle choices such as smoking, increased alcohol consumption and sedentary occupations (Jemal et al., 2011). Similarly, migration studies indicate that populations which have made the transition to a 'Western lifestyle' are at increased risk of developing CRC (Kolonel et al., 2004).

Approximately 608,000 deaths from CRC occur each year, making it the 4th most common cause of death from cancer (Ferlay et al., 2010). Mortality rates are higher in males than in females. Central and Eastern Europe have the highest mortality rates (20.3 per 100,000 for male, 12.1 per 100,000 for female), compared to Middle Africa, which have the lowest mortality rates for males and females (3.5 per 100,000 and 2.7 per 100,000 per year, respectively). In the UK, CRC is the third most common malignancy and the second most common cause of cancer-related death (Bray et al., 2002; Ferlay et al., 2010). Each year there are around 40,000 new cases and 16,000 deaths. Mortality rates vary considerably across the UK. This is thought to be due to disparities within the public healthcare system, and environmental and socio-economic differences (Mayer et al., 2007; Mayor, 2010). Whilst age-standardised 5-year survival rates have improved over the last 20 years, approximately 6% of the Western population will develop colorectal neoplasms during their lifetime and as such, CRC constitutes a major burden on public health organisations (Davies et al., 2005; Mayor, 2010).

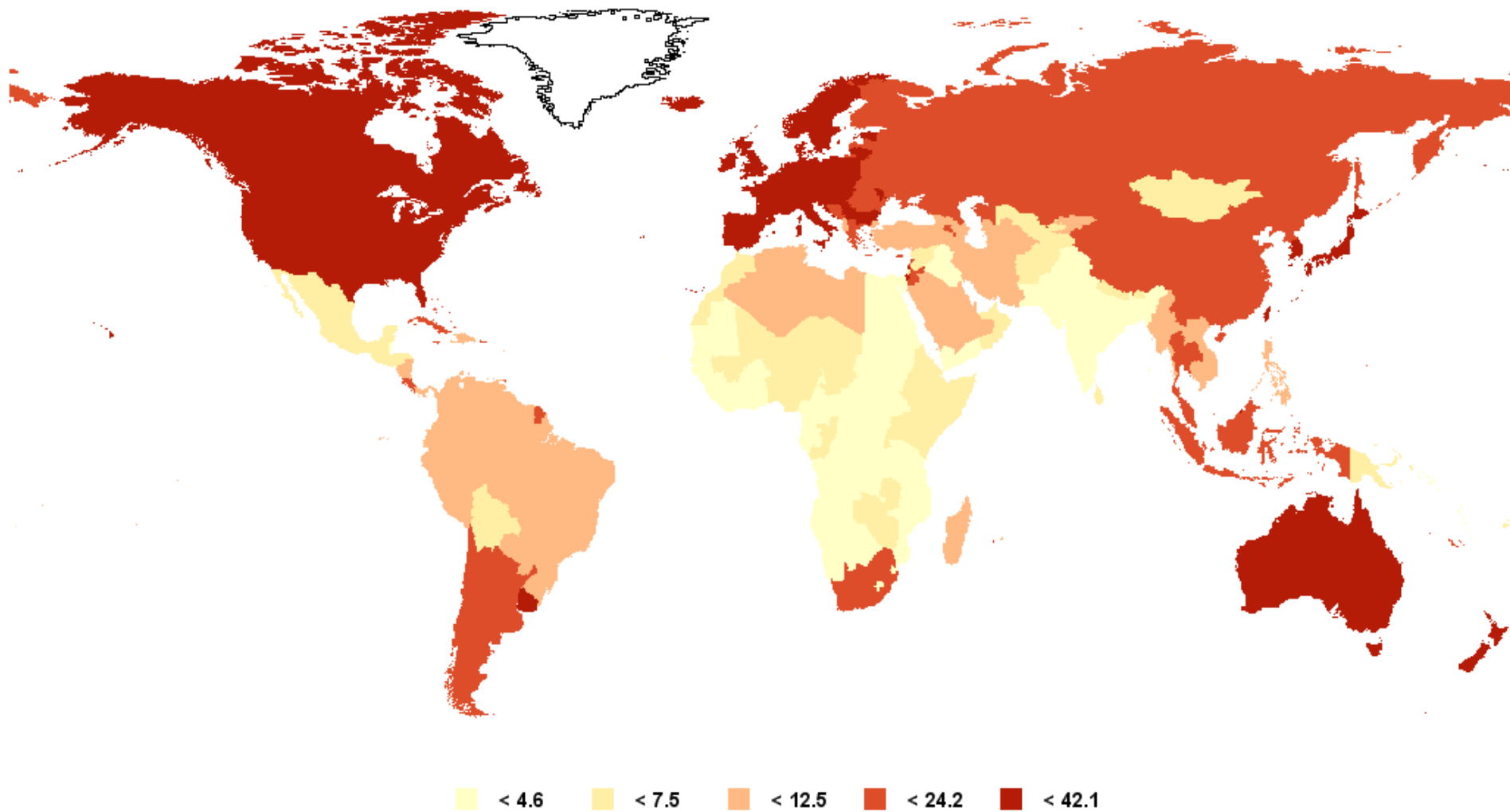
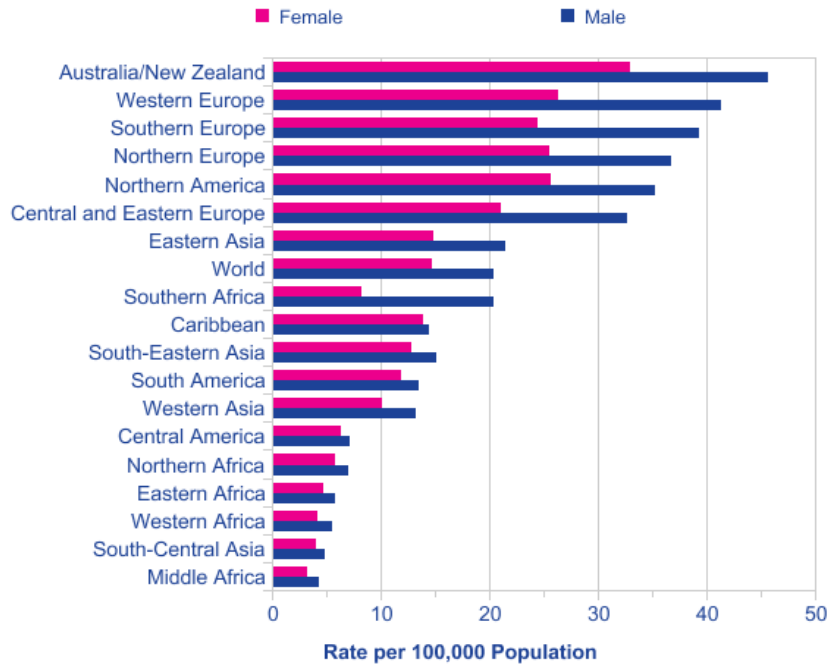


Figure 1.1: Global estimated age-standardised incidence rates for CRC: both sexes. Australia and New Zealand have over 42.1 cases per 100,000; Uganda and India have less than 4.6 cases per 100,000 (GLOBOCAN, 2008).

A



B

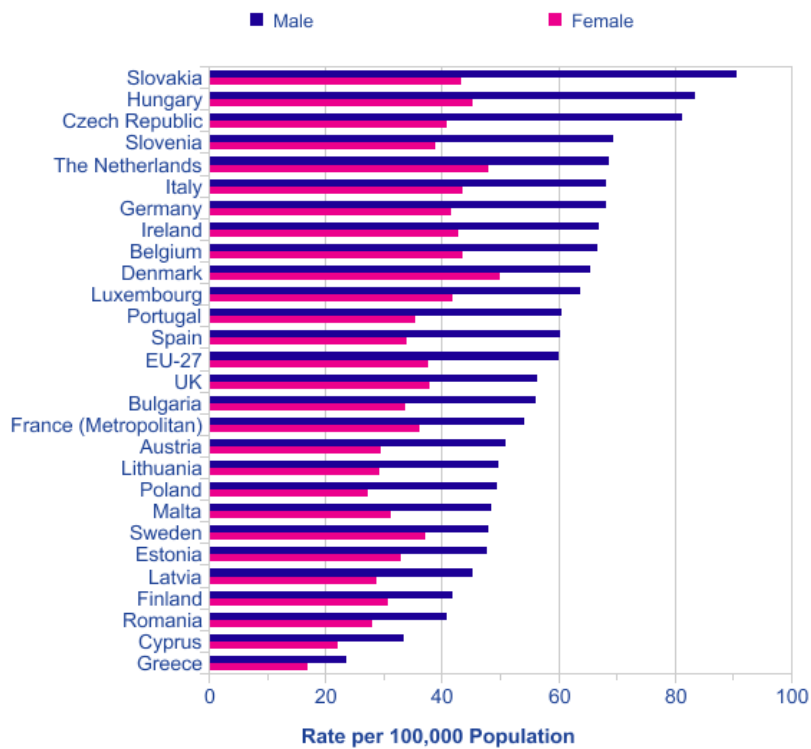


Figure 1.2: CRC incidence rates

(A) Global age-standardised incidence rates (B) European age-standardised incidence rates (adapted from Cancer Research UK, 2011).

1.2 Colorectal cancer risk factors

It is now well established that 5-10% of all CRC cases are due to genetic predisposition, and the remaining 90% of sporadic cases are intrinsically linked to environmental factors pertaining to diet and lifestyle (Smits et al., 2008). Epidemiological and pathological research has enabled the identification of several risk factors that may increase or decrease the risk of developing CRC. To date, the most comprehensive publication to examine such risk factors is the World Cancer Research Fund (WCRF)/American Institute for Cancer Research (AICR) report entitled 'Food, Nutrition, Physical Activity and the Prevention of Cancer: a Global Perspective' (2007). In summary, they reported the probability of a causal relationship between exposure and outcome. Here, we briefly review the pertinent risk factors associated with developing CRC.

1.2.1 Age

The biggest risk factor associated with developing CRC is an individual's age. The risk of CRC begins to increase at 40 years of age and rises dramatically beyond 50-55 years. Moreover, 83% of all cases arise in people over 60 years old (Cancer Research UK, 2011). Likewise, CRC mortality is strongly associated with age (Figure 1.3). CRC takes between 10-15 years to develop, and symptoms do not present themselves until the disease has reached an advanced stage. Although CRC cases do arise in the younger population, these cases are predominantly due to well-defined hereditary CRC syndromes (Chapter 1, Section 1.3).

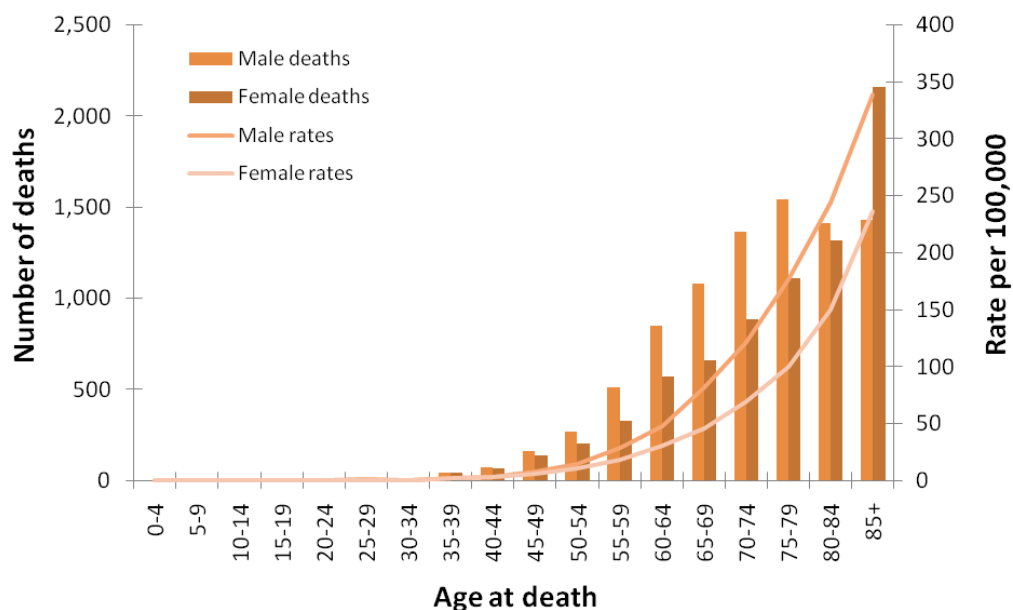


Figure 1.3: Age-specific mortality rates of CRC, UK, 2008 (adapted from Cancer Research UK, 2011).

1.2.2 Gender

Although the lifetime risk of CRC is similar between the sexes (Davies et al., 2005), age-adjusted incidence and mortality rates are higher in men than in women (Ferlay et al., 2010). Thus, male gender is an important risk factor for the development of CRC. It is thought that lower consumption of vegetables and increased alcohol or tobacco consumption amongst men may partly explain why males have a higher risk of CRC than females (Cai et al., 2012). In addition, there are sex-specific differences with regard to tumour location (Section 1.4.1). The frequency of proximal (right-sided) CRC is higher in men than in women. Moreover, patients with right-sided CRCs usually have a more aggressive disease and worse prognosis than patients with left-sided (distal) CRCs. The mechanism that underlies the sex-specific differences remains to be elucidated (Benedix et al., 2010).

1.2.3 Adult-attained height

According to the WCRF report, there is convincing evidence to suggest that adult-attained height increases the risk of CRC. Meta-analysis of cohort data from 16 case-control studies revealed a 9% increased risk per 5cm of height. In Western society, populations have become collectively taller with the increase in nutritional intake. Height may act as a proxy for energy balance because it is a reflection of nutritional and environmental exposures that occurred *in utero*, early childhood and puberty. In addition, taller individuals have a longer intestinal tract, undergoing more cellular divisions. This may simply increase the likelihood of polyp formation and malignant transformation (Hughes, 2011).

1.2.4 Obesity

Obesity has reached epidemic proportions in the Western world. In the UK alone, the prevalence of obesity has increased dramatically. Figures indicate that 59% of women and 69% of men have a Body Mass Index (BMI) of 25 or more. There is convincing epidemiological evidence, with a clear dose-response relationship, that subcutaneous fat (as indicated by BMI) and abdominal fatness (as indicated by waist circumference and or/hip to waist ratio) increases the risk of CRC. Meta-analyses from 60 cohort studies demonstrated a 15% increase in risk per 5 kg/m². Meta-analysis of four cohort studies showed an increased risk of 5% per inch of waist circumference. Furthermore, meta-analysis of 5 cohort-studies showed an increased risk of 40% per 0.1 increment of waist to hip ratio.

Obesity in general is linked to type II diabetes. It is well established that abdominal fatness decreases insulin sensitivity which can lead to increase insulin production. This hyperinsulinaemia increases the risk of CRC (Ortiz et al., 2012). The mechanisms that underlie the association between obesity and colon cancer remain to be fully established, but it has been suggested that the metabolic burden caused by an increased number of adipocytes creates an environment in which uncontrolled cell growth and survival are favoured (Sung et al., 2011). In addition, obesity promotes the production of pro-inflammatory factors and facilitates activation of the NLRP3 inflammasome, an interleukin-1 β family cytokine-activating protein complex (De Nardo and Latz, 2011). Pro-inflammatory cytokines are produced by activated macrophages that are frequently found in the adipose tissue of obese individuals. A recent study of inflammatory cytokines in colorectal tumours found that at least nine inflammatory cytokine genes were dysregulated compared with normal tissue. This study also noted that macrophages found in the cancerous tissue had a pro-inflammatory signature (McLean et al., 2011). The association between inflammation and CRC has also been investigated using knockout mice that lack regulators of inflammatory signalling. For example, the NOD-like receptor NLRP12 functions to downregulate many pro-inflammatory cytokines, and mice lacking this receptor become susceptible to colon inflammation and increased colorectal carcinogenesis. This study also highlighted the emerging importance of macrophages in controlling inflammation and hence cancer development.

1.2.5 Red and processed meat

There has been a great amount of scientific interest related to the consumption of red meat and processed foods in relation to CRC risk. The epidemiological studies to date conclude that there is increased risk of 15% and 21% per 50 g/day of red meat and processed meat consumed, respectively. Cohort and case-control studies indicate a dose-response relationship, and a conclusion from the WCRF/AICR report is that both red and processed meats are 'convincing' causes of CRC. However, this notion remains controversial. Some publications suggest that epidemiologic evidence does not support a clear association between consuming processed meat and CRC. Several hypotheses have been proposed to explain the mechanism underlying the link between red meat and CRC development, most of which are based around the primary constituents of the meat such as protein, fat or possibly iron (Williams et al., 2010). It has also been suggested that heterocyclic amines and

polycyclic aromatic compounds could contribute to the onset of CRC. These compounds form during the cooking and processing of meat and are potent carcinogens. There is considerable variability on how processed meat is defined but it generally refers to any mechanical, chemical, enzymatic or microbiological treatment of meat. This includes smoking, curing, salting, and the addition of preservatives such as salt, nitrate and nitrites. Amino acid derivatives can react with nitrite and nitrate, forming potentially carcinogenic compounds and excess iron in the diet can also lead to the production of free radicals (Cross et al., 2003; Nelson, 2001). A recent risk analysis for those individuals that consume high amounts of meat suggests that reducing meat intake to 70 g/week should, in theory, decrease the risk of CRC by up to 25% (Norat et al., 2005).

1.2.6 Alcohol

Some epidemiological studies indicate that there is a positive association between alcohol consumption and CRC occurrence, but not all investigators agree (Crockett et al., 2011; Fedirko et al., 2011; Otani et al., 2003; Su and Arab, 2004). The AICR report concludes that there is convincing evidence that more than 30 g/day of alcohol increases CRC risk in men, whilst the risk is 'probable' in women. Men generally consume more alcohol than women. In addition, there are differences in types of alcoholic drink consumed between the sexes and there may be hormone-related differences in alcohol metabolism or susceptibility to alcohol. Ethanol is carcinogenic as it can inhibit DNA methylation (Liu et al., 2009), alter retinoid signalling (Kane et al., 2010), and produce toxic metabolites such as acetaldehyde (Seitz and Stickel, 2007).

1.2.7 Smoking

It is estimated that tobacco causes approximately 20% of all cancer deaths. Globally, around 80% of lung cancer cases in men and 50% in women are caused by cigarette smoking. Cigarette smoke contains at least 80 known mutagenic carcinogens (e.g. cadmium, arsenic, ammonia, formaldehyde, benzopyrene) and is a source of oxidative stress. Whilst the association between smoking and lung cancer is universally accepted, the association between CRC has been controversial. Smokers have increased risk of CRC according to a recent study (Liang et al., 2009). In general, tobacco use is likely to increase tumour growth by inducing angiogenesis and suppressing the immune system (O'Byrne et al., 2000).

1.2.8 Energy restriction

Energy restriction appears to be one of the most convincing interventions for lowering CRC risk (Kritchevsky, 1993). Numerous studies in animal models have demonstrated that this occurs through mechanisms such as inhibiting cell proliferation, accelerating apoptosis, enhancing DNA repair and lowering sex steroid hormones (Tammariello and Milner, 2010). Energy restriction at a young age appears to confer protection against CRC. Hughes et al. (2010) showed that exposure to the Hunger Winter period (1944-1945) in the Netherland's Cohort Study on Diet and Cancer (NLCS) was associated with a lower risk of developing colorectal neoplasms.

1.2.9 Physical activity

Physical activity is a major aspect of energy expenditure, and according to the WCRF report, there is convincing evidence that physical activity decreases CRC risk and equally a sedentary lifestyle increases CRC risk. However, the exact mechanisms by which physical activity can be attributed to lowering cancer risk are not fully understood (Eheman et al., 2012). It has been suggested that sustained physical exercise raises the metabolic rate, which in turn reduces hypertension and insulin resistance and obesity. Moreover, physical activity may improve immune function, reduce free radicals, increase prostaglandins and increase gut motility. It has also been shown that physical activity decreases the risk of recurrence and improves the quality of life in CRC survivors (Denlinger and Engstrom, 2011).

1.2.10 Fibre intake

The notion that dietary fibre intake can reduce the risk of CRC is long-standing. This hypothesis was first proposed by Burkitt in 1971, based on findings that of low rates of CRC were found among rural Africans who consumed a fibre-rich diet (Burkitt, 1971). Dietary fibre might protect against CRC by increasing stool weight, reducing transit time of material in the colonic lumen and through dilution of carcinogens. Fibre digestion by the colonic microflora can produce butyrate, a compound known to stimulate apoptosis (Avivi-Green et al., 2000; Hague et al., 1993). However, a number of epidemiological studies have reported no association between dietary fibre and CRC risk (Sanjoaquin et al., 2004). This may be partially explained by the lack of reproducible data and the difficulty in delineating the effects of other dietary components such as folate, selenium and flavonoids that are found

in plant-rich material (Bingham et al., 2005). Taken together, the evidence suggests that dietary fibre may reduce the risk of CRC but more evidence is required.

1.2.11 Aspirin

Aspirin is an acetyl derivative of salicylic acid that was shown in classical experiments by John Vane to inhibit prostaglandin synthesis (Vane, 1971). Later experiments demonstrated that aspirin irreversibly inhibits COX1 and modulates the activity of the inducible COX2 enzyme, which are primarily responsible for the production of prostaglandins and thromboxane by platelets. The original application for aspirin was as an analgesic and modulator of blood clotting in heart attacks and strokes (Vane and Botting, 2003). However, observational and epidemiological studies suggest that non-steroidal anti-inflammatory drugs (NSAIDs), including aspirin are associated with an overall reduction in the incidence of colonic polyps and the appearance of colorectal carcinomas (Thun et al., 2012). Two randomised control trials in the UK and Sweden showed that aspirin at a low dose of 75 mg/day, when taken between 1 and 8.6 years of age, is associated with a 39% decrease in CRC. The mechanism(s) of aspirin action in the prevention of CRC are incompletely understood, but it is thought that aspirin and other NSAIDs suppress COX-2 and hence inhibit polyp growth (Baron et al., 2003; Sandler et al., 2003). Regular aspirin usage has side-effects, including of gastro-intestinal haemorrhage, so both trials concluded it was too early to recommend widespread use of aspirin as a chemopreventive agent to prevent CRC.

1.2.12 Other dietary factors

The WCRF/AIRC report also evaluates the effect of other dietary factors and the risk of developing CRC. It is probable that consumption of foods containing garlic reduces the risk of CRC (Dietrich et al., 2011; Norat, 2010). Garlic contains allyl sulphur compounds, including diallyl disulphide and S-allylcysteine, which are derived from unstable thiosulfinates such as allicin when garlic cloves are disrupted (Amagase et al., 2001). The complex chemistry of garlic sulphur compounds has made it difficult to assess mechanism in CRC prevention, but some of these substances have been tested in animal cancer models. For example, C57BL/6J mice provided with diallyl sulphide prior to chemical induction of CRC had reduced incidence of adenocarcinoma, as did animals given S-allylcysteine (Sumiyoshi and Wargovich, 1990; Wargovich, 1987). Despite initial hope from tests in animal models, few clinical trials with

cancer patients have been conducted using garlic compounds and these have provided mixed results (Ngo et al., 2007). One confounding issue is that in many trials, the level of garlic intake (and metabolic processing) is heterogeneous, making it difficult to define a dose. Garlic sulphur compounds are thought to protect against cancer by inhibiting carcinogen-induced DNA modifications, preventing unregulated cell growth, proliferation and angiogenesis, inducing differentiation, apoptosis and carcinogen-detoxifying enzymes (Ngo et al., 2007). Garlic also contains other substances, including selenium, vitamins A and C, and fructooligosaccharides which are likely to protect against cancer (Ngo et al., 2007). In addition to garlic, other dietary components are likely to influence the risk of developing CRC. For example, milk and calcium consumption reduces the risk of this type of cancer (Dietrich et al., 2011; Norat, 2010). Calcium is thought to trap CRC-promoting bile acids in the colon and it has been reported that this metal can increase apoptosis as well as decrease the proliferation of epithelial cells (Bernstein et al., 2005; Lupton et al., 1996; Whitfield et al., 1995). Finally there is some evidence that fish consumption can protect against CRC. However, as with dietary fibre, there is heterogeneity in these epidemiological studies. This may be partly due to the wide variety of fish species and sources consumed, ranging from fresh fish to tinned and dried fish. Moreover, a high intake of fish may be associated with low meat consumption; a potential confounder that is not easy to adjust for. It is worth noting that whilst five portions of vegetables a day is recommended for a healthy diet, studies suggest that there is little or no association between fruit and vegetable consumption and CRC risk (Key, 2011).

1.3 Hereditary colorectal cancer

As previously mentioned, the majority of CRC cases (~90%) develop sporadically and are strongly associated with an ageing population. The remaining cases (~5-10%) are due to well-defined inherited cancer syndromes named familial adenomatous polyposis (FAP), hereditary nonpolyposis CRC (HNPCC) and hamartomatous polyposis syndromes (Potter, 1999; Rustgi, 2007). Whilst these conditions only affect a small number of the younger population, knowledge derived from investigating hereditary CRC has led to a vast increase in our understanding of the critical molecular pathways of sporadic CRC (to be discussed in Chapter 1, Section 1.4) (Kinzler and Vogelstein, 1996). In parallel fashion, the emergence of normal diagnostics and therapeutics has continued to develop (Rustgi, 2007).

1.3.1 Familial adenomatous polyposis coli (FAP)

Familial adenomatous polyposis coli (FAP) is an autosomal-dominant CRC syndrome, with a prevalence of 1 in 13,000 individuals (Bisgaard and Bulow, 2006; Jasperson et al., 2010). The most compelling feature is the development of hundreds to thousands of adenomatous polyps in the colon and rectum, usually within the second decade of life (Bisgaard and Bulow, 2006; Nieuwenhuis et al., 2007; Nieuwenhuis and Vasen, 2007). However, the majority of patients are asymptomatic for years until the adenomas are large and numerous, causing rectal bleeding or anaemia (Half et al., 2009). In addition, FAP may present with extra-intestinal manifestations such as dental abnormalities, congenital hypertrophy of the retinal pigment epithelium, desmoid tumours and other extra colonic malignancies (Biasco et al., 2004; Rustgi, 2007; Speake et al., 2007). Approximately 70% of FAP patients have a family history of colorectal polyps and cancer, with an almost inevitable progression to CRC unless this is dealt with by surgical intervention (Galiatsatos and Foulkes, 2006). FAP manifests equally in both sexes, and accounts for 0.2-1% of all CRC cases. The disease is caused by a germline mutation in the adenomatous polyposis coli (*APC*) gene located on chromosome 5q21 (Grodén et al., 1991; Herrera et al., 1986; Nishisho et al., 1991). *APC* is a classical tumour suppressor gene. FAP patients inherit one germ-line mutation and develop tumours from those cells in which loss of the other allele (a 'second hit') is somatically acquired (Knudson, 2001; Nieuwenhuis and Vasem 2007; Jasperson et al., 2010).

The *APC* gene encodes a 2843 amino acid protein, consisting of a variety of functional domains involved in a multitude of cellular processes including transcription, cell adhesion and signal transduction (Burgess et al., 2011; Half et al, 2009) (Figure 1.4). Notably, *APC* forms part of a protein complex involved in ubiquitin-mediated degradation of β -catenin in the canonical Wnt signaling pathway (Goss and Groden, 2000) (Chapter 1, Section 1.4.4). To date, over 300 different mutations have been identified (Beroud and Soussie, 1996). The majority of these mutations (e.g. deletions, nonsense mutations) result in a truncated protein. The most common mutation, occurring in about 10% of FAP patients, is a deletion mutation in codon 1309. Over 60% of *APC* mutations are located between codons 1250-1484 – the so-called mutational cluster region (MCR) (Beroud and Soussie, 1996; Bertario et al., 2003). The fact that FAP is caused by a wide range of mutations represents a problem for molecular genetic diagnosis (Half et al., 2009). Several studies have revealed an association between the location of the *APC* mutations and phenotype; however, the correlation is not

exact and differences do occur (Nishisho et al., 1991). Approximately 10% of FAP patients have a less aggressive version of the disease – termed attenuated FAP. Attenuated FAP is caused by mutations in either the extreme 5' or 3' ends of the APC exons and is characterized by delayed onset and fewer adenomatous polyps (typically less than 100), and a lower cancer risk (Burt et al., 2004). Importantly, since the discovery that germline mutations in *APC* give rise to FAP, it has been well documented that at least 70% of sporadic CRC cases also harbour mutations in *APC*, which has led to the association between *APC* and initiation of sporadic CRC (Powell, 1992) (Chapter 1, Section 1.4.3).

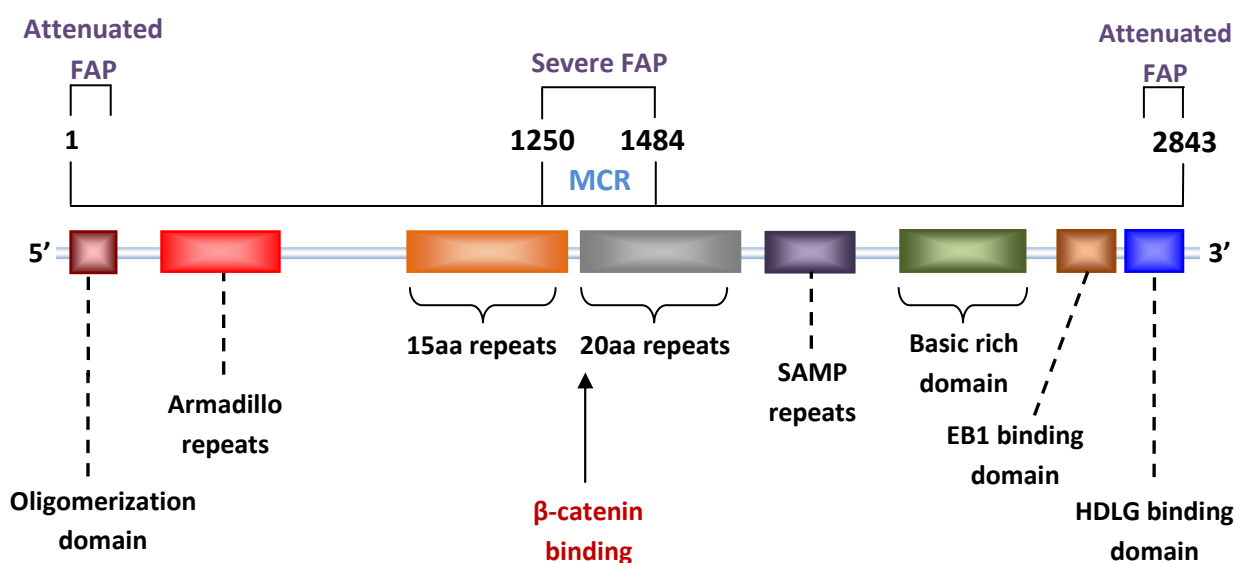


Figure 1.4: Adenomatous polyposis coli (APC) key functional domains

APC has eight functional domains which have important roles in fundamental cellular process such as cell migration (microtubule binding via the basic rich domain) and transcription (B-catenin binding via 20aa repeats). Severe FAP correlates with mutations between codons 1250-1884 found in the mutational cluster region (MCR), which is a common region for APC mutations in sporadic CRC. Attenuated FAP is highlighted by mutations in either the extreme 5' or 3' end of the APC exons. SAMP = serine alanine methionine proline. EB1 = end-binding protein 1. HDLG = Human Disc Large binding site (adapted from Half et al, 2009).

1.3.2 Hereditary non-polyposis colorectal cancer (HNPCC)

Hereditary non-polyposis colorectal cancer (HNPCC), also known as Lynch syndrome, was first described in 1966 (Lynch et al., 2009). The condition accounts for approximately 5% of all cases making it the most common inherited CRC predisposition and increases a patient's

life-time risk of cancer to 80% (Jasperson et al., 2010; Rustgi, 2007). HNPCC is characterized by an autosomal dominant inheritance of early-onset CRC (Lynch and Lynch, 2004; Stoffel et al., 2009). Patients have a markedly increased risk of developing other cancers including cancers of the endometrium, ovary, stomach, small bowel, urinary tract, pancreas and brain (Hampel et al., 2006; Kastrinos et al., 2009). The disease is caused by mutations in DNA mismatch repair (MMR) genes; predominantly MutL Homolog 1 (*MLH1*), MutS Homolog 2 (*MSH2*), MutS Homolog 6 (*MSH6*) and Postmeiotic segregation increased 2 (*PMS2*). Over 90% of HNPCC patients have germline abnormalities in *MLH1* or *MLH2*. The MMR system performs important recognition and editing functions during DNA replication, and thus plays a fundamental role in maintaining genomic stability. Upon DNA damage (e.g. as a result of oxidative stress) or following replication-associated errors, MMR proteins can recognize and repair both base-pair mismatches and small nucleotide (1-4 bp) insertion deletion loops (Figure 1.5). Briefly, MSH2 and MSH6 form a heterodimer which recognize single base mismatches or deletions, and MSH2 and MSH3 dimerize and extend the capability of the MMR systems to recognize 1- 4bp mismatches and deletions. Subsequently, MLH1 and PMS2 are recruited to form a complex with either MSH2-MSH6 or MSH2-MSH3 which ultimately triggers a cascade of events that leads to excision of the mismatched base(s), resynthesis and ligation. In HNPCC, mutations in MMR genes diminish the capacity to repair replication-associated errors, and as such mutations accumulate in short DNA tandem repeats known as microsatellites. Microsatellite instability (MSI) is a hallmark of HNPCC and is also observed in 15% of all sporadic CRCs (Chapter 1, Section 1.4.8). Ultimately, MMR deficiency mediates an overall increase in mutations that leads to the so-called 'mutator phenotype'. This has detrimental effects on 'normal' regulatory process (e.g. apoptosis) in the colonic epithelia which leads to a selective growth advantage and allows for neoplastic transformation.

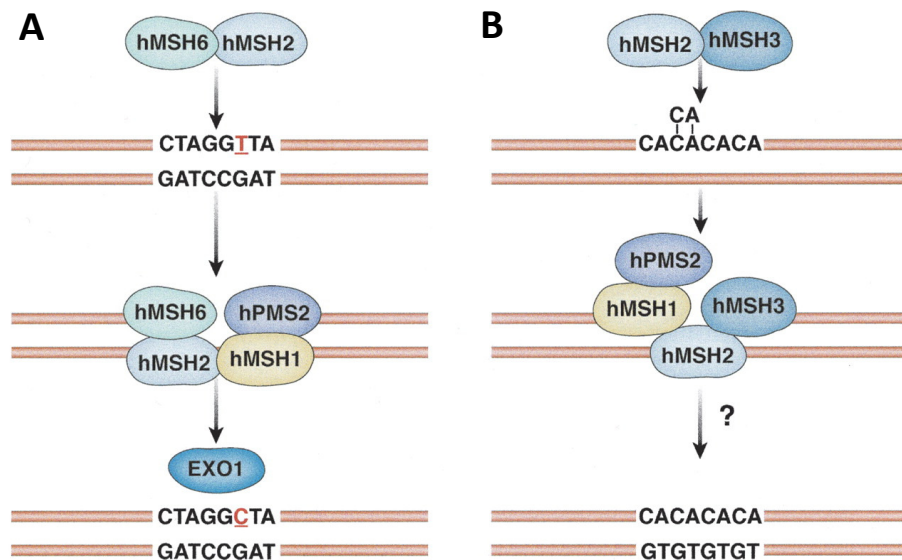


Figure 1.5: DNA mismatch repair system overview

The MMR system in mammalian cells functions to recognise and correct base-pair mismatches and small nucleotide (1-4 bp) insertion/deletion mutations that occur during DNA replication. (A) Key proteins involved in the recognition and repair of single-base mismatches and insertion/deletion mutations and (B) in 1-4 bp mismatches and insertion/deletion mutations. MLH1 and PMS2 form complexes with both MLH2-MLH6 and MLH2-MLH3, culminating in the excision of the mismatches base(s), resynthesis and ligation (adapted from Rugsti, 2007).

1.3.3 Hamartomatous polyposis syndromes

The hamartomatous polyposis syndromes are a heterogeneous group of disorders representing only a small fraction of the inherited gastrointestinal predisposition syndromes (<1%) (Jasperson et al., 2010). Nevertheless, many of these conditions exhibit a substantial risk of colorectal as well as extracolonic malignancies. These syndromes are characterised by the propensity to develop hamartomatous polyps of the gastrointestinal tract. Several syndromes have been documented; Juvenile Polyposis Syndrome (JPS), Peutz-Jeghers Syndrome (PJS), Bannayan-Riley-Ruvalcaba Syndrome (BRRS), Cowden Syndrome (CS), Cronkhite-Canada Syndrome (CCS), and Hereditary Mixed Polyposis Syndrome (HMPS) and PTEN Hamartoma Tumour Syndrome (PHTS) (Gammon et al., 2009; Schreibman, 2005). Whilst hamartomatous polyps are in themselves benign, they are associated with considerable morbidity and mortality from non-malignant manifestations, such as bleeding and bowel obstruction. Moreover, the transformation of these polyps to carcinoma is not well understood and represents a different mechanism than that seen in other hereditary syndromes.

1.4 The molecular basis of colorectal cancer

1.4.1 Anatomy of the colorectum

The colon is approximately 150 cm long and functions to absorb water and salts from faecal waste. In mammals, the colon comprises of four sections; the ascending colon, the transverse colon, the descending colon and the sigmoid colon (Figure 1.6). The ascending colon is positioned between the caecum and hepatic flexure. The transverse colon forms between the hepatic flexure and splenic flexure. The descending colon connects the splenic flexure to the sigmoid colon. Finally, the sigmoid colon terminates at the rectum. The walls of the sigmoid colon are muscular, and contract to increase the pressure inside the colon, causing the stool to move into the rectum. The rectum is approximately 12 cm long and functions as a temporary storage site for faeces.

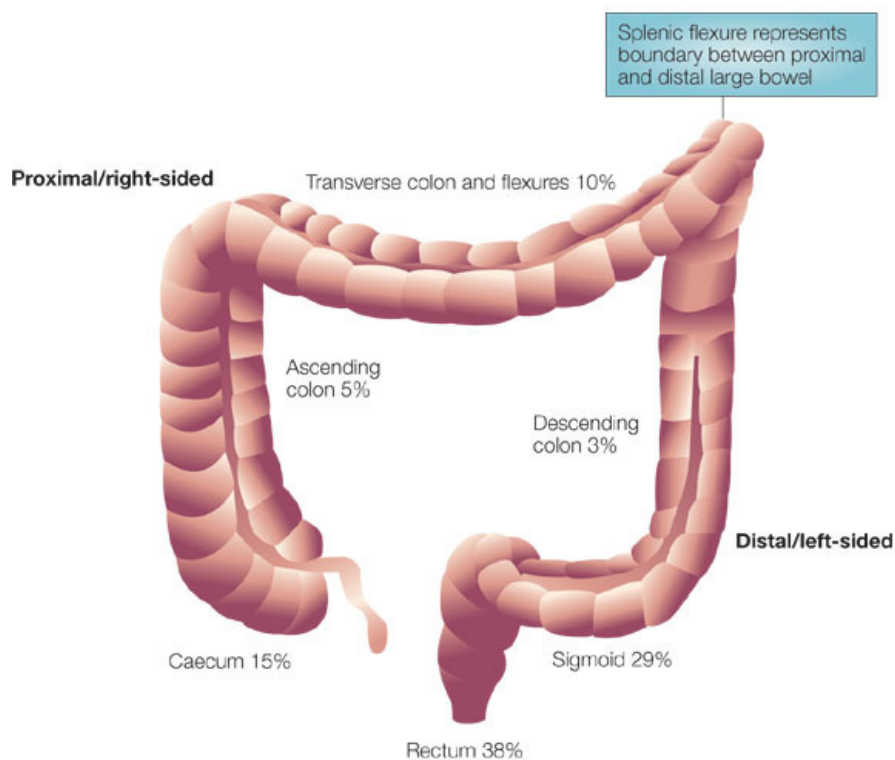


Figure 1.6: Anatomic structure of colorectum

Site distribution of CRC in England and Wales between 1971 and 1994 (adapted from Davies et al., 2005).

Over the last two decades, numerous studies have documented clinicopathological differences between proximal (right-sided) CRCs (caecum, ascending colon, hepatic flexure transverse colon) and distal (left-sided) CRCs (splenic flexure, descending colon, sigmoid colon, rectum) (Benedix et al., 2010; Bufill, 1990). The majority of CRCs originate in the rectum (38%) and sigmoid colon (29%) (Davies et al., 2005) (Figure 1.6). However, since the 1970's, there is growing evidence of a so-called 'distal-to-proximal shift' in the location of tumours (Jass, 1991; Levi et al., 1993; Meguid et al., 2008; Obrand and Gordon, 1998). The reasons behind this change are not entirely clear. It has been suggested that improved detection methods and an aging population are the likely explanations (Rabeneck et al., 2003).

The adult gastrointestinal tract is radially organised into several histologically distinct layers as depicted in Figure 1.7; the mucosa (including the lamina propria, and muscular mucosa), submucosa (loose connective tissue), *Muscularis propria* (circular and longitudinal smooth muscle) and serosa (Greene, 2002). At least 95% of CRCs originate from the mucosa and are classified as adenocarcinomas. Two rarer types of adenocarcinoma that exist include mucinous adenocarcinoma (MAC) and signet cell ring carcinoma (SCC). The prevalence of MAC is ~11% and is characterised by extracellular deposition of mucus constituting >50% of the tumour mass. By contrast, SCC is noted for the presence of individual neoplastic cells containing intracytoplasmic vacuoles with pleomorphic nuclei and accounts for just 1% of all CRC (Verhulst et al., 2012). Other rarer types of CRC include carcinoids, sarcomas and lymphomas. CRC in the context of this thesis refers to adenocarcinomas unless otherwise stated.

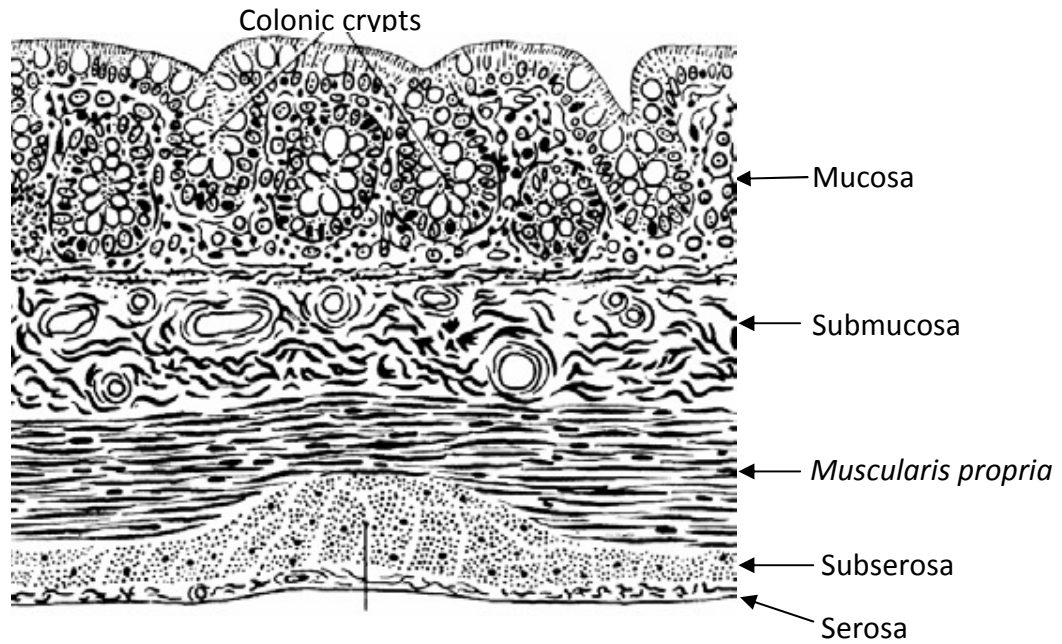


Figure 1.7: Schematic representation of gastrointestinal tract
(adapted from Centres for Disease Control and Prevention, 2011).

1.4.2 The colonic crypt

The colonic mucosa is a simple columnar epithelium adjacent to the luminal surface which is primarily composed of three differentiated cell types: goblet cells, enterocytes and enteroendocrine cells which function to lubricate the passage of waste material, absorb water and salts and secrete hormones, respectively (Marshman et al., 2002). Protruding into the lamina propria, the colonic epithelium forms millions of deep cavities termed colonic crypts (Potten and Hendry, 1995) (Figure 1.8). Each crypt consists of continuously renewing cells that are repeatedly exposed to a wide range of environmental perturbations. Cell turnover at the intercrypt table is very high, and the differentiated population at the crypt apex must be continuously replenished (Booth and Potten, 2000). This homeostatic environment is maintained by a stem cell niche, which cradles the base of the each crypt (Barker, 2007; Marshman et al., 2002). The colonic niche is composed of pericryptal myofibroblasts which surround the stem cell base (Powell, 1999). Pericryptal myofibroblasts probably influence the colonic stem cells by controlling their self-renewal and encouraging stem cell proliferation through a variety of signalling pathways, of which the canonical Wnt signalling pathway is of major importance (Bienz and Clevers, 2000; Pinto and Clevers, 2005; Zeki et al., 2011) (Chapter 1, Section 1.4.4). The stem cells undergo mitotic self-renewing

divisions and then migrate unilaterally up the crypt. They give rise to proliferating, undifferentiated progenitor (transit-amplifying) cells which continue to divide upwards towards the luminal surface where they function briefly to form the differentiated epithelial lining of the gastrointestinal tract (Marshman et al., 2002; Zeki et al., 2011). Eventually, the epithelial cells undergo apoptosis and are shed into the lumen. The entire process of proliferation, differentiation and apoptosis takes between 4-6 days. In essence, the colonic crypt has evolved as a defence mechanism against neoplastic formations (Weinberg, 2007). The stem cells are protected by their very location, and any cells harbouring mutations should be eradicated at the luminal surface. So why and how does CRC arise?

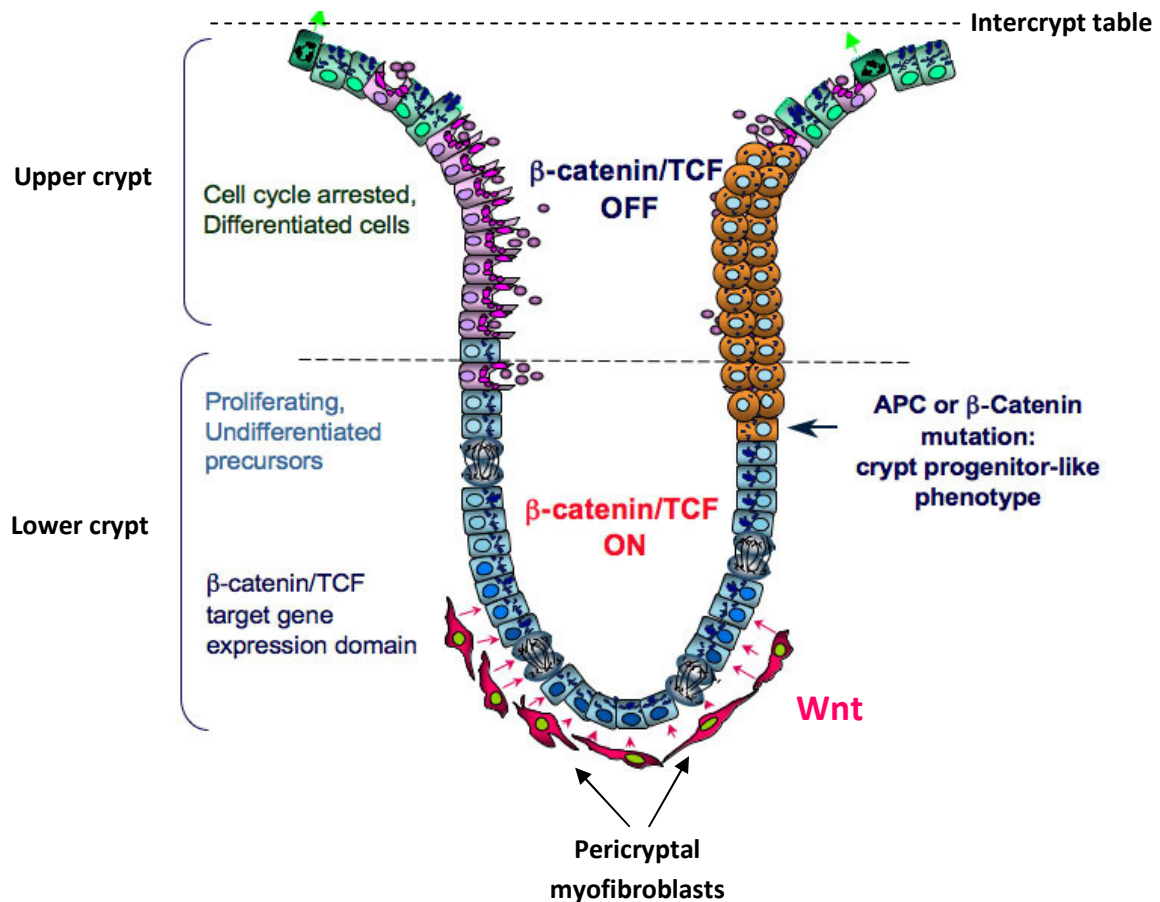


Figure 1.8: Colonic crypt architecture

Schematic representation and proposed model of colonic crypt regulation. The stem cell niche is located at the base of the crypt, and consists of pericryptal myofibroblasts, which produce signalling factors (e.g. Wnt) that maintain the stem cells in an undifferentiated state and control their proliferation. The concentration for these signalling factors decreases with distance from the niche so that the signalling environment (and thus cell behaviour) differs throughout the different crypt locations. In the lower third of the crypt, the progenitor proliferating cells are enriched in nuclear β -catenin, and hence they express β -catenin/TCF target genes. As the undifferentiated precursor cells migrate upwards towards the midcrypt region, β -catenin/TCF activity is downregulated. This ultimately results in cell cycle arrest and the transit amplifying cells subsequently differentiate to become the epithelial components of the gastrointestinal tract. Cells undergoing mutation in *APC* or *CTNNB1* (which encodes β -catenin) become independent of the physiological signals controlling β -catenin/TCF activity. As a consequence, they continue to behave as crypt progenitor cells in the surface epithelium, giving rise to aberrant crypt foci (ACFs) (adapted from van Wetering et al. 2002).

1.4.3 The adenoma-carcinoma sequence

Historically, CRC has been considered a genetic disease, resulting from the stochastic accumulation of mutations in tumour suppressor genes (loss of function) and oncogenes (gain of function). In 1990, Fearon and Volgenstein proposed a classic model that describes the evolution of benign adenomas to carcinomas through a step wise histological progression sequence (Figure 1.9). These genetic aberrations (e.g. *APC*, *KRAS*, *TP53*) ultimately transform normal glandular epithelium, and result in the clonal expansion of neoplastic cells with phenotypic hallmark characteristics including limitless replicative potential, evasion of apoptosis and immune surveillance, sustained angiogenesis and the ability to invade and metastasize (Fearon, 2011; Fearon and Vogelstein, 1990; Hanahan and Weinberg, 2000).

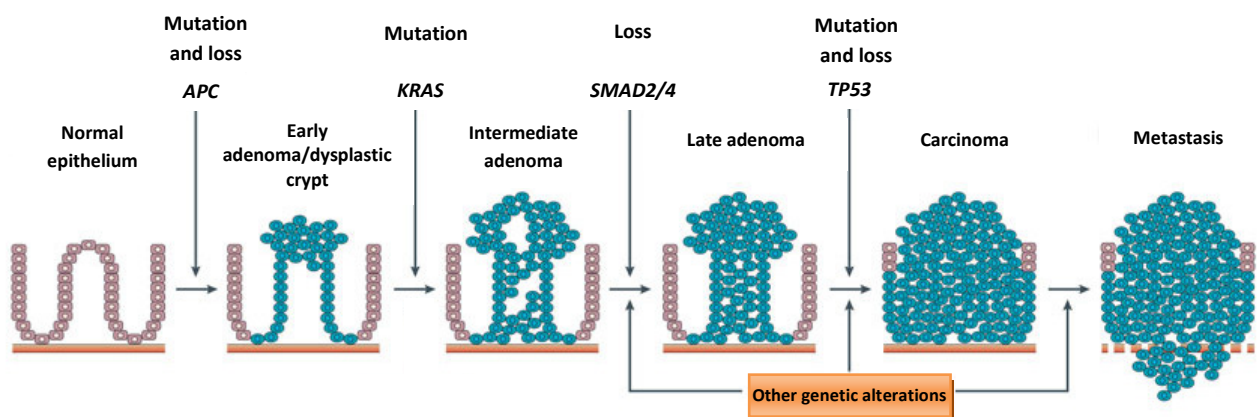


Figure 1.9: The colorectal adenoma-carcinoma sequence

The multistep genetic model of colorectal carcinogenesis is a well-defined sequence of mutational events that characterize the progression of normal colonic epithelium through pre-malignant adenoma to invasive adenocarcinoma. The initial step in CRC development is the inactivation of tumour suppressor gene *APC*, leading to activation of the Wnt signalling pathway and formation of ACF. Subsequent progression into early adenomas and carcinomas requires mutations in proto-oncogene *KRAS* and loss of tumour suppressor *SMAD2/4*. *TP53* mutations tend to occur late in the histological progression sequence and results in increased resistance of cancer cells to apoptosis (adapted from Davies et al 2005).

Adenomas (also referred to as polyps) can be described as elevated masses that protrude into the intestinal lumen (Davies et al., 2005). Dysplastic (neoplastic) polyps can either be pedunculated (with a stalk) or sessile (without a stalk). The epithelium of adenomas can take the form of tubular (glandular), villous (finger-like projections) or tubulovillous adenomas (a permutation of both). Occasionally, adenomas can be flat or depressed which can sometimes prove difficult to detect (Davies et al., 2005). Polyps are considered pre-malignant lesions and only a small percentage will actually progress to invasive adenocarcinomas (Kozuka et al., 1975). Moreover, the entire process of colorectal carcinogenesis takes somewhere in the region of 10-15 years. This has allowed for the identification and detailed analysis of the molecular events involved in the initiation and development of CRC (Soreide et al., 2009).

The earliest identifiable neoplastic lesion in CRC formation is the aberrant crypt focus (ACF) (Alrawi et al., 2006; Ranjana P, 1987; Roncucci et al., 1991). ACFs display expanded luminal openings compared to surrounding normal colonic mucosa (Takayama et al., 1998). Importantly, dysplastic crypts harbour mutations in APC and are most likely to give rise to CRC (Grady, 2005). APC is the most frequently mutated tumour suppressor gene in CRC, with a prevalence of 70-80% (Powell, 1992; Vogelstein, 1988). Mutations in APC were first identified as a germ-line abnormality in patients with familial adenomatous polyposis (Chapter 1, Section 1.3.1), and were subsequently recognized as a crucial initiating 'gatekeeper' mutation in sporadic carcinogenesis (Grodin et al., 1991; Herrera et al., 1986; Nishisho et al., 1991; Powell, 1992).

1.4.4 APC and the canonical Wnt signalling pathway

APC is a negative regulator of Wnt signalling – a critical pathway that is considered to be at the heart of crypt homeostasis and CRC initiation (Bienz and Clevers, 2000) (Figure 1.10). In the normal colonic epithelium, Wnt factors emanate at the base of colonic crypt, imposing a proliferative phenotype through the stabilization of β -catenin and subsequent transcription of Wnt target genes. As the progeny of the colonic stem cells differentiate and migrate towards the lumen, Wnt signalling and thus nuclear accumulation of β -catenin decreases (Batlle, 2002; Pinto and Clevers, 2005; van de Wetering et al., 2002; Zeki et al., 2011).

Upon activation of the Wnt signalling pathway, Wnt ligands interact with Frizzled (Frz) and the co-receptor low-density lipoprotein receptor-related protein (LRP5/6), recruiting Dishevelled (Dsh) to the plasma membrane. The multi-protein degradation complex, consisting of Axin (a scaffold protein) and two serine/threonine kinases glycogen synthase 3 β (GSK3 β) and casein kinase 1 (CK1), is therefore dissociated and cytoplasmic β -catenin cannot be marked for destruction. β -catenin is then free to translocate to the nucleus, where it displaces transcriptional repressor Groucho, and directly interacts with TCF/LEF transcription factors. This allows the transcription of Wnt target genes such as proto-oncogenes *CMYC* and *cyclin D1*, and Wnt pathway feedback regulators such as *AXIN2* and *Dickkopf-1*, ultimately maintaining a stem cell phenotype and proliferating progenitor population in the base of the crypt. In the absence of a Wnt signal, APC binds to Axin and presents β -catenin for phosphorylation and subsequent ubiquitination and proteosomal degradation. Thus, the transcription of the Wnt target genes is prevented (Bienz and Clevers, 2000; van de Wetering et al., 2002).

When APC is mutated in CRC, the resulting truncated protein is unable to bind to Axin, and so β -catenin is no longer marked for destruction, allowing the nuclear accumulation of β -catenin and the constitutive activation of Wnt target genes (Burgess et al., 2011; Korinek et al., 1997). Cells that would normally move out of the crypt are reprogrammed by the activated Tcf4 to remain crypt cells as a direct consequence of the loss of APC. This results in an increase in the size of the proliferating cell pool, and hence polyp formation (Bienz and Clevers, 2000).

APC is a multifunctional protein and controls other cellular activities in addition to regulation of β -catenin, for example, microtubule stability and cell migration (Burgess et al., 2011; Kroboth et al., 2007; Nathke et al., 1996). APC tagged with GFP has been shown to directly interact with microtubules and track along them to the cell periphery (Mimori-Kiyosue et al., 2000). This ability is inhibited by stably binding β -catenin mutants resulting in a decrease in migratory capacity. APC truncation disrupts interactions with microtubules and the actin cytoskeleton, giving rise to changes in microtubule stability, cell orientation and migration (Etienne-Manneville and Hall, 2003; Nathke, 2006; Sansom, 2004). However, the mechanism underlying changes in cytoskeletal dynamics via APC loss and formation of ACFs has not yet been explored (Burgess et al., 2011).

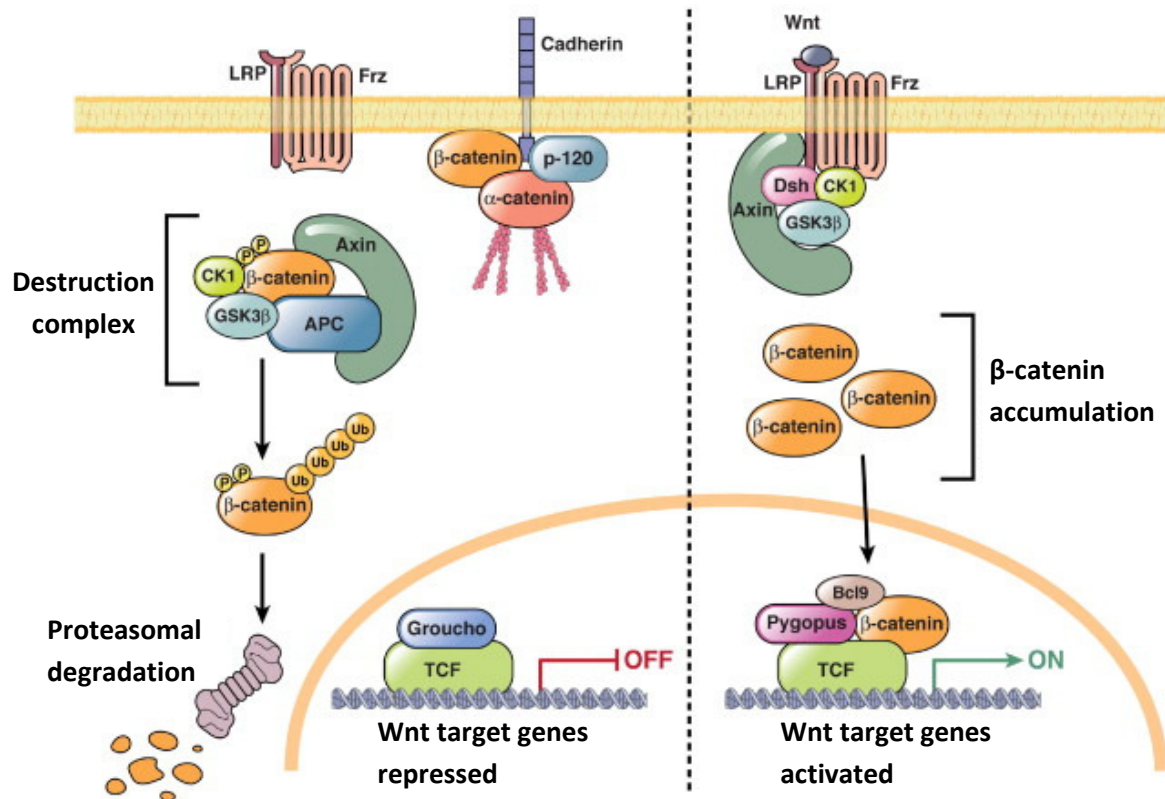


Figure 1.10: Overview of the canonical Wnt signaling pathway

In the absence of a Wnt signal, the APC destruction complex containing GSK-3 β and CK1 degrades cytoplasmic β -catenin in a proteasome-dependent manner. In the nucleus, Wnt target genes are silenced by Groucho interacting with TCF. When a Wnt ligand occupies Frz and the LRP co-receptor, this triggers the phosphorylation of LRP by CK1 and GSK-3 β , sequestering axin on the phosphorylated LRP complex. Phosphorylation of β -catenin is inhibited, leading to translocation of β -catenin to the nucleus. Increased nuclear β -catenin displaces Groucho to drive the transcription of Wnt target genes via interaction with TCF and LEF transcription factors (adapted from Pino and Chung, 2010).

1.4.5 KRAS and the MAPK pathway

As discussed, APC inactivation is important for CRC initiation in the classic adenoma-carcinoma model. However, APC mutations alone are insufficient for the progression of colorectal polyps into invasive adenocarcinomas (Smits et al., 2008). For example, oncogenic mutations in *KRAS* and *BRAF* occur in 37% and 13% of CRCs, respectively (Bos et al., 1987; Markowitz and Bertagnolli, 2009). *KRAS* is a member of the Ras family of guanine-triphosphate-binding signal transducing proteins. It is a down-stream effector of EGFR, and signals through *BRAF* (a serine/threonine kinase) to drive the mitogen-activated protein kinase (MAPK) signalling cascade. This pathway regulates various critical cellular events

including cell proliferation, differentiation, senescence, and apoptosis (Bos, 1989; Rajagopalan et al., 2002). In addition to *KRAS*, *RAS* oncogenes include *HRAS* and *NRAS* all of which are constitutively active and hence mediate dysregulated signaling. Ras is a small protein that transduces signals from the EGFR family proteins. Binding of ligand to EGFR results in dimerization and receptor tyrosine phosphorylation, as indicated in Figure 1.11. Ras activates a signaling cascade through phosphoinositol kinases (PI3K) as well as RAF and thus acts as a central signaling node. Activation of PI3K inhibits apoptosis, whereas RAF activation stimulates cellular proliferation and is therefore important in cancer. *KRAS* mutations lead to constitutive changes that promote cell proliferation and survival independent of the EGFR receptor. Codon 12 is the most common codon affected, usually by a missense mutation, but there are a large number of other mutations that have been identified in a variety of cancers. Since *KRAS* is downstream from EGFR, EGFR is bypassed and drugs that act by inhibiting EGFR signaling are rendered ineffective. Normally, Ras works as a GTPase that can exchange GDP for GTP. In this state, Ras can activate Raf, a member of the MAP3K family of tyrosine kinases. A MAP3K activates a MAP2K, which in turn activates a MAPK. In the Ras/Raf pathway, the MAPK target is ERK, which can dimerise upon activation, enter the nucleus and phosphorylate client transcription factors such as Elk1. This drives the production of various factors involved in cell growth and differentiation (Bos, 1989; Pino and Chung, 2010; Rajagopalan et al., 2002) (Figure 1.11).

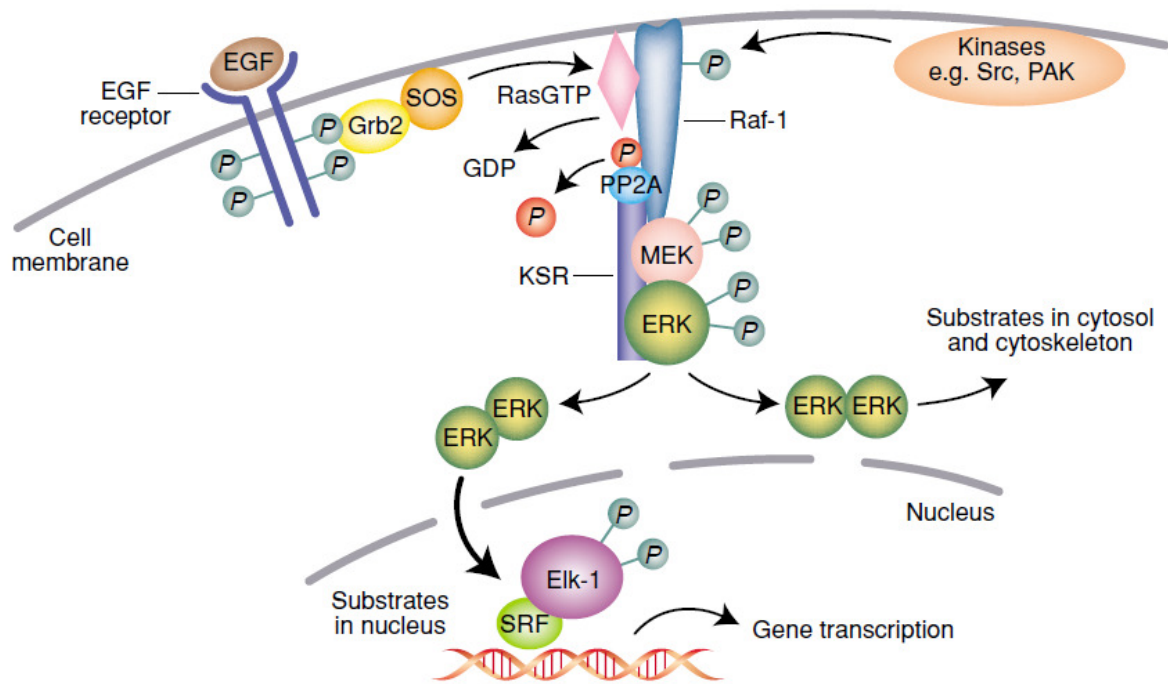


Figure 1.11: Overview of the Ras-Raf-MEK-ERK Pathway

EGF binds to its receptor EGFR and induces receptor dimerization and tyr autophosphorylation. The Grb-SOS complex docks onto the phosphorylated Tyr residues, activating Ras, which exchanges its GDP for GTP. Ras-GTP binds to Raf and recruits it to the cell membrane where Raf is activated. Activated Raf1 phosphorylates MEK, which in turn phosphorylates and activates ERK. ERK has a variety of targets including the transcription factor Elk1, which promotes the expression of genes involved in cell growth (adapted from Kolch et al., 2002).

1.4.6 Tumour suppressor *TP53*

Mutations of the tumour suppressor gene *TP53* are thought to be an almost universal hallmark of human tumours. *TP53* encodes the transcription factor p53, a classical tumour suppressor and central orchestrator of cellular responses to stress (Levine, 1997). Often referred to as ‘guardian of the genome’, p53 is a master regulator that mediates the transcription of hundreds of genes involved in DNA metabolism, cell cycle control, apoptosis, senescence, angiogenesis and cell migration (Levine, 1997; Menendez et al., 2009; Pino and Chung, 2010). In the majority of tumours, the two *TP53* alleles are inactivated, most commonly by a combination of two events: a missense mutation that inactivates the transcriptional activity of p53 and a 17p chromosomal deletion that takes out the second *TP53* allele (Baker et al., 1989; Baker et al., 1990). Loss-of-function of *TP53* is observed in approximately 50% of CRCs defining its role with the progression of adenomas to invasive carcinomas (Fearon and Vogelstein, 1990; Miranda et al., 2006). Mutant p53 disrupts cell

proliferation and leads to the failure of apoptotic mechanisms, resulting in high-level genomic instability and hence cancer progression. However, despite 30 years of investigation, the impact of this tumour suppressor gene on clinical outcome is far from conclusive (Munro et al., 2005).

1.4.7 The chromosomal instability pathway

Extensive research into the transition from benign adenoma to malignant carcinoma has revealed at least two distinct pathways underlying the development of CRC (Smits et al., 2008). The most common genetic pathway which accounts for approximately 75-85% of all CRC cases is the chromosomal instability pathway (CIN), also referred to as the microsatellite stability pathway (MSS) (Hermsen et al., 2002; Lengauer et al., 1997). Tumours with CIN exhibit aneuploidy, chromosomal losses, amplifications, translocations and deletions. Furthermore, loss of heterozygosity (LOH) of 17p and 18q is frequent. Chromosomal loss at 18q has been documented in up to 70% of CRC cases, and the *DCC* gene (deleted in colorectal cancer) which maps to 18q21 has long been implicated in colorectal carcinogenesis (Fearon, 2011). Furthermore, tumour suppressor genes *SMAD2/4* are located on chromosome 18q. *SMAD2/4* proteins are intracellular mediators of the transforming growth factor- β (TGF β) pathway which is involved in the regulation of cell growth, differentiation and apoptosis. Loss of the *SMAD* proteins perturbs the TGF β pathway as they are transcriptional activators of TGF β responsive genes. *SMAD2* and *SMAD4* are depleted in 20% and 10% of CRCs, respectively (Pino and Chung, 2010; Takagi et al., 1996; Takagi et al., 1998).

1.4.8 The microsatellite instability pathway

The second pathway implicated in approximately 15–20% of sporadic CRC cases is referred to as the microsatellite instability pathway (MIN) (Thibodeau et al., 1993). MIN is characterized by inactivation of MMR genes (Chapter 1, Section 1.3.2). Such tumours exhibit frameshift mutations and base-pair substitutions that are commonly found in short, tandemly repeated nucleotide sequences known as microsatellites. MIN in hereditary and sporadic CRC occurs through two different mechanisms (Markowitz and Bertagnolli, 2009). The autosomal dominant condition HNPCC is believed to account for 5-15% of CRC cases and typically exhibits a germline mutation in a mismatch-repair enzyme (*MSH2* and *MLH1* MMR

genes). In sporadic MSI CRC, instability in microsatellite sequences is frequently due to loss of expression of the mismatch-repair gene (most commonly *MLH1*) caused by epigenetic silencing (Miyakura et al., 2003).

Since the proposal of the classic adenoma-carcinoma model, our knowledge of CRC pathogenesis has advanced considerably. Numerous studies over the past few decades have revealed that there are 80 genes mutated in the average CRC genome, of which a subset of 15 are so-called driver mutations that are important in the initiation, progression and maintenance of colorectal tumours (Sjoberg, 2006; van Engeland et al., 2011; Wood, 2007). This has led to numerous revisions of the initial model, and the idea that CRC does not only arise via CIN or MSI, but can arise by other distinct molecular mechanisms and pathways (Smits et al., 2008; van Engeland et al., 2011).

1.5 Epigenetics and colorectal cancer

1.5.1 The role of epigenetics

As previously mentioned, CRC has been historically considered a genetic disease, characterised by sequential mutations in oncogenes and tumour-suppressor genes (Fearon and Vogelstein, 1990; Wood et al., 2007). It is now widely accepted that cancer initiation and progression can occur via an alternative epigenetic mechanism. The original definition of epigenetics was coined by Waddington in 1942 – the notion that ‘phenotypes arise from genotype through programmed change’. This idea was particularly important in the establishment of modern developmental biology. It is appreciated now that developmental processes are regulated largely by epigenetics, a consequence of this being that different cell types maintain their fate during cell division, even though the DNA sequence *per se* remains the same (Feinberg, 2007). Nowadays epigenetics is broadly defined as heritable changes in gene expression without changes in the DNA sequence itself (Feinberg and Tycko, 2004; Lao and Grady, 2011; van Engeland et al., 2011). These modifications can be imagined as a molecular signature superimposed on the DNA sequence that ultimately influences gene expression (Hughes, 2011). Epigenetic modifications play a key role in DNA regulation including replication DNA repair and transcription. Abnormalities in the epigenetic profile can lead to misregulation of these critical processes. Indeed, epigenetic silencing is

recognised as the ‘third hit’ in Knudson’s model of tumour-suppressor gene inactivation, and characterises a subgroup of CRCs with a distinct etiology and prognosis (Kondo and Issa, 2004). The first epigenetic alteration in cancer was discovered by Feinberg and Vogelstein in 1983. They reported the overall depletion in 5-methylcytosine, so-called global DNA hypomethylation, in CRC compared with normal colon. Since then, extensive research has revealed that the ‘epigenetic landscape’ is more complex than was first appreciated (Suzuki and Bird, 2008). There are a variety of epigenetic regulatory mechanisms that both up-regulate and down-regulate gene expression in both normal and cancerous tissue. The overall epigenetic backdrop of a cell results from factors that determine the condensation state of chromatin. Chromatin status is a critical determinant of whether the DNA is accessible to the transcription factors and accessory molecules that control gene activity. Put simply, an open or relaxed chromatin (euchromatin) state permits a gene to be transcribed, whereas a closed or condensed state (heterochromatin) prevents gene transcription (Lao and Grady, 2011; Sharma et al., 2010).

In cancer, epigenetic regulation is organised at multiple levels and includes: DNA methylation; loss of imprinting; post-translational histone modifications; chromatin looping; microRNA’s; and nucleosomal positioning (Kaneda and Feinberg, 2005; Kouzarides, 2007; Rana, 2007; Tiwari et al., 2008). Moreover, the mechanistic interaction between these epigenetic alterations coupled to genetic mutations is hugely complex, with abundant crosstalk (Lao and Grady, 2011). This thesis will focus mainly on DNA methylation, as by far the most extensively studied epigenetic alteration in CRC. However, the reader can be directed to an excellent review for describing the complex interplay between other epigenetic factors (van Engeland et al., 2011).

1.5.2 DNA methylation and CpG islands

DNA methylation is defined as the post-replicative addition of a methyl group to the 5-carbon position on the cytosine ring, resulting in 5-methylcytosine (Lao and Grady, 2011; Smits et al., 2008; van Engeland et al., 2011). The transfer of a methyl group from S-adenosylmethionine (methyl donor) to cytosine (methyl receptor) is mediated by enzymes called deoxynucleotide methyltransferases (DNMTs) including DNMT1, DNMT3a and DNMT3b, which recognise CG dinucleotide sequences called CpG dinucleotides (Bestor, 2000; Jones and Baylin, 2002). CpG dinucleotides are found less frequently than expected by

chance alone in the genome, probably because they are vulnerable to spontaneous deamination of the $-NH_2$ group of 5-methylcytosine (Herman and Baylin, 2003; McCabe et al., 2009). In humans, the majority of CpGs are methylated, with unmethylated CpGs typically restricted to small regions known as CpG islands. By definition, CpG islands are 0.5 Kb – 2 Kb sequences with a G:C content >55% and a higher than expected ratio of > 0.6. CpG islands are associated with the promoter region in 60% of all genes (Gardiner-Garden and Frommer, 1987; Lao and Grady, 2011).

Importantly, DNA methylation is present throughout the majority of the genome and is essential for normal mammalian development (Bird, 2002). This epigenetic alteration is associated with genomic imprinting, transcriptional inactivation of the X-chromosome and aging (Lao and Grady, 2011; Reik and Lewis, 2005). Homozygous deletion of the murine DNA methyltransferase, *Dnmt1*, results in demethylation and embryonic lethality, demonstrating that DNA methylation is critical during development (Li et al., 1992).

1.5.3 Aberrant DNA methylation and colorectal cancer

In CRC, epigenetic instability presents itself in a variety of ways including global DNA hypomethylation and aberrant promoter hypermethylation at CpG islands (Herman and Baylin, 2003; van Engeland et al., 2011). As previously mentioned, DNA hypomethylation was one of the first recognised epigenetic alterations in CRC and refers to the loss of 5-methylcytosine content (Feinberg and Vogelstein, 1983). In contrast to normal tissues, cancer DNA is globally hypomethylated at CpG dinucleotides in repetitive sequences (e.g. satellite- and LINE- repeats, these being endogenous retroviral elements), and is locally hypermethylated at discrete CpG sites that normally exist in the unmethylated state (Baylin et al., 1998) (Figure 1.12). In the colon, changes in the DNA methylation pattern arise early on, initially in histologically normal mucosa (Toyota and Issa, 1999). For example, aberrant methylation of *IGF2* (Insulin growth receptor), *ESR1* (Estrogen receptor) and *TUSC3* (Tumour suppressor candidate 3) has been shown to occur in histologically normal colon in age-dependent manner (Fink, 1996; Issa, 1994; Toyota and Issa, 1999). Thus, it has been suggested that CpG islands may exhibit a stochastic predisposition to methylation. One notion is that for 'old' cancer cells, methylation could be a 'molecular clock' that denotes their advanced age (Kondo and Issa, 2004). This idea is supported by the fact that one of the estrogen receptor genes, ERalpha, becomes increasingly methylated as the colonic mucosa

ages, and is particularly densely methylated in CRC causing the gene to become transcriptionally silenced (Issa, 1994).

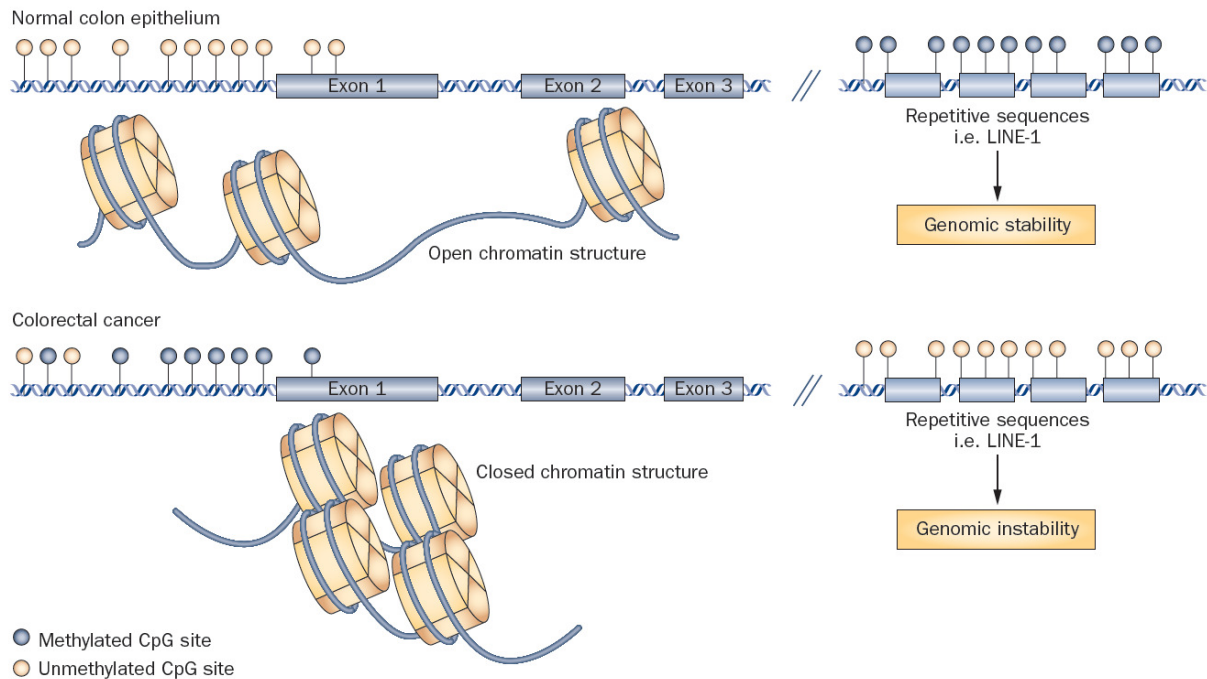


Figure 1.12: CpG island DNA hypermethylation and global DNA hypomethylation in normal colonic epithelium and CRC

Unmethylated CpG islands are correlated with an open chromatin structure (euchromatin), whereas methylated CpG islands are correlated with a condensed, closed chromatin structure (heterochromatin) and transcriptional silencing. Normal colonic epithelium predominantly contains unmethylated CpG islands in the promoter regions of genes, whereas aberrant hypermethylation of promoter associated CpG islands is a hallmark of colorectal neoplasms. In addition to the aberrant hypermethylation seen in CRCs, global hypomethylation at LINE-1 sequences is also observed which is frequently associated with genomic instability. Interestingly, an inverse association exists between CpG promoter hypermethylation and global LINE-1 hypomethylation with the progression of CRC (adapted from Lao and Grady, 2011).

1.5.3.1 DNA Hypomethylation

DNA hypomethylation has been attributed to genomic instability, which may predispose to CIN and aneuploidy. Loss of methylation at sites located close to the centromere may predispose the cell to chromosomal recombination and replication events. Evidence attributing genomic instability to DNA hypomethylation comes from experimental work in

mice. For example, *Dnmt1* hypomorphic *Apc*^{Min/+} mice develop small adenomas associated with LOH of APC (Eads et al., 2002).

In addition, DNA hypomethylation has been associated with loss of imprinting (LOI) (Cui, 2002; Sakatani, 2005). LOI is a key state that arises in cancer and refers to either inappropriate activation of a silent allele of an imprinted growth-promoting gene, or the silencing of a tumour suppressor gene that is normally expressed. An example of LOI in CRC is hypomethylation of the promoter of the insulin-like growth factor II (IGF2) gene which leads to its abnormal activation (Nakagawa et al., 2001). IGF2 expression then activates the IGF1 receptor (IGFR), which becomes autophosphorylated and triggers the PI3K and GRB2/RAS/ERK pathway. In this way, LOI can lead to inappropriate growth factor sensitivity and dysregulated growth factor receptor signalling.

1.5.3.2 DNA promoter hypermethylation

Aberrant promoter methylation is associated with transcriptional silencing and is functionally equivalent to coding-region mutations or deletions (Herman and Baylin, 2003; Lao and Grady, 2011). Numerous studies have revealed a wide range of epigenetically silenced genes by aberrant promoter CpG island methylation (Table 1.1). Many of the genes frequently affected are integral to a number of molecular/cellular events including cell cycle control, regulation of transcription, adhesion, invasion and metastasis, apoptosis and chromatin organisation (van Engeland et al., 2011). It is now widely acknowledged that epigenetic changes co-operate with the classical genetic changes to drive the progression of normal colonic epithelium towards invasive adenocarcinoma. In the average cancer genome, thousands of genes are thought exhibit aberrant methylation. However, only a proportion of these genes are likely to play fundamental roles in CRC pathogenesis (Smits et al., 2008).

Table 1.1: Representative genes commonly methylated and silenced in CRC

Gene	Protein	Function	Effect of loss of function
APC	Adenomatous polyposis coli	Wnt signalling pathway inhibition	Increased Wnt/ β -catenin signalling
MLH1	MutL homolog 1	DNA mismatch repair	Microsatellite instability
MGMT	O-6 methylguanine DNA methyltransferase	Repair of alkylation in DNA damage	Increased G>A mutation frequency
RUNX3	Runt-related transcription factor 3	Transcription factor	Decreased TGF β /BMP signalling
MINT1*	Methylated in tumour locus 1	NA	NA
MINT31*	Methylated in tumour locus 31	NA	NA
CDH1	E-cadherin	Calcium-dependent cell-cell adhesion glycoprotein	Loss of cell adhesion
CDKN2A/p16	Cyclin-dependent kinase inhibitor 2A	Regulated cell cycle G1 progression	Increased cell proliferation
TIMP3	Tissue inhibitor of metalloproteinase 3	Inhibition of MMPs and ADAMs	Increased EGFR signalling and TNF signalling
ID4	Inhibitor of DNA binding 4	Transcription factor	Not Known
IRF8	Interferon regulatory factor 8	Transcription factor	Interferon signalling
THBS1/TSP1	Thrombospondin 1	Cell-to-cell and cell-to-matrix adhesive glycoprotein	Decreased TGF β 1 signalling
DAPK	Death associated protein kinase	Induction of cell death	Interferon gamma signalling, TNF alpha signalling
VIM	Vimentin	Stabilising cytoskeleton	No known biological effect
SEPT9	Septin 9	GTPase, formation of filaments	Impaired cytokinesis of loss of cell cycle control
SFRP1	Secreted frizzled-related protein 1	Wnt antagonist	Increased Wnt/ β -catenin signalling
SFRP2	Secreted frizzled-related protein 2	Wnt antagonist	Increased Wnt/ β -catenin signalling
CDH13	Cadherin 13	Selective cell recognition and adhesion, antiapoptotic	Increased PI3K/Akt/mTOR signalling, increased MAPK signalling
HLTF	Helicase-like transcription factor	dsDNA translocase, fork remodelling activity, ubiquitin ligase	Impaired DNA repair

*MINTs are 'methylated in tumour' loci and are not specific genes. Abbreviations: ADAM, A Disintegrin and Metalloproteinase; MMP; mitogen-active protein kinase; TNF, tumour necrosis factor. Table adapted from Lao and Grady, 2011.

Aberrant CpG island methylation of the MMR gene *MLH1* is one of the best characterised epigenetic alterations in CRC (Herman et al., 1998). It is associated with both microsatellite instability and *BRAF* mutations in sporadic colorectal carcinogenesis, as well as the hereditary syndrome HNPCC. Once *MLH1* is inactivated, the rate of progression to malignant transformation is rapid (Hughes, 2011). As previously discussed (Chapter 1, 1.3.2), dysregulation of *MLH1* has profound clinical implications because of its critical role in DNA repair. Normally, the *MLH1* protein dimerises with the *PMS2*, *PMS1* or *MLH3* proteins to form the DNA mismatch repair dimers MutLalpha, MutLbeta and MutLgamma, respectively. These complexes can form part of the BRCA1-associated genome surveillance complex in combination with a variety of other proteins. The specific role of *MLH1* is to help activate the endonuclease activity of *PMS2*. *PMS2* then introduces single strand breakages in mismatched DNA that can be recognized by the exonuclease *EXO1*, enabling the mismatched strand to be degraded. Furthermore, *MLH1* may have a role in DNA damage signalling, which leads to cell cycle arrest and apoptosis if the damage cannot be repaired (Li, 2008).

In addition, hypermethylation of O⁶-methylguanine DNA methyltransferase (*MGMT*) has been observed in histologically normal colonic tissue adjacent to tumour tissue, suggesting that *MGMT* methylation may occur early in the polyp-adenocarcinoma sequence (Giovannucci and Ogino, 2005; Shen et al., 2005). The O⁶-*MGMT* enzyme catalyses the removal of alkyl adducts from the O⁶ position of guanine, and thus prevents G:C > A:T point mutations. Vogel et al. (2008) showed that *MGMT* promoter hypermethylation is associated with G:C > A:T mutations in *KRAS* but not *APC*, suggesting that *MGMT* silencing may succeed *APC* mutation but precedes *KRAS* in the polyp-adenocarcinoma sequence.

Two mechanisms have been proposed to explain the epigenetic silencing by CpG island promoter methylation. The first is by direct inhibition between methylated promoters and transcription factors such as activator protein-2 (AP-2), cAMP-response-element-binding-protein (CREB) and nuclear factor κB (NF-κB) (Comb and Goodman, 1990; Kondo and Issa, 2004). CpG island promoter hypermethylation can also mediate transcriptional silencing through the co-operative interactions with enzymes that induce changes in the chromatin structure. A family of methyl-CpG binding proteins including MeCP2, MBD1, MBD2 are involved in this process, and can bind to methylated DNA with high affinity (Lao and Grady, 2011; van Engeland et al., 2011). These proteins initiate a sequence of events that can alter

the structure of chromatin by recruiting proteins that regulate histone acetylation e.g. HDACs (histone deacetylases) and chromatin remodelling, thereby condensing the chromatin and impeding the access of transcription factors to the promoter (Tsai and Baylin, 2011). Experimental evidence for the importance of methyl-CpG binding proteins in CRC comes from *APC*^{MIN/+} mice, which suppress intestinal carcinogenesis in the absence of MBD2 (Sansom et al., 2003).

1.5.4 CpG island promoter methylator phenotype (CIMP)

The discovery that some colorectal tumour subsets display widespread promoter methylation whilst others do not has led to the concept of a CpG island methylator phenotype (CIMP). CIMP was first suggested to be involved in colorectal carcinogenesis in 1999 by Toyota et al., but the idea was met with initial scepticism (Issa et al., 2005; Samowitz, 2007b). However, the validity of this phenotype has now gained wide acceptance as the epidemiological and epigenetic evidence has accumulated (Ogino and Goel, 2008; Samowitz et al., 2005). Tumours characterised by CIMP probably arise through the serrated adenoma pathway and have a markedly different histology than adenoma-carcinoma pathway tumours of traditional origin (Smits et al., 2008). The 'classic' panel of markers that are used to assess CIMP status are *MINT1*, *MINT2*, *MINT31*, *P16*^{INK4A}, and *MLH1*. It is now thought that there are actually two general types of CIMP that can be seen in sporadic tumours: CIMP high, which relate to *BRAF* mutations and *MLH1* methylation; and CIMP low, which involve *KRAS* mutations (Jass, 2006; Ogino et al., 2006; Shen, 2007). Another commonly used panel is the Weisenberger CIMP panel, which focuses on methylation in *CACNA1G*, *IGF2*, *NEUROG1*, *RUNX3* and *SOCS1* genes (Weisenberger, 2006). However, the clinical utility of CIMP in CRC has been controversial, because universally accepted standard definitions have been lacking (van Engeland et al., 2011). CIMP tumours have a high frequency of *BRAF* V600E mutations, tend to occur in the right (proximal) colon and are less common in men than in women. This is independent of the panel of CIMP markers that are used (Barault, 2008; Samowitz, 2007a; Weisenberger, 2006). Understanding the biological cause of CIMP will allow scientists to quantify and define CIMP and a better definition of relevant CIMP panels should lead to a substantial improvement on the development of diagnostics and treatments for CRC (Smits et al., 2008).

1.6 Clinicopathological staging of colorectal cancer

There are two major staging systems currently employed throughout the world to classify cancer patients according to clinical and histopathological characteristics: the Dukes staging system and the Tumour Node Metastasis (TNM) system. Clinicopathological staging of newly diagnosed CRC is predominantly used to predict patient prognosis and ultimately plan the most effective treatment regimen (Compton and Greene, 2004).

The Dukes' staging system was originally devised by Cuthbert Dukes in 1932 and today remains one of the most influential strategies in the field of cancer therapeutics. The classification system was first used for rectal cancer, and was based on the degree of penetration into the wall of the rectum and metastatic spread to the surrounding lymph nodes. The original staging system consisted of three categories denoted A-C. Dukes' A carcinomas were confined to the wall of the rectum with no lymph node metastasis, Dukes' B carcinomas had progressed to the extra-rectal tissues with no invasion to regional lymph nodes and Dukes' C tumours were classified as such if metastasis was present in the regional lymph nodes. This system was subsequently applied to all intestinal carcinomas. Since its inception, numerous modifications have been made, by Dukes himself and other investigators. In 1949, Kirklin and co-workers revised stage A to designate carcinomas limited to the mucosa and subdivided stage B into B1 and B2; carcinomas extending to the *Muscularis propria* and penetrating the *Muscularis propria*, respectively. Stage C was later subdivided into C1 (regional nodes contain metastases) and C2 (apical lymph nodes contain metastases) (Zinkin, 1983).

The Aster-Coller staging system is an alternative staging system that was originally proposed in 1954. However, this method of classification is less frequently implemented, perhaps due to the misinterpretation that can arise. Aster and Coller extended Kirklin's classification by dividing Dukes C into C1 (carcinoma confined to the wall with positive lymph nodes) and C2 (carcinomas penetrating all layers with lymph node metastases) (Astler and Coller, 1954). These are, however, different to the C1 and C2 categories proposed by Dukes. In 1967, Dukes' stage D was added by Turnbull et al. which refers to patients with distant metastasis. In 1974, the Aster and Coller system was further refined by Gunderson and Sosin who added the additional categories B3 (lesions adherent to and invading adjacent organs) and C3

(gross nodal disease with extension and invasion of distant organs). Taken together, the revisions to the original staging system constitute the Modified Aster Coller System (MAC).

The other major classification system used globally is the International Union against Cancer (IUCC) and American Joint Committee on Cancer's (AJCC) TNM staging, and is frequently described as having many advantages over the other staging system (Puppa et al., 2010). Although TNM assessment was originally developed to predict patient prognosis, its function has been expanded to aid in pre-operative clinical trials. Moreover, it is multidisciplinary in design and is continuously being updated to incorporate new data (Chapuis et al., 2011). The latest TNM manual describes 9 stages (I, IIA, IIB, IIC, IIIA, IIIB, IIIC, IVA and IVB). CRC patients are classified based on tumour penetration (T), lymph nodes involved (N), and extent of distant metastases (M).

The 5-year survival rate for patients with CRC is intimately linked with the Dukes' staging system, and varies significantly between Dukes' A (>90%) to Dukes' D (8%) patients (Table 1.2). In intermediate-grade CRC (Dukes' B and C), survival varies from approximately 75% to 44% and therefore this group requires the most careful management (Smits et al., 2008). In addition to Dukes' staging, several other tumour-related features have also been suggested to offer prognostic value. These histological factors include venous and lymphatic invasion, tumour budding, tumour border configuration/tumour budding and the number of lymph nodes examined (Deschoolmeester et al., 2010). However, tumour classification based on the Dukes' staging system in the UK still remains the most significant prognostic factor for CRC.

Table 1.2: Clinicopathological staging and 5-year survival of CRC patients

Dukes' stage	Penetration	Frequency of diagnosis	5-year survival
A	<i>Muscularis mucoase</i>	11%	>90%
B	Visceral tissues	35%	75%
C	Lymph nodes	25%	44%
D	Metastasis	29%	8%

1.7 Screening

CRC prognosis is predominantly determined by clinicopathological staging, with early detection frequently resulting in excellent outcome. However, patients usually present with advanced stage disease as bleeding and/or other symptoms often occur when the adenomas are large and cause physical obstruction. CRC arises from a defined and predictable histopathological progression sequence, which lends itself to early detection by screening of asymptomatic individuals who are at high risk (e.g. those above 60 years or age). The majority of CRC originate from adenomatous polyps which if detected early, can be removed by surgical intervention to prevent malignant transformation. There is now universal agreement that population-based screening can significantly reduce CRC morbidity and mortality (Davies et al., 2005; Hawkes and Cunningham, 2010). However, the choice of screening modality remains contentious, with little evidence to favour one technique over another (Hawkes and Cunningham, 2010). Various procedures exist to facilitate the detection of early asymptomatic disease, including faecal occult blood testing (FOBT), double-contrast barium anaemia, flexible sigmoidoscopy and colonoscopy. Other approaches such as DNA testing of the stool and virtual colonography are also being developed though they require further testing and evaluation (Bressler et al., 2004; Davies et al., 2005; Seeff et al., 2004; Whitney et al., 2004).

In the UK, national screening programmes were implemented between 2007 and 2010. At present, individuals in England aged 60-74 and in Scotland aged 50-74 are invited to take the stool-based FOBT biennially. The FOBT is a relatively cost-effective method with a sensitivity of detecting CRC at approximately 50%. The test is based on the peroxidase-like enzymatic activity of haemoglobin and is able to detect non-visible or occult blood in the stool (Ahlquist et al., 1985). If individuals test positive, patients are invited for a colonoscopic examination. Colonoscopy is frequently referred to as the 'gold standard' for diagnosis of CRC (Seeff et al., 2004). This invasive procedure involves direct observation of the rectum and colon using a flexible fibre optic device. Colonoscopy has been shown to detect CRC with a sensitivity and specificity of 97% and 98%, respectively (Winawer et al., 2003). Although colonoscopy is considered by most experts to be the preferred method for detecting CRC, the use of this technique for average-risk populations (i.e. under 50 years of age) has been questioned because potential procedural complications may occur (such as perforation of bowel wall)

and the appropriate frequency for testing has not yet been established. In addition, concerns have been raised about high costs and variable capacities of the healthcare providers to make colonoscopy available routinely.

In 2011, the NHS bowel cancer screening programme introduced flexible sigmoidoscopy screening to those aged 55 and over. This procedure enables the detection and removal of all visible colorectal adenomas and precursor lesions within the distal colon and rectum using a flexible endoscope (Davies et al., 2005). Flexible sigmoidoscopy is a relatively safe procedure (with perforation rates half that of colonoscopy) and is reported to be cost effective. However, a potential pitfall of this method of intervention is that, unlike colonoscopy, it does not examine the entire colon/colorectum, an important consideration given that 30% of tumours arise in the proximal colon (Smits et al., 2008). Nevertheless, the rationale for implementing this screening modality appears robust. Atkin et al. recently published the long-term follow-up data from a large randomised, controlled, UK-based trial assessing the use of flexible sigmoidoscopy. That study showed that flexible sigmoidoscopy screening reduces CRC incidence by 33% and mortality by 43% and that 489 people need to be screened to prevent one CRC death (Atkin et al., 2010).

1.8 Treatment

Improvements in therapeutics and surgical techniques have led to an overall change in the management of CRC and consequently a (small) increase in survival rates. Surgical resection is the mainstay of treatment for CRC patients. In the majority of cases surgical resection is performed with curative intent, with primary tumour, adjacent bowel and lymph node removal. However, the chance of survival by surgery alone decreases with advancing stage (Nelson et al., 2001).

For early-stage CRC (Dukes' A) patients, surgery alone is often effective at curing the disease. These patients show a 95% survival rate. For Dukes' C patients, standard treatment requires adjuvant chemotherapy after surgical resection. Treatment with 5-FU (5-Fluorouracil) and leucovorin has reduced overall mortality rate by ~10% and the recurrence rates by 40-50% (Loupakis et al., 2008). More recently, oxaliplatin-based chemotherapy has been shown to further improve disease-free and overall survival (Andre et al., 2009). However, Dukes' B

patients do not routinely receive adjuvant post-operative chemotherapy as the benefits have been difficult to prove and the treatment remains controversial (Macdonald, 1999). Even so, approximately 30% of Dukes' B patients are likely to die within 5 years and hence this group would benefit from a strategy to identify individuals at high risk who may relapse and thus benefit from chemotherapy. It should also be noted that the majority of CRC cases affect the elderly (>60 years of age) and in this age group chemotherapy is considered dangerous and is avoided (Smits et al., 2008).

It has been proposed that Dukes' B patients with high risk features such as obstruction, tumour perforation, serosal tumour penetration (T4) and lymphovascular invasion may be more likely to relapse and should be considered for follow-up therapy (Figueredo et al., 2008). The identification of novel high-risk features would help improve the management and screening of this group of patients.

1.9 Prognostic biomarkers in colorectal cancer

Significant advances in the diagnosis, treatment and management of CRC has been made in recent years. Nevertheless, CRC is still a major health burden with over 1 million cases in the world, and a disease specific mortality of 50% (Draht et al., 2012; Ferlay et al., 2010; Jemal et al., 2010). At present, the Dukes'/TNM classification system is the main tool for predicting patient prognosis and determining treatment regimen (Graziano and Cascinu, 2003). Whilst Dukes' staging is very effective at predicting prognosis for Dukes' A and Dukes' D patients, there is considerable variability between the prognostic outcomes between intermediate stage CRC patients. Currently, in the UK Dukes' B patients do not receive adjuvant chemotherapy as it is thought that these patients have a good prognosis. However, 30% of Dukes' B patients will experience relapse and die within 5 years of diagnosis from CRC-related causes (Fretwell et al., 2010; Smits et al., 2008). Moreover, there is considerable heterogeneity in the natural course of the disease and treatment response between patients with histologically identical tumours. This can be explained, in part, by the fact that CRC is a heterogeneous disease (Draht et al., 2012; Newton et al., 2010). At least three pathways through which CRC can arise have been described; CIN, MSI and CIMP. The genetic and epigenetic alterations described in these pathways are likely to be important for neoplastic

formation and cancer progression and thus are attractive for the development of biomarkers (George and Kopetz, 2011; Smits et al., 2008).

A biomarker can be defined as an objectively measured substance used as an indicator of normal biological processes, or as a pharmacological response to a specified therapeutic intervention (George and Kopetz, 2011; Lee and Chan, 2011; Newton et al., 2010). Biomarkers are usually categorized as either prognostic or predictive. A prognostic biomarker is used to assess the clinical outcome, such as tumour aggressiveness or death, and can be considered to define the 'natural history' of the disease. Validation of prognostic biomarkers is usually performed using a retrospective cohort study (George and Kopetz, 2011). By contrast, a predictive biomarker is used to indicate the likelihood of a given response or to judge the efficacy of a given therapeutic. Predictive biomarkers therefore require the analysis of prospective cohort studies to exclude prognostic effects (George and Kopetz, 2011; Lee and Chan, 2011; Newton et al., 2010).

In recent years, research has intensified to identify prognostic biomarkers that improve the assessment of prognosis, and to identify Dukes' B patients with risk of recurrence who would benefit from adjuvant chemotherapy (Smits et al., 2008). Carcinoembryonic antigen (CEA), a glycoprotein involved in cell adhesion, is one of the first biomarkers suggested for CRC (Chau et al., 2004). However, the clinical utility of CEA as a prognostic biomarker remains controversial. Post-operative CEA expression has been championed as a prognostic biomarker in patients after resection of colorectal liver metastases (Oussoultzoglou et al., 2008). However, a subsequent meta analysis suggested that whereas CEA is a highly specific biomarker, it lacks sensitivity to predict recurrence of the disease (Tan et al., 2009). An additional complication is that elevated CEA levels are present in patients with breast, lung, and pancreatic cancer, diabetes type I and II, pancreatitis and liver cirrhosis (Newton et al., 2010). It therefore remains unclear whether CEA is suitable for routine clinical practice, and hence the identification of more robust and reliable prognostic biomarkers remains a priority.

1.9.1 Genetic Biomarkers

Numerous genetic markers have been evaluated for their prognostic influence. Scientists have been particularly interested in the relationship between *TP53* mutations and patient

prognosis (Lee and Chan, 2011). Inactivation of *TP53* has been associated with poor CRC prognosis. However, the results are frequently inconsistent and inconclusive. One study showed that *TP53* mutation status was associated with lower RFS in Dukes' B and C cancer (RR = 1.49, $p = 0.01$) yet there was no difference in overall survival (Allegra et al., 2003). Conversely, Russo et al., showed that *TP53* mutation was associated with lower overall survival in the Cancer International Collaborative Study that looked at 3583 CRC patients ($p = 0.06$) (Russo et al., 2005). Similarly, chromosomal loss of 18q, which occurs in at least 70% of CRCs, is one of the best-studied prognostic biomarkers (Popat and Houlston, 2005). Numerous retrospective studies have demonstrated that loss of 18q is associated with poorer prognosis in Dukes' B and Dukes' C patients (Smits et al., 2008; Sun et al., 1999). Using a retrospective tissue archive, one group found that Dukes' B and Dukes' C patients with intact 18q had a significant 5-year overall survival advantage compared to those with allelic loss of 18q. Moreover, Popat and co-workers demonstrated that loss of 18q was associated with poor prognosis in a meta-analysis of 2189 patients (HR = 2.0; $p = 0.0001$). However, despite promising results from both studies, a recent prospective study showed that 18q status was not a prognostic factor in Dukes' B and Dukes' C CRC patients (Roth et al., 2009). The prognostic value of *KRAS* has also been evaluated, again showing conflicting results. A number of studies indicate that *KRAS* is linked to poor survival, and that this is independent of other prognostic factors such as Dukes' stage. However, follow-up studies were not able to replicate these findings and the clinical relevance of *KRAS* mutation status is still uncertain (Anwar et al., 2004; Castagnola and Giaretti, 2005; McLeod and Church, 2003). Other biomarkers not implicated in the CIN pathway have also been investigated, for example, vascular endothelial growth factor (VEGF). VEGF is a pro-angiogenic factor whose downstream signalling cascades involve endothelial cell proliferation and migration and vascular permeability (Roskoski Jr, 2007). Studies have shown that increased expression of VEGF is associated with tumour aggressiveness, metastatic spread, and poor disease-free and overall survival (Zlobec and Lugli, 2008). However, data on the expression status of VEGF is limited and more studies are needed to confirm these findings (Lee and Chan, 2011).

1.9.2 DNA methylation biomarkers

In parallel to genetic markers being investigated, the expanding knowledge in our understanding of the CRC epigenome has led the pursuit of an epigenetic mark or signature which can accurately predict patient prognosis. Within this setting, DNA promoter

methylation has received the most attention. Methylation occurs at CpG islands and because these sequences are essentially fixed and stable, they lend themselves to analysis in most tissues and cell types. The advent of high throughput PCR and sequencing technologies means that the detection of CpG methylation is relatively fast and simple (Draht et al., 2012; Herman and Baylin, 2003).

Methylation has been suggested to play a role in determining CRC prognosis, although the validity of some candidate markers is debated. Notably, one group found that epigenetic inactivation of the DNA-binding protein inhibitor *ID4* is prevalent in CRC and is associated with poor tumour differentiation and overall survival (Umetani et al., 2004). However, Tanaka et al. found no correlation between *ID4* methylation and recurrence-free or overall survival. In the same study, promoter methylation of the E3 ubiquitin-protein ligase *CHFR* was associated with a worse recurrence free-survival in patients (Tanaka et al., 2011). Another group observed that CRC patients with CpG island promoter methylation of genes in the extracellular matrix (ECM) remodelling pathway exhibited worse survival. The genes tested in this study included insulin-like growth factor-binding protein 3 (*IGFBP3*), Ena/VASP-like protein (*EVL*), CD109 antigen precursor (*CD109*) and Filamin-C (*FLNC*). This data suggests that epigenetic regulation of the ECM pathway in general might constitute a prognostic signature in CRC (Yi et al., 2011). In addition, methylation of *MGMT* has previously been suggested to be a suitable prognostic biomarker, although results remain inconclusive. Finally, the role of CIMP (Chapter 1, Section 1.5.4) in predicting recurrence and disease-free survival remains controversial.

The plethora of genetic and epigenetic alterations that drive CRC carcinogenesis has led to the emergence of numerous potential biomarkers that may offer prognostic or predictive value. However, the majority of studies to date on the clinical utility of biomarkers are far from conclusive. Problems with poor study design, methodological differences, lack of reproducibility, small sample sizes and discrepancies in the evaluation of immunoreactivity from antibody studies have held back large-scale prospective studies. Many challenges remain, including standardization of techniques, integration across laboratories and validation of new biomarkers against robustly accepted clinical and pathological parameters (Soreide et al., 2008; Newton et al., 2010; Lee and Chan, 2011).

1.10 Lamins and colorectal cancer

1.10.1 Lamins and the nuclear envelope

The nucleus is the hallmark of all eukaryotic cells (Dahl and Kalinowski, 2011). It is the site of many fundamental cellular processes including DNA replication, transcription and ribosome assembly (Lamond and Earnshaw, 1998). This multifaceted dynamic organelle encompasses a three-dimensional interphase chromatin structure which is encapsulated by the nuclear envelope (Dahl and Kalinowski, 2011). The nuclear envelope is composed of an outer nuclear membrane (ONM) that is continuous with the endoplasmic reticulum, and an inner nuclear membrane (INM), which contains an extensive array of proteins and provides a physical attachment point for chromatin. The ONM and INM are separated by a luminal space which acts as a physical barrier between the nucleoplasm and the cytoplasm, thus separating the various metabolic processes in the cell (Worman and Courvalin, 2005) (Figure 1.13). The nuclear envelope is punctuated by a multi-protein complex called the nuclear pore complex that tightly controls nuclear export and import (Lim and Fahrenkrog, 2006). In metazoans, underlying the inner nuclear membrane lies a dense, filamentous meshwork termed the nuclear lamina. The nuclear lamina is primarily composed of lamins and lamin-binding proteins (Broers et al., 2006; Hutchison and Worman, 2004).

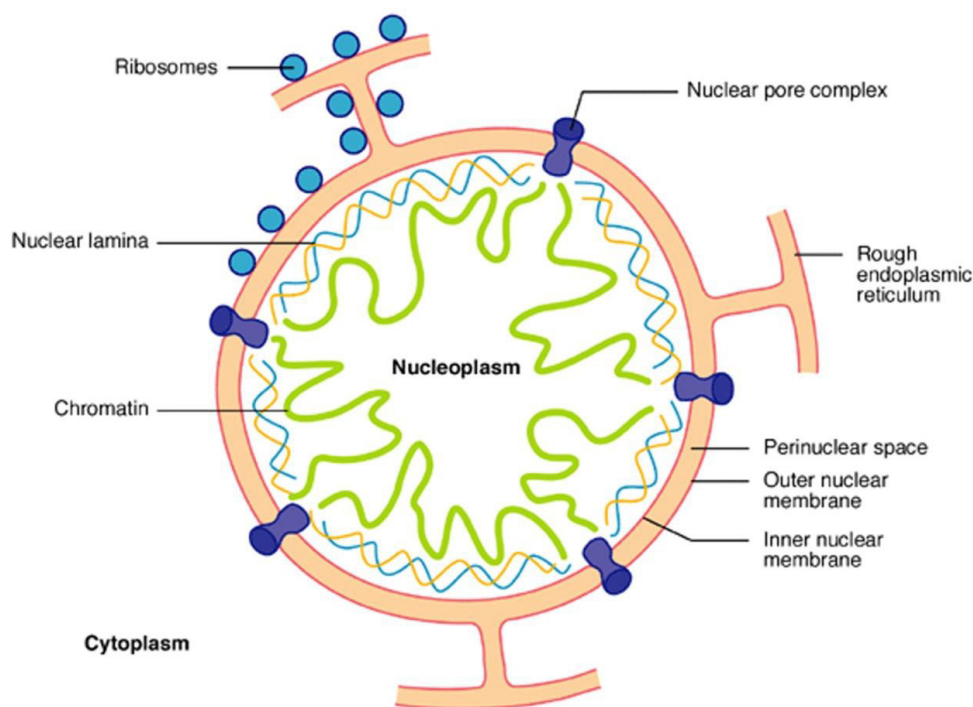


Figure 1.13: Overview of the structure of the nucleus (Maidment and Ellis, 2002).

1.10.2 Lamin structure and function

Lamins are type V intermediate filament (IF) proteins, which consist of A- and B-type lamins that can be functionally and biochemically distinguished (Hutchison, 2002). In humans, several lamin polypeptides are encoded by three distinct genes: A-type lamins, predominantly A and C, are alternatively spliced products of a single gene (*LMNA*), whereas B-type lamins, lamin B1 and lamin B2, are encoded by two distinct genes (Dechat et al., 2008). Lamin polypeptides have a conserved tripartite structure consisting of an alpha-helical coiled-coil rod domain made of four segments of heptad repeats. This is flanked by a short amino-terminal head and a large globular carboxy-terminal tail domain which contains a nuclear localisation signal (NLS) (Hutchison and Worman, 2004; Krimm, 2002; McKeon, 1991) (Figure 1.14). The NLS facilitates the targeting and transport of lamins into the nucleus (Broers et al., 2006). Lamins also contain a unusual Ig-like fold between the rod domain and C-terminal, which has been implicated in both lamin-protein interactions and lamin-DNA interactions. With the exception of lamin C, the lamin proteins are characterized by the presence of a CAAX motif at the C-terminus, which is subject to unique post-translational processing events (Rusiñol and Sinensky, 2006).

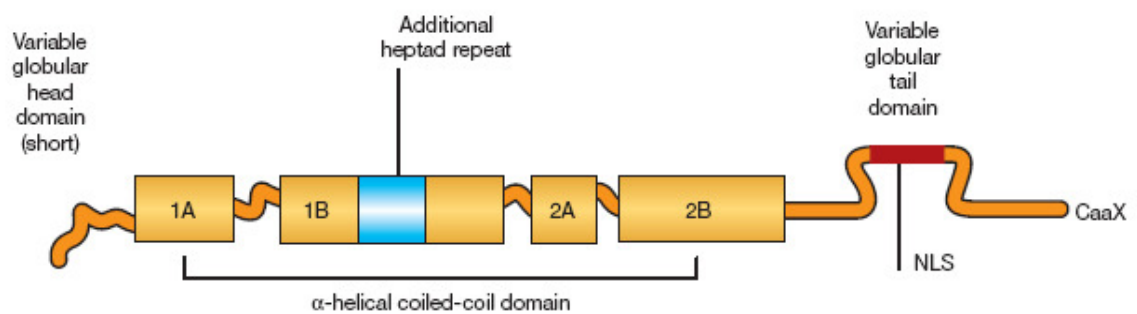


Figure 1.14: General structure of lamin polypeptide (adapted from Hutchison and Worman 2004)

B-type lamins are ubiquitously expressed in metazoan cells and are essential for cell survival. This is demonstrated by experiments in mice. Homozygous *Lmnb1* mutant mice survived embryonic development but died at birth with lung and bone defects (Vergnes et al., 2004). Furthermore, lamin B1 depletion by RNAi severely inhibits RNA polymerase I and II activity in HeLa cells, showing that lamin B1 is essential for RNA synthesis (Tang et al., 2008). In contrast to the B-type lamins, A-type lamins are not essential for development but are required for certain functions, particularly for the muscle and heart. *In vitro*, cells are able to

survive and proliferate in the absence of lamin A/C. However, *Lmna*^{-/-} mice suffer from muscular dystrophy and cardiomyopathy (Sullivan, et al. 1999). Furthermore, loss of A-type lamin expression compromises nuclear envelope integrity, leading to decreased bone formation as well as muscular dystrophy (Li et al., 2011; Nikolova, 2004).

Described as 'guardian of the soma', the dense lamin meshwork acts as an elastic shell, which in essence functions to maintain the structural integrity of the nucleus, thus preserving genomic stability (Dahl and Kalinowski, 2011; Hutchison and Worman, 2004). In support of this concept, loss of lamin A/C has been shown to play a role in nuclear mechanical support which likely contributes to its importance in muscle and heart tissue (Dechat et al., 2008). *Lmna*^{-/-} mouse embryonic fibroblasts (MEFs) have a significantly decreased mechanical stiffness. When these mutant MEFs are mechanically stretched, the degree of nuclear deformation increases compared with wild-type MEFs (Lammerding et al., 2004). In addition, nuclear rupture under high force is commonly seen in MEFs lacking *Lmna*, demonstrating the importance of lamin A/C to nuclear integrity (Lammerding et al., 2004).

Research into lamins intensified after it was found that mutations in *LMNA* cause an array of human degenerative diseases termed laminopathies, including Hutchinson-Gilford Progeria Syndrome (Dechat et al., 2008; Gonzalez-Suarez and Gonzalo, 2010; Hutchison et al., 2001). A substantial body of evidence suggests that these proteins are fundamental to a myriad of molecular and cellular processes such as spatial organisation and anchorage of the nuclear pores and nuclear envelope proteins, chromosome segregation and cytokinesis, regulation of gene expression, DNA replication, DNA repair, the DNA damage response and aging (Gonzalez-Suarez and Gonzalo, 2010; Hutchison, 2002; Liu et al., 2005; Liu et al., 2000; Scaffidi and Misteli, 2006; Spann et al., 1997; Varela et al., 2005).

An important aspect of lamin biology is how they help to connect the nucleus to the cytoskeleton. A-type lamins do this through their interaction with LINC (linker of nucleoskeleton and cytoskeleton) complexes allowing communication from the inside of the nucleus to the cytoskeleton (Burke and Roux, 2009). The so-called LINC complex is critical in forming the nucleo-cytoskeletal tether. This complex is comprised of SUN (Sad1 and UNC-84 homology) domain proteins, located at the INM, and nesprins, which mainly sit in the ONM (Burke and Roux, 2009). SUN1 and SUN2 proteins, together with nesprins-1,-2 and -3α

interact via their KASH domains in the perinuclear space (Hodzic et al., 2004; Worman and Gundersen, 2006). A recent crystallographic study of the SUN2-KASH1/2 complex, published in *Cell*, has revealed that KASH2 peptides sit in three grooves that are formed between the SUN domains (Sosa et al., 2012). This trimeric arrangement is probably the building block for higher order SUN-KASH structures and likely provides the molecular basis for generating force that is required for the control of nuclear movement and chromosomal positioning. Studies have shown previously that mutations perturbing the LINC complex can lead to impaired nuclear positioning, defective cell migration and sensitivity to mechanical stress (Dahl and Kalinowski, 2011). Nesprins can connect to all major cytoskeletal components by either binding to actin directly (nesprin-1/2), or to intermediate filaments (nesprin-3) or microtubules (nesprin-1/2/4) via plectin and kinesin, respectively (Taranum, 2012). Importantly, this physical connection between lamins-SUNs-nesprins effectively creates a mechanical stress transducer that stretches from the plasma membrane to the nucleus via the cytoskeleton (Dahl and Kalinowski, 2011; Lammerding et al., 2004).

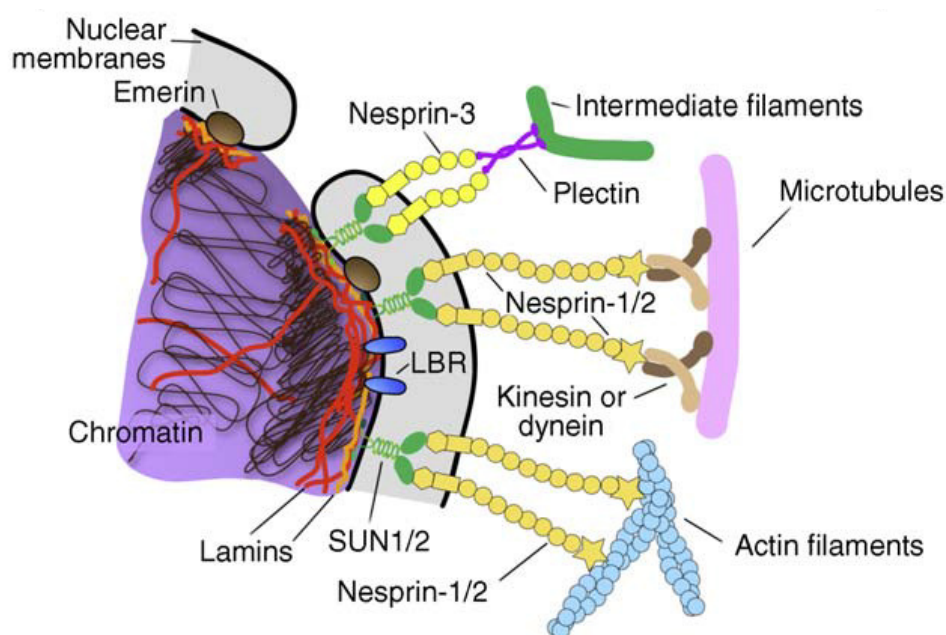


Figure 1.15: Schematic representation of the nuclear envelope

Lamins are juxtapositioned at the INM and are therefore well positioned to form stable structures with the nuclear interior. In addition to SUN1/2, membrane proteins such as emerin and LBR are retained at the inner nuclear membrane through their interactions with lamins, chromatin and other nuclear proteins. Nesprins can interact with all three components of the cytoskeletal via SUN proteins (adapted from Friedl et al. 2011).

Having considered the role of lamins in the organisation of the nuclear envelope and in communication with the cytoskeleton, it should be noted that lamin A may also be important as a chromatin scaffold. A-type lamins and the lamin-binding LEM (LAP2, Emerin, MAN) domain proteins bind to BAF (barrier-to-autointegration factor) (BAF), which can bind DNA and organise chromatin structure (Holaska et al., 2003; Zheng et al., 2000). Densely packaged heterochromatin tends to correlate with gene silencing, and it has been suggested that the A-type lamins may help to organise chromatin into these active and inactive domains (Kind and van Steensel, 2010). Studies using anchored reporters have shown that genes at the nuclear periphery tend to be repressed, although this can vary depending on regulatory sequences and chromatin context (Finlan et al., 2008; Reddy et al., 2008). The function of A-type lamins in chromatin positioning and regulation of gene expression has been attributed to the lamin Ig domain, based on truncation and mutational studies (Ludérus et al., 1994; Taniura et al., 1995).

1.10.3 A-type lamins and cancer

Numerous studies have documented aberrant expression of A-type lamins in a variety of cancers including small cell lung carcinoma, skin basal cell and squamous carcinoma, leukaemia, lymphomas and CRC, and in some cases lamin expression has been linked to tumour progression and survival (Broers et al., 1993; Moss et al., 1999). Some studies suggest that a lack of lamin A/C expression is associated with poor prognosis. Wu et al. (2009) documented that lamin A/C expression is significantly lower in patients with gastric cancer tissue compared to non-cancerous gastric tissue, and that loss of lamin A/C expression correlates with histological classification and poor prognosis (Wu et al., 2009). Moreover, epigenetic silencing of *LMNA* and thus loss of lamin A/C expression has been correlated with a decrease in overall survival in patients with nodal diffuse large B-cell lymphoma (Agrelo et al., 2005). In contrast, another study found that lamin A was highly discriminatory between low and high-grade prostate tumours, and in this cancer type, up-regulation of lamin A is a potential indicator of poor prognosis (Skvortsov et al., 2010). Recent studies in our laboratory have suggested that lamin A/C is a prognostic biomarker for CRC. By interrogating the Netherlands Cohort Study on Diet and Cancer (NLCS) tissue archive, Willis et al. found that patients expressing lamin A/C in their tumours were twice as likely to die of cancer related causes compared to clinicopathologically identical patients with negative expression (Hazard ratio [HR] 1.85; 95% confidence interval [C.I.] 1.16-2.97) (P

= 0.05) (Willis et al., 2008). In order to shed light on the potential mechanisms responsible for this observation, an *in vitro* model system approach was taken. Downstream investigations revealed that over-expression of lamin A in the SW480 CRC cell line caused the cells to adopt a significantly more motile phenotype. It was then shown that expression of GFP-lamin A led to an increase in expression of the actin-bundling protein T-plastin, which in turn gives rise to a decrease in expression of the cell-adhesion molecule E-cadherin (encoded by *CDH1*) (Willis et al., 2008). The study by Willis et al. (2008) suggest that lamin A may act as a master regulator of a metastatic pathway which promotes tumour invasiveness through dynamic reorganisation of the actin cytoskeleton.

Loss of E-cadherin is a hallmark of cancer and frequently associated with epithelial to mesenchymal transition (EMT), resulting in increased metastatic behaviour and poor prognosis (Bhangu et al., 2012; Yilmaz and Christofori, 2009). EMT is an orchestrated series of events whereby stationary polarised epithelial cells, communicating by cell-cell junctions, break up their junctions and switch to a non-polarised, mobile and invasive mesenchymal cell state (Kalluri and Weinberg, 2009; Thiery and Sleeman, 2006). During EMT, the adhesion molecule repertoire of the cancer cell changes considerably, underpinned by developmental reprogramming that gives rise to a wholesale reorganisation of the actin cytoskeleton (Yilmaz and Christofori, 2009). These cytoskeletal rearrangements are accompanied by the formation of membrane protrusions, which are required for invasive growth. Once the cancer cell has detached from the primary tumour mass, it uses chemotactic signals to move through the extracellular matrix and secretes proteinases that assist the migration by breaking down the proteins of the matrix. EMT can be initiated by both intrinsic signals (e.g. gene mutations in *CDH1*) as well extrinsic signals (e.g. growth factor signalling) (Yilmaz and Christofori, 2009). Among the molecules that induce EMT in cancer are TGF β , Wnt, members of the EGF family and the transcription factor SNAI2 (also known as Slug), a repressor of E-cadherin gene expression (Cui et al., 1996; Huber et al., 2005; Kim et al., 2002; Savagner et al., 1997; Zavadil and Bottinger, 2005).

1.11 Plastins: actin bundling proteins

1.11.1 The actin cytoskeleton: overview

Actin is one of the most abundant cellular proteins and all eukaryotes maintain genes for actin (Pollard et al., 1994). The ancestral prokaryotic actin gene *MreB* arose over 3 billion years ago and as an ancient fundamental protein actin and its homologues are essential for cell viability (van den Ent et al., 2001a). In animals, actin filaments complement two other cytoskeletal components, microtubules and intermediate filaments, which together make up the cytoskeleton. The actin cytoskeleton of eukaryotic cells is a dynamic meshwork that is involved in fundamental biological phenomena such as cell shape, cell division, cell motility, contraction, cell substrate adhesion, intracellular transport, cytokinesis and signal transduction (Doherty and McMahon, 2008).

First discovered in 1940s alongside myosin in muscle, early x-ray studies of actin showed that it formed highly organised arrays of filaments that hinted at its role in cellular organisation (Astbury, 1947). Vertebrates have three main actin isoforms, α -, β - and γ . There are three α -isoforms of skeletal, cardiac, and smooth muscle actin and the β - and γ -isoforms are found in both nonmuscle and muscle cells. Actin isoforms differ by only a few amino acids, mostly toward the N terminus. Actin belongs to a structural superfamily defined by a characteristic 375-amino-acid $\beta\beta\beta\alpha\beta\alpha$ fold together with sugar kinases, hexokinases, and Hsp70 proteins (Bork et al., 1992). The family also includes the prokaryotic actin-like proteins *MreB* (van den Ent et al., 2001b) and *ParM* (van den Ent et al., 2002) and the actin-related Arp proteins (Robinson et al., 2001).

Actin itself consists of two major domains, each comprising two smaller subdomains. The two major domains are known as the outer and inner subdomains, according to their arrangement within the actin filament. Monomeric actin (G-actin) is a globular 42 kDa ATP-ADP-binding protein. Under physiological conditions, actin monomers spontaneously polymerise into long polarised filaments (F-actin), with a helical arrangement of subunits, as first visualised *in vivo* in striated muscle (Hanson et al., 1964). The actin filament is asymmetric and can be seen as either a short, single left-handed helix with consecutive lateral subunits staggered by a half monomer length, or as two long right-handed helices of

actin subunits ordered head-to-tail. Actin cytoskeletal dynamics within a cell are regulated by controlling the homeostatic balance between G-actin and F-actin states in response to extracellular environmental cues (Lee and Dominguez, 2010).

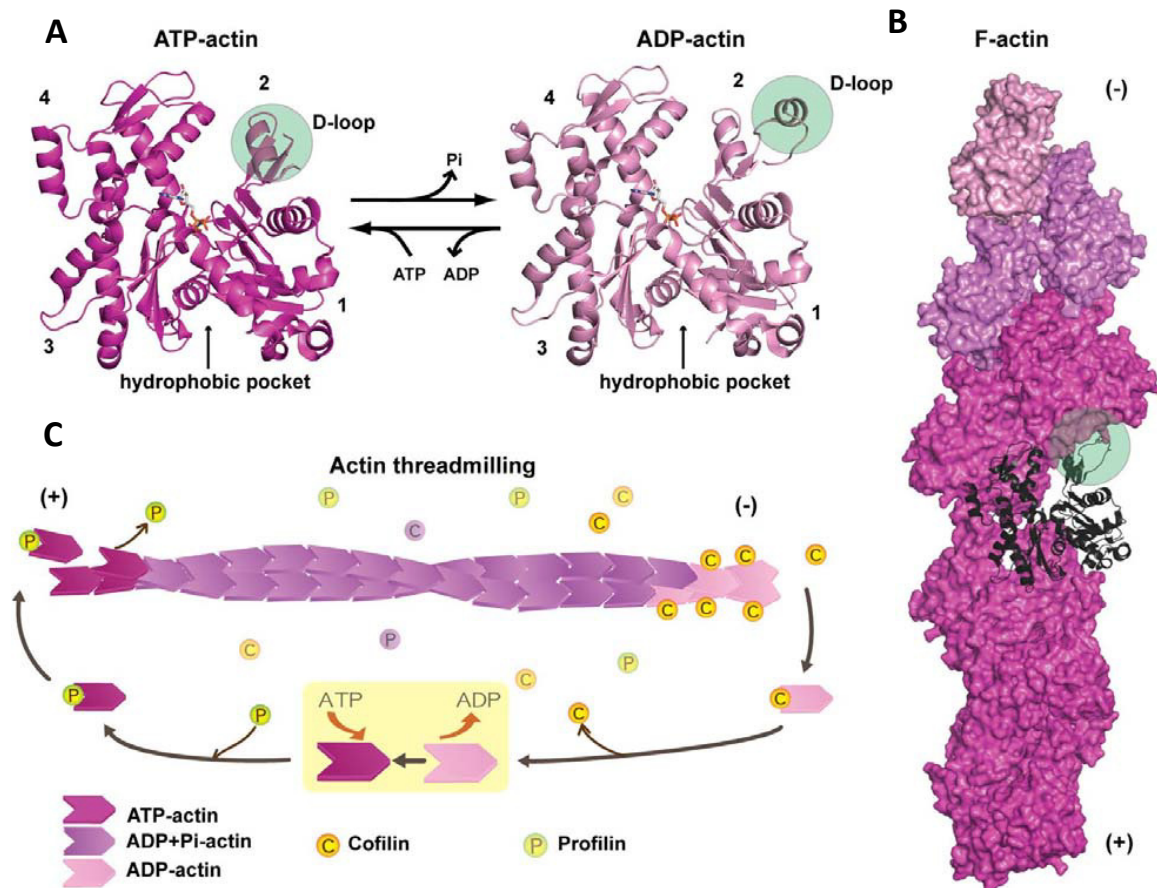


Figure 1.16: Monomeric and filamentous actin

(A) The actin monomer consists of two major and structurally related domains, the outer and inner domains. Subdomains 1 and 2 (outer domain) and subdomains 3 and 4 (inner domain) are illustrated. A large cleft between subdomains 2 and 4 constitutes the nucleotide-binding site. The hydrophobic pocket opposite the ATP binding site is the site for interaction with most ABPs. (B) F-actin, modelled on diffraction studies of actin filaments and fitting of the actin monomer structure. The D-loop (shaded in A) is disordered in most structures of actin but is likely to be involved in actin-actin interactions in the filament. An actin monomer is represented by a black ribbon. (C) Model showing actin filament treadmilling. The barbed (+) end exposes subdomains 2 and 3 of the actin monomer and adds actin monomers bound to ATP. The pointed (-) end exposes subdomains 2 and 4 of the actin subunits. This region has net dissociation of actin-ADP monomers. In cells, however, actin filament treadmilling is tightly regulated by ABPs (adapted from Lee and Dominguez, 2010).

In vitro, actin polymerisation initiates in a slow manner owing to the instability of small actin oligomers. However, once an actin trimer (the nucleus) is formed, actin polymerisation is rapid (Pollard and Cooper, 2009). Actin binds to its nucleotide (ATP or ADP) and as filament assembly is initiated, it hydrolyses the terminal phosphate from the bound ATP to provide energy for the polymerisation process. Actin filaments are polar because the subunits are all oriented in the same direction. Polymerisation is fast at the growing barbed (+) end, and is slower at pointed (-) end of the filament. Mechanical force is generated at the plus end by the incorporation of new actin subunits into the filament, generating membrane protrusions that give directionality to migrating cells (or contracting muscle cells) (Lee and Dominguez, 2010; Pollard and Cooper, 2009). This dynamic yet steady-state mechanism of actin polymerization/depolymerization is called actin filament treadmilling. However, treadmilling does not explain the full picture of dynamic filament assembly observed in all cell types. Actin cytoskeletal dynamics are tightly controlled and regulated by a plethora of accessory proteins, known as actin-binding proteins (ABPs) (Lee and Dominguez, 2010; Pollard and Cooper, 2009). There are over 100 ABPs known to date which perform a multitude of functions including actin filament nucleation (e.g. Arp2/3 complex, formin), elongation (e.g. Ena/VASP), capping (e.g. gelsolin), severing (e.g. ADF/cofilin) and cross-linking (e.g. plastin) which is summarised in Figure 1.17 (Pollard and Borisy, 2003). The biological interplay between actin and all its accessory proteins is too vast an area to cover in the context of this thesis. Here, we will focus on a subset of ABPs known as actin-bundling proteins. Actin-bundling proteins function to cross-link actin filaments into loose/tight networks or bundles and are often localised to dynamic actin-rich cellular regions (Delanote et al., 2005). Indeed, actin bundling proteins are important in the formation of specialised structures such as filopodia (long, thin actin-based protrusions), lamellipodia (sheet-like protrusions), stress fibres (elastic contractile bundles of parallel actin filaments) and microvilli (finger-like projections) (Stevenson et al., 2012). In cancer, the 'normal' functions of the actin cytoskeleton and its constituent parts are subverted to promote tumour invasion and metastasis (Hall, 2009; Stevenson et al., 2012). A number of actin bundling-proteins have been linked to cancer progression, as summarised in Table 1.3.

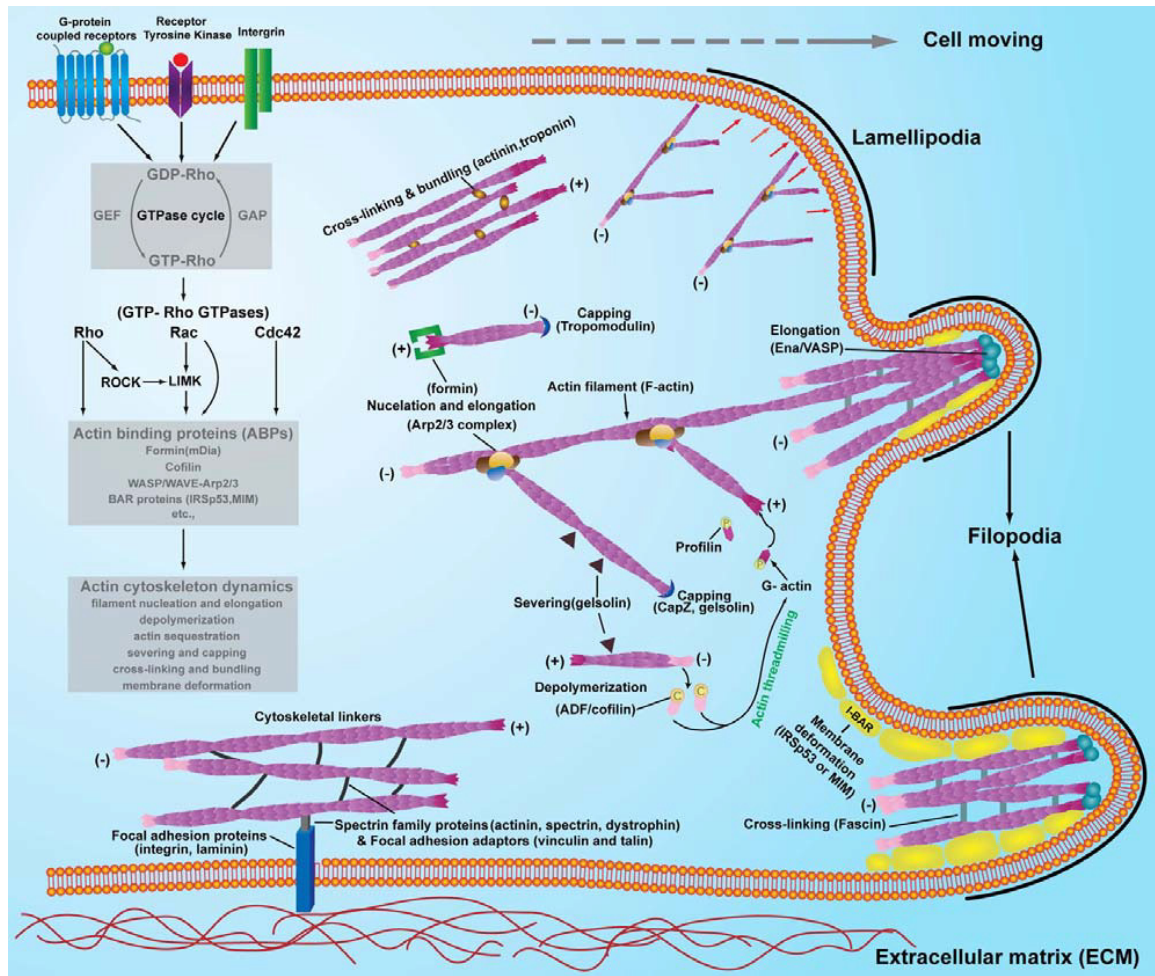


Figure 1.17: Actin filament networks

Three major types of actin network are shown above, including lamellipodia, filopodia and focal adhesions (shown at the ECM). These actin networks are regulated by rho-family GTPases signalling via ABPs and in response to various ligands that stimulate G-protein coupled receptors, receptor tyrosine kinases and integrins (adapted from Lee and Dominguez, 2010).

Table 1.3: Clinical correlations between actin-bundling proteins and cancer

Protein	Structures and cell type	Function	Role in cancer
α-Actinin-1 and α-actinin-4	Cellular protrusions, stress fibres, lamellipodia, microvilli, invadopodia of multiple cells	Crosslinks actin into parallel bundles by forming dimers head to tail	Expression in breast, ovary, pancreas, astrocytoma cancers. Associated with poor prognosis and tumour resistance (ovary)
Eplin	Stress fibres in multiple cell types	Actin filament bundling and side binding	Eplin downregulation correlates with progression and metastasis in prostate cancer and eplin might be angiogenic. Potential tumour suppressor in breast cancer
Fascin	Neurons, dendritic cells, endothelial cells and cancer cells	Crosslinks actin into parallel bundles. Thought to be a monomer with two actin-binding sites	Significant independent prognostic indicator of poor outcome of cancers of the liver, ovary, lung, pancreas, colon, head and neck squamous cell carcinoma and brain
Filamin-A	Cell cortex, filopodia of many cell types	Crosslinks into orthogonal gels	Prostate cancer metastasis correlates with low nuclear and high cytoplasmic filamin-A. A secreted variant of filamin-A in the blood correlates with high-grade astrocytomas in metastatic breast cancer
Formins	Stress fibres and filopodia of multiple cell types	Actin nucleation and parallel bundling. Also interacts with microtubules	Downregulation of formin-like-2 correlates with a poor prognosis in hepatocellular carcinoma. Higher expression correlates with tumour differentiation
Spectrin	Microvilli and terminal web of intestinal epithelial cells and cell cortex of many cell types	Crosslinks actin into orthogonal networks by forming tetramers.	Reduced expression of spectrin associated with poor prognosis in pancreatic cancer and progression in hepatocellular cancer
Supervillin	Stress fibres and focal adhesions of multiple cell types. Implicated in nuclear architecture.	Actin bundling into parallel bundles	Androgen receptor co-regulator that might be important in androgen-dependent prostate cancer
Villin	Epithelial cells of the gastrointestinal tract that possess brush border microvilli	Crosslinks filaments in low Ca^{2+} and severs filaments at high Ca^{2+}	Expression altered in Barrett's oesophagus, bladder cancer, colorectal and intestinal cancer

1.11.2 Early biochemical studies of plastins

Plastins belong to the family of actin-bundling proteins, which are conserved from lower eukaryotes to mammals. In general, plastins are found in cells with high actin turnover, associated with polarized actin filaments. Our understanding of the function of these proteins is largely inferred from early biochemical studies on chicken fimbrin which was discovered in 1979 as a protein that was involved in the organisation of microvilli in the intestinal brush border (Matsudaira and Burgess, 1979). Fimbrin was shown to localise with surface structures such as membrane ruffles and focal adhesions in chicken embryo fibroblasts (hence the name). Independent to the studies on chicken fimbrin, a related protein was identified from immortalised fibroblasts. The protein was given the name L-plastin because it was found to be abundantly expressed in lymphocytes (Goldstein et al., 1985). It was only with the advent of molecular cloning techniques, coupled with amino acid sequencing, that fimbrin and plastin were revealed to be two related members of the same family. Today, the terms fimbrin and plastin are used interchangeably. In humans, three plastin isoforms exist; T-, L- and I-plastin.

Biochemical characterisation of chicken fimbrin was stimulated by the desire of researchers to understand the composition of brush borders, which were relatively abundant and easy to extract from chicken intestines (Bretscher and Weber, 1978). Initial studies showed that core microfilaments extracted in the absence of calcium contained three main F-actin-associated proteins: villin, calmodulin and fimbrin (Glenney et al., 1980; Howe et al., 1980). The first evidence for the calcium binding ability of fimbrin came in 1981, when chicken fimbrin was purified by classical ammonium sulphate precipitation and sepharose/affinity chromatography and was shown to bind to ^{45}Ca by equilibrium dialysis. The authors suggested a dissociation constant of 9 μM , and showed that fimbrin-bound calcium could be displaced by magnesium. The results suggested that there was one calcium binding site per protein. However, comparison of the three plastin sequences shows that the calcium binding sites between the plastins are weakly conserved (Giganti et al., 2005) provided some evidence to suggest that T-plastin is relatively insensitive to calcium levels, but more work is required to determine directly whether (and why) the plastins are differentially regulated by calcium (Giganti et al., 2005).

In the Glenney et al paper, the authors demonstrated (by sucrose density gradient centrifugation) that purified fimbrin could bind to purified actin at a ratio of one fimbrin molecule per two-three actin molecules (Glenney et al., 1980). This interaction was dependent on calcium/magnesium ions *in vitro*. Low speed centrifugation followed by electron microscopy of the pellets showed that fimbrin-actin mixtures formed polymerised fibrils. Including villin in the mixture enhanced polymerisation. Incubation of these filaments with the actin-binding domain of myosin also indicated that the filaments always maintained the same polarity. This was the first evidence that fimbrin could cross-link, organise and bundle actin, and that fimbrin contributed to the rigidity of the stereocilium (Bretscher, 1981; Glenney et al., 1981).

1.11.3 Plastin structure

Understanding the structural basis of these early biochemical studies has been held back by the lack of complete and comprehensive crystal structures for the mammalian plastins. However, crystal structures of the N-terminal actin binding ABD1 domain (comprising the two calponin homology domains CH1 and CH2) have been solved for the yeast *Saccharomyces cerevisiae* plastin and the plant *Arabidopsis thaliana* plastin (Klein et al., 2004). In addition, the N-terminal region of human T-plastin has been solved by X-ray crystallography (Goldsmith et al., 1997). Plastins have a modular structure comprising of two EF-hands, and two tandem actin-binding domains (ABDs), each consisting of two calponin homology (CH) domains (Korenbaum and Rivero, 2002) (Figure 1.18). Each CH domain is composed of four α -helical segments. Three of these stretches form a loose bundle of helices, with the fourth α -helix laying perpendicular to the main bundle. Similar CH domains are found in other actin binding cytoskeletal proteins such as dystrophin, α -actinin and spectrin; thus the CH domain has been repeatedly used during evolution as an actin binding module (Delanote et al., 2005; Shinomiya, 2012). The actin cross-linking core of plastin is compact, contacting actin through the CH1 domain and the CH4 domain using conserved residues at the CH1-CH4 interface. The regions that join the CH domains are poorly defined in the crystallographic studies, indicating that this region is highly dynamic. Having demonstrated that the binding sites for plastin on the actin molecule reside in two independent subdomains, workers have suggested that differential binding of plastin to actin may help control actin turnover and assembly, independent of plastins role as a simple bundling protein (Hanein et al., 1998). Recent support for this idea comes from a high-

resolution cryo-EM structure of the human L-plastin ABD2 domain bound to F-actin, which suggests that ABD2 binding induces the closure of the actin cleft. This stabilisation effect is then transmitted co-operatively to neighbouring subunits to stabilise local regions of the filament (Galkin et al., 2008). The interaction of the plastin ABD1 domain with actin remains to be defined; thus high-resolution structures of the plastin ABD1-ABD2 domains in combination with F-actin will be required to establish how the two domains work together to bind, stabilise and subsequently protect F-actin from depolymerisation.

Further evidence for a role for plastin beyond simple bundling comes from Giganti and colleagues, who suggested that T-plastin increased the Arp2/3 (actin-nucleating protein) induced movement of actin (Giganti et al., 2005). In this study, the authors used beads asymmetrically coated with the VCA domain of the WAS protein to establish an *in vitro* assay for actin motility. The mobility of the beads was observed by phase-contrast microscopy. The coated beads could bind to purified Arp2/3, and polymerized actin on the bead, showing directed movement when incubated in a HeLa cell free extract. Introducing T-plastin to the assay stimulated the movement of the beads by ~1.5 fold and stabilised actin comets. Interestingly, the T-plastin ABD1 domain also had the same effect as full-length T-plastin on bead velocity and actin comet length, even though alone it lacked actin-bundling activity. Taken together with the observations that T-plastin could displace cofilin, an actin-depolymerizing protein, this paper supports the hypothesis that T-plastin does more than simply bundle the actin filament and may induce cell motility. However, comparative biochemical studies and crystal structures of T, L and I-plastin from the same organism, preferable in combination with actin, will be required to deduce whether the plastins show any degree of specialization in their binding to actin.

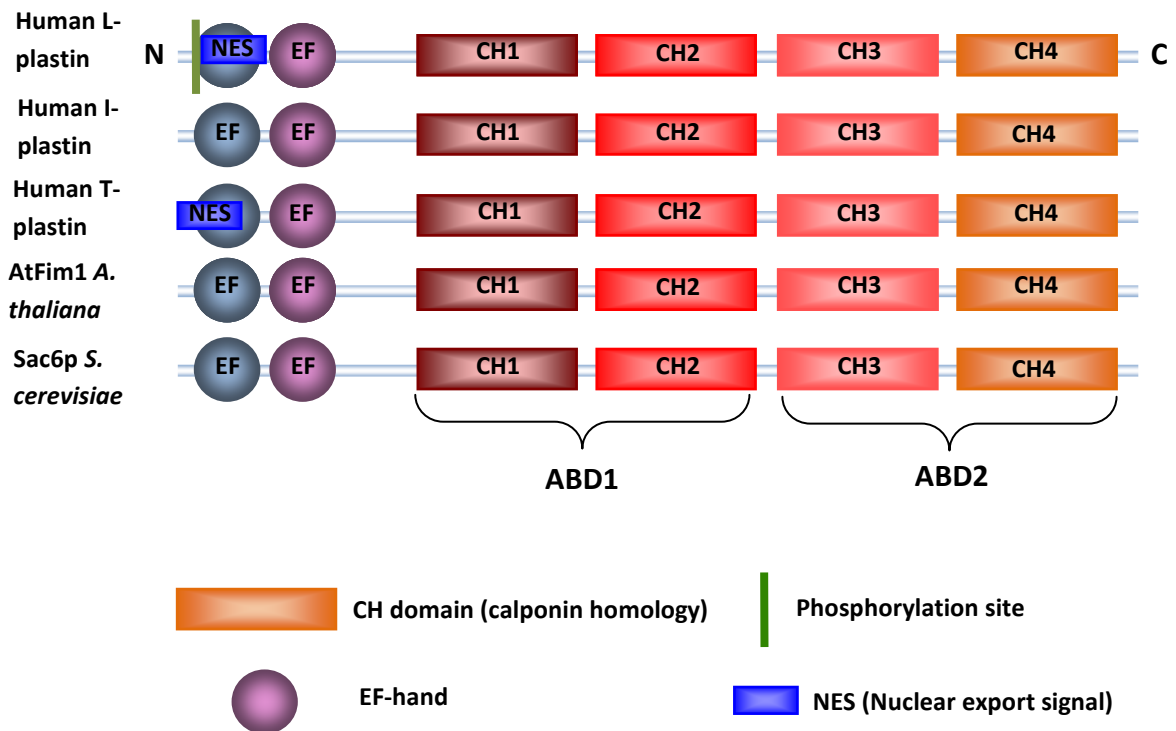


Figure 1.18: Schematic representations of human plastin isoforms

Each plastin contains two amino-terminal EF hands, and two actin binding (ABD) domains. Each ABD consists of two calponin (CH) domains. Human T-plastin contains an NES, and L-plastin contains a phosphorylation site (adapted from Delanote et al., 2005).

1.11.4 Tissue-specific expression and localisation

In general, plastins normally localise to various actin-rich membrane structures involved in locomotion, signalling, adhesion and immune defense, including focal adhesions, ruffling membranes, filopodia and the phagocytic cup. Moreover, plastins are also located in highly specialized surface structures with ordered microfilament bundles such as stereocilia. This is of particular interest, as actin bundles formed by plastin may also have a mechanosensory function by sensing mechanical alterations in signals during chemosensory signal transduction (Daudet and Lebart, 2002). However, the three plastin isoforms (T, L and I) exhibit a tissue-specific expression pattern that suggests that they may have functional specialisation. T-plastin (encoded by *PLS3*) is normally expressed in cells derived from solid tissue and L-plastin (encoded by *PLS2*, also known as *LCP1*) is confined to hematopoietic cell lineages. In macrophages, for example, L-plastin is found in podosomes and filopodia. Finally, I-plastin (encoded by *PLS1*) is predominantly found in the small intestine, colon and

kidney (Grimm-Gunter et al., 2009; Lin et al., 1994) and is required for the regulation and morphology of brush borders, as demonstrated from studies of *Pls1*^{-/-} mice (Grimm-Gunter et al., 2009). During the early stages of intestinal epithelial cell differentiation, both T- and L-plastin are expressed at the apical and basal membranes, respectively. However, these plastins disappear after day 16.5 and are replaced by I-plastin at the apical surface. This suggests that plastin isoforms play different roles during epithelial cell differentiation. It is thought that both T- and I-plastin are needed for the formation and extension of the intestinal microvilli, whereas L-plastin might be needed to control cell adhesion (Chafel et al., 1995). I-plastin and T-plastin, but not L-plastin, are also found in cochlea auditory hair cell stereocilia (Daudet and Lebart, 2002). However, T-plastin is absent from mature hair cell stereocilia, suggesting that T-plastin could have a particular role in stereocilia formation. Importantly, human plastin isoforms share approximately 70% homology at the protein level but are encoded by three distinct genes located on chromosomes 3 (I-plastin), 13 (L-plastin), and X (T-plastin) (Delanote et al., 2005). The three plastin genes have evolved from a common ancestor, but their tissue specific expression is regulated differently. T-plastin is under the control of upstream enhancer elements and is methylated at a CpG island (Lin et al., 1999). Conversely, L-plastin is under control of a strong promoter, can be modulated by steroid hormone receptors, and is regulated by an upstream repressor (Lin et al., 1993a).

1.11.5 Plastin function

T- L- and I-plastin have similar sequences, but this does not mean that they are functionally equivalent. Arpin and colleagues overexpressed T- and L-plastin in the fibroblast-like cell line, CV-1, and in a polarized epithelial cell line, LLC-PK1 (Arpin et al., 1994). Both isoforms induced cell rounding and the reorganization of the actin cytoskeleton in both cell types. However, in epithelial cells, T-plastin altered the shape of microvilli and maintained its association with actin filaments even after detergent treatment. These studies demonstrate that the cell type and other cell-specific proteins can be important in determining the function of protein homologs.

Both T-plastin and L-plastin have a role in immunity. L-plastin is involved in the motility of B cells, and has recently been shown to be required for marginal zone B cell development (Todd et al., 2011). These authors used L-plastin knockout mice to analyse the behaviour of B cells in the absence of L-plastin. They found that the B cells failed to respond properly to the

chemokines CXCL12 and CXCL13, as well as the lipid sphingosine -1-phosphate. As a result, the L-plastin knockout mice had a deficiency of B cells in the spleen, with a 40% reduction in the follicles and an 80% reduction in marginal zone B cells. These mice could not respond effectively to *Streptococcus pneumoniae* infections, demonstrating that L-plastin is required for proper function of the immune system. The importance of T-plastin in immunity is demonstrated by the fact that T-plastin is linked with Sezary's disease. Sezary's disease is a cutaneous lymphoma of the skin characterised by CD4+ T cells that overproduce mucopolysaccharides (Wong et al., 2011). Sezary's disease is rare, affecting ~3 people per 1,000,000 and its cause is unknown. T-plastin protein expression is not found in normal lymphocytes but is found in T cells from Sézary syndrome patients (Kari et al., 2003; Su et al., 2003). However, no coding mutations associated with the *PLS3* gene have been found in individuals with the disease. In preparation of this thesis, it was discovered that CpG dinucleotides within the *PLS3* promoter are hypomethylated in T-plastin overexpressing patients (Jones et al., 2012). The mechanisms underlying this phenomenon in Sezary syndrome patients remain to be elucidated.

Post-transcriptional regulation of T-plastin is important for its function, and has a crucial bearing on human health. For example, the survival motor neuron protein, SMN, modulates the half-life of T-plastin mRNA, as shown in both human cells and in a zebrafish model (Hao et al., 2012). In addition, a paper in Science showed that loss of SMN causes spinal muscular atrophy, identifying T-plastin as an important modifier of this motor neuron disease (Oprea et al., 2008). Expressing T-plastin in motor neurons rescues movement deficits in *smn* zebrafish mutants, raising the prospect that T-plastin could be used therapeutically for the human disease. Evidence has also emerged to support the regulation of T-plastin at the post-transcriptional level by ROD1, a polypyrimidine tract binding protein that plays a role in the nonsense-mediated mRNA decay (NMD) pathway. Interestingly, cofilin1 and various nuclear pore/envelope proteins also emerge as putative targets for ROD1 from this study, suggesting that post-transcriptional regulation might influence nuclear-cytoskeletal remodelling processes (Brazao et al., 2012).

Plastins are also regulated at the post-translational level. Intriguingly, L-plastin, but not T- or I-plastin, is phosphorylated (at the N-terminal residues Ser5 and Ser7) and high levels of phosphorylated L-plastin have been found in haematopoietic cells and in cancer cells (Jones

et al., 1998). Protein kinase A can phosphorylate L-plastin *in vitro* (Wang and Brown, 1999), but whether Protein kinase A is the *in vivo* phosphate donor is not certain. Other investigators have suggested that Protein kinase C phosphorylates L-plastin in the MCF-7 breast cancer cell line (Janji et al., 2010). Although it has been suggested that phosphorylation of L-plastin is important in leukocyte function/adhesion and might regulate actin binding or interactions between L-plastin and other accessory proteins, the physiological significance of L-plastin modification by phosphorylation is not fully understood (Delanote et al., 2005). However, it does appear that in the MCF-7 cells, L-plastin phosphorylation increases during the reorganization of the actin cytoskeleton and may induce the transition of L-plastin to sites of *de novo* actin polymerization (Al Tanoury et al., 2010).

Plastins are expressed in all eukaryotes, including yeast and plants. In *S. cerevisiae*, the sole plastin homolog Sac6p co-localises with both actin cables and cortical actin patches (Drubin et al., 1988). Yeast lacking Sac6p have various temperature sensitive defects in morphology, endocytosis and sporulation (Adams et al., 1991; Kubler and Riezman, 1993). Although overexpression of Sac6p is lethal, yeast deficient in Sac6p can be rescued by the expression of human T and L-plastin, but not I-plastin (Adams et al., 1995). The functional dynamics of plastins have probably been best visualised in plant cells, in experiments where the actin-binding domain 2 of Arabidopsis fimbrin has been tagged with GFP (Sheahan et al., 2004; Voigt et al., 2005). Although the fimbrin domain was essentially used as a probe in these studies, they do demonstrate that fimbrins are recruited to motile regions of the actin cytoskeleton. The same probe has been used in a recent study of the effect of calcium on actin-mediated organelle movement (Jung et al., 2012). An interesting point from this work is that ABD2-GFP localized to F-actin patches close to the nucleus when calcium concentrations were increased by UTP treatment. Although the functional significance of this observation was not investigated further, it would be consistent with a role for plastin(s) in cytoskeletal-nuclear communication.

1.11.6 Plastins and cancer

In cancer, remodelling of the cytoskeletal architecture is a vital step in the acquisition of invasive capabilities and metastasis. Given the function of plastins as important cross-linkers of actin filaments, it has been suggested that these proteins may play an important role in

cancer. Indeed, aberrant plastin expression has been documented in a number of carcinomas (Delanote et al., 2005; Lin et al., 1993b; Otsuka et al., 2001; Shinomiya, 2012). As discussed, human T-, L- and I-plastin are expressed in a tightly controlled tissue-specific fashion. For example, L-plastin is normally found in haematopoietic cells (e.g. peripheral blood leukocytes, B-lymphocytes, macrophages). Interestingly, many authors report that L-plastin is frequently expressed in transformed cells of non-haematopoietic origin. A study by Lin et al. found aberrant expression of L-plastin was present in 69% of cancers investigated (Lin et al., 1993b). This is further supported by the presence of L-plastin in a number of human neoplastic cancer cell lines (Park et al., 1994). In addition, Zheng and co-workers demonstrated that L-plastin expression was regulated by steroid hormone receptors and linked to malignant progression of prostatic epithelial cells (Zheng et al., 1997). More recently, DNA microarray expression profiling revealed that L-plastin was significantly upregulated in tumour necrosis factor (TNF)-alpha resistant breast adenocarcinoma MCF-7 cells. RNAi/overexpression experiments showed that L-plastin protected MCF-7 cells from TNF α induced cell death in a manner that required L-plastin phosphorylation (Janji et al., 2010). This study suggests that upregulation of L-plastin can protect tumors from cytokine mediated cell death. The kinases upstream of L-plastin were not identified in this work, but could be explored further as targets to prevent EMT, since TNF α resistance correlates with the gain of mesenchymal behaviour. Importantly, L-plastin expression has also been observed in CRC. Using a tissue microarray of 58 clinically stratified CRC specimens, Otsuka and colleagues found that L-plastin expression was associated with tumour progression (Otsuka et al., 2001).

In addition to L-plastin, T-plastin has been implicated in a number of cancers. Enhanced expression of T-plastin has been associated with both drug and radiation resistant cells. Firstly, T-plastin expression is enhanced in cisplatin-resistant human bladder, prostatic, head and neck cancers (Hisano et al., 1996). Secondly, increased expression of T-plastin has been observed in Chinese hamster ovary (CHO) cells in which G2 arrest has been induced by X-radiation and by etoposide, a topoisomerase inhibitor. When T-plastin expression was down-regulated, radiation induced G2 arrest was decreased in CHO cells, indicating a correlation between G2 arrest and cell cycle control. This group also showed that *PLS3* promoter methylation controls gene expression in the CRC cell SW948. A follow-up study showed that T-plastin was differentially expressed in various liver cancer cells, and that those cells with

low levels of T-plastin were also more susceptible to DNA damage (Ikeda et al., 2005; Sasaki et al., 2002b). Taken together, these results imply that down-regulation of T-plastin facilitates cancer development through the G2/M cell-cycle checkpoint in mammalian cells. The studies discussed above highlight an interesting idea; that T-plastin may influence cancer progression by perturbing the cell cycle, perhaps through changes in the nuclear-cytoskeletal framework that impacts upon chromatin organisation and hence gene activation. This concept contrasts with the hypothesis that T-plastin solely contributes to cell motility as part of the actin machinery that enables cells to migrate and metastasise.

Although various studies have reported that plastin expression may be dysregulated in epithelial cancers and immortalised cell lines, none to date have demonstrated a clear causal relationship between *PLS3* promoter methylation and/or plastin expression and tumour development.

1.12 Rationale and aims of thesis

As outlined in the introduction, we have previously found that positive expression of A-type lamins is predictive of poor prognosis in CRC (Willis et al, 2008). In order to understand this finding, an *in vitro* model system based upon the expression of GFP-lamin A in CRC cells was established. Downstream investigations revealed that CRC cells overexpressing lamin A were significantly more motile, and this increase in motility was, in part, caused by upregulation of actin bundling protein T-plastin. Thus, T-plastin was identified as a candidate gene for further exploration. The main aims of this thesis were to investigate *PLS3* promoter methylation and plastin expression in CRC, using a combination of both epigenetic and immunohistochemical approaches. Furthermore, we sought to examine their potential as prognostic biomarkers to be used in conjunction with lamin A/C. At the onset of this project, we hypothesised that the *PLS3* promoter would be demethylated, and that plastin would be aberrantly expressed in colorectal carcinomas. In addition, we hypothesised that the high risk of mortality in CRC patients who exhibit A-type lamin expression in their tumours, arises because lamin A is a master regulator of a pathway that co-ordinates the cytoskeletal changes required for cell motility and tumour invasiveness. The main objectives of this thesis were:

- 1) To determine the methylation status of the CpG island within the *PLS3* promoter in both CRC cell lines and tissues.
- 2) To investigate whether there is an association between *PLS3* promoter methylation and clinicopathological staging, using DNA samples obtained from the Netherlands CRC archive.
- 3) To raise and test polyclonal plastin antibodies for their ability to detect T/L-plastin in cell lines and tissues.
- 4) To use polyclonal plastin antibodies developed in objective 3 to investigate the expression pattern of T/L plastin by immunohistochemical analysis, and to determine its utility as prognostic biomarker in CRC
- 5) To generate a candidate gene network based on the differential expression of genes when lamin A is introduced into a CRC cell line, and to validate this network by both real-time PCR and immunoblotting techniques.

Chapter 2: Materials and methods

2.1 General chemicals and materials

The majority of routine chemicals were purchased from BDH Laboratory Supplies (VWR International Ltd, Leicestershire, England), Melford (Melford Laboratories Ltd, Suffolk, England) and Sigma-Aldrich (Sigma-Aldrich Company Ltd, Dorset, England) unless otherwise stated. Chemicals from BDH were AnalaR[®] analytical grade and all other reagents were Molecular Biology Grade. All plastic ware for tissue culture was supplied by Greiner Bio-One Ltd, Gloucestershire, UK.

2.2 The Netherlands Cohort Study on Diet and Cancer

In 1986, a prospective cohort study on diet and cancer was initiated in the Netherlands. The study design is described in detail elsewhere (van den Brandt et al., 1990). Briefly, the cohort of 55-69 year old men (n = 58,279) and women (n = 62,573) originated from 204 municipal population registries throughout the Netherlands. At baseline, participants completed a self-administered questionnaire on dietary habits and lifestyle. Subsequently, incident CRC cases were identified by monitoring the entire cohort for cancer through annual record linkage to the Netherlands Cancer Registry (NCR); nine regional cancer registries throughout the Netherlands and the Pathologisch Anatomisch Landelijk Geautomatiseerd Archief (PALGA); the nationwide registry for histopathology and cytopathology in the Netherlands (van den Brandt et al., 1990). For patient follow-up, the first 2.3 years were excluded due to incomplete nationwide coverage of PALGA. However, from January 1989 until January 1994, 819 incident cases with histologically confirmed CRC were identified, and the patient follow-up was complete and subsequently obtained for the period of 1st January 1989 to 31st December 1996 (7 years).

2.2.1 Tissue samples

Tumour material of CRC patients was collected after approval by the Ethical Review Board of Maastricht University, PALGA and the Netherlands NCR. Tissue samples from 819 identified CRC patients were requested from 54 pathology laboratories throughout the Netherlands. Tumour tissue collection started in August 1999 and was completed in December 2001.

Forty four tumour tissue samples (5%) were untraced. Of the 775 traceable tissue samples, 737 (90%) contained sufficient tumour material as confirmed by senior pathologist Professor Adriaan de Bruïne (University Hospital Maastricht, Netherlands) for histological and molecular analysis. All specimens had been previously processed according to standard Dutch pathology guidelines. Briefly, specimens were grossly dissected and immersed in 10% formalin fixative for 30 minutes at 35°C. Dehydration and embedding of tissues was fully automated and the procedure was as follows: 70% ethanol, 60 minutes at 35°C, 70% ethanol, 60 minutes at 37°C, 96% ethanol, 60 minutes at 37°C, 96% ethanol, 1 hour and 30 minutes at 40°C, 100% ethanol, 1 hour 30 minutes at 40°C and 100% ethanol, 2 hours at 45°C. Thereafter, samples were cleared in xylene for 15 minutes at 45°C, 15 minutes at 50°C, followed by another 30 minutes in fresh xylene at 50°C before embedding in paraffin at 60°C for two 60-minute periods, and finally for 1 hour 30 minutes. The clinical stage of the tumours was then confirmed histologically by a resident pathologist.

2.2.2 The CREAM database and retrospective study

Information regarding age at diagnosis, sex and other clinicopathological features was retrieved from the NLCS database. Information concerning tumour sub-localisation, Dukes'/TNM stage and differentiation state of the tumour was retrieved from the NCR database. DNA had been previously isolated from 737 tissue specimens for biochemical analysis. Information regarding the molecular status of tumours (e.g. *KRAS* oncogene mutations), along with clinicopathological characteristics described above, was collated and entered into a new database entitled the Colorectal Epidemiology and Mutation (CREAM) database. Within the CREAM database, a subset of 161 genomic DNA samples and 70 CRC tissue slides were analysed for *PLS3* promoter methylation (Chapter 3) and T/L-plastin expression (Chapter 5), respectively.

2.2.3 Statistical analysis

The patients from the analysis included in this study developed cancer between 1989 and 1994. Information on mortality from 1st January 1989 until 1996 (7 years) was retrieved through linkage with the Central Bureau for Statistics. CRC-related death was concluded if CRC was determined to be either the primary cause of death or as a primary, secondary or tertiary complication, using the International Classification of Diseases (ICD) system.

Differences in patient, tumour and follow-up characteristics were analysed using the Chi-square (χ^2) test. In order to investigate survival, two statistical analyses were performed. Firstly, Kaplan-Meier curves were produced to estimate survival probability. Kaplan-Meier curves are an estimate of the survivor function. The time in the study represents a clinical endpoint, in this case death from CRC. The study baseline is $t = 0$. Survivor function $S(t)$ is the proportion of the population still alive at time t . Secondly, Cox regression analysis using the Breslow method for ties was performed to estimate the cumulative hazard. Cox regression (or proportional hazards regression) is the method for investigating the effect of several variables upon the time a specified event takes to happen, i.e. death from CRC. The cumulative hazard at time t is the risk of dying between time 0 and time t , and the survivor function at time t is the probability of surviving to time t . Co-efficients or hazard ratios (HR) above 1 indicate a worse prognosis and a coefficient of less than 1 indicates a protective effect of the variable with which it is associated. A coefficient of 1 indicates no effect of the variable on the likelihood of hazard occurrence. All analyses were performed using SPSS in collaboration with senior epidemiologist, Dr Kim Smits (University Hospital Maastricht, Netherlands).

2.3 Mammalian cell culture and transfections

2.3.1 Cell lines and subculture

The human CRC cell lines SW480, SW620, and SW948 were originally obtained from the European Collection of Cell Cultures (ECACC), Wiltshire, UK, as growing cultures (Table 2.1). The SW480 cells had been stably transfected previously with DNA constructs encoding either EGFP-lamin A (SW480/lamA) or EGFP (SW480/cntl) (Willis et al, 2008). The GFP-lamin A full length cDNA was a kind gift from Dr M Izumi, Institute of Physical and Chemical Research, Saitama, Japan. Cells were routinely cultured in 75 cm² plastic tissue culture flasks under the following conditions: SW480, SW480/cntl, SW480/lamA and SW620 cells were cultured in L-15 (Leibovitz medium) with 2 mM L-Glutamine (Invitrogen, UK) and HT29 and SW948 in DMEM (Dulbecco's modified Eagle's medium) (Invitrogen, UK) supplemented with 10% foetal calf serum (FCS) lot 057K3395 (Sigma), 100 Uml⁻¹ penicillin and 100 µgml⁻¹ streptomycin. All cultures were maintained in a humidified environment at 37°C in either the presence of 5% CO₂ (SW498) or absence of CO₂ (SW480, SW480/cntl, SW480/lamA, SW620).

Upon 90% confluency, culture media was removed, cells were washed in Versene (137 mM NaCl, 2.7 mM KCl, 8 mM Na₂HPO₄, 1.5 mM KH₂PO₄, 1.5 mM EDTA pH 7.4) and subsequently detached from the flask in Versene containing 10% (v/v) trypsin in a humidified environment at 37°C for 3 minutes. Thereafter, cells were neutralised with either serum-containing L-15 or DMEM media and centrifuged (Eppendorf 5810R) at 200 x g for 5 minutes. Supernatants were removed and cells were resuspended in fresh medium and seeded into new flasks.

At the Department of Pathology, University Hospital Maastricht, Netherlands, human CRC cell lines HT29, LS and CaCo-2, all obtained from LGC (Teddington, UK), were cultured in DMEM supplemented with 10% FCS, 100 Uml⁻¹ penicillin and 100 µgml⁻¹ streptomycin (Table 2.1). All cultures were maintained in a humidified environment at 37°C in the presence of 5% CO₂. At approximately 90% confluency, cells were washed, trypsinised and seeded into new flask (as described above). Cells were routinely split 1:3 – 1:4.

Table 2.1: CRC cell lines

Cell line	Description	Dukes' Stage	Age	Gender	Ethnicity	Reference
SW480	Human colon adenocarcinoma	B	50	Male	Caucasian	(Leibovitz et al., 1976)
SW620	Derived from a metastasis of the same tumour from which the SW480 was derived	C	51	Male	Caucasian	(Leibovitz et al., 1976)
SW948	Human colon adenocarcinoma	C	81	Female	Caucasian	(Leibovitz et al., 1976)
HT29	Human colon adenocarcinoma	-	44	Female	Caucasian	(Chen et al., 1987)
LS	Human colon adenocarcinoma	B	58	Female	Caucasian	(Rodrigues et al., 1976)
CaCo-2	Human colon adenocarcinoma	-	72	Male	Caucasian	(Fogh et al., 1987)

2.3.2 DAC treatment

In order to investigate whether DNA methylation of the *PLS3* promoter controlled T-plastin expression, two CRC cell lines (HT29 and SW948) were subjected to drug treatments that enable the detection of epigenetic modifications. Cells were seeded and allowed to reach 30% confluency. At 30% confluency, HT29 and SW948 cells were treated with both 0.5 µM

and 2.0 μM of the methylation inhibitor 5-Aza-2'-deoxycytidine (DAC) (Ikeda et al., 2005). The culture medium containing DAC was replenished every 24 hours. Control cells were left untreated and replenished with fresh media. At 96 hours, cells were harvested, washed in 1 x phosphate buffered saline (PBS), and RNA was isolated in order to examine T-plastin expression by quantitative real-time PCR (Chapter 2, Section 2.6).

2.4 Nested methylation-specific PCR (N-MSP)

2.4.1 Primer design

Methylation specific PCR (MSP) is a quick and cost effective method which can rapidly assess the methylation status of a group of CpG sites within a given CpG island (Herman et al., 1996). The assay consists of initial modification of DNA by sodium bisulphite, which converts all of the unmethylated cytosines to uracil, whereby methylated cytosines remain unchanged (Derks et al., 2004). This is followed by detection of unmethylated versus methylated DNA by PCR using primers specific for both. Since the DNA was obtained from formalin-fixed, paraffin-embedded tissues, a two-stage nested MSP was performed. Nested PCR was used because it can detect methylation more effectively in clinical samples, where DNA quality and quantity is limited (1 methylated allele in 50,000 unmethylated alleles). The first round of primers are designed to amplify sodium bisulphite-modified DNA and do not discriminate between methylated and unmethylated DNA (Table 2.2). Careful primer design is crucial for ensuring the success and specificity of MSP. Primers were designed with the following considerations:

- (a) The primers should be 23-30 bp in length to ensure specificity.
- (b) Primers should contain one to three CpG dinucleotides in the 3' region of the primers. This allows for discrimination between methylated (M) and unmethylated (U) DNA and ensures specific annealing.
- (c) Primers must contain non-CpG cytosines in their sequence to retain specificity for sodium bisulphite converted DNA.
- (d) Both U and M primers should have similar melting temperatures (T_m). The GC content of the U primers is decreased upon sodium bisulphite conversion, so the U primer should to be extended into the 5' region. Although this leads to variation in the start site it allows paired

analysis in a single thermocycler and ensures that products can be easily recognised after gel electrophoresis.

(e) Primers for both methylated and unmethylated DNA should contain the same CpG sites to ensure sensitivity and specificity.

(f) To facilitate MSP on fragmented DNA from formalin-fixed, paraffin embedded tissue sections, amplicons should be no more than 150 bp.

Table 2.2: N-MSP *PLS3* primer set

Outside	Flank up	Flank down
	YGGAGAAATTTTAGTTGGAGTTTT	CCACTTAATACAATAAAATACAAAAAAC
Inside	Unmethylated (U)	Methylated (M)
Sense	TGGAGTTTTTGGGTGTTTGGT	TTTCGGGCGTTCGGGC
Antisense	CTTAATACAATAAAATACAAAAACATATCTACA	AATACAATAAAATACAAAAACGTATTCTACG

2.4.2 DNA isolation

A 4 µm section of each tissue block was previously stained with hematoxylin and eosin and reviewed by the senior pathologist, Professor Adriaan de Bruïne. Five sections (20 µm thick) were deparafinised and subjected to genomic DNA extraction by using a Puregene® DNA isolation kit (Qiagen) according to the manufacturer's instructions. This method was also used to isolate DNA from CRC cell lines SW480, SW620, SW948, LS, CaCo2 and HT29. Briefly, CRC cells were harvested at 70% confluency then cell pellets were resuspended in culture medium in a 15 ml tube. Thereafter, cells were centrifuged at 500 x g for 3 minutes. The supernatant was removed leaving behind 100-200 µl residual liquid. The tubes were then vortexed to resuspend the cells in the residual supernatant. 3 ml of Cell Lysis Solution was added to each sample and pipette-mixed until no cell particulates were visible. Once the lysates were homogenous, 15 µl RNase A Solution was added to each sample, inverted 25 times then incubated at 37°C for 1 hour. Once the samples had cooled to room temperature (RT), 1 ml Protein Precipitation Solution was added and vortexed vigorously for 20 seconds to mix the Protein Precipitation Solution uniformly with the cell lysates. Following this, samples were centrifuged at 2000 x g for 10 minutes. The supernatant containing the DNA was poured into a 15 ml tube containing 3 ml 100% isopropanol (2-propanol) then inverted gently 50 times. The samples were then centrifuged at 2000 x g for 3 minutes. Thereafter, the supernatant was discarded and the tube drained briefly on clean absorbent paper. Three ml 70% ethanol (EtOH) was added to the pellet and the tube inverted several

times to wash the DNA. Samples were then centrifuged a final time at 2000 x g for 1 minute. The EtOH was carefully discarded and the tube pellet was allowed to air dry for 15 minutes. Following this, 250 µl of DNA Hydration Solution was added to each sample, and heated at 65°C for 1 hour (tapping the tube periodically to aid in dispersing the DNA). The DNA was stored at 4°C.

2.4.3 Sodium bisulphite conversion

Sodium bisulphite modification, which converts unmethylated cytosine residues to uracil residues, was carried out on 500 ng genomic DNA isolated from CRC and normal tissue sections, in addition to CRC cell lines (HT29, SW620, SW948, SW480-GFP, SW480/lamA, CaCo2) with the use of an EZ DNA methylation™ kit (Zymo Research Co) according to the manufacturer's instructions. Briefly, DNA samples were diluted to a concentration of 500 ng in a volume of 45 µl with sterile H₂O. Five µl of M-Dilution Buffer was added to 45 µl of DNA samples in 1.5 ml DNase-free tubes, mixed gently by pipetting up and down and incubated at 37°C for 15 minutes. Meanwhile, 750 µl of sterile water and 210 µl of M-Dilution Buffer was added to 1 tube of CT Conversion Reagent and mixed by vortexing for 10 minutes. Subsequently, 100 µl of the prepared CT Conversion Reagent was added to each sample and lightly vortexed. Samples were incubated at 55°C for 16 hours in the dark, followed by incubation on ice for 10 minutes. Thereafter, 400 µl of M-Binding buffer was added to each sample pipette mixed. The samples were transferred to Zymo-Spin I Columns, and the columns were placed into 2 ml collection tubes and centrifuged at 12,000 x g for 15-30 seconds. The flow-through was discarded. Two hundred µl of M-Wash Buffer was added to each column, centrifuged for 30 seconds, and again the flow through was discarded. Then 200 µl of M-Desulphonation Buffer was added and the samples were incubated at RT for 15 minutes. After incubation, the samples were centrifuged at 12,000 x g for 30 seconds. Following this, samples were washed again with M-Wash Buffer and centrifuged at 12,000 x g for 30 seconds. The flow-through was discarded and the washing step was repeated, with columns centrifuged for an additional 1 minute to remove any excess buffer and dry the samples. The columns were then placed in fresh 1.5 ml sterile tubes, and 20 µl of M-elution buffer was added directly to the column matrix. Finally, samples were spun at 12,000 x g, the columns were discarded and the eluted DNA was stored at -20°C.

2.4.4 N-MSP

In order to examine *PLS3* promoter methylation, N-MSP was performed on sodium bisulfite-modified DNA. The PCR procedure requires both an outside and an inside primer pair and thus two 'nested' reactions. N-MSP was carried out in Multiplate® 96-well PCR plates (Bio-Rad). For the outside MSP, 50 ng (4 µl) bisulphite treated DNA was added as a template to a total volume of 21 µl of the following reaction mix: 11.75 µl nuclease-free H₂O, 2.5 µl 10x Magic buffer (166 mM NH₄SO₄, 670 mM Tris pH 8.8, 67 mM MgCl₂, 100 mM beta-mercaptoethanol), 1.25 µl of 6.25 mM dNTPs, 2.5 µl sense and antisense primers at a concentration of 20 µM and 0.5 µl Immolase™ DNA polymerase (Bioline) at 1U ul⁻¹. The reaction mix was subjected to the following PCR conditions: 95°C for 3 minutes; then 35 cycles of 95°C for 30 seconds, 56°C for 30 seconds, 72°C for 30 seconds, followed by 72°C for 4 minutes. The PCR products from the outside reaction were subjected to a second 'inside' round of PCR, with unmethylated and methylated reactions being prepared separately. Each PCR product was diluted 1:1000 in 0.1x TE (1 mM Tris, 0.1 mM EDTA, pH 8.0). Four µl of template was added to 21 µl of the following reaction mix: 16.5 µl nuclease-free H₂O 2.5 µl 10x Magic buffer [166 mM NH₄SO₄, 670 mM Tris pH 8.8, 67 mM MgCl₂, 100 mM beta-mercaptoethanol], 0.25 µl dNTPs at 6.25 mM, 0.5 µl 50% glycerol, 0.5 µl each of sense and antisense primer (U or M) at 20 µM and 0.5 µl of 1U ul⁻¹ Immolase™. The mix was subjected to the following PCR conditions: 95°C for 3 minutes; 35 cycles of 95°C for 30 seconds, 66°C for 30 seconds, 72°C for 30 seconds, followed by 72°C for 4 minutes. After thermocycling, the PCR products were stored at 4°C prior to analysis by agarose gel.

2.4.5 DNA gel electrophoresis

All amplified PCR products were run on 2% agarose gels in 0.5x TBE (45 mM Tris, 45 mM Boric acid, 1 mM EDTA pH 8.0) containing 5µl/100 ml GelStar™ stain to visualise DNA, at 100 Volts (V) for 20 min. A loading dye was not required because Immolase™ is coloured. Product size was compared to a 100 bp DNA ladder (Promega Cat #G2101) and bands were visualised using a Gel Doc™ transilluminator and Quality One™ software, version 4.0.3 (Bio-Rad).

2.5 Bisulphite sequencing

2.5.1 Primer design

In order to validate the N-MSP data, bisulphite sequencing was performed on sodium bisulphite modified DNA, as previously described. This assay allows for the exact positions of the 5-methylcytosine to be determined. The bisulphite sequencing primers are shown in Table 2.3. Primers were designed taking the following criteria into consideration:

- (a) To prevent unbiased amplification of either methylated or unmethylated DNA the primers should not hybridise across CpG sites.
- (b) Primers must contain an adequate number of non-CpG cytosines in their sequence to retain specificity for sodium bisulphite converted DNA.
- (c) Primers must flank the N-MSP primer site.
- (d) Primers products should be ~400 bp in length and contain a minimum of five CpG sites for analysis.

Table 2.3: Bisulphite sequencing primers

Gene ID	Forward	Reverse
<i>PLS3</i>	AGTYGGGTTAGATTTAGGATTTTG	ACCACTTAATACAATAAAATACAAAAAAC

2.5.2 Amplification of sodium-bisulphite modified DNA and ligation into pCR[®]2.1 vector

Bisulphite-modified DNA containing the *PLS3* promoter was amplified from SW948 and SW620 cell lines, or patient normal and tumour tissue, using methylation specific primers just described. The PCR reaction was comprised of 18.75 µl water, 2.5 µl 10x Magic buffer (166 mM NH₄SO₄, 670 mM Tris pH 8.8, 67 mM MgCl₂, 100 mM beta-mercaptoethanol), 0.25 µl dNTPs at 5 mM, 0.5 µl each of forward and reverse primers at 2.5 µM and 1 µl of 1U µl⁻¹ Immolase™ with 2 µl of sodium bisulphite-treated template. The PCR protocol consisted of an initial denaturation at 95°C for 3 minutes; followed by 40 amplification cycles of 30 seconds at 95°C, 30 seconds at 62°C, 30 seconds at 72°C and a final extension at 72°C for 10 minutes. PCR products were checked by 2% agarose gel (as described in Chapter 2, Section 2.4.5) and products from positive PCR reactions were directly ligated into the pCR[®]2.1 cloning vector using a TOPO TA[®] Cloning Kit (Invitrogen, Breda, the Netherlands) according

the manufacturer's instructions. Briefly, the 10 µl ligation reaction was composed of 1 µl PCR product, 0.5 µl Ligation buffer, 0.5 µl (2U) T4 DNA ligase, 1 µl linearised vector and 2 µl water. The ligation reactions were incubated at 14°C for 4 hours or overnight.

2.5.3 Transformation

The ligation mix (described in the Section 2.5.2) was used to transform TOP10 (Invitrogen) competent bacteria according to the following procedure. An aliquot of bacterial cells was thawed on ice and 1 µl ligation reaction was added gently to 15 µl of bacterial suspension. The mixture was left on ice for 30 minutes followed by heat shock for 30 seconds at 42°C. The cells were replaced on ice for 5 minutes prior to the addition of 125 µl SOC medium (0.5% yeast extract, 2% tryptone, 10 mM NaCl, 2.5 mM KCl, 10 mM MgCl₂, 10 mM MgSO₄, 20 mM glucose). The mixtures were incubated for 1 hour at 37°C in an Innova 4430 Incubator Shaker (Brunswick Scientific). Thereafter, 100 µl of the transformed bacterial suspension was spread onto LB (10 g bacto-tryptone, 5 g yeast extract, 10 g NaCl, 15 g agar per litre, pH 7.5) agar plates containing 40 µl of 40 mg ml⁻¹ X-gal dissolved in dimethylformamide. The plates were incubated at 37°C overnight. The next morning, the ratio of blue/white colonies was examined, with 5-25 blue colonies normally expected. A ratio of less than 1:10 blue:white colonies indicated an efficient transformation.

2.5.4 Colony PCR

The validity of recombinants were checked by PCR using universal M13 primers. Approximately 20 white colonies per plate were picked with a toothpick and used to inoculate both a PCR reaction mixture and 120 µl LB containing 100 µg ml⁻¹ ampicillin. The culture plates were incubated at 37°C with shaking at 270 rpm for several hours and the cultures were kept until the results from the PCR were known. The PCR reaction was composed of: 2.5 µl of PCR Buffer, 0.6 µl of 50 mM MgCl₂, 1 µl of 5 mM dNTPs, 0.5 µl of 10 µM of both M13 forward and reverse primers, 0.4 µl of Platinum® Taq (Invitrogen) and 15 µl water. The PCR profile consisted of a 95°C denaturation step for 10 minutes; 32 cycles of 94°C for 30 seconds, 48°C for 45 seconds and 72°C for 45 seconds; followed by 10 minutes at 72°C. The PCR products were analysed on a 2% agarose gel and compared with empty vector (245 bp). PCR products containing the correct insert (~550 bp) were selected for DNA sequencing.

2.5.5 Purification of recombinant DNA

Two ml LB supplemented with $100 \mu\text{g ml}^{-1}$ ampicillin was inoculated with $5 \mu\text{l}$ of the appropriate miniculture suspension from the 96 well plate. After overnight growth at 37°C in a 270 rpm shaking incubator, purification of recombinant plasmids was performed using a GenElute™ Plasmid Mini-Prep Kit according to the manufacturer's instructions (Sigma). The bacteria were pelleted at $12,000 \times g$ for 1 minute and the supernatant removed. The cells were resuspended in $200 \mu\text{l}$ Resuspension Solution to which $200 \mu\text{l}$ lysis solution was added. Samples were inverted gently and allowed to clear for ~ 5 minutes. Following this, $350 \mu\text{l}$ Neutralisation Solution was added to each sample, inverted 4-6 times to mix and the debris removed by centrifugation at maximum speed for 10 minutes. A binding column was prepared by adding $500 \mu\text{l}$ of Column Preparation Solution and centrifuging the column at $12,000 \times g$ for 1 minute. The flow through was discarded and the lysate added to the column, prior to centrifugation at $12,000 \times g$ for 1 minute. The column was washed with $750 \mu\text{l}$ wash solution, and centrifuged again at $12,000 \times g$ for 1 minute, discarding the flow through. After drying the column by centrifugation at $12,000 \times g$ for 1 minute, each column was transferred to a fresh collection tube. The DNA was eluted using $50 \mu\text{l}$ of nuclease-free water, by centrifuging the column for 1 minute at $12,000 \times g$. The DNA concentration of the eluate was measured using a NanoDrop spectrophotometer (Thermo Fisher Scientific, UK) and the DNA was stored at -20°C .

2.5.6 DNA amplification and sequencing analysis

The DNA amplification and sequencing was performed in collaboration with Mr Peter Moerkerk, University Hospital Maastricht, Netherlands. One hundred ng of recombinant DNA was used as a template for PCR in the following reaction mixture: $1.5 \mu\text{l}$ ABI reaction buffer, $1 \mu\text{l}$ ABI reaction mix, $3.2 \mu\text{l}$ of $1 \mu\text{M}$ M13 forward and reverse primers, made up to $10 \mu\text{l}$ with nuclease-free water. The template was amplified by PCR according to the following parameters: 96°C for 3 minutes, 25 cycles of 96°C for 30 seconds, 50°C for 5 seconds and 60°C for 3 minutes. The PCR products were purified on sephadex G50. Two grams of G50 were mixed with 25 ml water and swollen for several hours at RT or overnight at 4°C . Three hundred μl of mixed sephadex solution was pipetted into a 96 well filter plate with a dummy elution plate fixed beneath it. The plates were centrifuged for 3 minutes at 1840 rpm and the flow through discarded. The dummy plate was replaced by a Corning

elution plate. Ten microlitres of water was added to each well of the filter plate containing sephadex, followed by loading of the DNA samples. The plates were spun at 1840 rpm for 3 minutes to elute the DNA and the elution plate was sealed and taken for DNA sequencing by an automated DNA sequencer (Applied Biosystems, Foster City, CA).

2.6 Quantitative real-time PCR

2.6.1 Primer design

Quantitative real-time PCR (qPCR) was performed to analyse mRNA expression levels of T-plastin in 0.5 and 2.0 μM DAC-treated HT29 and SW948 CRC cell lines (Chapter 3.2.1). In addition, qPCR was also chosen to examine the mRNA expression levels of 11 genes from a microarray dataset (Chapter 6). To assist primer design, the PrimerBank was utilised to search for validated qPCR primers corresponding to the genes of interest, taking into account the possibility of alternatively spliced transcripts. PrimerBank is a public database containing over 300,000 human and mouse primer pairs for the detection and quantification of mRNA expression (<http://pga.mgh.harvard.edu/primerbank>). The programme selects suitable primers based on the following parameters:

- (a) Primers should be 19-23 nucleotides in length, to facilitate gene specificity and minimise the potential for primers to cross-react.
- (b) the primer GC content should be between 35-65%.
- (c) the ΔG threshold value for the last five residues at the 3' end should be -9 kcalmol^{-1} to minimise non-specific primer extension.
- (d) T_m values of should be similar (between 60-63°C) to reduce non-specific amplification.
- (e) PCR products should be 150-350 bp.
- (f) Primer cross-reactivity should be minimised by checking the primers by BLAST analysis
- (g) Primers giving secondary structures in the target or primer should be avoided to maximise PCR efficiency.

Gene Runner[®] (Hastings Software Inc.) was used to facilitate the examination of possible secondary structure formations (e.g. hairpin loops, self-dimers) between and within primer pairs. In some cases, primers were optimised by removing or adding 1-2 extra nucleotides to the end of the sequence. The final primer sequences used in this chapter are detailed in

Table 2.4. Fifty nmol primers were synthesised (Invitrogen) and the primers were diluted in sterile water to produce a 10 μ M working solution.

Table 2.4: Primers for qPCR analysis

Gene ID	Forward Primer	Reverse primer
<i>AREG</i>	CCCAAAACAAGACGGAAAGTGA	GCTGACATTTGCATGTTACTG
<i>BMP4</i>	TGGTCTTGAGTATCCTGAGCG	CTGAGGTAAAGAGGAAACGA
<i>CDH1</i>	TCTTCCCCGCCCTGCC	CTAGCAGCTTCGGAACCGC
<i>COL18A1</i>	GGCTGGCCTACGTCTTTGG	CGGATGTGGAACAGCAGTGAG
<i>EGFR</i>	AAGGAAATCCTCGATGAAGCCT	TGTCTTTGTGTTCCCGGACATA
<i>EIF4E</i>	AGGATGGTATTGAGCCTATGTGG	CACAGAAGTGTCTCTAGCCAAAA
<i>EREG</i>	GCTCTGACATGAATGGCTATTGT	TGTTACATCGGACACCAGTAT
<i>FN1</i>	GGCCTGGAACCGGAAACCGA	AGGGTGGGTGACGAAAGGGGT
<i>GAPDH</i>	CATGAGAAGTATGACAACAGCCT	AGTCCTTCCACGATACCAAAGT
<i>IGF2</i>	CCTCCAGTTCGTCTGTGGG	CACGTCCCTCTCGGACTTG
<i>PLS3</i>	ACTCATGCTGGATGGTGACA	GTTCCACCCAGAGCACAAAT
<i>SERPINE1</i>	CATCCCCATCCTACGTG	CCCCATAGGGTGAGAAAACC
<i>SNAI2</i>	ATACCACAACCAGAGATCCTCA	GACTCACTCGCCCCAAAGATG

2.6.2 Total RNA isolation

Total RNA was isolated from SW480/cntl, SW480/lamA, HT29 and SW948 CRC cell lines using the RNeasy mini kit (Qiagen) according to the manufacturer's instructions. Briefly, CRC cells were grown to approximately 70% confluency in 75 cm² tissue culture flasks and harvested as described in Chapter 2, Section 2.3.1. Cells were washed in 4 ml PBS prior to centrifugation at 200 x g for 5 minutes (Eppendorf 5810R). After the supernatant was removed, the cell pellets were resuspended in 600 μ l RLT buffer and lysates were homogenised by vortexing for 1 minute. Subsequently, 600 μ l of RNase-free 70% ethanol (molecular biology grade) was added to each homogenised lysate and pipette mixed. Samples were transferred to an RNeasy spin column placed in a 2 ml collection tube, then centrifuged for 15 s at 8,000 x g. The flow through was discarded. Thereafter, 700 μ l RW1 buffer was added to the spin column and centrifuged for 15 s at 8,000 x g. Again, the flow through was discarded. Following this step, 500 μ l RPE buffer was added to each spin column and centrifuged for 15 s at 8,000 x g. The membrane was washed again in 500 μ l RPE buffer and centrifuged for 2 minutes at 8000 x g. After discarding the flow through, the spin column was placed into a fresh 2 ml collection tube and centrifuged at 12,000 x g for 1 minute ensuring that no residual RPE buffer was left and the membrane was fully dry. The

spin column was carefully removed and placed into a new 1.5 ml collection tube. The RNA was eluted by adding 30 μ l RNase-free water and centrifuging for 1 minute at 8000 x g. Samples were stored at -80°C.

2.6.4 Quantification and purity of RNA

The concentration and purity of RNA was measured using a NanoDrop spectrophotometer (Thermo Fisher Scientific, UK). Briefly, 1 μ l of sample was loaded onto the optical pedestal, the absorbance at 260 nm and 280 nm was measured, and the concentration of RNA was calculated. The $A_{260}:A_{280}$ ratio was used to assess RNA purity, with a value of 1.7-2.0 taken to indicate that the sample was sufficiently pure.

2.6.3 cDNA synthesis

Synthesis of cDNA was performed using an iScript kit (Biorad) in accordance with the manufacturer's instructions. Briefly, 4 μ l 5x iScript buffer, 1 μ l iScript MMLV reverse transcriptase and 11 μ l nuclease-free water were added to 4 μ l (2 μ g) of RNA template in 0.5 ml PCR tubes. Reactions were incubated at 25°C for 5 minutes, followed by 42°C for 30 minutes and then 85°C for 5 minutes. Synthesized cDNA samples were diluted in nuclease-free water (Sigma) to give a final concentration of 20 ng μ l⁻¹. Aliquots were stored at -80°C.

2.6.5 qPCR primer validation

Prior to performing qPCR on the biological samples of interest, it is important to assess the efficiency of the primers. For each primer set, qPCR was performed on a cDNA dilution series (0.1 ng – 100ng diluted to 1000x dilution). Quantitative real-time PCR was carried out in a MicroAmp® optical 96 well reaction plates (Applied Biosystems). Twelve point five μ l Fast SYBR® Green Master Mix (Applied Biosystems, Nieuwekerk a/d IJssel, NL), 5 μ l cDNA, 5.5 μ l nuclease-free water, 1 μ l forward primer (1000 μ M) and 1 μ l reverse primer (1000 μ M) were added to each well. A negative control containing no cDNA was run for each primer pair that was used. MicroAmp® optical adhesive film (Applied Biosystems) was placed on the top of the 96 well reaction plate to reduce contamination and evaporation. The plate was centrifuged briefly to remove bubbles. Reactions were run in a 7500 Fast Real-Time PCR System (Applied Biosciences). The qPCR profile was as follows: 95°C for 20 seconds, 40 cycles of 95°C for 3 seconds followed by 60°C for 30 seconds. Following this, a melt curve stage was

performed in which the samples were heated to 95°C for 15 seconds, cooled to 60°C for 1 minute, slowly heated up to 95°C, and cooled to 65°C for 15 seconds. The baseline and threshold values were checked to confirm the validity of the automatically generated parameters. In a qPCR reaction, the fluorescence signal is measured during the exponential amplification phase because it provides the most accurate data for quantification. Cycle threshold (C_T) values indicate the amplification cycle at which the fluorescent signal exceeds a threshold above the background signal (baseline). Thus, the lower the C_T value, the higher the gene expression. A standard curve was plotted where X axis = $\log_{10}[\text{cDNA}]$ and Y axis = C_T values. Primers passed quality control testing if the gradient of the graph was between -3.3 +/- 0.3 as this indicates that the efficiency of the PCR reaction is 100% +/- 10% and hence allows for meaningful gene comparison. All primers used within this thesis were deemed suitable for qPCR analysis (Supplementary Figure S1 A).

2.6.6 qPCR

Quantitative real-time PCR was carried out as described in 2.6.5 with 30 ng cDNA added to each well on the PCR plate. A negative control containing no cDNA was also run for each primer used. Three to five biological replicates were run in separate plates and three technical replicates were carried out in each individual plate. In order to establish the integrity of the qPCR product, melt curve analysis was automatically performed by the 7500 Software v2.0.5 (Applied Biosystems). After the PCR cycling was complete, the temperature was raised at 1°C increments from 65°C to 95°C. As temperature rises, the PCR products denature, leading to a decrease in fluorescence. A single peak represents the decreased fluorescence at the melting point of the qPCR product, whereas primer-dimers or non-specific products may appear as multiple peaks. Within our experimental data, single peaks were observed confirming the specificity of the primers and integrity of the qPCR products. A representation of melt curve analysis is shown in Supplementary Figure S1 B. Furthermore, the progression of the qPCR reaction can be observed in realtime in the form of an amplification plot where $Y = \Delta R_n$ and $X = \text{number of cycles}$ [$\Delta R_n = (\text{ROX}^{\text{TM}} \text{ fluorescence} / \text{SYBR Green fluorescence}) - \text{baseline}$] (Supplementary Figure S1 C). ROXTM is a reference dye within the mastermix that provides an internal fluorescence reference against which the SYBR green fluorescence can be normalised. A baseline can be obtained from the first cycles of qPCR in which fluorescence remains relatively constant. The C_T values (as described above) can be obtained from this graph and were used to calculate the relative changes in gene

expression using the $2^{-\Delta\Delta CT}$ method (Livak and Schmittgen, 2001a). Relative quantification compares the gene expression in two or more samples and contrasts with absolute quantification, which calculates the number of copies of a specific RNA. The relative changes were normalised to an endogenous control gene, *GAPDH*.

2.7 Generation of plastin polyclonal antibodies

2.7.1 Animal selection

Polyclonal antibodies are commonly produced in mammalian and avian species. To raise antibodies against plastins, the rabbit was chosen as it responds to a wide range of immunogens and yields large quantities of antibody. Two animals per antigen were selected in order to maximise the likelihood of a strong and specific response to the antigen.

2.7.2 Peptide immunogen design

Peptides were used to raise the plastin antibodies (Table 2.5). In a peptide of 15-20 residues, there will be a limited number of potential epitopes and thus polyclonal sera raised against a short peptide sequence may have specificity and affinity characteristics similar to a monoclonal antibody. Plastin protein sequences were sent to Cambridge Research Biochemicals and three antigenic peptides were chosen using standard bioinformatic algorithms. Potentially immunogenic plastin peptides were designed to minimise unwanted cross-reactivity with unrelated proteins. The sequences of the peptides and testing of the resulting sera are discussed in detail in Chapter 4. The antigenic peptides were designed bearing in mind the following principles:

- (a) Peptides should correspond to loops in the parent protein to mimic the exposed sequences in the native protein.
- (b) Hydrophilic sequences are likely to be exposure at the surface.
- (c) N and C termini tend to be surfaced exposed.
- (d) Y and P residues help give structure to the peptide.
- (e) Repetitive sequences (three or more identical residues) should preferably be avoided as this often results in poor quality peptide and non-specific antibodies.

(f) Ideally, peptides should not include aspartic acid, as these residues may form aspartimides.

(g) Long amino acid repeats, such as poly Q residues, should be avoided as hydrogen bonding can occur resulting in poor peptide synthesis and low solubility.

Table 2.5: Peptides sequences for generation of plastin polyclonal antibodies

Ab name	Residues	Peptide sequence
Dann1	110-127	SELSSEGTQHSYSEEEKY
Dann2	310-322	APKGQKEGEPRID
Dann3	674-589	SGNLTEDDKHNNAKYA

2.7.3 Conjugation and antibody production

Peptides are small molecules which would only elicit a very weak immune response. To circumvent this problem, 5 mg of antigen was conjugated to 5mg of a carrier, keyhole limpet haemocyanin (KLH), via the side chain thiol (-SH) of a cysteine residue with m-Maleimidobenzoic acid N-hydroxysuccinimide ester (MBS). A standard CRB immunisation schedule was followed to yield a high affinity antibody after the secondary immune response. The antibodies were affinity purified on peptide conjugated sepharose beads to remove additional serum proteins and help reduce background staining. The antisera from the final bleed were purified using a peptide affinity column and eluted using a TEA buffer at pH 10. The purified antibody eluates were stored at -20°C at the following concentrations; Dann1a: 1.76 mgml⁻¹, Dann1b: 1.11 mgml⁻¹, Dann2a: 2.73 mgml⁻¹, Dann2b: 0.96 mgml⁻¹, Dann3a: 1.20 mgml⁻¹ and Dann3b at 0.55 mgml⁻¹. The antisera from all immunised animals were screened for anti-peptide antibody responses using an Enzyme-Linked Immunosorbent Assay (ELISA) in which the peptide antigen was adsorbed onto the ELISA plate (performed by Cambridge Research Biochemicals, UK). ELISA methods are immunoassays used for the detection and quantification of a substance based on antibody:antigen interactions (Hornbeck, 2001). Antibody binding to the peptide was quantified using an alkaline phosphatase labelled secondary antibody which was detected by the action of the enzyme on a chromogenic substrate (p-nitrophenyl phosphate). Affinity-purified antibodies were characterised by ELISA over a range of dilutions up to 1/100,000 and compared with the crude antisera. In addition, unbound antisera and TEA pH 4 eluates were tested against the immunising peptides. The antibody titre was determined by calculating the point at which

absorbance of the chromagenic substrate was 50% of maximum. Antiserum obtained from each animal showed a relatively high titre of anti-peptide antibody, varying from 1:4283 (Dann1a) to 1:43658 (Dann2a) (Supplementary Figure 2). The results from the ELISA analysis suggested that antibodies had been successfully raised against all three plastin peptides.

2.8 Immunohistochemistry

2.8.1 Antigen retrieval

Formalin-fixed, paraffin-embedded tissue specimens obtained from the NLCS archive were previously sectioned into 4 μm slices and left overnight at 50°C to bond to Starforst® adhesive microscope slides (Knittel Glaser, Braunschweig, Germany). CRC tissue sections were then de-paraffinised in xylene, 2 x 5 minutes followed by 100% EtOH 2 x 5 minutes. Endogenous peroxidase activity was quenched by submerging the slides in 0.3% H₂O₂ in methanol for 20 minutes, followed by 3 minutes in distilled H₂O. Thereafter, antigen retrieval was performed by immersing the tissue sections in Tris-EDTA buffer (10 mM Tris, 1 mM EDTA pH 8) or in 0.01 M citrate buffer (pH 6) that had been pre-heated for 3 minutes in a microwave (850W). The slides were heated for 10 minutes at 360W. Following this the slides were allowed to cool to room temperature (RT) for 30 minutes before washing in 1 x PBS. Non-specific antibody binding was blocked using 5% bovine serum albumin (BSA) in PBS. After 30 minutes of blocking, slides were gently tapped onto blotting paper to remove the blocking solution.

2.8.2 Antibody incubation and antigen visualisation

Primary antibodies were diluted in 0.5% BSA in PBS and each section was incubated with 120 μl primary antibody at 4°C overnight. Negative controls were incubated in 0.5% BSA/PBS, omitting the primary antibody. Post incubation, unbound primary antibody was removed by washing 3 x 3 minutes in PBS. Thereafter, each slide was incubated with 120 μl BrightVision (ImmunoLogic, NL) poly-HRP-anti-mouse/rabbit/rat IgG for 30 minutes at RT. Slides were then washed 3 x 3 minutes in PBS. Immunological detection was achieved by adding 120 μl activated 3,3-diamino-benzidine-tera hydrochloride (DAB) chromagen (Sigma). DAB was applied directly to tissue sections, and reactions were stopped by immersing sections in distilled H₂O.

2.8.3 Counterstaining and mounting

In order to visualise cell nuclei, sections were counterstained in haematoxylin for 20 seconds then rinsed in tap water for a few minutes. Slides were then dehydrated through a graded ethanol series: 70% EtOH for 3 minutes, 96% EtOH for 3 minutes and 2 x 100% EtOH for 1 minute. Thereafter sections were cleared in 2 x xylene for 3 minutes. Specimens were mounted and covered with Entellan® (Merck kGaA, Darmstadt, Germany) and left to dry overnight.

2.8.4 Photography

CRC tissue sections were analysed using a Nikon Diaphot inverted microscope (Nikon Corporation, Tokyo, Japan) equipped for bright field microscopy with Plan 4x/0.13, 10x/0.25, 20x/0.4 and 40x/1.3 lenses. Images were taken with a Nikon DXM1200 digital camera controlled by Nikon Act-1, version 2.20 software. Image processing was carried out using Adobe® Photoshop® 7.0 imaging software (Adobe Systems Inc, San Jose, CA, US).

2.9 One-dimensional SDS-PAGE and immunoblotting

2.9.1 Preparation of recombinant plastin proteins

E. coli expressing GST fusion proteins of T-plastin (human), I-plastin (human) and L-plastin (mouse; the N-terminal half of the protein), plus a GST-only expressing control, were a kind gift from Dr Francisco Rivero, University of Hull. The fusion proteins have a molecular mass of ~96 kDa, with exception of the GST-L-plastin fusion protein (40 kDa). Stabs from each of these *E.coli* strains were grown up in a shaking incubator at 37°C in 5ml of sterile LB medium (10 g tryptone, 5 g yeast extract, 10 g NaCl per litre) supplemented with 100 µg ml⁻¹ ampicillin. Fusion protein synthesis was induced by the addition of 1 mM Isopropyl β-D-thiogalactoside (IPTG) and 1 ml aliquots were harvested at 0 hour, 1 hour, 2 hours and 3 hours post-induction. The aliquots were centrifuged at 500 g for 5 min at 4°C. The supernatants were removed and the pellets were resuspended in 500 µl PBS, spun down at 12,000 g for 2 minutes at 4°C and the pellets freeze-thawed using liquid nitrogen. The thawed pellets were resuspended in bacterial lysis buffer (PBS supplemented with 20 µg ml⁻¹ DNase, 0.1% Triton X-100, 100 µg ml⁻¹ lysozyme and 1 µg ml⁻¹ of protease inhibitor cocktail).

Aliquots of the bacterial lysate were taken up in an equal volume of 2X Laemmli sample buffer (4% SDS, 20% glycerol, 10% 2-mercaptoethanol, 0.004% bromophenol blue and 0.125 M Tris HCl, pH 6.8.) for SDS PAGE/Western blotting analysis or were snap frozen for future use. Glycerol stocks of the *E. coli* strains were made by diluting 250 µl of exponentially growing cultures with an equal volume of sterile glycerol. The glycerol stocks were stored at -80°C.

2.9.2 Preparation of mouse tissue

Mouse tissue from liver, kidney, muscle and spleen was obtained from C57BL/6 mice. The tissues were rinsed in PBS, drained of excess fluid, cut into small pieces where necessary and snap frozen in liquid nitrogen. Frozen tissue was weighed, pulverised in a cold pestle and mortar and resuspended in lysis buffer (20 mM MES, 30 mM Tris, 100 mM NaCl, pH 7.4) with 1% Triton X-100, supplemented with 20 µg ml⁻¹ DNase and the following protease inhibitors: 10 µgml⁻¹ each of chymostatin, leupeptin, antipain and pepstatin A (Sigma). Lysates were homogenised with a syringe and needle and supernatants obtained by centrifugation for 10 min at 4°C, 12,000 x g. The amount of protein present in the lysates after centrifugation was confirmed by colloidal Coomassie staining (Chapter 2, Section 2,9.6).

2.9.3 Preparation of whole cell extracts

Cultured SW480/lamA, SW480/cntl and SW620 cells in 72 cm² dishes at 70-80% confluency (~ 8 x 10⁶ cells per cell line) were washed in PBS, and scraped in lysis buffer (20 mM MES, 30 mM Tris, 100 mM NaCl, pH 7.4, with 1% Triton X-100 (Sigma), supplemented with the following protease inhibitors: 10 µgml⁻¹ each of chymostatin, leupeptin, antipain and pepstatin A) using a blunt-ended plastic scraper. The cell lysates were transferred to 1.5 ml tubes and centrifuged at 12,000 x g for 10 minutes at 4°C to remove debris. Post nuclear supernatants were transferred to fresh tubes and either snap frozen in liquid nitrogen for later use, or mixed with an equal volume of 2X Laemmli buffer [125 mM Tris-HCL (pH 6.8), 2% Sodium dodecyl sulphate (SDS), 2 mM dithiothreitol (DTT), 20% glycerol, and 0.25% bromophenol blue (w/v)] and boiled for 5 minutes prior to SDS-PAGE analysis. The amount of protein present in the lysates after centrifugation was verified by Bradford assay or Coomassie staining described below in Sections 2.9.4 and 2.9.6, respectively.

2.9.4 Bradford assay

A BioRad DC assay kit (Biorad) was used to assess protein content prior to SDS-PAGE. Standard curves were obtained using BSA as a protein standard. BSA solutions were made up from 0.5 mgml^{-1} to 1.5 mgml^{-1} in lysis buffer. Twenty microliters of Reagent S (5% SDS) were added to each ml of Reagent A (alkaline copper tartrate) that was required for the assay. Twenty μl of standards or samples were pipetted into fresh tubes, to which 100 μl of reagent A(S) was added. After vortexing, 800 μl reagent B (Folin reagent) was added and the tubes were vortexed again. After 15 minutes, the samples were transferred to cuvettes and the absorbance was read at 750 nm using a Biophotometer (Eppendorf).

2.9.5 SDS-PAGE

Cells or tissues were lysed in lysis buffer as previously described. Nuclei and cell debris were pelleted by centrifugation at $12,000 \times g$ (Eppendorf) for 10 minutes at 4°C . Post-nuclear cell lysates, murine tissue supernatants or proteins from *E. coli* were taken up with an equal volume of 2X sample buffer (4 ml 10% SDS, 2 ml glycerol, 1.2 ml 1 M Tris, pH 6.8, 2.8 ml distilled H_2O , 0.01% bromophenol blue) and 50 mM DTT as a reducing agent, heated at 95°C for five minutes and analysed by SDS-PAGE. The SDS-PAGE resolving gel consisted of 10% ProSeive[®] 50 acrylamide gel solution (Cambrex Bio Science Wokingham Ltd., Berkshire, UK), 0.375 M Tris pH 8.8, 0.1% SDS, 0.1% APS, 0.04% TEMED. The stacking gel consisted of 5% ProSeive[®], 0.125 M Tris pH 6.8, 0.1% SDS, 0.075% APS and 0.075% TEMED. The proteins were separated on a mini-gel system (Biorad) using Tris-Glycine SDS running buffer (25 mM Tris, 192 mM glycine, 0.1% SDS, pH 8.6, Sigma). The gels were run at a 100 V per gel for ~2 hours, until the dye front reached the bottom of the gel. Page Ruler pre-stained ladder was used as a molecular weight marker (Fermentas).

2.9.6 Coomassie blue staining

To visualise proteins post-SDS-PAGE, colloidal Coomassie staining was used. First, SDS-PAGE gels were fixed in 7% glacial acetic acid in 40% (v/v) methanol for 1 hour. The gels were transferred to colloidal Coomassie solution (Sigma product B2025) activated in 20% methanol and incubated with rocking for 4 hours or overnight. Gels were destained with 10% acetic acid in 25% (v/v) methanol for 60 seconds, rinsed twice with 25% methanol and

destained for up to 24 hours. The destained gels were briefly rinsed with distilled water prior to drying down onto Whatman paper (GE Healthcare) with a gel drier for 40 minutes at 80°C.

2.9.7 Western blotting

Proteins run on SDS-PAGE gels were transferred to PVDF (Millipore) membranes for 2 hrs using a wet mini-blotting apparatus and powerpack (Biorad PowerPac 300) set at 240 mA. The PVDF membranes were preprimed for 20 seconds in methanol and rinsed in transfer buffer (190 mM glycine, 25 mM Tris in 20% methanol). PVDF membranes were subsequently washed once in Tris buffered saline (25 mM Tris, 137 mM NaCl, 2.7 mM KCl, pH 8.0) with 0.1% Tween®20 and blocked in 4% milk/TBST overnight at 4°C with constant agitation. After blocking, PVDF membranes were washed once in TBST.

Detection of proteins was accomplished using a series of antibodies (Table 2.6). Membranes were incubated with primary antibodies diluted to their optimum working concentrations in a 50 ml tube containing 3 ml 1% milk/TBST for 1 hour at RT on a roller. After washing a five times with TBST, membranes were incubated with corresponding secondary antibodies GAMPO (Goat anti-mouse peroxidase) or SARPO (swine anti-rabbit peroxidase) from DAKO at 1:3000 in 1% milk/TBST for 1 hour. Thereafter, PVDF membranes were washed five times in TBST and visualised by ECL Plus (GE Healthcare). Solutions A and B from the ECL plus kit were mixed in a ratio of 40:1, with 500 µl solution being applied per membrane. After brief incubation under saranwrap (Dow) the membranes were drained of excess fluid, sandwiched in fresh saranwrap. Immunoreactivity was measured by recovering the signal of chemiluminescence on Biomax Light film (Kodak). Multiple exposures were made in the range of 20 seconds to 15 minutes and the films were developed using a compact X4 Automatic X-ray Film Processor (Xograph Imaging Systems Ltd, Gloucestershire, UK).

2.9.8 Peptide inhibition assay

To test antibody specificity of the Dann antibodies raised against plastin, the following assay was used. Recombinant proteins were resolved on 10% SDS-PAGE gels as described above in Section 2.9.5. The separated proteins were transferred electrophoretically onto PVDF membranes and subjected to western blotting, as described in Section 2.9.7. After transfer and blocking with 4% milk/TBST, the membranes were incubated with antibody alone

(positive control), or antibody pre-blocked with peptide, for 30 minutes at RT with constant agitation. Since the plastin antibodies were used at an optimal dilution of $\sim 1 \text{ ug ul}^{-1}$, the peptides were used at a concentration of $\sim 3 \text{ } \mu\text{g ml}^{-1}$ (2x) and $30 \text{ } \mu\text{g ul}^{-1}$ (10x). Non-specific peptides were used as a control. The peptides used in the assay were the same as those used for immunisation to generate the Dann1, Dann 2 and Dann 3 antibodies (Chapter 4). After incubating the PVDF membranes with antibody or with antibody blocked with peptide for 1 hour, the membranes were probed with swine anti-rabbit peroxidase (SARPO; DAKO) and developed by ECL Plus as described in Section 2.9.7.

Table 2.6: Primary antibodies for Western blotting

Antibody	Target	Antibody type	Dilution	Source
AC-40	β -actin	Mouse monoclonal	1:2000	Sigma
Jol 2	Lamin A/C	Mouse monoclonal	1:200	Dyer et al., 1997
HECD-1	E-cadherin	Mouse monoclonal	1:500	Abcam [®]
ab54532	Cofilin	Mouse monoclonal	1:200	Abcam [®]
sc-8979	PAI-1	Rabbit polyclonal	1:200	Santa Cruz
sc-03	EGFR	Rabbit polyclonal	1:200	Santa Cruz
L40C6	SNAI2	Mouse monoclonal	1:1000	Cell signalling
HC10	MHC class 1	Mouse monoclonal	1:100	Kind gift from Dr Adam Benham
ab45769	T-plastin	Rabbit polyclonal	1:1000	Abcam [®]
LPL4A.1	L-plastin	Mouse monoclonal	1:500	Abcam [®]
Dann1a	Plastin	Rabbit polyclonal	*	Cambridge Research Biochemicals
Dann1b	Plastin	Rabbit polyclonal	*	Cambridge Research Biochemicals
Dann2a	Plastin	Rabbit polyclonal	*	Cambridge Research Biochemicals
Dann2b	Plastin	Rabbit polyclonal	*	Cambridge Research Biochemicals
Dann3a	Plastin	Rabbit polyclonal	*	Cambridge Research Biochemicals
Dann3b	Plastin	Rabbit polyclonal	*	Cambridge Research Biochemicals

*assay dependent (see Chapter 4).

2.10 Bioinformatics

2.10.1 DNA microarray dataset

A genome-wide DNA microarray was previously carried out on SW480/cntl and SW480/lamA cell lines using the Human Genome U133 Plus high-density oligonucleotide Affymetrix GeneChip[®] array technology (Affymetrix, Santa Clara, CA, UDS) by Dr N Willis and Dr Thomas Cox, Durham University. The Affymetrix guidelines for the HG-U133 Plus 2.0 GeneChip were

consulted to help filter and normalise the data, using the Affymetrix GeneChip Operation Software (GCOS). The microarray dataset analysis was briefly carried out in collaboration with Dr Dan Swan, Newcastle University and Dr Clare Foster, Durham University. Each gene on the microarray is represented by a probe set composed of eleven probe pairs, which provides for separate measurements of each transcript. These sequences are 25 bases long and cover ~600 bases of target sequence. The probe pairs include Perfect Match (PM) and Mismatch (MM) oligonucleotides, which differ in the central base pair only. The MM probes control for non-specific hybridisation. Constitutively expressed human genes are present on the microarray, as normalisation controls.

The data arising from the microarray analysis was obtained as Cell Intensity files. These files contained the results of the microarray experiment as intensity calculations of the pixel values. The data were interrogated with GeneSpring GX10 (Agilent) and processed with the MAS5 algorithm to give the following values: Present (if the transcript was detected), Marginal (if the transcript was barely detectable) and Absent (if the transcript was undetected). Probes with one or more Present or Marginal values were analysed further after renormalisation using GCRMA (Guanine Cytosine Robust Multi-Array Analysis). This produced an intensity value for each set of probes. Genes were considered differentially expressed if there was a 2-fold or greater change in value between probesets when comparing the two cell lines.

2.10.2 Ingenuity Pathway Analysis

In order to extract the most relevant biological information, computational analysis of probesets showing greater than a 2.5-fold differential expression was performed by Ingenuity Pathway Analysis (IPA®). IPA is a web-based application which makes use of a database of biological interactions derived from an extensive network of modelled relationships between proteins, genes and metabolites as well as complexes, cells, tissues and diseases. The dataset was uploaded into IPA® and analysis was performed using standard settings to examine significance against biological functions, disease and canonical pathways (using Fischer Exact tests, and a p -value of <0.05). Eligible molecules or genes were algorithmically clustered into networks based on literature-curated interactions (Chapter 6).

Chapter 3: *PLS3* promoter methylation in colorectal cancer

3.1 Introduction

Despite therapeutic innovations and increasing education on diet and lifestyle, CRC remains one of the most prevalent malignancies in the Western world (Jemal et al., 2010; Smits et al., 2008). Prognosis of newly diagnosed cases principally relies on the Duke's classification system, yet the 5-year survival rate of patients with CRC varies from 90% to 10% with tumour progression. Much effort has been made to identify molecular biomarkers that can predict patient prognosis and/or response to therapy (McLeod (Anwar et al., 2004; McLeod and Church, 2003; Zlobec and Lugli, 2008). Although many publications have claimed that various biomarkers offer prognostic or predictive value, the results are often inconclusive due to publication bias against negative results, false-positives and inappropriate study design owing to a lack of large sample sizes (Soreide et al., 2008; Newton et al., 2010; Lee and Chan, 2011). Discovering sensitive and specific biomarkers that enable the stratification of patients into appropriate screening or surveillance programmes will improve the detection, treatment and prognosis of CRC (Zlobec and Lugli, 2008). It is now well established that CRC is a heterogeneous disease, and can arise via at least three distinct pathways, CIN, MSI and CIMP (Draht et al., 2012). Whilst epigenetic alterations have received less attention than their classical genetic counterparts, they are perhaps more interesting as they can potentially be reversed by therapeutic intervention (Smits et al., 2008). This, coupled with improved high-throughput technologies for the detection of methylation in cancer cells, offers great potential for use in the clinic (van Engeland et al., 2010).

DNA methylation is the most studied epigenetic alteration in CRC. It refers to the post-replicative addition of a methyl group to the carbon 5'-position of cytosine, resulting in 5-methylcytosine. DNA methylation is catalysed by DNMTs, which recognises CG dinucleotide sequences. CpG dinucleotides are not uniformly distributed throughout the genome, but instead are concentrated in CpG dinucleotide dense regions called CpG islands (Bird 1986). CpG islands are generally defined as 0.5 Kb – 2Kb sequences with a G:C content of >55%, located at the 5' region in approximately half of all genes. In cancer, many of these CpG

islands become aberrantly methylated which results in transcriptional silencing. This is recognized as an important mechanism for the inactivation of tumour suppressor genes (Momparker, 2003). In contrast to normal tissues, cancer DNA is both globally hypomethylated at CpG dinucleotides in repetitive sequences (e.g. satellite repeats, endogenous retroviral elements) and is locally hypermethylated at discrete CpG sites that normally exist in the unmethylated state (Baylin et al., 1998). The recognition that a clinically distinct subset of tumours have a high degree of DNA methylation has led to the concept of CIMP (Issa, 2004). Tumours characterised by CIMP are thought to arise by the serrated adenoma pathway and have a different histology than tumours of the adenoma-carcinoma pathway (Hughes, 2012).

Previous studies in our laboratory have revealed that lamin A/C is a prognostic biomarker of CRC (Willis et al., 2008). Subsequent downstream investigations revealed that over-expression of lamin A in the SW480 CRC cell line caused the cells to adopt a significantly more motile phenotype. In addition, T-plastin (encoded by the *PLS3* gene) was upregulated in SW480/lamA compared with SW480/cntl cells, thus identifying *PLS3* as a candidate gene for further exploration. T-plastin belongs to a family of actin binding proteins and is normally expressed in epithelial and mesenchymal cells but not in the colon; I-plastin is detected in the small intestine and colon but L-plastin is chiefly found in hematopoietic cells (Delanote et al. 2005). T-plastin has been implicated in a number of malignancies, and its expression is raised in cisplatin-resistant human bladder, prostatic, head and neck cancers (Hisano et al., 1996). T-plastin is differentially expressed in some liver cancer cell lines, and cells with low levels of T-plastin become susceptible to DNA damage (Sasaki, et al. 2002; Ikeda et al, 2005). It has been suggested that down-regulation of T-plastin assists cancer development by encouraging entry into mitosis, but a mechanism to explain this theory has not been established.

The *PLS3* gene (which encodes T-plastin) is located on chromosome Xq23, spans 60 kilobases and contains 16 exons. The *PLS3* promoter contains one CpG island (Lin et al., 1999). It has previously been shown that *PLS3* gene expression was suppressed in a human CRC cell line because of promoter-specific DNA methylation (Sasaki *et al.* 2002). To our knowledge, *PLS3* promoter methylation has never before been studied in primary human colorectal tumours. The aim of this chapter was to investigate *PLS3* promoter methylation in both CRC cell lines

and primary human CRCs using the NLCS tissue archive and to test the hypothesis that aberrant methylation of the *PLS3* promoter leads to dysregulation of T-plastin gene expression (Figure 3.1). Given the importance of lamin A/C and T-plastin in CRC, we explored the potential of *PLS3* methylation as a risk biomarker to be used in combination with lamin A/C.

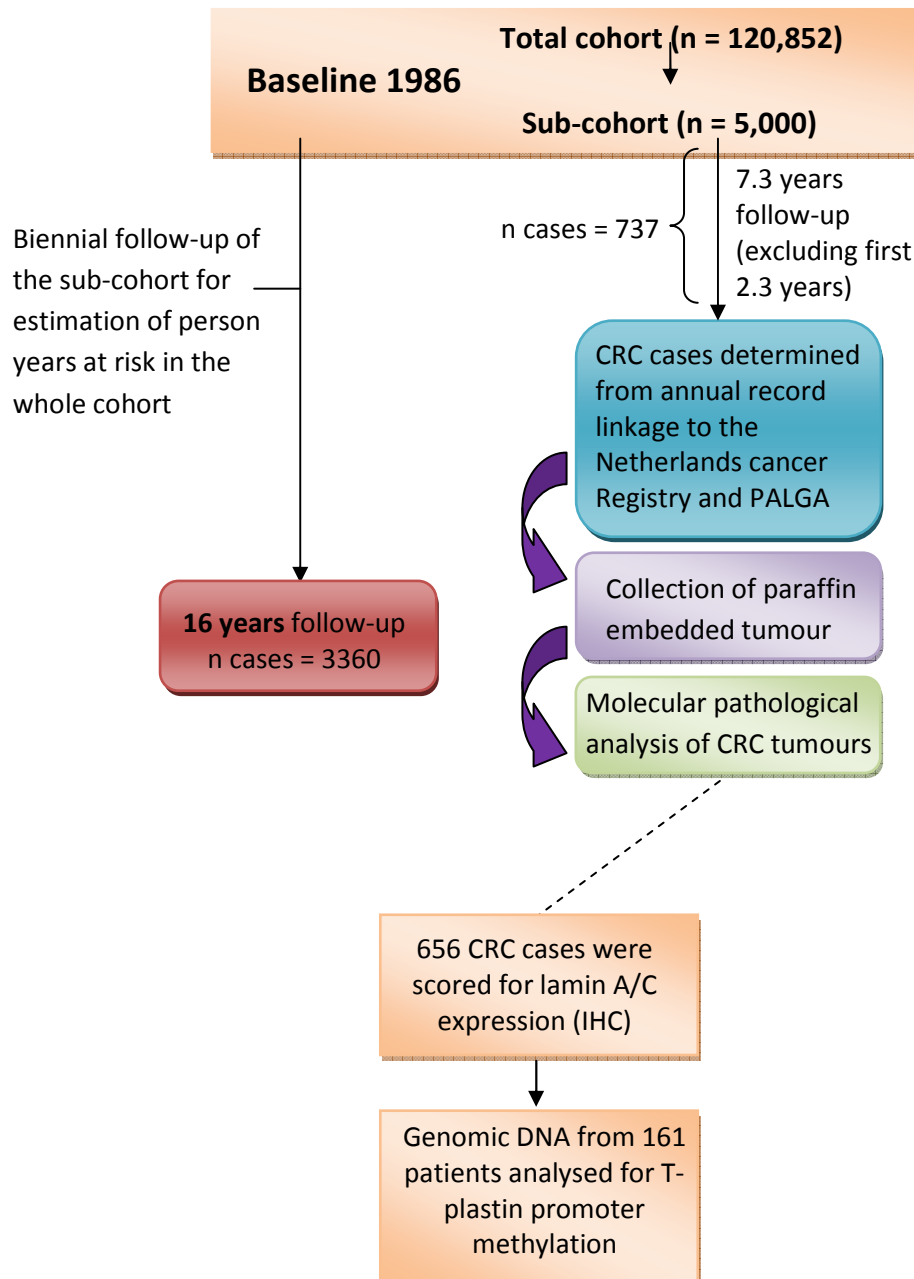


Figure 3.1: Study design of the Netherlands Cohort Study on Diet and Cancer (NLCS) (adapted from Hughes, 2011).

3.2 Results

3.2.1 *PLS3* promoter methylation and mRNA expression in CRC cell lines

The promoter region of the *PLS3* gene (National Centre for Biotechnology Information [NCBI] accession number NM_005032.3) contains a 431 bp CpG island located in the promoter from nucleotides -70 to +361 relative to the transcription start site (TSS) (Figure 3.2). Primer sets 1 and 2 were designed in a region within the promoter and tested by nested methylation-specific PCR (N-MSP) on sodium-bisulphite treated genomic DNA. These primers were tested by a Masters student in Maastricht. It was concluded that primer pairs 1 and 2 were not suitable for further use as they were unable to amplify and discriminate between methylated and unmethylated DNA (data not shown). Consequently, we designed and optimised primer set 3b (Supplementary Figures S3-S5). This primer pair was determined to be optimal with 35 cycles of amplification and an annealing temperature of 66°C (data not shown).

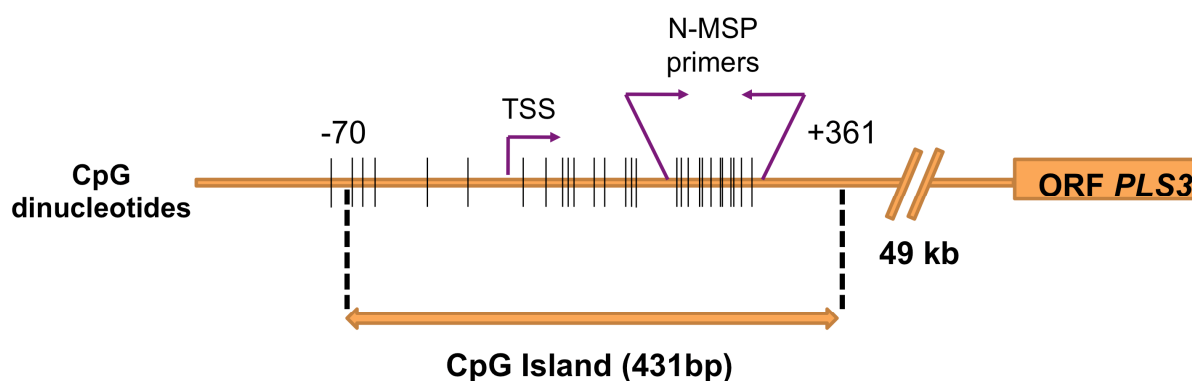


Figure 3.2: *PLS3* promoter structure and N-MSP primer location

Schematic representation of the *PLS3* (T-plastin) promoter. A CpG island is located between nucleotides -70 to +361 relative to the transcription start site (TSS). Vertical lines represent the approximate locations of the CpG dinucleotides, the orange rectangle represents the open reading frame (ORF) of *PLS3*, and paired arrows indicate the location of the amplicons identified by N-MSP.

To assay this region for potential methylation, we examined six CRC cell lines by N-MSP using primers located from nucleotides +239 to +351 relative to the transcription start site (TSS). A representative panel of CRC cell lines were chosen for analysis: the male cells lines SW480, SW620 and CaCo-2 and the female cell lines LS, HT29 and SW498 (Chapter 2, Table 2.1). The PCR products were analysed on a 2% agarose gel. The *PLS3* promoter was found to be methylated in SW948 and HT29 CRC cell lines. All the other cell lines (SW620, SW480, LS, CaCo-2) were unmethylated (Figure 3.3). In order to validate this finding and investigate the pattern of CpG methylation within the *PLS3* promoter, we designed sequencing primers to detect sodium bisulphite-modified genomic DNA isolated from SW620 (*PLS3* promoter methylation negative) and SW948 (*PLS3* promoter methylation positive) (Supplementary Figure S6). This assay allows the analysis of the *PLS3* promoter methylation at single molecule resolution. The promoter region spanning 26 CpG sites (+47 to +355 relative to the TSS) was amplified by PCR using sodium bisulphite-modified genomic DNA as a template (Figure 3.4). PCR products were ligated into the pCR[®]2.1 cloning vector using a TOPO TA[®] cloning kit and transformed into *E. coli* (Chapter 2, Section 2.5.2-2.5.3). Colony PCR was performed to check the integrity of the recombinants (Supplementary Figure S7). Plasmid DNA minipreps were prepared from six independent bacterial clones harbouring the inserts. The clones were sequenced to determine the sites that had been methylated using an automated DNA sequencer (Supplementary Figures S8-S10). Bisulphite sequencing confirmed the N-MSP PCR data in that SW948 cells showed almost complete methylation. For example, one clone had 26/26 sites methylated whereas SW620 cells showed no methylated CpGs (Figure 3.5). It should be noted that some CpG islands in the *PLS3* promoter from SW948 cells were always methylated (e.g. sites at 71, 99, and 102 bp) whereas other sites were variably methylated. Next, we sought to examine the relationship between aberrant promoter methylation and gene expression. Cells lines that were methylated (SW948 and HT29) (Figure 3.3) were subjected to epigenetic drug treatment. CRC cell lines HT29 and SW948 were incubated with and without the DNA methylation inhibitor 5-aza-2'-deoxycytidine (DAC). DAC is an analogue of cytosine, that when incorporated into DNA, irreversibly binds to DNA methyltransferase. This prevents the enzyme from functioning, resulting in passive de-methylation and gene restoration (Santi et al., 1983). In both cell lines, endogenous T-plastin mRNA was significantly higher in DAC treated cells than in untreated cells, as determined by quantitative real-time PCR (qPCR). For example, in the SW948 cells, 0.5 μ M treatment of DAC led to approximately 4-fold increase

($p = 0.05$) and 2 μM led to 8-fold increase ($p = 0.01$). Similar results were obtained for the HT29 cell line, showing a 3-fold and 4-fold increase in T-plastin mRNA expression after 0.5 μM and 2 μM DAC treatment, respectively ($p = 0.02$ and 0.001) (Figure 3.6).

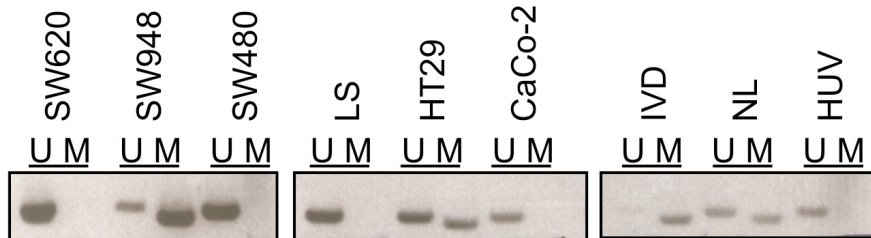


Figure 3.3: *PLS3* promoter methylation in CRC cell lines

Electrophoretic analysis of N-MSP amplification products in six CRC cell lines: SW620, SW948, SW480, LS, HT29, and CaCo-2. IVD (*in vitro* methylated) and NL (normal lymphocytes) are methylated controls and HUVEC (human umbilical vein endothelial cells) is an unmethylated control. U = unmethylated, M = methylated. Data shows that the *PLS3* promoter is methylated in SW948 and HT29 CRC cell lines.

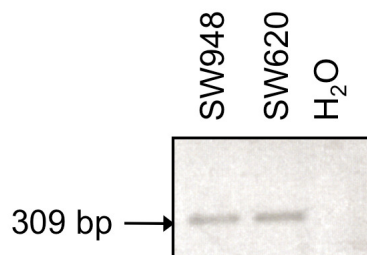


Figure 3.4: Amplification of bisulphite-modified DNA from CRC cell lines

Electrophoretic analysis of bisulphite-modified DNA containing the *PLS3* promoter from SW948 and SW620 cell lines. Negative H₂O control indicates no contamination in the samples. The 309 bp PCR products were ligated into the pCR[®]2.1 cloning vector using a TOPO TA[®] Cloning Kit for subsequent transformation into *E. coli* and bisulphite sequencing analysis.

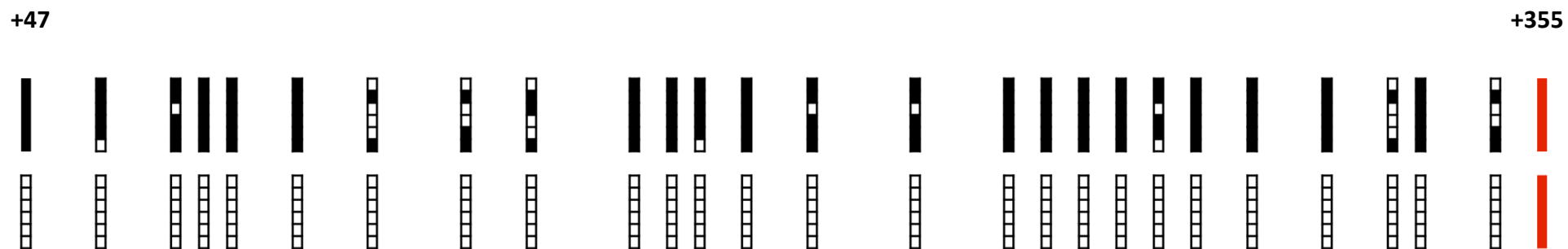


Figure 3.5: Bisulphite sequencing of SW948 and SW620 CRC cell lines

Schematic representation of bisulphite sequencing in SW948 (upper panel) and SW620 cell lines (lower panel). Six different bacterial clones per tissue sample were sequenced. Each row represents an individual cloned allele that was sequenced following sodium bisulphite DNA modification. Each box indicates a CpG dinucleotide (black box = methylated CpG site, white box = unmethylated CpG site). Data shows that the *PLS3* promoter in the SW948 cell line is predominantly methylated, whereas the *PLS3* promoter in the SW620 cell line is exclusively unmethylated. Red boxes indicate the end of the amplicons.

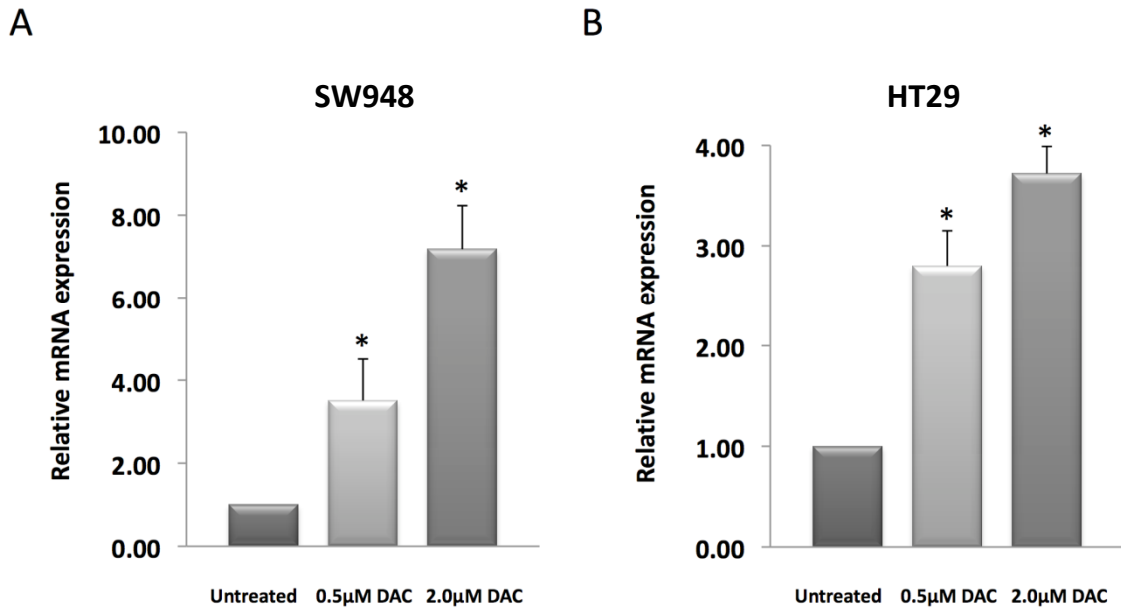


Figure 3.6: T-plastin mRNA expression is restored after treatment with 5-aza-2'-doxycytidine

T-plastin mRNA expression in SW948 and HT29 CRC cells with and without treatment with the DNA methylation inhibitor 5-aza-2'-doxycytidine (DAC). Quantification is presented as mean values relative to untreated cells from three independent experiments (normalisation was against GAPDH). Statistical analysis was performed using the student t-test (two-sided). Error bars correspond to the standard error of biological replicates. * = statistical significance. Data shows that in the SW948 and HT29 cell lines, T-plastin was increased approximately 3-4 fold with 0.5 μM of DAC compared to controls cells (SW498; 0.5 μM $p = 0.05$, 2 μM $p = 0.01$. HT29; 0.5 μM $p = 0.02$, 2 μM $p = 0.001$).

3.2.2 *PLS3* promoter methylation in normal colonic mucosa and primary colorectal carcinomas

After establishing that the *PLS3* promoter was methylated in CRC cell lines SW948 and HT29, *PLS3* promoter methylation status was investigated in non-cancerous colonic mucosa and in a subset of genomic DNA samples extracted from the NLCS tissue archive. We performed N-MSP using the same primer pair used to assess the methylation status in CRC cell lines (Figure 3.2). This was done firstly on non-cancerous (normal) colonic mucosa. As methylated controls, *in vitro* methylated DNA and DNA from normal lymphocytes was used. DNA from human umbilical cord was used as a negative control (as in Figure 3.3). The frequency of promoter methylation in normal mucosa was 13/20 (65%) (Figure 3.7). Next, the prevalence of *PLS3* promoter methylation was examined in bisulphite-treated genomic DNA from 161 primary tumours (a subset from the CREAM archive, Figure 3.1). A selection of the results from this analysis is shown in Figure 3.8 and the entire data set is shown in Table 3.1. The frequency of methylation in this cohort was approximately 50%.

As with the cell lines, we wanted to validate the N-MSP data by bisulphite sequencing and provide a high-resolution map of the methylated sites within the *PLS3* promoter in both normal and tumour tissue. The bisulphite sequencing primers that were shown to work previously (see Figure 3.4 and 3.5) were used to amplify a 309 bp product within the CpG island located in the *PLS3* gene promoter. Initially, we tried to amplify a 309 bp region from the patients DNA (previously isolated from 'fixed' paraffin-embedded, formalin-fixed tissue). However, it was not possible to detect any amplification products from either methylated or unmethylated examples with the sequencing primers, due to poor quality, fragmented DNA (Figure 3.9 lanes 5-8). In contrast, DNA could be amplified from frozen material (Figure 3.9, lanes 1-4) and from the cell lines that were analysed previously (Figure 3.9), confirming that the PCR itself worked. As it was not possible to obtain DNA from any fixed samples, it was decided to investigate and compare the pattern of methylation between frozen tumour material and the corresponding normal colonic mucosa. To do this, an additional subset of CRC and matching normal colon tissue (unfixed, frozen material) was screened for their methylation status (Figure 3.10). Five of the eight patients were methylated at the *PLS3* promoter in both normal and tumour tissues. However, three of the eight patients showed methylation differences. Patient 1 lacked any methylation of both tumour and normal tissue

whereas patients 4 and 7 were methylated in normal colonic tissue and were unmethylated in the tumour tissue. These were taken for further analysis. The relative T-plastin mRNA expression of these three patients was measured by qPCR (Figure 3.11). Data shows that there was no difference between T-plastin mRNA expression between normal and tumour tissue in Patient 1 (Figure 3.11 A). In contrast, the relative expression of T-plastin was significantly higher in tumour tissue from patients 4 and 7, compared to their corresponding normal colonic mucosa ($p = 0.03$ and 0.04 , respectively). These results are consistent with the methylation data shown in Figure 3.10 and suggest that the *PLS3* promoter is demethylated in CRC, which results in aberrant expression of T-plastin.

The PCR products of normal and tumour DNA from patients 1, 4 and 7 were subjected to bisulphite sequence analysis, using the same primer set as previously described. The promoter region spanning 26 CpG sites (+47 to +355 relative to the TSS) was amplified by PCR using sodium bisulphite-modified genomic DNA as a template (Figure 3.12). PCR products were ligated into a TOPO-TA cloning vector, and transformed into *E. coli*. Colony PCR was performed to check the validity of the recombinants (Supplementary Figure S11). Plasmid DNA minipreps were prepared from six independent bacterial clones harbouring the correct inserts. These clones were subsequently sequenced using an automated DNA sequencer (Supplementary Figures S12-S13). Data showed that there was no methylation in the *PLS3* promoter region in any of the clones analysed (Figure 3.13). This was unexpected and does not confirm the N-MSP data. This may be due to the fact that bisulphite sequencing is not sensitive enough to detect low levels of methylation from formalin-fixed DNA samples.

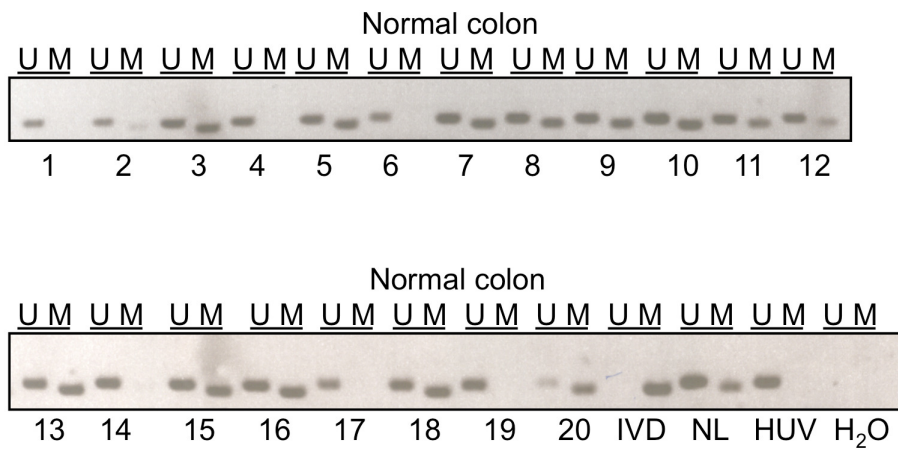


Figure 3.7: *PLS3* promoter methylation in normal colonic mucosa

Electrophoretic analysis of MSP amplification products of normal colonic mucosa from 20 patient samples. IVD (*in vitro* methylated DNA) and NL (normal lymphocytes) are methylated controls and HUVEC (human umbilical vein endothelial cells) are an unmethylated control. U = unmethylated, M = methylated. Data shows that the prevalence of methylation in normal colonic mucosa was 65%.

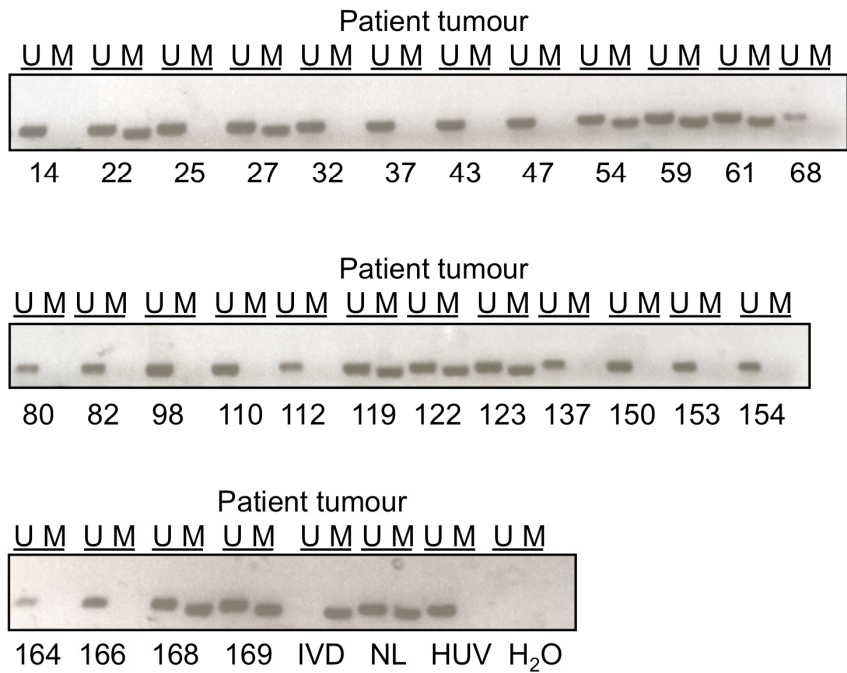


Figure 3.8: *PLS3* promoter methylation in primary colorectal tumours

Electrophoretic analysis of MSP amplification products in 28 patient tumour samples. Numbers refer to the patient sample identity. IVD (*in vitro* methylated DNA) and NL (normal lymphocytes) are methylated controls and HUVEC (human umbilical vein endothelial cells) is an unmethylated control. U = unmethylated, M = methylated. Data shows that the prevalence of *PLS3* methylation is approximately 50%.

Table 3.1: Prevalence of *PLS3* promoter methylation in 161 CRC patient samples

3	U	98	U	232	U	312	I	382	U	544	M	643	M	765	U
4	M	110	U	234	M	315	U	384	I	546	I	645	M	768	U
6	M	112	U	237	U	318	M	390	U	548	U	650	M	774	U
7	U	119	M	238	M	319	I	395	U	558	M	652	M	778	M
8	U	122	M	239	M	321	M	405	U	560	I	657	U	784	U
11	M	123	M	241	M	334	U	406	M	563	M	660	U	785	U
12	M	137	U	242	M	336	U	408	U	564	U	665	M	790	M
13	U	150	U	243	M	338	I	411	U	566	I	666	M	791	U
14	U	153	U	251	M	340	I	418	U	567	U	675	U	802	U
17	I	154	U	256	I	342	U	432	I	571	U	681	M		
22	M	164	U	257	M	344	M	435	U	574	U	689	M		
23	I	166	U	260	M	345	M	446	U	576	I	693	U		
25	U	168	M	263	M	348	U	448	M	579	I	696	U		
27	M	169	M	273	U	350	U	450	M	581	M	697	U		
32	U	173	I	275	U	353	U	458	M	587	U	699	M		
37	U	174	M	277	U	359	U	459	M	590	U	700	M		
43	U	184	M	279	M	360	M	462	M	594	U	712	U		
47	U	185	M	280	M	364	M	473	U	598	I	717	U		
54	M	187	M	281	U	368	I	488	M	600	U	719	M		
59	M	194	U	286	M	371	M	491	U	602	M	731	U		
61	M	196	U	287	M	374	M	503	I	606	U	738	U		
68	U	198	I	298	U	375	M	505	M	618	M	739	U		
80	U	213	M	308	M	376	M	509	U	623	M	744	U		
82	U	221	M	309	M	379	U	532	I	626	M	748	I		
84	I	230	M	310	U	380	I	540	M	642	M	754	M		

I = Insufficient DNA

n = 161

Methylated (M) =
78 (48%)

Unmethylated (U)
= 83 (52%)

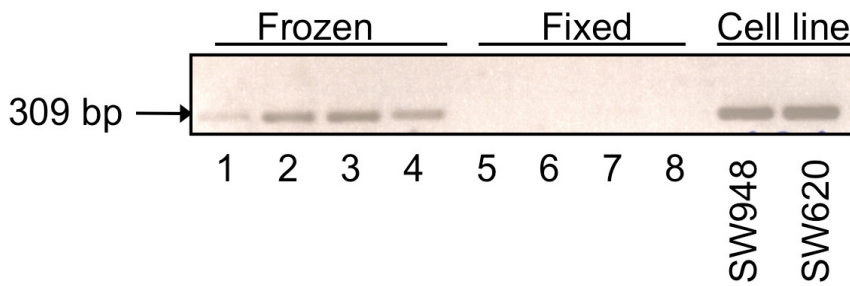


Figure 3.9: Amplification of bisulphite-modified DNA from human CRC tissue and cell lines

Electrophoretic analysis of bisulphite-modified DNA containing the *PLS3* promoter from sequencing amplification products from frozen tissue (lanes 1-4), formalin-fixed tissue (lanes 5-8) and CRC cell lines (SW948 and SW620). No PCR products were obtained for fixed tumour material (paraffin-embedded), compared with unfixed (frozen) material and CRC cell lines.

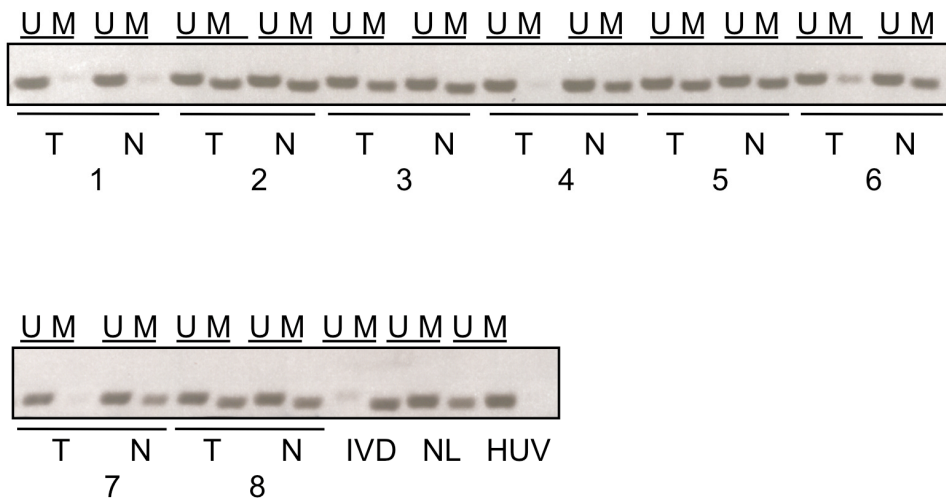


Figure 3.10: *PLS3* promoter methylation in colorectal carcinomas and corresponding normal colonic mucosa from a small independent subset

Electrophoretic analysis of N-MSP amplification products from carcinomas and adjacent normal colon from eight colorectal cancer patients. All material is from fixed samples. IVD (*in vitro* methylated DNA) and NL (normal lymphocytes) are methylated controls and HUVEC (human umbilical vein endothelial cells) is an unmethylated control. U = unmethylated, M = methylated. T = tumour, N = normal. Data shows that five of the eight patients were methylated at the *PLS3* promoter in both normal and tumour tissue. Three patients exhibited differences in their methylation pattern.

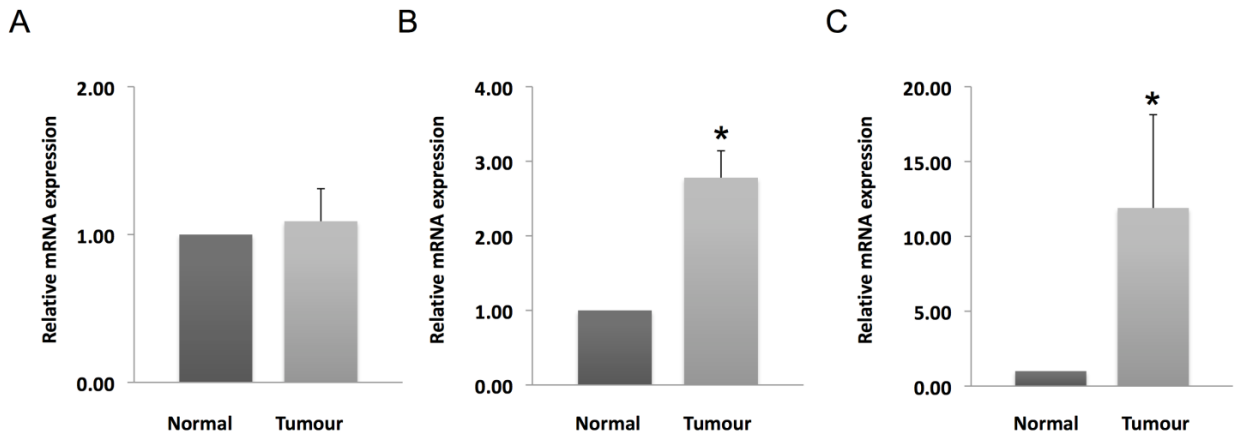


Figure 3.11: T-plastin mRNA expression in colorectal carcinomas and corresponding normal colonic mucosa from three patients

T-plastin mRNA expression measured by qPCR in human tumour versus normal tissue from (A) patient 1 (B) patient 4 and (C) patient 7 (from Figure 3.10). For each patient, the level of T-plastin expression in normal mucosa tissue was set to 1. Data are presented as mean values relative to normal mucosa from 3 independent experiments. Normalisation was against GAPDH. Error bars correspond to standard error of technical replicates. Statistical analysis was done using the student t-test (2-sided). * = statistical significance. Data shows that relative T-plastin expression is elevated in tumour samples from patients 4 and 7 compared to their corresponding normal mucosa. Patient 1: $p = 0.69$; Patient 4: $p = 0.03$, Patient 7: $p = 0.04$.

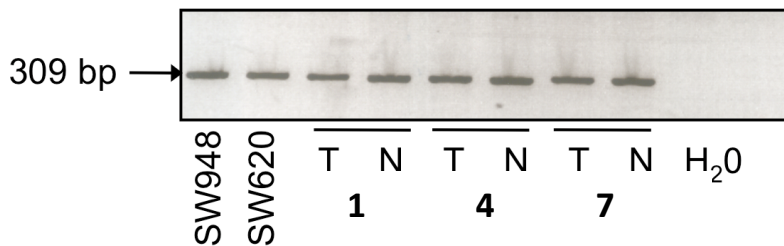


Figure 3.12: Amplification of bisulphite-modified DNA from frozen normal and tumour tissue and CRC cell lines

Electrophoretic analysis of bisulphite sequencing amplification products. CVRC cell lines (SW948 and SW620) and tumour versus normal tissue from patients 1, 4 and 7 (Figure 3.11) was analysed. PCR products were obtained from all samples. Negative H₂O control indicates no contamination in the samples. The 309 bp PCR products were ligated into the pCR[®]2.1 cloning vector using a TOPO TA[®] Cloning Kit for subsequent transformation into *E.coli* and bisulphite sequencing analysis.

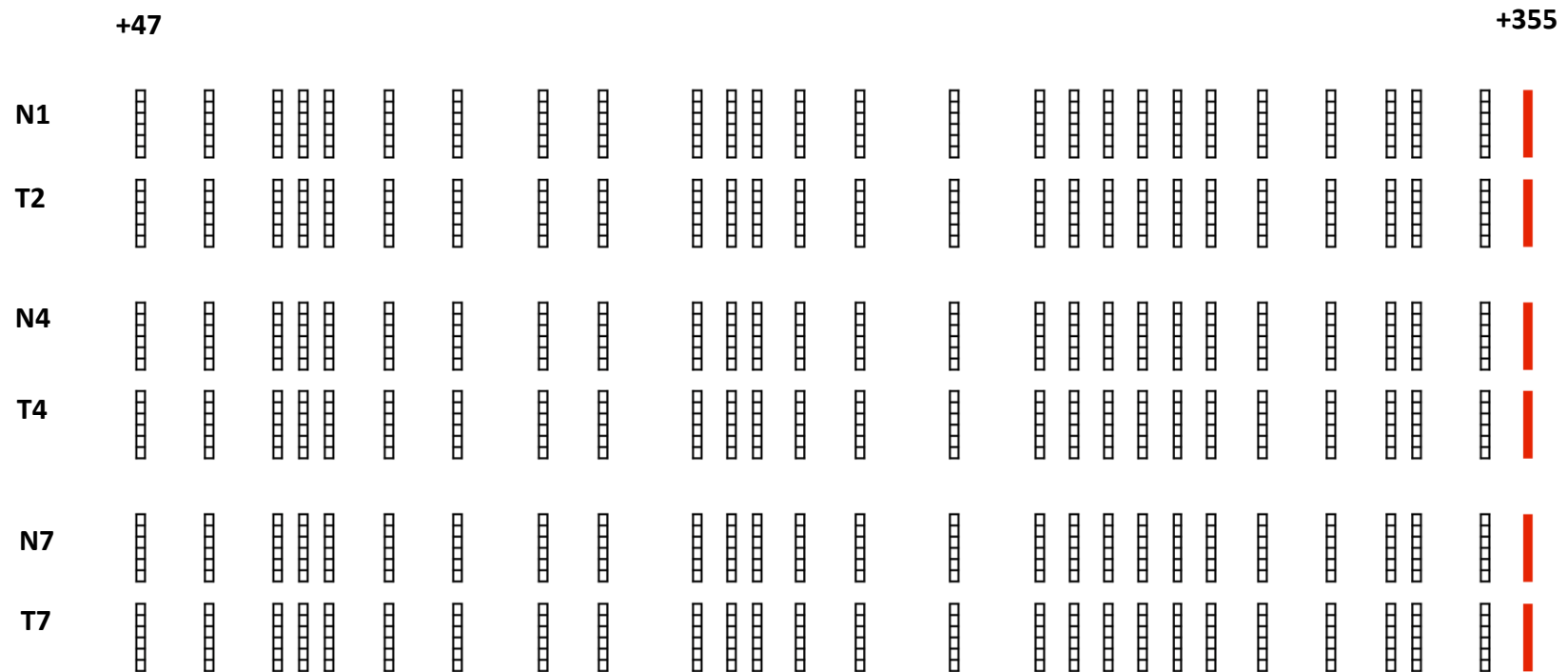


Figure 3.13: Bisulphite sequencing of normal colon versus tumour tissue from three CRC patients

Bisulphite sequencing of tumour (T1, T4 and T7) and the matched normal colonic mucosa (N1, N4 and N7) from three CRC patients. Six different bacterial clones per tissue sample were sequenced. Each row represents an individual cloned allele that was sequenced following sodium bisulphite DNA modification. Each box indicates a CpG dinucleotide (black box = methylated CpG site, white box = unmethylated CpG site). No methylated residues were found in any of the replicates. Red boxes indicate the end of the amplicon.

3.2.3 Patient analysis

The 161 patients from the N-MSP analysis included in this study developed cancer between 1989 and 1994. Information on mortality from 1st January 1989 until 1996 (7 years) was retrieved through linkage with the Central Bureau for Statistics. CRC related death was concluded if CRC was determined to be either the primary cause of death or as a primary, secondary or tertiary complication, using the ICD system. Differences in patient, tumour and follow-up characteristics were analysed using the Chi-square (χ^2) test. Kaplan-Meier analysis was selected to investigate survival. This is a more comprehensive statistical approach compared with Chi-square (χ^2) cross-tabulation. This is due to the fact that Kaplan-Meier analysis takes into account censored data, that is otherwise lost from the sample before the final outcome is observed (e.g. if a patient dies before the end of the follow-up, but not as a result of CRC). Hazard ratios (HR) (an estimate of the relative effect of a variable [e.g. *PLS3* methylation status] on an event [e.g. CRC mortality]) and corresponding 95% confidence intervals (CI) for CRC-related mortality according to *PLS3* status were estimated using Cox regression analysis. All analysis was performed using SPSS. This work was carried out in collaboration with senior epidemiologist, Dr Kim Smits, University Hospital Maastricht.

3.2.3.1 *PLS3* methylation versus tumour progression and location

Initial baseline analysis was performed on all patient and tumour characteristics in relation to CRC-related mortality (outlined in Table 3.2). The study population characteristics appeared to be normal with 53% (n = 84) of patients being male and 47% (n=77) of patients being female. Interestingly, there was a statistically significant difference between *PLS3* promoter methylation status and sex (Figure 3.14 A; Table 3.2). Male patients were predominantly unmethylated for *PLS3*; 72/84 (86%) and female patients were predominantly methylated for *PLS3*; 66/77 (85%) ($p = <0.0001$). There was no difference in age at diagnosis and CRC-related mortality ($p = 0.566$). Similarly, there was no statistically significant difference between CRC-related death and methylation status ($p = 0.512$).

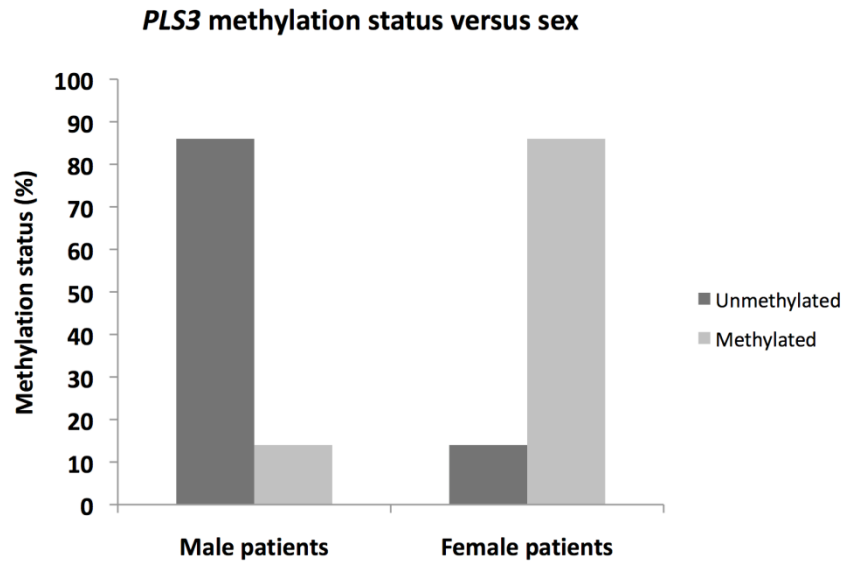
Classification using Dukes' staging system were as follows: Dukes' A, 49% methylation (n = 17), Dukes' B, 42% methylation (n = 22), Dukes' C, 52% methylation (n = 27) and Dukes' D, 60% methylation (n = 9) of the *PLS3* promoter. There was no association between *PLS3* promoter methylation *PLS3* expression status and Dukes stage ($p = 0.557$) (Figure 3.14 B).

However, there does appear to be a striking difference between *PLS3* promoter methylation status and tumour location ($p = 0.044$). Methylation of the *PLS3* promoter is highest in the proximal (right-sided) colon with a prevalence of 58% and decreases to 28% in the rectum (left-sided). Conversely, the *PLS3* promoter is unmethylated with a prevalence of 42% in the proximal (right-sided) colon which increases to 72% in the rectum (Figure 3.15).

Table 3.2: *PLS3* promoter methylation in relation to clinicopathological characteristics

	<i>PLS3</i> (U)	<i>PLS3</i> (M)	<i>p</i> -value
CRC related death, No	50	43	
CRC related death, Yes	33	35	0.512
Lamin A/C expression	43	43	
Lamin A/C lack of expression	34	24	0.309
Age at diagnosis, mean (SD)	68.1 (4.3)	67.8 (4.3)	0.566
Proximal	24	32	
Distal	23	28	
Rectosigmoid	12	9	
Rectum	23	9	0.044
Dukes' A, N	18	17	
Dukes' B, N	31	22	
Dukes' C, N	25	27	
Dukes' D, N	6	9	0.557
Male patients, N	72	12	
Female patients, N	11	66	<0.0001

A



B

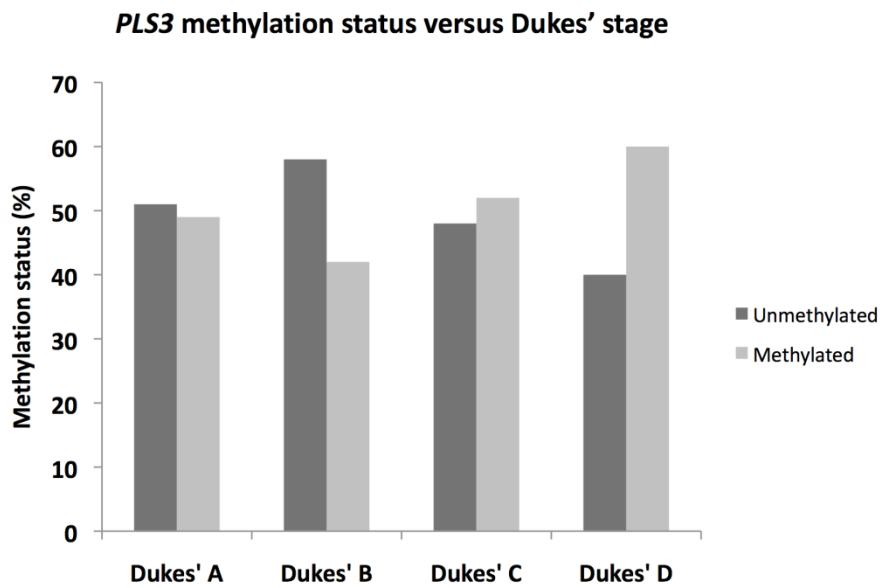


Figure 3.14: *PLS3* promoter methylation in relation to sex and Dukes' stage

(A) Histogram of *PLS3* promoter methylation by sex assessed using 161 patient tumour samples. There is a statistically significant difference between *PLS3* promoter methylation and sex ($p = <0.0001$). (B) Histogram of *PLS3* promoter methylation by Dukes' stage. There is no association between the prevalence *PLS3* promoter methylation and Dukes' stage ($p = 0.557$). Statistical analysis was performed using the Chi (χ^2) test. All p -values are two-sided.

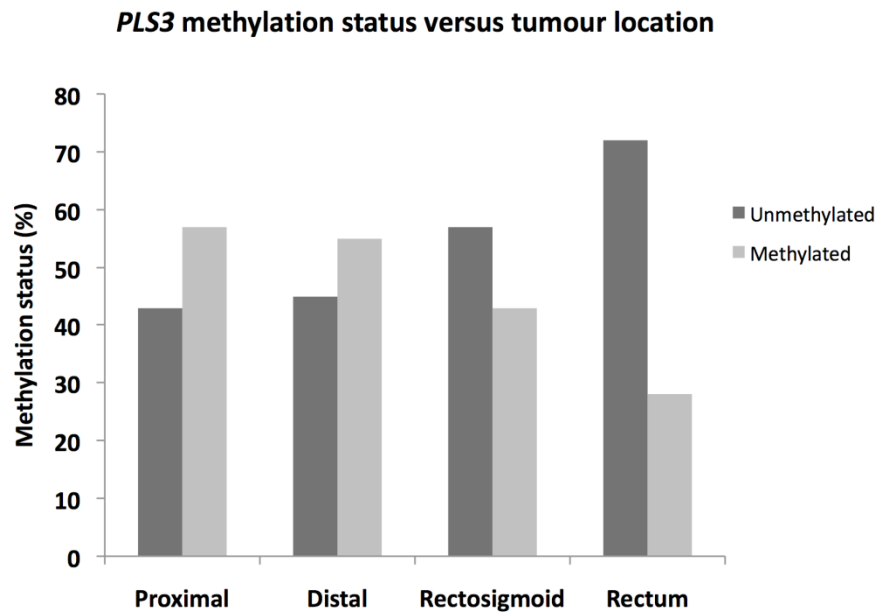


Figure 3.15: *PLS3* promoter methylation in relation to tumour location

Histogram of *PLS3* promoter methylation by tumour location assessed using 161 patient samples. There is a statistically significant difference between *PLS3* promoter methylation and tumour location (proximal, distal, rectosigmoid and rectum) ($p = 0.044$). Statistical analysis was performed using the Chi (χ^2) test. All p -values are two-sided.

3.2.3.2 *PLS3* promoter methylation and patient survival

In order to examine whether *PLS3* promoter methylation could be an independent prognostic biomarker, two statistical analyses were carried out. Firstly, Kaplan-Meier curves were produced to estimate survival probability. Kaplan-Meier curves are an estimate of the survivor function. The time in the study represents a clinical endpoint, in this case, death from CRC. The study baseline is $t = 0$. Survivor function $S(t)$ is the proportion of the population still alive at time t . Secondly, Cox regression analysis using the Breslow method for ties was performed to estimate the cumulative hazard. Cox regression (or proportional hazards regression) is the method for investigating the effect of several variables upon the time a specified event takes to happen, i.e. death from CRC. The cumulative hazard at time t is the risk of dying between time 0 and time t , and the survivor function at time t is the probability of surviving to time t . Co-efficients or hazard ratios above 1 indicate a worse prognosis (i.e. the hazard, CRC-related mortality, is more likely to occur) and a coefficient of less than 1 indicates a protective effect of the *PLS3* promoter methylation. A coefficient of 1 indicates no effect of *PLS3* promoter methylation on the likelihood of hazard occurrence. Data shows that there is no statistically significant correlation between *PLS3* promoter methylation in a population where expression of lamin A/C is a biomarker for CRC cancer (Willis et al., 2008) (Figures 3.16-3.17; Table 3.2).

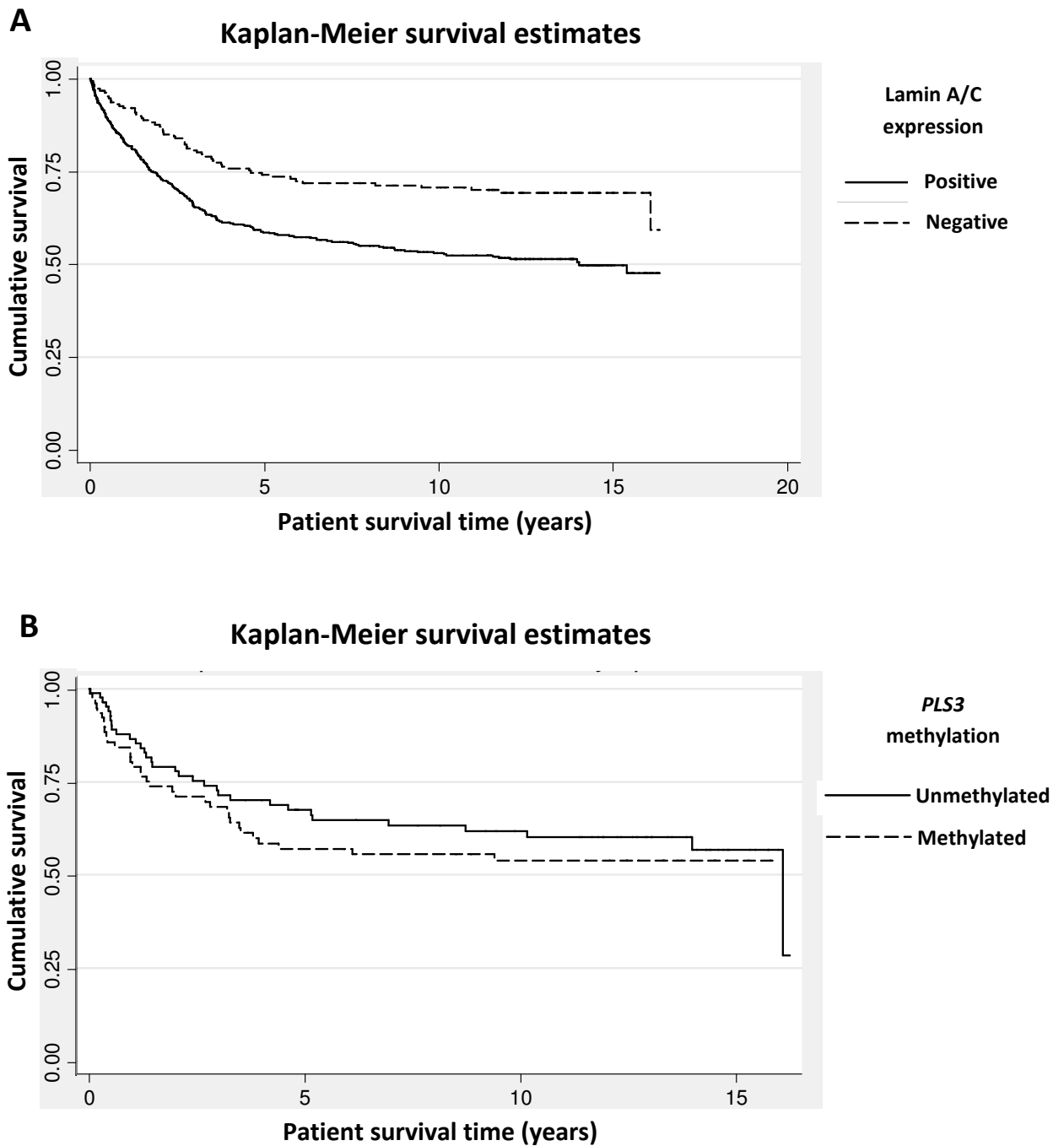


Figure 3.16: Kaplan-Meier survival analysis for all Dukes' stages

(A) Kaplan-Meier plots of cumulative survival for CRC patients in relation to lamin A/C expression. Data shows that there is a statistically significant correlation between lamin A/C expression and survival. Relative hazard ratio (HR) = 0.48 (95% C.I. = 0.27 – 0.73), $p = <0.001$ (adjusted for gender and age at diagnosis). (B) Kaplan-Meier plot of cumulative survival for CRC patients in relation to differential *PLS3* promoter methylation. Data shows that there is no statistically significant correlation between *PLS3* methylation and survival. Relative hazard ratio (HR) = 1.13 (95% C.I. = 0.58-2.23, $p = 0.438$) (adjusted for gender and age at diagnosis).

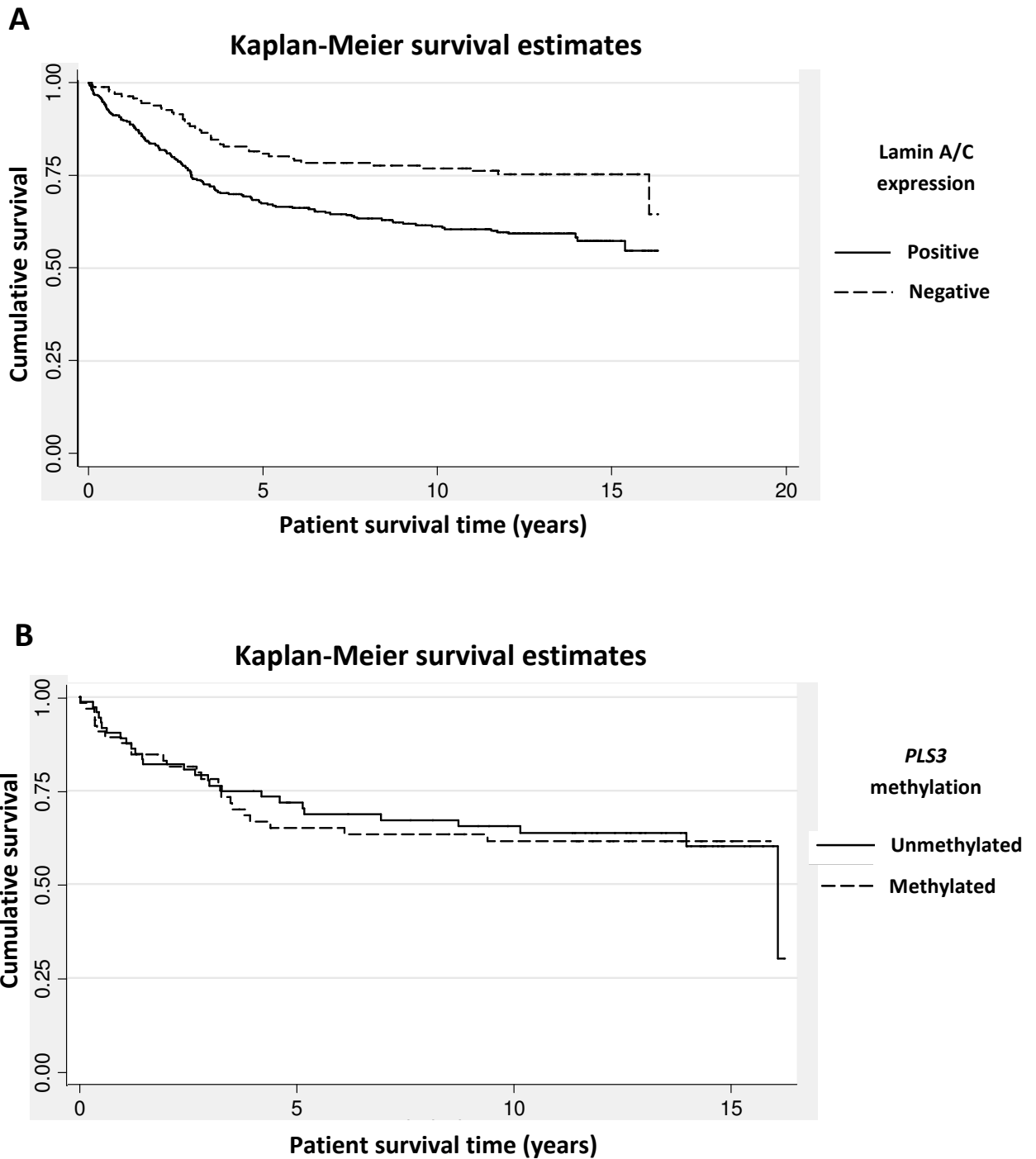


Figure 3.17: Kaplan-Meier survival analysis for Dukes' A, B and C patients

(A) Kaplan-Meier plots of cumulative survival for CRC patients in relation to lamin A/C expression. Data shows that there is a statistically significant correlation between lamin A/C expression and survival. Relative hazard ratio (HR) = 0.52 (95% C.I. = 0.27-0.86), $p = 0.0003$ (adjusted for gender and age at diagnosis). (B) Kaplan-Meier plot of cumulative survival for CRC patients in relation to differential *PLS3* methylation. Data shows that there is no statistically significant correlation between *PLS3* promoter methylation and survival. Relative hazard ratio (HR) = 0.89 (95% C.I. = 0.41-1.93, $p = 0.767$) (adjusted for gender and age at diagnosis).

3.3 Discussion

Aberrant CpG island promoter hypermethylation can result in transcriptional silencing, and this phenomenon has been widely investigated with respect to both CRC progression and prognostic and therapeutic applications (Lao and Grady, 2011). In this study, the aim was to investigate *PLS3* promoter methylation in CRC. N-MSP was the method of choice as this approach allows robust and sensitive genomic DNA from formalin-fixed, paraffin-embedded clinical samples (Derks et al., 2004). However, it should be noted that the *PLS3* gene contains only one CpG island of just 431 bp (Figure 3.2). Designing appropriate primer pairs to assess the methylation within the CpG island was difficult, due to the small size of this stretch of DNA. However, following successful optimisation of previously established protocols, we showed that methylated and unmethylated alleles could be discriminated, and that the technique was both reliable and reproducible. Of the CRC lines analysed by N-MSP, two were methylated in the *PLS3* promoter (SW948 and HT29; Figure 3.3). However, although N-MSP is quick and simple to use, there are limitations. It is not a quantitative assay and should normally be confirmed by bisulphite sequencing, which allows for quantitative analysis of methylation status at single molecule resolution. To this end, unmethylated (SW620) and methylated (SW948) CRC cell lines were chosen for bisulphite sequencing analysis. Bisulphite sequencing primers were successfully designed, allowing for the examination of 26 methylation sites. Data confirmed that the *PLS3* promoter in the SW948 cell line is indeed methylated and exclusively unmethylated in the SW620 cell line (Figure 3.5).

In order to investigate the relationship between *PLS3* promoter methylation and gene expression, SW948 and HT29 cells were subjected to epigenetic drug treatment. Our data demonstrates that epigenetic silencing of the *PLS3* promoter by methylation occurs in CRC cell lines and can be reversed by inhibiting DNA methyltransferases (Figure 3.6). This is consistent with the finding by a Japanese group, who demonstrated by PCR that the *PLS3* gene in SW948 cells is deactivated by methylation (Sasaki et al., 2002; Ikeda et al., 2005).

In the SW948 clones that were analysed, there were clearly two methylation ‘hotspots’ towards the transcription initiation start site. Whether *PLS3* promoter methylation initiates at a particular region within the CpG island then spreads downstream toward the transcription start site cannot be deduced from these data. It would be interesting to see

whether methylation-associated transcriptional silencing occurs in a region-specific manner. Moreover, it would be useful to explore how these sites relate to the binding of transcription factors, and also how the methylation machinery gains access to the *PLS3* CpG island. It is also worth bearing in mind that the methylation pattern in SW948 varies between the six replicates (Figure 3.5). This is common in methylation analysis, and reflects the fact that the assay is an 'average' of material from heterogeneous cells, which may all have slightly different methylation patterns (Herman et al., 1996; Derks et al., 2004). Improvements in single cell PCR and sequencing techniques, coupled with laser capture micro-dissection, will eventually allow us to visualize the methylation landscape of *PLS3* (and other promoters) in a tumour in finer detail in the future.

In order to investigate the *PLS3* methylation in human CRC, we analyzed a subset of DNA samples from the NLCS archive. To the best of our knowledge, no-one has investigated *PLS3* promoter methylation in a large cancer series to date. This study allowed *PLS3* promoter methylation to be investigated in a population in which lamin A/C was known to be a predictor of poor prognosis. Again, utilising the N-MSP method, we found that the prevalence of *PLS3* promoter methylation was 65% in normal colonic mucosa (13/20) and 48% (78/161) in tumour tissue (Figure 3.7; Table 3.1). Given that T-plastin is reported to be absent from normal colonic epithelia (where the I-plastin isoform is normally expressed), the frequency of *PLS3* promoter methylation is expected to be higher. However, sample sizes for normal colon (n=20) were much lower than the tumours (n=161). Moreover, there are likely to be other mechanisms controlling gene expression and an unmethylated gene promoter does not necessarily mean that T-plastin expression is switched on in any given cancer cell. Additional mechanisms such as mRNA and protein half-life, or regulation by microRNAs could be involved in modulating T-plastin expression. Indeed, a small nucleolar RNA, SNORA64, lies just upstream of the *PLS3* gene; one possibility is that the methylation status of the *PLS3* promoter (and the surrounding DNA) might influence the transcription and activity of SNORA64 (Kiss, 2002). It would be informative to explore whether SNORA64 transcription is reduced in SW948 compared with HT29 cells, and if so whether inhibition of methylation restores its expression.

We attempted to validate the methylation status of *PLS3* in the human DNA samples by bisulphite sequencing analysis. However, a limitation of this approach is that it is often

difficult to retrieve enough DNA for sequencing from formalin fixed tissue held in historical archives. This proved to be the case for the analysis of *PLS3* promoter methylation in tumour samples (Figure 3.9). To solve this problem, a prospective, rather than retrospective, study could be performed and the methylation status of *PLS3* could be analyzed using DNA from fresh frozen tissue. However, the disadvantage of such a prospective study would be that little or no survival data would be available at the time of sampling, and as such, may be of limited statistical use.

By using qPCR, we showed that T-plastin mRNA expression in two CRC patients was significantly elevated in tumour tissue, compared with its normal counterpart (Figure 3.11). The N-MSP analysis corroborated this finding (Figure 3.10), suggesting that *PLS3* promoter methylation may silence gene transcription. However, this conclusion was made on the assumption that methylation status, as determined by N-MSP, is indeed correct. Surprisingly, bisulphite sequencing analysis did not confirm the N-MSP data; the *PLS3* promoter from patients 4 and 7 appeared to be methylated by N-MSP analysis, but unmethylated by bisulphite sequencing analysis (Figure 3.12). This discrepancy could be due to several reasons. Firstly, although bisulphite sequencing is highly specific, the information obtained for each clone is from one amplicon. PCR products from the N-MSP however, represent thousands of amplicons. Thus, if there are only small levels of methylation in the patient material, it may be difficult to detect using the bisulphite sequencing approach. Secondly, it is possible that CpG sites up or downstream of the promoter are methylated and that the full landscape of *PLS3* methylation is different from the region that has been sequenced in this chapter. It has recently been shown that methylation of CpG sites outside of the well-defined CpG island can be responsible for gene inactivation (Rach et al., 2011). This may call into question the definition of a CpG island (Fernandez et al., 2011).

It is clear from the data in this chapter that *PLS3* promoter methylation is involved in silencing T-plastin expression *in vitro* (Figure 3.6), although we saw no prognostic effect in tumour samples (Table 3.2). Analyses of clinicopathological characteristics revealed that there was no association between *PLS3* promoter methylation and survival. However, some of the observations made during the analysis in this chapter merit further investigation. For example, there was a remarkable difference in *PLS3* promoter methylation between the sexes ($p = <0.0001$) (Figure 3.14). Over 85% of the female samples analysed were methylated

for *PLS3* and over 85% of male samples were unmethylated for *PLS3*. The T-plastin gene is expressed on the X-chromosome, so it would be very interesting to see whether X chromosome inactivation of *PLS3* occurs and how this is affected by the onset of CRC. Of the cell lines examined in this Chapter, two female cell lines (HT29 and SW498) were methylated whereas one female cell line (LS) was unmethylated, suggesting that there is no simple relationship between X-inactivation and *PLS3* methylation. Interestingly, a recent meta-analysis of 5 genome-wide association studies (GWAS) identified a new common variant linked to CRC risk on the X chromosome at Xp22.2 (Dunlop et al., 2012). The risk loci on Xp22.2 does not reside near the *PLS3* gene but is close to the *SHROOM2* gene, whose normal function is to regulate melanosome biogenesis and endothelial morphogenesis. Of note, Shroom2 localises to cell-cell adhesion loci and binds to cortical actin (Etournay et al., 2007; Farber et al., 2011). Farber and co-investigators showed that loss of Shroom2 activity leads to an increase in migration and angiogenesis. The Nature Genetics report (Dunlop et al., 2012) was the first published example of an X-chromosome variation in a non-sex linked cancer. This lends weight to the notion that T-plastin, a gene on the X-chromosome, can be involved in both male and female cancer development.

It was also notable from our study that *PLS3* methylation status appeared to differ between tumour locations, there being least methylation in the left-sided (LCC) and more methylation in right-sided (RCC) CRC (Figure 3.15). It has been known since the 1980s that there are sex-specific differences between left-sided and right-sided CRCs. More women than men tend to have RCC, RCCs tend to be more advanced and survival of patients with LCCs tends to be greater (Benedix et al., 2010). Our finding that *PLS3* is more likely to be methylated in females and more likely to be methylated in RCC is consistent with this observation. These findings should be followed up to determine T-plastin protein expression in female right sided CRC, and it remains possible that *PLS3* methylation status could be useful as part of the CIMP biomarker panel in this cohort. As the number of samples within each category is small, further sampling and analysis is important to validate these findings. It would also be necessary to include information about smoking, alcohol consumption and obesity in any subsequent analysis since these risk factors may have independent associations with either LCC or RCC.

In summary, we have investigated *PLS3* promoter methylation in a large CRC cohort, and whilst *PLS3* promoter methylation cannot be used as an independent prognostic biomarker, our data suggests that *PLS3* promoter methylation is an important mechanism of transcriptional silencing. Moreover, demethylation of the *PLS3* promoter may lead to aberrant expression of T-plastin in tumour tissue. Given that T-plastin functions as an actin-bundling protein, once may hypothesise that increased expression of the protein, brought about by demethylation of the promoter, results in changes in the cytoskeletal architecture that favours growth and metastasis.

Chapter 4: Characterisation of polyclonal plastin antibodies

4.1 Introduction

The actin cytoskeleton is a dynamic meshwork that is an essential component of all eukaryotic cells and is involved in many biological phenomena such as cell division, organisation of cytoplasmic organelles and intracellular compartments, cellular motility, cellular adhesion, and control of cell shape (Pollard and Cooper, 1986). In cancer, many of these characteristics of normal cell behaviour are lost or perturbed. For example, in tumour metastasis, cancer cells acquire migratory and invasive capabilities in order to leave the primary tumour and disseminate through the body to a secondary site (Toyooka et al., 2006). This process involves a dramatic reorganization and remodelling of the actin cytoskeleton and the concomitant formation of membrane protrusions required for invasive growth. Importantly, this overall organization of the actin cytoskeleton is tightly controlled by a plethora of actin-binding proteins including α -actinin and filamins, which are involved in cross-linking and anchoring glycoproteins to the cytoskeleton (Dos Remedios et al., 2003). Plastins also belong to this family of actin-binding proteins (known as actin-bundling proteins) which are conserved from lower eukaryotes to humans (Lin et al., 1999; Shinomiya et al., 1994). These polypeptides function to stabilize and rearrange the organization of the actin cytoskeleton in response to external stimuli (Bretscher, 1981; Delanote et al., 2005; Glenney et al., 1981; Namba et al., 1992).

Members of the plastin family have a modular structure which consists of an amino terminal domain (10 kDa) with two EF-hand motifs, and two ABDs, each divided into two tandemly arranged CH domains. Each CH domain is composed of four α -helical segments, three of which form a loose bundle of helices, with the fourth α -helix sitting perpendicular to the main bundle. These segments are connected by extended and variable loops (Delanote et al., 2005).

Plastins normally localise to various actin-rich membrane structures involved in locomotion, signalling, adhesion and immune defense, including focal adhesions, ruffling membranes, filopodia and the phagocytic cup. Moreover, plastins are also located in highly specialized

surface structures with ordered microfilament bundles such as stereocilia. This is of particular interest, as actin bundles formed by plastin may also have a mechanosensory function by sensing mechanical alterations in signals during chemosensory signal transduction (Daudet and Lebart, 2002).

As previously mentioned, the different plastin isoforms have been implicated in a number of cancers (Ikeda et al., 2005; Leavitt, 1994; Otsuka et al., 2001; Sasaki et al., 2002a). The expression of L-plastin, for example, is induced in many types of malignant human cells of non-hematopoietic origin, suggesting that its expression accompanies tumourigenesis in solid tissues. Foran and co-workers (2006) found that overexpression of L-plastin in SW480 cells leads to the loss of E-cadherin and hence increased proliferation and invasiveness. T-plastin has been associated with both drug and radiation resistance in cancer cells; increased expression of T-plastin has also been reported in cisplatin-resistant human cancers (Hisano et al., 1996). In our laboratory, we have shown that RNAi knockdown of T-plastin results in decreased motility in CRC cells (Willis et al., 2008). Moreover, qPCR analysis demonstrated that T-plastin mRNA expression is elevated in tumour tissue compared to matching normal colonic mucosa (Chapter 3, Figure 3.11). Given that both increased T and L-plastin expression may be important in the progression of CRC, plastin isoform-specific antibodies might be useful as tools for biomarker studies. Antibodies can be used in a wide range of situations where characterisation, quantification, and localisation of proteins are required (Brehm-Stecher and Johnson, 2004; Norman E, 1999). Importantly, the use of antibodies has proved invaluable in diagnostic and therapeutic applications. The aim of this chapter was to characterise six commercially produced rabbit polyclonal antibodies raised against three immunising peptides and to examine their plastin isoform specificity (Figure 4.1).

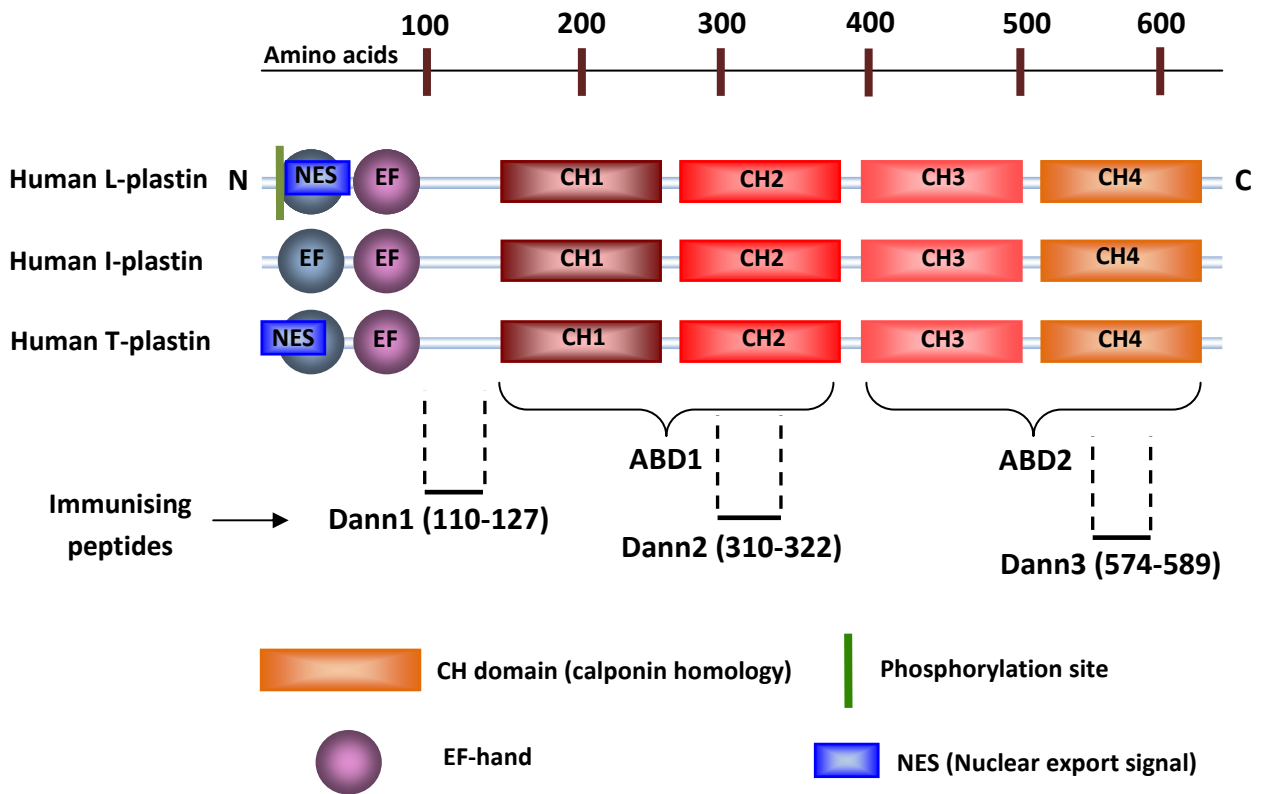


Figure 4.1: Schematic representations of human plastin isoforms

Domain organisation in human plastin isoforms. A scale (in amino acids) is displayed at the top of the schematic. Each plastin contains two amino-terminal EF hands, and two actin binding (ABD) domains. Each ABD consists of two calponin (CH) domains. Human T-plastin contains an nuclear export signal (NES), and L-plastin contains a phosphorylation site. The locations of the immunising peptides used to produce the antibodies are shown. The number in parenthesis corresponds to the amino acid residues. Dann1 is located in the N-terminus, Dann2 is located in ABD1, and Dann3 is located in ABD2 (adapted from Delanote et al. 2005).

4.2 Results

4.2.1 Sequence alignments of plastin isoforms

As shown in Figure 4.2, T-, L- and I-plastin are homologous proteins. A sequence alignment of the human plastin isoforms using UniProt shows that they share approximately 70% homology in the amino acid sequence. T and L-plastin are 83% identical. Three human peptides to be used for immunisation were designed against exposed regions of the protein that were likely to be antigenic. For the Dann1 peptide, four out of 18 residues vary between T, L- and I-plastin. Only two of these residues vary between T and L-plastin. For the Dann2 peptide, four of the 13 residues are different. The Dann3 peptide resides in a region that differs in five of the 16 residues.

To verify whether antibodies against these peptides would be likely to recognise both human and rodent cells and tissues, an alignment of T-plastin in human, mouse and rat was performed (Figure 4.3). The alignment confirms that the sequences are highly similar (highlighted in grey). There are no differences in the human, mouse and rat T-plastin in the peptide sequence corresponding to Dann1 or Dann2. Just two out of 16 residues differ between rat and human in the Dann3 peptide, with this region being identical between human and mouse. The alignment suggests that T-plastin is not under rapid natural selection, and confirms that the antibodies have the potential to be used on human or mouse material.

1	MDEMATTQISKDELDELKEFAKVDLNSNGFICDYELHELKFKEANMPLPGYKVREIIQKL	60	P13797	PLST_HUMAN
1	MDEMATTQISKDELDELKEFAKVDLNSNGFICDYELHELKFKEANMPLPGYKVREIIQKL	60	Q99K51	PLST_MOUSE
1	MDEMATTQISKDELDELKEFAKVDLNSNGFICDYELHELKFKEANMPLPGYKVREIIQKL	60	Q63598	PLST_RAT

61	MLDGDNRNKDGKISFDEFVYIFQEVKSSDIAKTFRKAINRKEGICALGGTSELSSEGTQHS	120	P13797	PLST_HUMAN
61	MVDGDRNKDGKISFNEFVYIFQEVKSSDIAKTFRKAINRKEGICALGGTSELSSEGTQHS	120	Q99K51	PLST_MOUSE
61	MLDGDNRNKDGKISFNEFVYIFQEVKSSDIAKTFRKAINRKEGICALGGTSELSSEGTQHS	120	Q63598	PLST_RAT
:				
121	YSEEEKYAFVNWINKALENDPDCRHVIPMNPNTDDLKFAVGDGIVLCKMINLSVPDTIDE	180	P13797	PLST_HUMAN
121	YSEEEKYAFVNWINKALENDPDCRHVIPMNPNTDDLKFAVGDGIVLCKMINLSVPDTIDE	180	Q99K51	PLST_MOUSE
121	YSEEEKYAFVNWINKALENDPDCRHVIPMNPNTDDLKFAVGDGIVLCKMINLSVPDTIDE	180	Q63598	PLST_RAT

181	RAINKKKLTFFIIQENLNLAALSASAIGCHVVNIGAEDLRAGKPHLVGLLWQIIKIGLF	240	P13797	PLST_HUMAN
181	RAINKKKLTFFIIQENLNLAALSASAIGCHVVNIGAEDLRAGKPHLVGLLWQIIKIGLF	240	Q99K51	PLST_MOUSE
181	RAINKKKLTFFIIQENLNLAALSASAIGCHVVNIGAEDLRAGKPHLVGLLWQIIKIGLF	240	Q63598	PLST_RAT

241	ADIELSRNEALAALLRDGETLEELMKLSPPELLLRWANFHLENSGWQKINNFSAIDKDSK	300	P13797	PLST_HUMAN
241	ADIELSRNEALAALLRDGETLEELMKLSPPELLLRWANFHLENSGWQKINNFSAIDKDSK	300	Q99K51	PLST_MOUSE
241	ADIELSRNEALAALLRDGETLEELMKLSPPELLLRWANFHLENSGWQKINNFSAIDKDSK	300	Q63598	PLST_RAT

301	AYFHLLNQIAPKGQKEGEPRIDINMSGFNETDDLKRAESMLQQADKLGCRQFVTPADVVS	360	P13797	PLST_HUMAN
301	AYFHLLNQIAPKGQKEGEPRIDINMSGFNETDDLKRAESMLQQADKLGCRQFVTPADVVS	360	Q99K51	PLST_MOUSE
301	AYFHLLNQIAPKGQKEGEPRIDINMSGFNETDDLKRAESMLQQADKLGCRQFVTPADVVS	360	Q63598	PLST_RAT

361	GNPKLNLAFLVANLNFNKPALTKPENQDIDWTLLEGETREERTFRNWMNSLGVNPHVNHL	420	P13797	PLST_HUMAN
361	GNPKLNLAFLVANLNFNKPALTKPENQDIDWTLLEGETREERTFRNWMNSLGVNPHVNHL	420	Q99K51	PLST_MOUSE
361	GNPKLNLAFLVANLNFNKPALTKPENQDIDWTLLEGETREERTFRNWMNSLGVNPHVNHL	420	Q63598	PLST_RAT

421	ADLQDALVILQLYERIKVPVDWSKVNKPPYPKLGANMCKLENCNYAVELGKHPAKFSLVG	480	P13797	PLST_HUMAN
421	ADLQDALVILQLYERIKVPVDWSKVNKPPYPKLGANMCKLENCNYAVELGKHPAKFSLVG	480	Q99K51	PLST_MOUSE
421	VDLQDALVILQLYERIKVPVDWSKVNKPPYPKLGANMCKLENCNYAVELGKHPAKFSLVG	480	Q63598	PLST_RAT
.*****:*				
481	IGGQDLNDGNPTLTLAVVWQLMRRYTLNVLEDLGEGQKANDDIIVNWVNTLSEAGKSTS	540	P13797	PLST_HUMAN
481	IGGQDLNDGNPTLTLAVVWQLMRRYTLNVLEDLGEGQKANDDIIVNWVNTLSEAGKSTS	540	Q99K51	PLST_MOUSE
481	IGGQDLNDGNPTLTLAVVWQLMRRYTLNVLEDLGEGQKATDDIIVNWVNTLSEAGKSTS	540	Q63598	PLST_RAT
***** *:*				
541	IQSFKDKTISSSLAVVDLIDAIQPGCINYLKSGNLTEDDKHNNAKYAVSMARRIGARV	600	P13797	PLST_HUMAN
541	IQSFKDKTISSSLAVVDLIDAIQPGCINYLKSGNLTEDDKHNNAKYAVSMARRIGARV	600	Q99K51	PLST_MOUSE
541	IQSFKDKTISSSLAVVDLIDAIQPGCINYLKSGNLTEDDKHNNAKYAVSMARRIGARV	600	Q63598	PLST_RAT
*****:*				
601	YALPEDLVEVKPKMVMVTFACLMGRGMKRV	630	P13797	PLST_HUMAN
601	YALPEDLVEVKPKMVMVTFACLMGRGMKRV	630	Q99K51	PLST_MOUSE
601	YALPEDLVEVKPKMVMVTFACLMGRGMKSV	630	Q63598	PLST_RAT
***** *				

Figure 4.3: Alignment of human T-plastin with mouse and rat T-plastin

The full-length protein sequences of human T-plastin (PLST, P13797), mouse T-plastin (PLST, Q99K51) and rat T-plastin (PLST, Q63598) were aligned using the Uniprot program. Regions of identity are shaded dark grey. The sequences corresponding to the Dann1 peptide (red) and Dann2 peptide are identical in human, mouse and rat T-plastin. The sequences corresponding to the Dann3 peptide (green) are identical between human and mouse, but not rat.

4.2.2 Characterisation of the polyclonal Dann antibodies

4.2.2.1 Producing recombinant plastins to test reference antibodies

To assess the reactivity and specificity of the Dann antibodies, recombinant proteins against T-, L- and I-plastin were expressed in *E. coli*. The plastin-expressing bacteria were obtained as a kind gift from Dr Francisco Rivero (University of Hull). Bacterial protein expression was induced by adding IPTG to the cultures, and samples were taken at 0 hr, 1 hr, 2 hr and 3 hr post-induction. After lysis, the bacterial proteins were analysed by SDS-PAGE and Coomassie stained to verify the expression of the fusion proteins. Figure 4.5 shows that each recombinant plastin and the GST-fusion control had been expressed. Note that expression was detected prior to induction in all four cases (Figure 4.4 A-D), since recombinant protein was visible at the 0 hr time points. Each fusion protein was expressed at the predicted molecular weight, and they were the most abundant proteins in the lysates. The GST-control was expressed at 25 kDa, GST-T-plastin at 96 kDa, GST-L-plastin (only N-terminal) at 40 kDa, and GST-I-plastin at 96 kDa.

The protein lysates from the 3-hour time point were tested using antisera against T-plastin, L-plastin, and an affinity-purified antibody against I-plastin, kindly provided by Dr. Francisco Rivero (Figure 4.5 A-C) and commercially available antibodies from Abcam (Figure 4.5 D-E). The T-plastin antisera strongly recognised T-plastin as expected, resulting in an intense smear on Western blot (Figure 4.5 A, lane 2). This antibody also detected recombinant L-plastin. Surprisingly, more background was detected in the GST-only lane than in the I-plastin lane (Figure 4.5 A, lanes 1 and 4). In contrast, the L-plastin antisera did not specifically detect L-plastin at the 1:1000 dilution used in these experiments (Figure 4.5 B). This antibody did recognise a background band present in all bacterial lysates; hence this antibody was used as a control for protein loading in subsequent peptide inhibition experiments. The I-plastin antibody did specifically recognise the recombinant I-plastin at ~96 kDa (Figure 4.5 C, lane 4), consistent with the recombinant protein band seen on Coomassie (Figure 4.4). The Abcam antibody against GST-T-plastin was specific (Figure 4.6 D), as was the Abcam antibody against GST-L-plastin, both producing a signal at ~96 kDa (Figure 4.5 E). Note that both Abcam antibodies recognised likely degradation products.

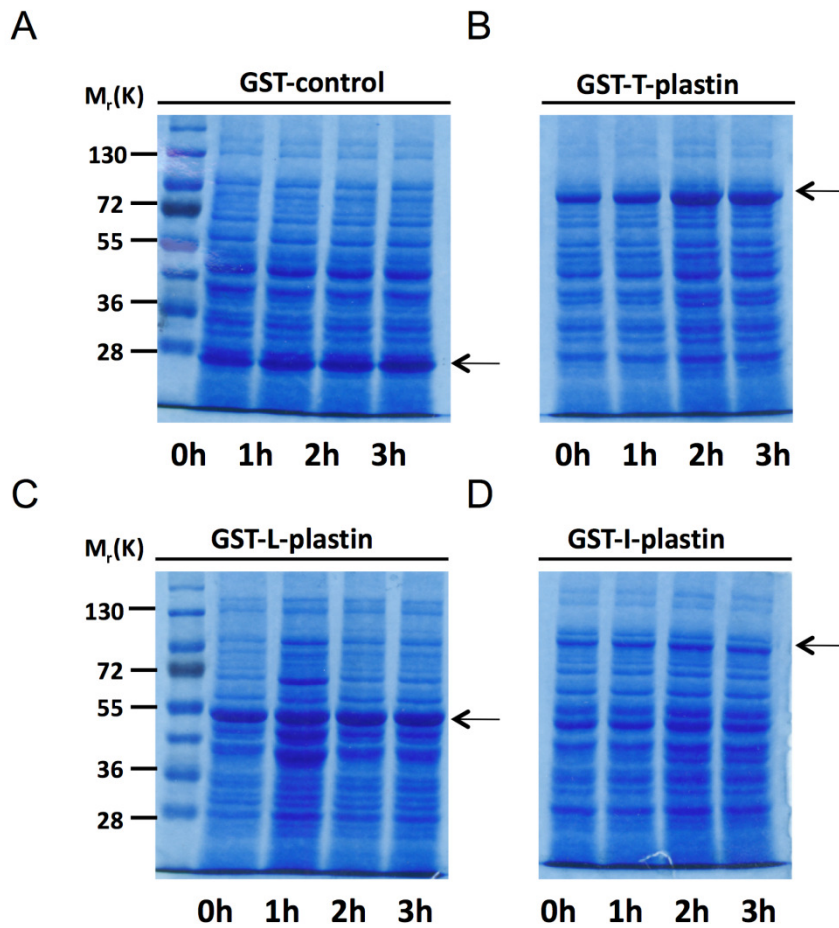


Figure 4.4: Coomassie staining of recombinant plastin proteins

Plastin expression was induced for 0 hr, 1 hr, 2 hr or 3 hr with 1 mM IPTG. Protein lysates were resolved by 10% SDS-PAGE prior to staining with colloidal Coomassie. (A) GST-control (B) T-plastin (C) L-plastin (D) I-plastin. Arrows indicate specific GST-fusion expression. Molecular weight markers are given in kDa. The recombinant proteins are induced at each time point analysed. Each fusion protein was expressed at the predicted molecular weight; GST-control at 25 kDa, GST-T-plastin (human) at 96 kDa, GST-L-plastin (mouse) at 40 kDa and GST-I-plastin (human) at 96 kDa.

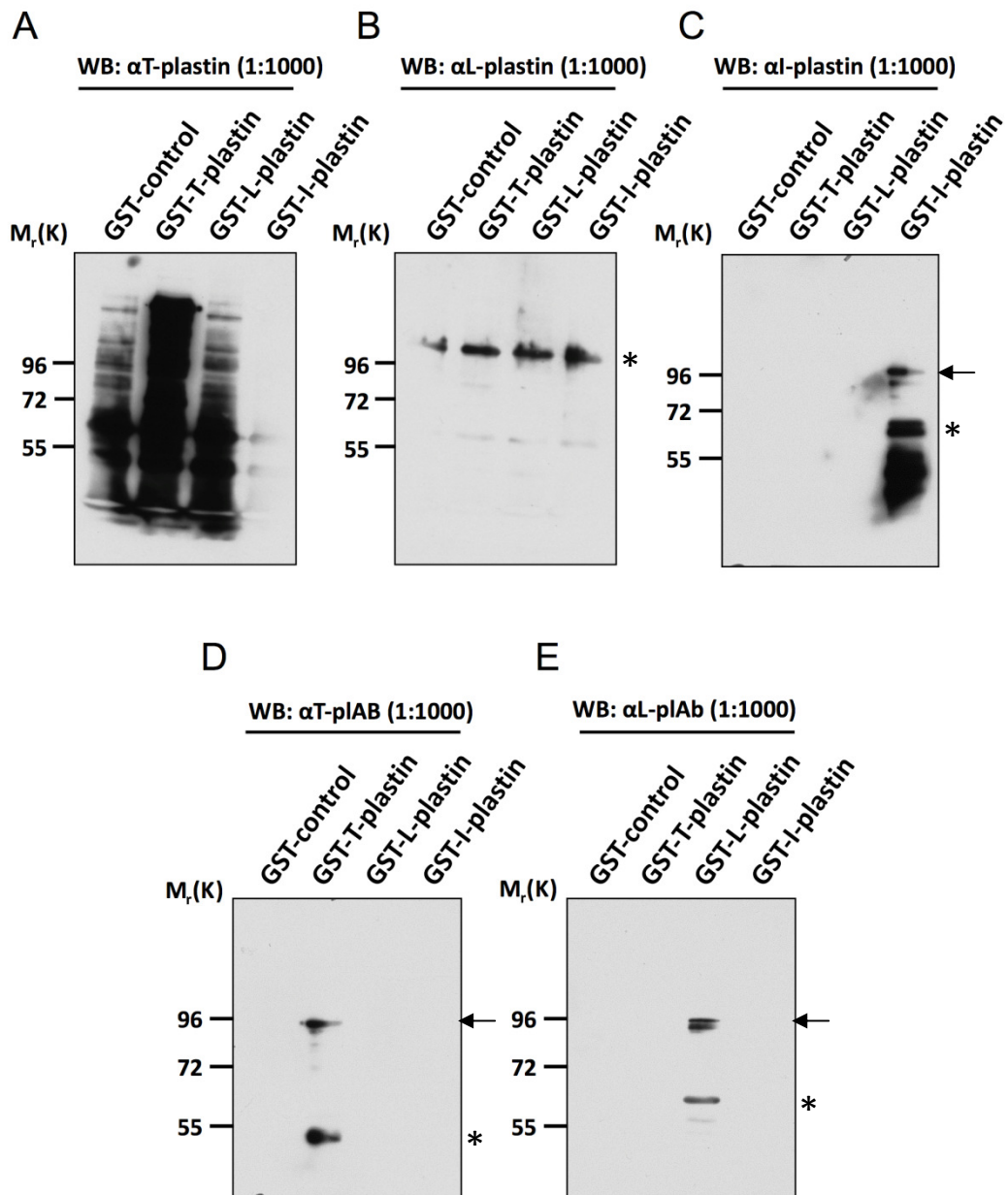


Figure 4.5: Western blotting analysis of plastin GST-fusion proteins

Lysates from bacteria three hours after induction with IPTG were analysed by 10% SDS PAGE, transferred to PVDF membrane and immunoblotted. GST-cntl, GST-T-plastin, GST-L-plastin, and GST-I-plastin with probed with (A) crude T-plastin antisera. (B) L-plastin antisera (C) affinity purified I-plastin antibody (D) a commercially available T-plastin antibody and (E) a commercially available L-plastin antibody. Molecular weight markers are given in kDa. Arrow denotes specific band at predicted molecular weight. Asterisk denotes background band. Note that the T-plastin antisera gave a strong background; the L-plastin antisera gave a signal in all lysates including the GST control. The I-plastin antibody gave a specific signal against the GST-fusion protein at the predicted molecular weight of 96 kDa. Both Abcam antibodies produced a signal at the predicted molecular weight of 96 kDa.

4.2.2.2 Characterising the Dann1a antibody against recombinant plastins

The recombinant proteins were used to test the specificity of the Dann antibodies, starting with Dann1a. Bacterial lysates containing each recombinant GST-fusion protein were run on 10% SDS-PAGE as before, transferred to PVDF membranes and immunoblotted with Dann1a at 1:100, 1:500 and 1:1000 dilution (Figure 4.6). The 1:100 dilutions gave a strong signal for both L-plastin and T-plastin (Figure 4.6 A, lanes 2 and 3). No signal was detected against the GST-only lysate or the I-plastin lysate, demonstrating the specificity of the antibody for T- and L-plastin (Figure 4.6 A, lanes 1 and 4). At 1:100 dilution, four bands were seen in the T-plastin lane, most likely corresponding to degradation products or truncated protein products. Titrating the antibody out to 1:1000 gave a clear single band for both T and L-plastin, at the expected molecular weights for the fusion proteins (~96 kDa and ~40 kDa, respectively). This experiment demonstrates that the Dann1a antibody detects both T-plastin and L-plastin, as expected from the sequence alignment (Figure 4.2). The antibody did not detect any non-specific bacterial proteins, since no signal was observed in the GST-control lysate.

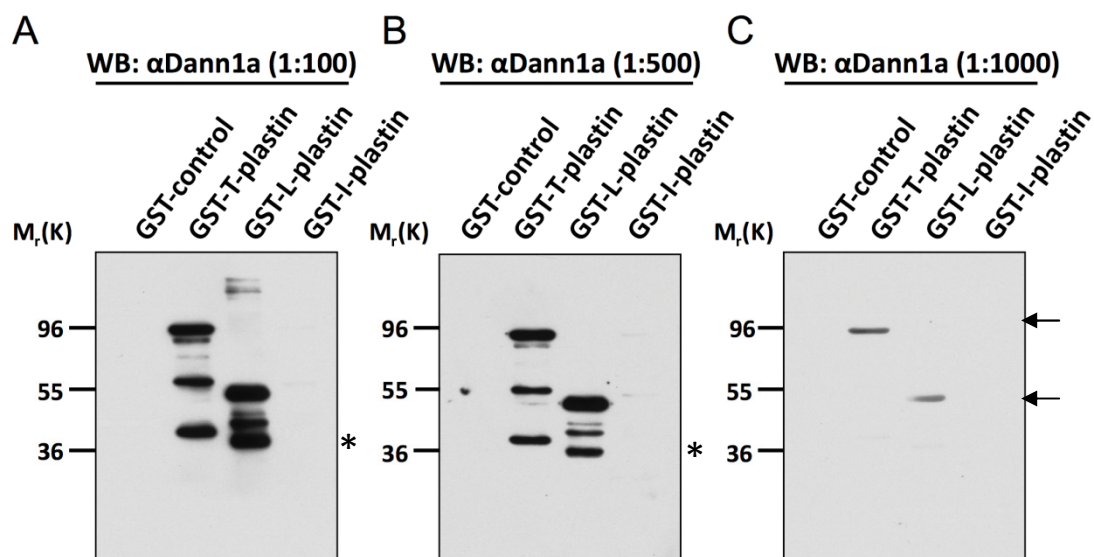


Figure 4.6: Characterisation of Dann1a antibodies by Western blot analysis

Lysates from bacteria expressing GST-fusion proteins were analysed by 10% SDS-PAGE, transferred to PVDF membrane and immunoblotted. GST-cntl, GST-T-plastin, GST-L-plastin, and GST-I-plastin were probed with (A) Dann1a at 1:100 dilution (B) Dann1a at 1:500 dilution and (C) Dann1a antibody at 1:1000 dilution. Molecular weight markers are given in kDa. Arrow denotes specific band at predicted molecular weight. Asterisk denotes background band. Dann1a specifically recognised both GST-T-plastin at a predicted molecular weight of 96 kDa and GST-L-plastin at a predicted molecular weight of 40 kDa. The optimal dilution was 1:1000.

4.2.2.3 Characterising the Dann1b, Dann2a, Dann2b, Dann3a and Dann3b antibodies against recombinant plastins

Having demonstrated that the Dann1a antibody recognises T-plastin and L-plastin, Dann1b, Dann2a, Dann2b and Dann3a were taken for analysis (Figure 4.7 A-D). At 1:500 dilution, the Dann1b antibody recognised T-plastin and L-plastin as expected (Figure 4.7 A, lanes 2 and 3). Multiple bands were observed in this experiment and some signal was detected in the L-plastin lane (Figure 4.7 A, lane 4). The Dann3b antibody at 1:500 recognised T-plastin at the predicted molecular weight. However, this antibody also produced multiple background bands (Figure 4.7 E, lane 2). In contrast, the Dann2a and Dann3a antibodies did not recognise the recombinant plastins at all (Figure 4.7 B and D). The most promising result was obtained with the Dann2b antibody, which recognised a single band at the expected molecular mass for T-plastin (Figure 4.7 C). The Dann2 and Dann3 antibodies were not expected to recognise the GST-L-plastin fusion protein, because only the N-terminus of L-plastin was encoded in the fusion protein.

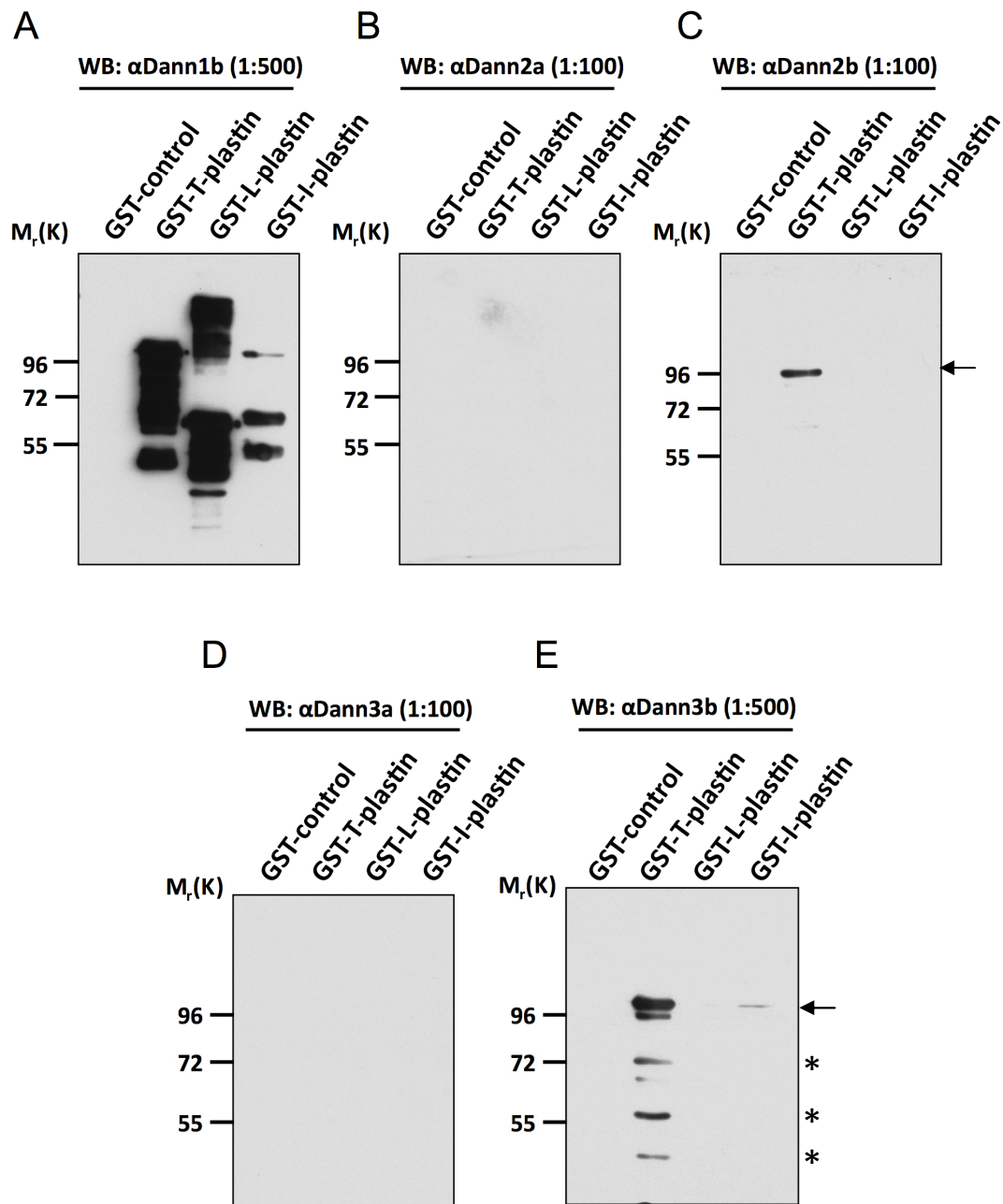


Figure 4.7: Characterisation of Dann1b-3b antibodies by Western blot analysis

Lysates from bacteria expressing GST-fusion proteins were analysed by 10% SDS-PAGE, transferred to PVDF membrane and immunoblotted. GST-cntl, GST-T-plastin, GST-L-plastin and GST-I-plastin were probed with (A) Dann1b at 1:500 dilution (B) Dann2a at 1:100 dilution (C) Dann2b antibody at 1:100 dilution (D) Dann3a antibody at 1:100 dilution and (E) Dann3b antibody at 1:500 dilution. Molecular weight markers are given in kDa. Arrow denotes specific band at predicted molecular weight. Asterisk denotes background band. Dann1b was unspecific as a signal was detected in all three lysates. Dann2a and Dann3a produced no signal against the lysates. Dann2b was specific against GST-T-plastin at a predicted molecular weight of 96 kDa. Dann3b detected multiple bands against GST-T-plastin. Note that the GST-L-plastin construct only encodes the N-terminal half of the protein and the Dann 2 peptide is located in the ABD1.

4.2.2.4 Confirming the specificity of Dann antibodies by peptide inhibition assay

Having demonstrated that Dann1a, Dann2b and Dann3b recognise recombinant T-plastin and/or L-plastin, peptide inhibition assays using the immunogenic peptides were performed to determine the specificity of each antibody. For Dann1a, the antibody was pre-incubated with 2-fold and 10-fold Dann1a peptide for 1hr prior to immunoblotting. *E.Coli* lysates expressing the GST-fusion proteins were used as the source of the plastin antigens. In the absence of peptide, Dann1a recognised proteins in both the T-plastin and L-plastin lysates, as seen before (Figure 4.8 A). In the presence of 2-fold (Figure 4.8 B) or 10-fold (Figure 4.8 C) SELSSEGTQHSYSEEEKY, the Dann1a antigen, the antibody signal was completely blocked. Re-probing the membranes with the L-plastin antibody first shown in Figure 4.5 B gave a background signal in all lysates, confirming that proteins were present on the PVDF membranes (data not shown). When the Dann3 antigen SGNLTEDDKHNNAKYA was used, there was no reduction in the Dann1a antibody signal, demonstrating the specificity of the antibody for its antigen (Figure 4.8 D). The same assay was performed for the Dann2b antibody. In the absence of any peptide, Dann2b recognised T-plastin and not L-plastin or I-plastin (Figure 4.9 A) as expected from previous experiments (Figure 4.7 C). When the Dann2b antibody was pre-incubated with the Dann2b peptide APKGQKEGEPRIID prior to Western blotting, the antibody signal was only partially blocked (Figure 4.9 B and C). This is consistent with the high titre of Dann2b found in the ELISA experiments (Supplementary Figure S2). The specificity of Dann2b for its antigen was demonstrated by incubating the antibody with the non-specific Dann3 antigen, SGNLTEDDKHNNAKYA. No inhibition of binding to the recombinant protein occurred in the presence of this control peptide (Figure 4.9 D). A third peptide inhibition experiment was conducted using the Dann3b antibody. In the absence of any peptide, a strong signal with multiple bands was seen for T-plastin, but not for L-plastin or I-plastin (Figure 4.10 A). In the presence of the Dann3 antigen SGNLTEDDKHNNAKYA, the major T-plastin band at 96 kDa disappeared, but a band at ~55 kDa remained. This suggested that the 55 kDa band was a non-specific protein rather than a degradation product of T-plastin. To confirm the specificity, incubating the Dann3b antibody with the control Dann1 peptide SELSSEGTQHSYSEEEKY had no effect on the detection of T-plastin from the bacterial lysate. Taken together, the results confirm Dann1a and Dann2b are specific antibodies, whereas Dann3b might also recognise a non-specific bacterial protein.

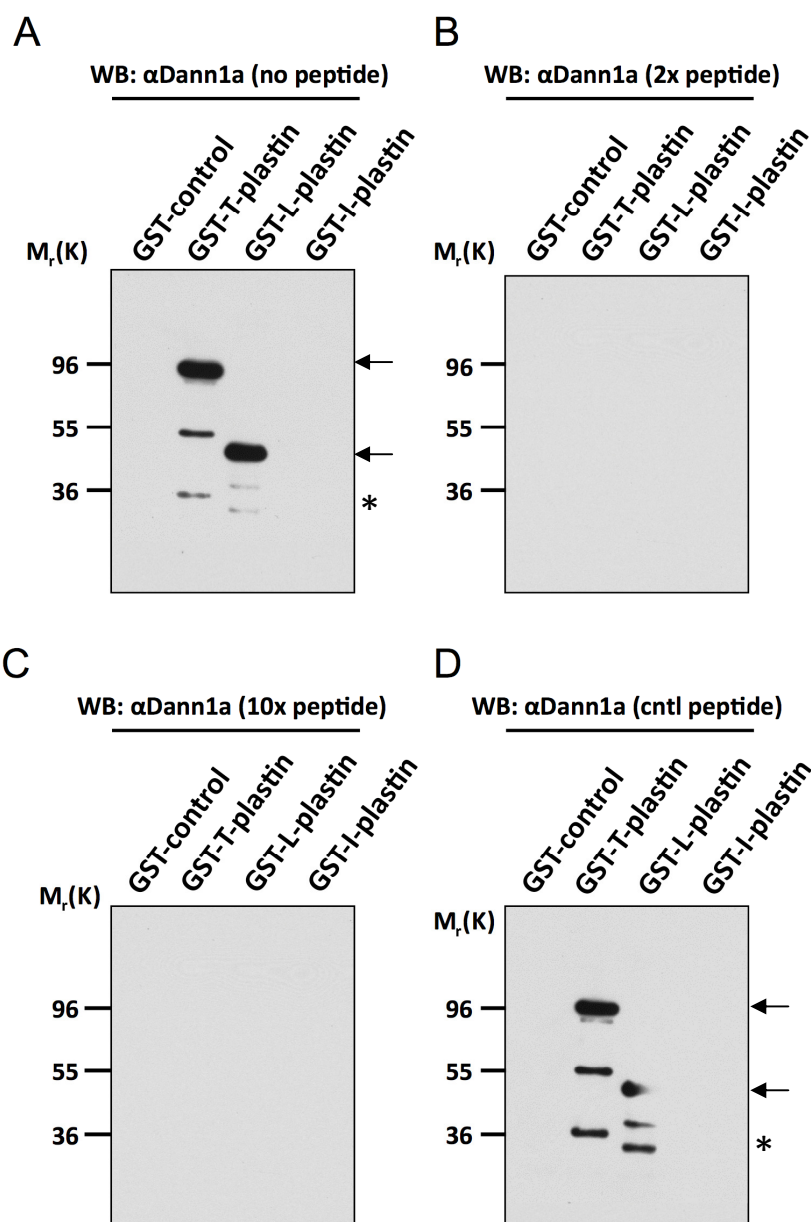


Figure 4.8: Confirmation of the specificity of Dann1a antibody by peptide inhibition assay

Lysates from bacteria expressing GST-fusion proteins were analysed by 10% SDS-PAGE, transferred to PVDF membrane and immunoblotted. GST-cntl, GST-T-plastin, GST-L-plastin and GST-I-plastin were incubated with (A) Dann1a antibody and no peptide (B) Dann1a antibody and 2x concentration of Dann1 peptide (C) Dann1a antibody and 10x concentration of Dann1 peptide and (D) Dann1a antibody and Dann3 peptide as a control. Molecular weight markers are given in kDa. Arrow denotes specific band at predicted molecular weight. Asterisk denotes background band. Dann1a was specific for the Dann1 peptide as no signal was detected in either the 2x or 10x concentration of Dann1 peptide. Moreover, it had no affinity for the Dann3 peptide (control) as a signal in the GST-T-plastin and GST-L-plastin lanes was detected.

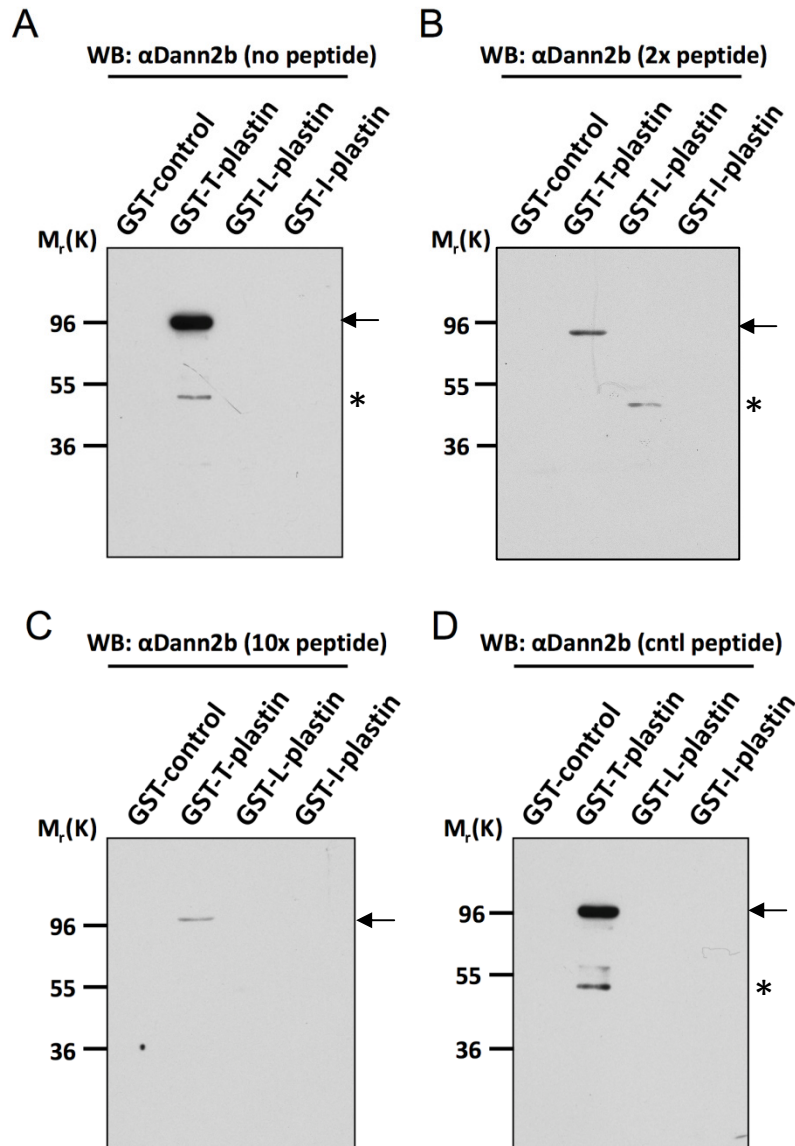


Figure 4.9: Confirmation of the specificity of Dann2b antibody by peptide inhibition assay

Lysates from bacteria expressing GST-fusion proteins were analysed by 10% SDS-PAGE, transferred to PVDF membrane and immunoblotted. GST-cntl, GST-T-plastin, GST-L-plastin and GST-I-plastin were incubated with (A) Dann2b and no peptide (B) Dann2b antibody and 2x concentration of Dann2 peptide (C) Dann2b antibody and 10x concentration of Dann2 peptide and (D) Dann2b antibody and Dann1 peptide as a control. Molecular weight markers are given in kDa. Arrow denotes specific band at predicted molecular weight. Asterisk denotes background band. Dann2b antibody binding was not completely inhibited by the peptide as there was a signal detected in both the 2x and 10x concentration panels. The control peptide gave no inhibition of Dann2b binding to T-plastin.

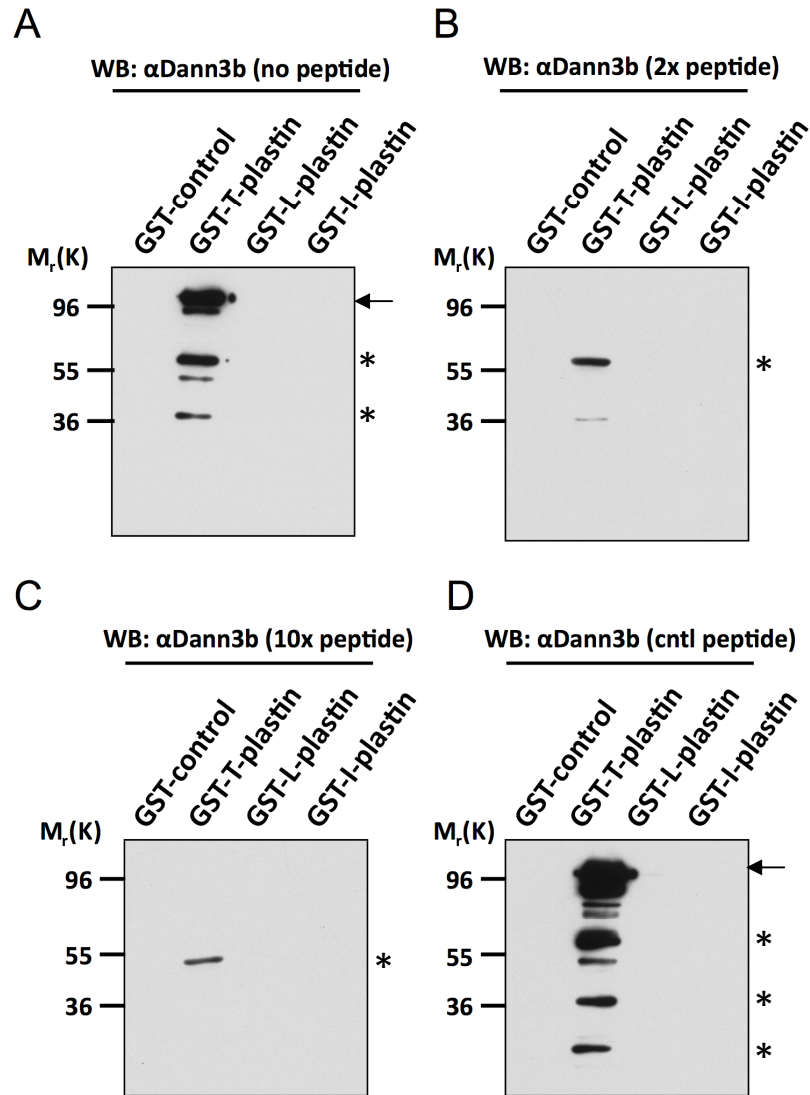


Figure 4.10: Confirmation of the specificity of Dann3b antibody by peptide inhibition assay

Lysates from bacteria expressing GST-fusion proteins were analysed by 10% SDS-PAGE, transferred to PVDF membrane and immunoblotted. GST-cntl, GST-T-plastin, GST-L-plastin and GST-I-plastin were incubated with (A) Dann3b antibody and no peptide (B) Dann3b antibody and 2x concentration of Dann3 peptide (C) Dann1a antibody and 10x concentration of Dann3 peptide and (D) Dann3b antibody and Dann1 peptide as a control. Molecular weight markers are given in kDa. Arrow denotes specific band at predicted molecular weight. Asterisk denotes background band. Dann3b antibody binding was partially inhibited by the peptide as there was a signal detected in both the 2x and 10x concentration panels. The control peptide gave no inhibition of Dann3b binding to T-plastin.

4.2.2.5 Detection of plastins in mouse tissue using the Dann antibodies

Having shown that the Dann1a antibody recognised its target antigens, and was largely specific in the context of a bacterial lysate, the next step was to test them against mouse tissue. Muscle, spleen, kidney and liver were selected as the tissues to test because T-plastin is expressed in normal muscle, L-plastin is expressed in normal spleen and I-plastin is expressed in normal kidney (Shinomiya, 2012). Liver was taken as an additional tissue since T-plastin is expressed in immortalised (cancer) liver cell lines (Ikeda et al., 2005).

Mouse tissue samples were analysed by SDS-PAGE and stained by coomassie to confirm that protein had been recovered post-lysis (Figure 4.11 A). Equivalent samples were run on SDS-PAGE, transferred to PVDF membranes and immunoblotted using the Abcam T-plastin antibody (Figure 4.12 B), the I-plastin antibody from Dr. Francisco Rivero (Figure 4.11 C) and the Dann1a antibody (Figure 4.11 D). The Abcam antibody recognised a ~70 kDa band in muscle, spleen and kidney, but not in liver. Additional bands were also seen in spleen and kidney (Figure 4.11 B). Thus, the Abcam antibody did not appear to be very specific. The I-plastin antibody detected a single band in kidney, as expected, and a weak band in spleen (Figure 4.11 C). The Dann1a antibody detected the same ~70 kDa band in spleen, confirming that it detected L-plastin cleanly. The Dann1a antibody also decorated a single band in mouse muscle, but this protein ran at ~50 kDa rather than the expected molecular mass of T-plastin which is ~70 kDa (Figure 4.11 D). Although it is possible that some degradation of the muscle plastin occurred during lysis, the Abcam antibody did detect a ~70 kDa protein in muscle. It should also be noted that no signal was detected in liver for T, L or I-plastin. The overall con

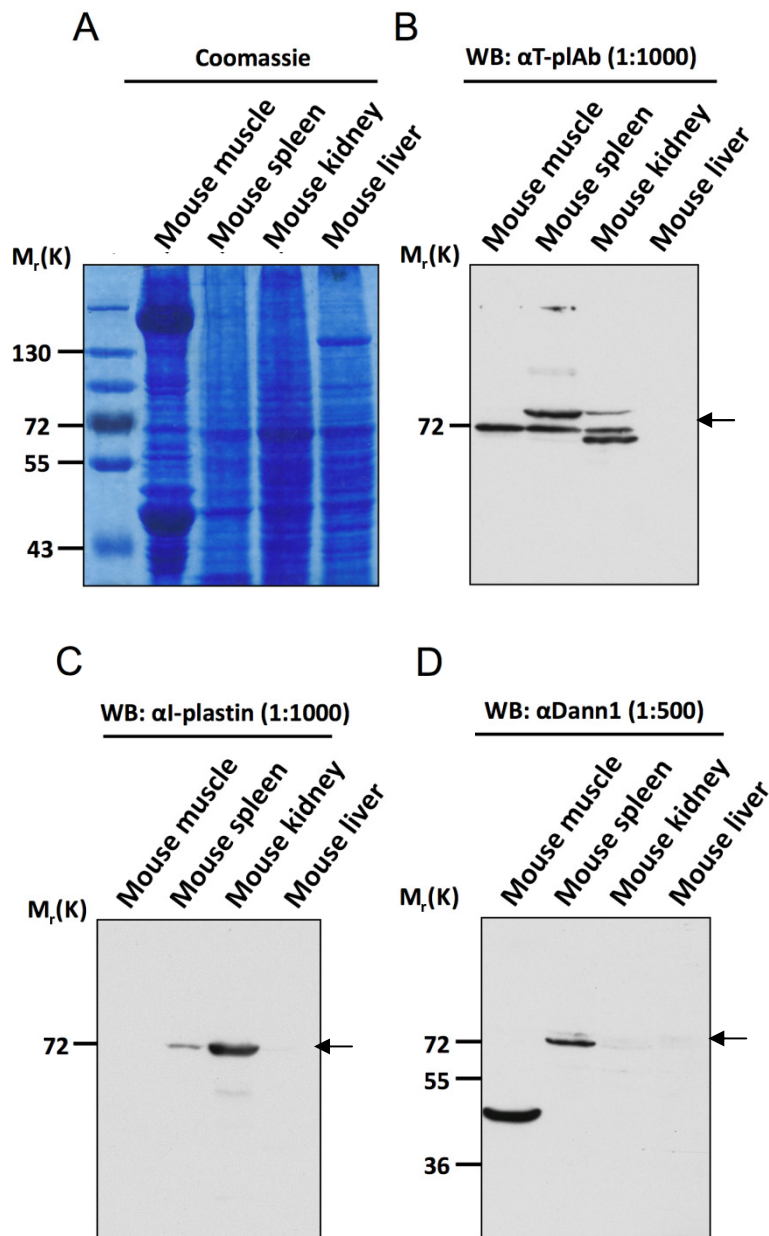


Figure 4.11: Confirmation of the specificity of Dann1a using mouse tissue

(A) Lysates from mouse muscle, spleen, kidney and liver tissue were analysed by 10% SDS PAGE prior to staining with colloidal coomassie. Lysates from mouse muscle, spleen, kidney and liver tissue were analysed by 10% SDS PAGE, transferred to PVDF membrane and probed with (B) T-plastin antibody (Abcam) (C) I-plastin antibody as used in Figure 4.6 and (D) Dann1a 1:500 dilution. Molecular weight markers are given in kDa. Arrow denotes specific band at predicted molecular weight. Dann1a recognised a ~50 kDa in muscle and a ~70 kDa band in spleen.

4.2.2.6 Detection of plastins in cell lines

The Dann1a antibody gave a signal at the expected molecular weight against spleen tissue, but an unexpected specific signal against a protein of ~55 kDa from muscle. To investigate the size of the plastin protein being detected by Dann1a, the antibody was tested against immortalised cell lines (Figure 4.12). The CRC cell lines SW480/lamA, SW480/cntl and SW620 were used for this analysis. Willis et al. previously showed that T-plastin was upregulated in the SW480/lamA compared SW480/cntl cells, as determined by RT-PCR (Willis et al., 2008). In addition, Foran and colleagues have shown that L-plastin is absent in the SW480 cell line but elevated in its metastatic counterpart SW620. Cell lysates were generated and equal amounts were taken for Coomassie staining (Figure 4.12 A) and for Western blotting (Figure 4.12 B and C). As expected, no Dann1a signal could be detected in the SW480/cntl cell line, whereas a doublet at ~70 kDa could be detected in the SW620 cells, most likely corresponding to T-plastin and L-plastin. A single band was seen in the SW480/lamA cell line, consistent with the induction of T-plastin but not L-plastin by lamin A expression.

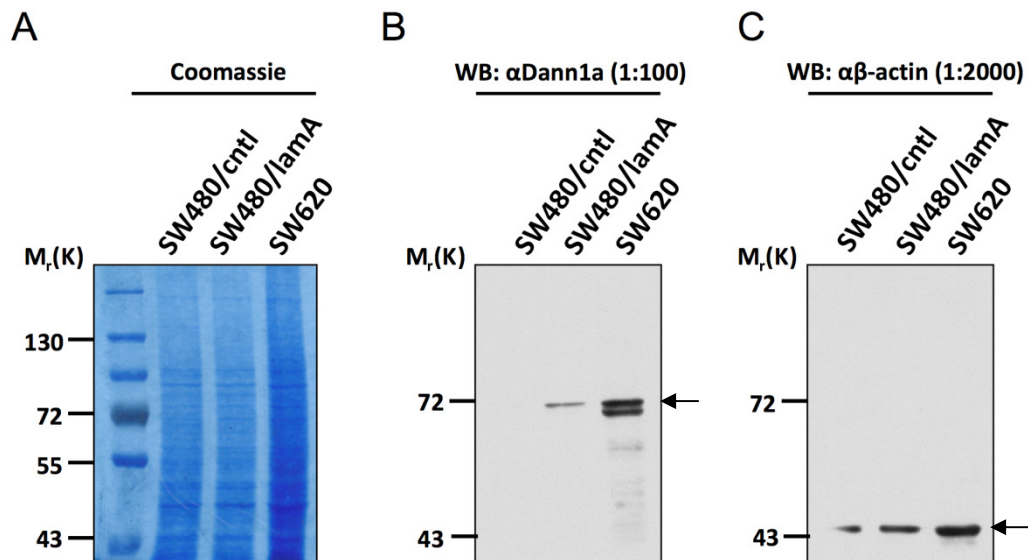


Figure 4.12: Confirmation of the specificity of Dann1a using CRC cell lines

(A) Lysates from SW480/cntl SW480/lamA and SW620 were analysed by 10% SDS PAGE prior to staining with colloidal coomassie. Lysates from SW480/cntl SW480-lamA and SW620 were analysed by 10% SDS PAGE, transferred to PVDF membrane and probed with (B) Dann1a 1:100 dilution and (C) β -actin as a control. Molecular weight markers are given in kDa. Arrow denotes specific band at predicted molecular weight. Dann1a recognised a single band of ~ 70 kDa in the SW480/lamA and a doublet at a similar molecular weight in the SW620 cells.

4.3 Discussion

In this chapter, we characterised polyclonal plastin antibodies raised against three immunising peptides and demonstrated their specificity by a combination of Western blotting and peptide inhibition assays. The antibodies were tested against recombinant proteins in an *E. coli* lysate, murine tissues and CRC cancer lines. Sequence analysis of the plastins showed that they are well conserved, both within the plastin family and between species (Figures 4.2 and 4.3). This makes designing isoform-specific antibodies challenging. The central region of T-plastin is the most divergent, and the Dann2 peptide designed in this region was only 54% identical to the equivalent peptide sequence in L-plastin. The Dann2b antibody raised against this peptide showed high affinity by ELISA (Supplementary Figure S2) and gave a specific signal when used for Western blotting against recombinant GST-T-plastin (Figure 4.7). The interaction between Dann2b and its antigen could be partly inhibited by pre-incubating the antibody with the immunising peptide (Figure 4.9), providing further evidence of a high affinity interaction with the GST-T-plastin protein. To explore this further, experiments could be performed to titrate the antibody with even higher concentrations of peptide, if desired, or by using higher dilutions of the antibody. Unfortunately, although the Dann2b antibody looked the most promising in the fusion protein analysis, it did not work in immunoblotting on cell lysates, despite numerous attempts using different extraction protocols (data not shown). This finding highlights the fact that while antibody reactivity may be excellent in the context of a bacterial lysates, this does not necessarily mean that there will be a positive result when the antibody is tested on mammalian cells.

In contrast to the Dann2b antibody, the Dann2a antibody did not recognise GST-T-plastin (Figure 4.7), despite having a high titre when measured against the peptide in ELISA (Figure S2). This finding demonstrates that the context of an epitope within a protein sequence is important for its antigenicity. It may be that some secondary structure is lost in the SDS-denatured protein, since although the Dann2 peptide is only 13 residues in length, it does have 2 proline residues and a glycine that may introduce kinks in its secondary structure. The difference between the Dann2a and Dann2b antisera also demonstrate that individual animals can raise very different antibody responses to the same peptide. The B cell repertoires of the two animals used to raise these antibodies will not be the same, due to B cell specific antibody gene rearrangement and somatic hypermutation in the germinal

centres (Manz et al., 2005). The different antibody responses made by individual rabbits also highlight the potential problem in using polyclonal antisera as potential biomarkers. Each time a new antibody is raised against the same peptide, an equivalent antibody response cannot be guaranteed. Therefore, the preferred choice is to raise a monoclonal antibody through hybridoma technology. Although this is more time consuming, the immortalised B cell hybridoma produced will continue to secrete the same antibody throughout the cells lifetime, ensuring a consistent antibody product. Alternatively, phage display or yeast surface display technologies could be used to try and develop specific antibodies to closely related sequences such as those found in the plastins (Baird et al., 2009).

The Dann3 peptide did not produce a useful antibody. Dann3a gave no signal, whereas Dann3b gave a background band that could not be blocked by the immunogen (Figure 4.10). Interestingly, the antibody response to Dann3 did seem to be specific to T-plastin and Dann3b did not bind to GST-L-plastin or GST-I-plastin despite the peptide sequences being ~75% identical in this C-terminal region. To probe the nature of the Dann3b epitope (or any of the Dann antibodies) further, one could synthesise a nested series of truncated peptides to see at what point the antibodies ceased to recognise the antigens. Similarly, alanine mutations in the immunising peptide could be introduced at different positions to determine which amino acids were specifically required for antibody binding, either by ELISA or by western blotting.

The most promising antibody arising out of the work in this Chapter was Dann1a. Although this antibody recognised both T-plastin and L-plastin, it did not cross-react with any bacterial or mammalian proteins, and it could be specifically inhibited by the immunising peptide (Figures 4.6-4.8). Dann1a also detected plastins in muscle and spleen (Figure 4.12). The role of T-plastin in muscle is worthy of further investigation. Dann1a recognised a ~55 kDa species in bacterial lysates and in muscle (Figure 4.8 and Figure 4.11). This band looked specific, at least in the recombinant protein blots, because it was inhibited by the peptide. Since lamin A/C mutations often give rise to muscle phenotypes (Benedetti and Merlini, 2004) and lamin A/C expression may be linked to that of T-plastin, it might be worth studying T-plastin function in the muscle to determine whether or not unusual alternative splicing or protein processing of T-plastin is occurring in this tissue. T-plastin has been shown to be upregulated in failing hearts compared with non-failing hearts, in patients with end-

stage dilated cardiomyopathy (Tan et al., 2002). Since proteolytic stress responses are induced during heart failure by mechanical injury and neurohormonal perturbations (Vatner and Vatner, 1998), one explanation for the 55 kDa band in muscle might be that T-plastin is regulated by proteolysis. Further experiments to study the half-life and post-translational modification of T-plastin in heart muscle could be performed by taking cardiomyocytes in culture and subjecting them to pulse-chase metabolic labeling experiments. It might also be possible to compare T-plastin protein expression and regulation in skeletal and heart muscle in animals, for example by performing muscle 'work rate' experiments in mice. Another possible explanation for the 55 kDa T-plastin band in muscle is that the protein is regulated by alternative splicing, and that muscle expresses a different form to spleen. Consultation with the human protein atlas (www.proteinatlas.org) shows that at least nine *PLS3* alternative splice variants have been annotated, potentially giving rise to a range of protein species in addition to the regular 71 kDa form (*PLS3-001*). However, whether these additional splice variants are functionally expressed in muscle or other tissues is not clear. T-plastin is also subject to post-transcriptional regulation by the mRNA decay pathway and this process could have a degree of transcript or tissue specificity (Brazao et al., 2012). The expression of plastins in normal liver is also worthy of further investigation, since no signal was detected in liver with any of our antibodies (Figure 4.11). The absence or presence of plastins in this organ could be tested by RT-PCR. If no mRNA were to be detected, liver could be investigated as a model for how the cytoskeleton is organised in the absence of plastin expression. If mRNA is detected, it would be interesting to investigate why the Dann1a and the Abcam antibody do not detect it. Perhaps T-plastin is alternatively spliced or rapidly turned over in this tissue.

The induction of T-plastin expression by GFP-lamin A was also confirmed by immunoblotting, using the Dann1a antibody, and the result suggested that T-plastin but not L-plastin was upregulated (Figure 4.12). Why lamin A expression should selectively induce only one of the plastin genes is not known, and is worthy of further exploration. The fact that Dann1a detects a doublet in the SW620 cells suggests that it could be a good tool to probe the relative levels of T-plastin and L-plastin in various cell types. Taken together, the data in this Chapter suggest that Dann1a is specific to both T and L-plastin isoforms and this antibody can now be used for the further study of plastin in CRC cell lines and tumour tissues.

Chapter 5: Immunohistochemical analysis of plastin expression in colorectal cancer

5.1 Introduction

Plastins belong to a family of actin bundling proteins, which function to cross-link actin filaments in networks (Delanote et al., 2005). This is essential for the formation of specialised cell structures and remodelling of the actin cytoskeleton (Stevenson et al., 2012). Three plastin isoforms exist, sharing approximately 70% similarity in their amino acid sequence, each of which is expressed in a tissue specific manner. Importantly, the different plastin isoforms have been implicated in a number of cancers (Lin et al., 1993; Shinomiya et al., 2012). The expression of L-plastin, for example, is induced in many types of cancerous human cells of non-haematopoietic origin (Lin et al., 1993). In addition, Osuka and colleagues identified L-plastin as a metastatic marker for CRC progression in a tissue microarray consisting of 58 clinically stratified specimens (Otsuka et al. 2001). This group showed that L-plastin gene expression correlated with cancer stage, and suggested that L-plastin is a potential metastatic marker. However, the antibody stainings in this paper are not entirely clear.

It has been shown previously that T-plastin mRNA expression is increased upon stable transfection of GFP-lamin in the SW480 CRC line (Willis et al., 2008). Moreover, we have observed that T-plastin mRNA expression is significantly upregulated in human colorectal tumours, compared to the corresponding normal colonic mucosa (Chapter 3, Figure 3.11 B and C). Given the potential importance of plastin in cancer, we sought to examine T/L-plastin expression in the NLCS cohort (Figure 5.1), using the Dann1a antibody characterised in Chapter 4. The overall aims of this chapter were to examine the expression pattern of T/L-plastin in human CRC tumours, investigate the relationship between expression and tumour progression and explore the potential of T/L-plastin as a prognostic biomarker in CRC.

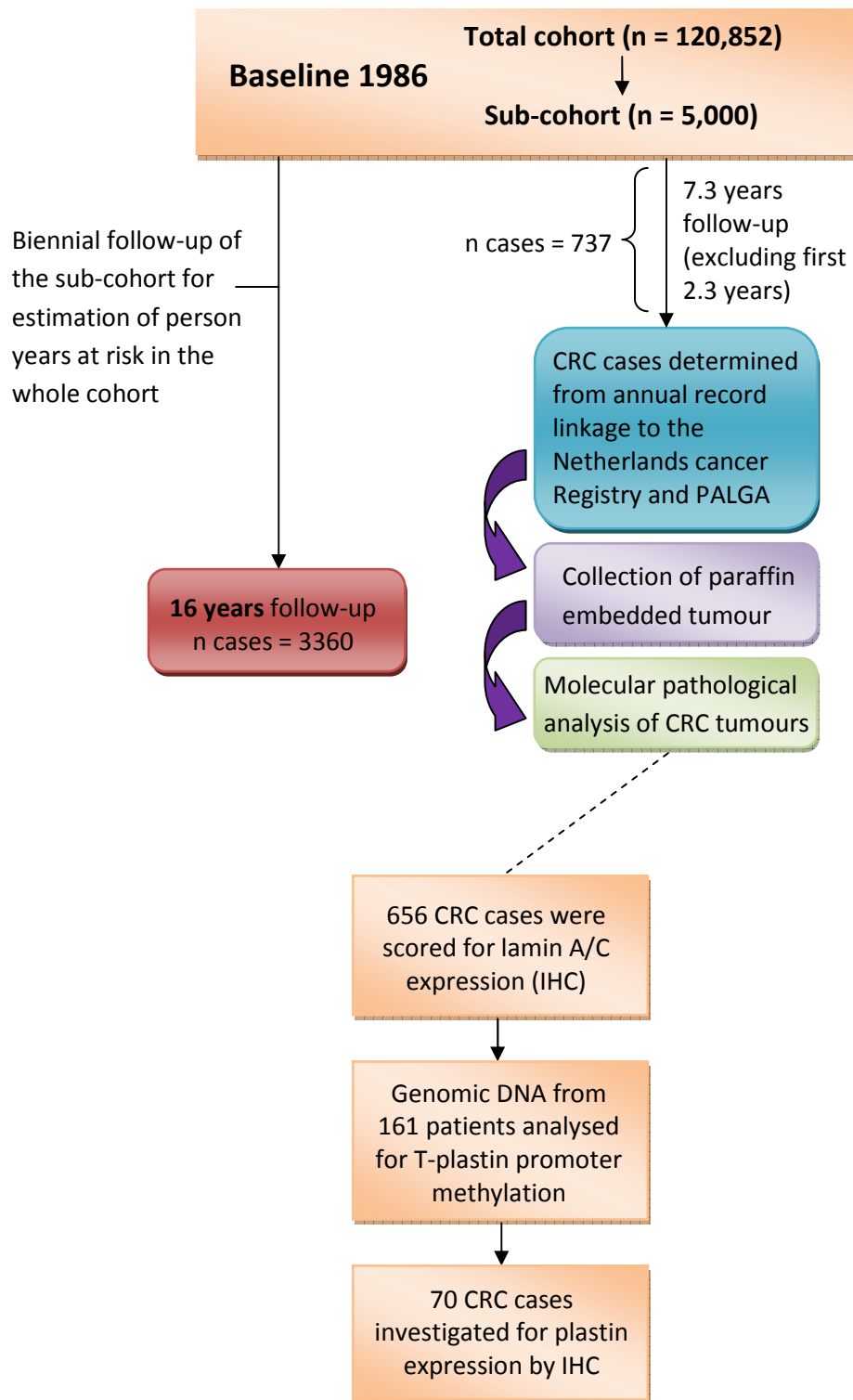


Figure 5.1: Study design of the Netherlands Cohort Study on Diet and Cancer (NLCS)
 (adapted from Hughes, 2011)

5.2 Results

5.2.1 Characterisation of platin antibodies in normal human skin and colon

In the previous chapter, we successfully characterised the Dann1a antibody by Immunoblotting. Here, we wanted to establish whether this antibody could recognise platin in human tissues. Prior to assessing the platin expression status in human colorectal carcinomas from the NLCS archive, normal human skin was used to further characterise the Dann1a antibody, as T and L-platin platin were known to be expressed in the epidermis and infiltrating leukocytes, respectively (Shinomiya, 2012). Initially, tissues were subjected to different antigen retrieval techniques. Skin sections exposed to primary antibody Dann1a produced highly specific staining after microwave digestion with Tris-EDTA buffer pH 8.0, and a specific but weaker stain with citrate buffer pH 6.0. Thus, it was deduced that antigen retrieval using Tris-EDTA pH 8.0 was optimal and would be used in further experiments (data not shown).

Once an optimal antigen retrieval technique had been established, skin sections were then subjected to different antibody dilutions. Figure 5.2 shows that 1:100 antibody dilution was optimal. Omitting the primary antibody produced negative staining. In the skin sections, Dann1a decorated the epidermal cells and was present in leukocytes, as expected. Interestingly, T/L-platin appeared to be strongly expressed in the nucleus, as well as the cytoplasm of skin epithelial cells (Figure 5.2 A-C). Having optimised the antibody dilution for Dann1a, we then wanted to examine the expression pattern in normal human colonic epithelia. The data showed that T/L-platin expression was absent in normal colon (Figure 5.3).

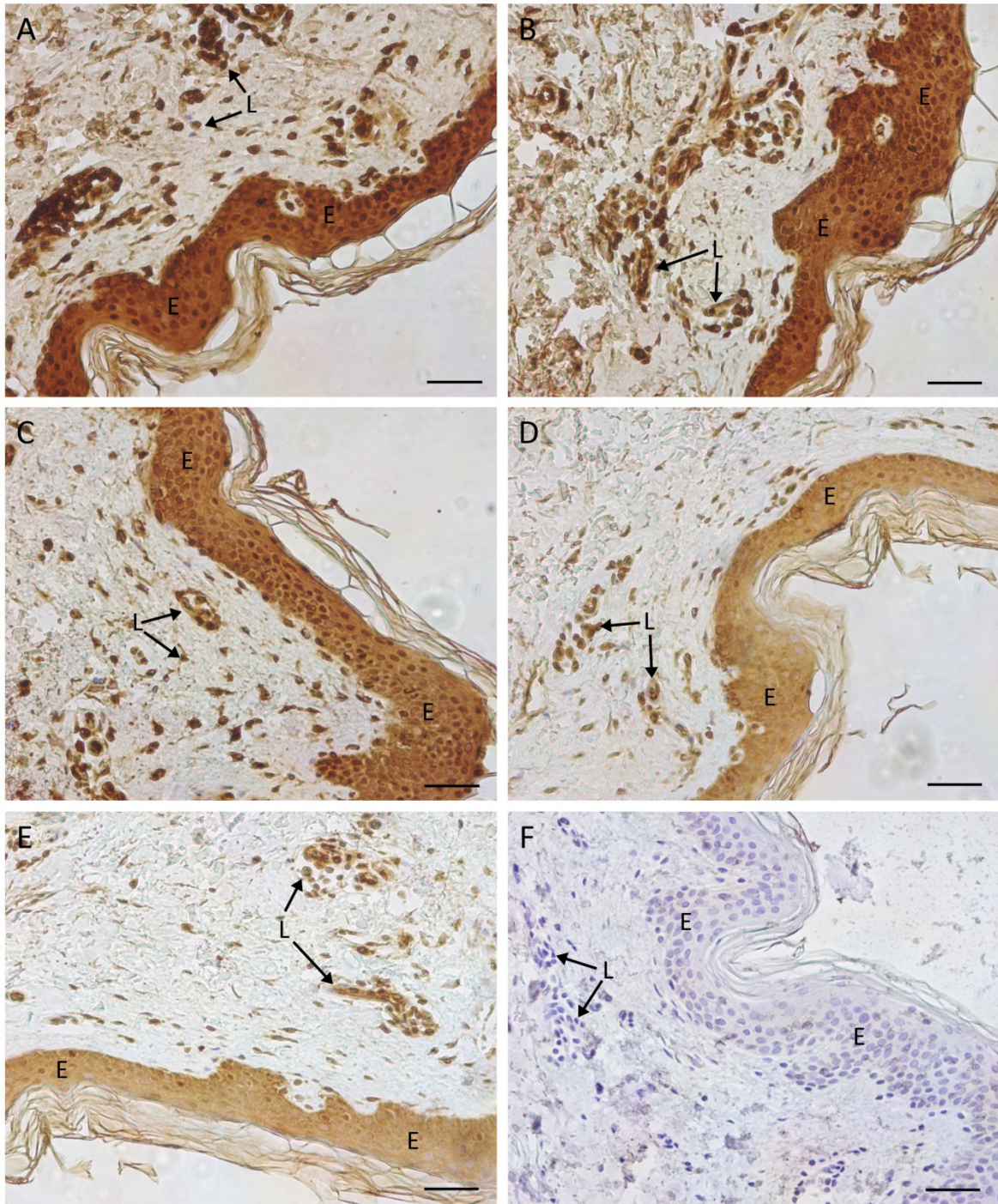


Figure 5.2: Optimisation of Dann1a antibody in normal human skin

Formalin-fixed, paraffin-embedded human skin sections were deparaffinised by xylene, followed by 100% ethanol and endogenous peroxidase activity was quenched in 0.3% hydrogen peroxide. Antigen retrieval was performed by microwave with Tris-EDTA buffer pH 8.0. Sections were incubated with Dann1a antibody at (A-C) 1:50 dilution and (D-E) 1:100 dilution and (F) with no primary antibody, before detection with DAB and photography at x20 magnification. Blue (hematoxylin) staining represents the nuclear staining and brown (DAB) staining represents the antibody (Dann1a). E = skin

epidermis, L = leukocytes. Data shows that Dann1a at 1:100 produced optimal staining. Scale bar = 50 μm .

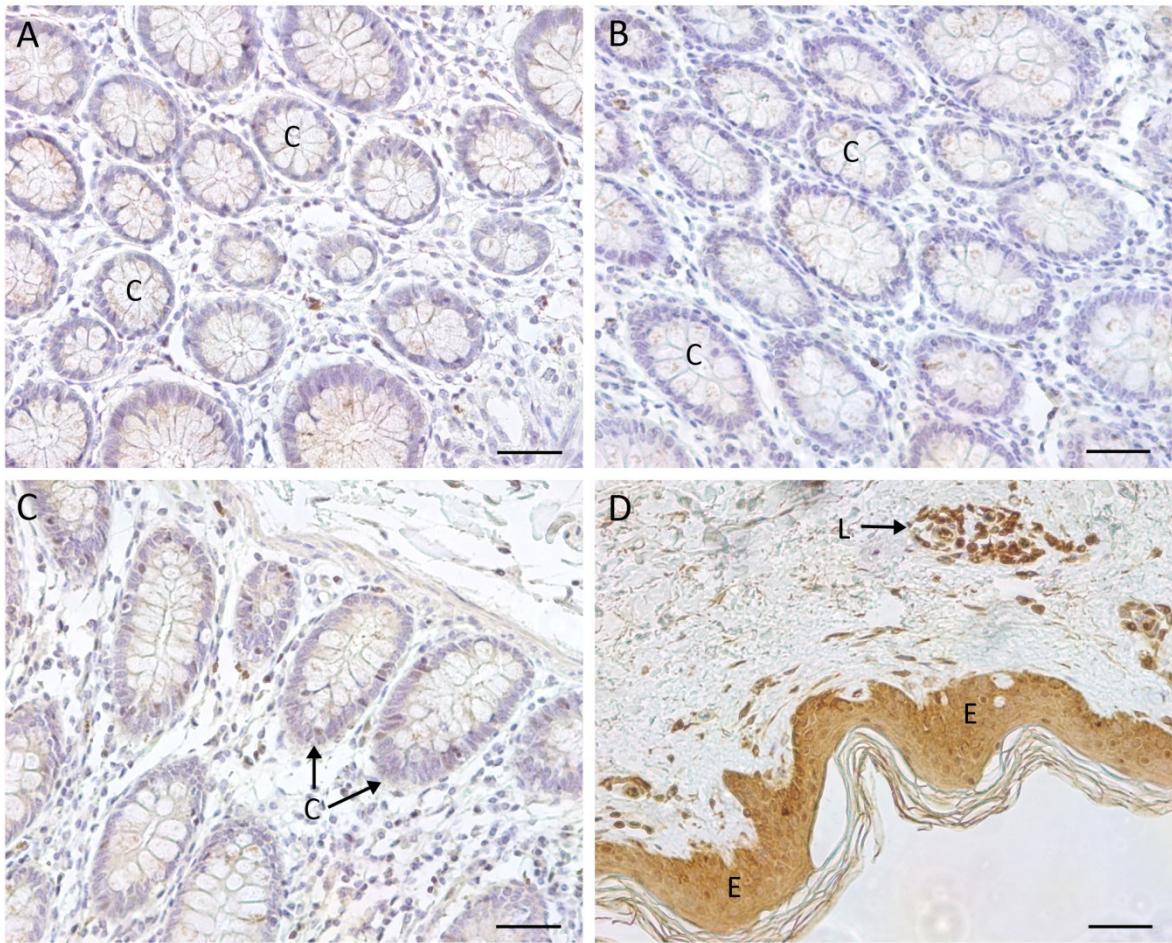


Figure 5.3: T/L-plastin is absent in normal colonic epithelia

Formalin-fixed, paraffin-embedded human colon and skin sections were deparaffinised by xylene, followed by 100% ethanol and endogenous peroxidase activity was quenched in 0.3% hydrogen peroxide. Antigen retrieval was performed by microwave with Tris-EDTA buffer pH 8.0. Sections were incubated with Dann1a antibody at (A-C) 1:100 dilution (normal colon). (D) skin section incubated with Dann1a at 1:100 dilution as a positive control. Images were photographed at x20 magnification. Blue (hematoxylin) staining represents the nuclear staining and brown (DAB) staining represents the antibody (Dann1a). E = skin epidermis, L = leukocytes, C = colonic crypts. Data shows that T/L-plastin is absent from normal colonic crypts. Scale bar = 50 μm .

5.2.2 Immunohistochemical analysis of T/L-plastin expression in CRC

To investigate the pattern of plastin expression in CRC, immunohistochemical analysis was performed on tissues from 70 CRC patient samples from the NLCS archive that had previously been stained for lamin A/C (Figure 5.1). After quenching of endogenous peroxidase activity followed by antigen retrieval, slides were stained for T/L-plastin with Dann1a antibody, exactly as described in Chapter 2, section 8. An example of the staining pattern is shown in Figure 5.4. Muscle always stained strongly and thus was used as a positive control. The availability of an internal positive control demonstrated that a negative stain in tumour tissue corresponded to an absence of antigen rather than poor staining (Figure 5.4 C and D). Normal colonic epithelial cells within the section always stained negatively and hence were used as an internal negative control. Adjacent stromal nuclei stained positively or negatively, depending on the expression pattern of the surrounding tumour tissue. Leukocytes sometimes stained positively (possibly indicating the presence of L-plastin). Out of the 70 slides processed, not all specimens were available for analysis. This was due to either insufficient tumour material, or the lack of an internal control. In addition, the subsequent retrieval of information from the NLCS archive and PALGA databases led to a further reduction to 58 due to incomplete information or the duplication of administrative codes. Slides were scored blind on two separate occasions, in consultation with senior pathologist Dr Robert Reidl (University Hospital Maastricht, Netherlands). A scoring criterion was established, based on the following descriptors; absent, weak, positive, and heterogeneous (Figure 5.5). Tumour cells can be clearly recognised due to the dense staining of haematoxylin (denoted by T, Figure 5.5). However, there were clearly some tissues where tumour cells were present that did not express plastin (Figure 5.5 A-B). Antigen retrieval had occurred in these cases because staining of muscle was seen in the sample. In other examples, tumour tissue stained very strongly for T/L-plastin, when the antibody was used at the same dilution (Figure 5.5 E-F). Of the available 58 specimens immunohistochemically assessed, plastin was found to be positive in 47 (81%) and negative in 11 (19%) patients. This is a remarkable result given that T/L-plastin is not seen in normal colonic tissue.

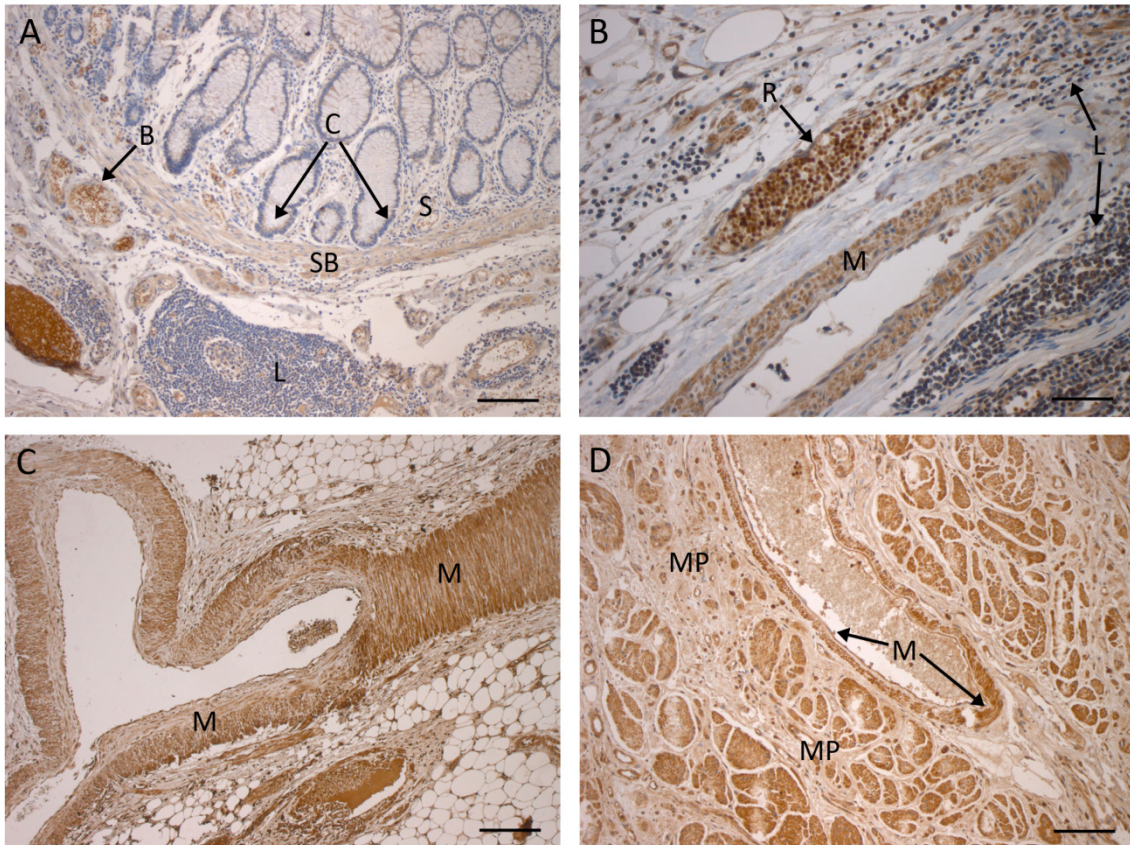


Figure 5.4: Positive plastin expression in muscle and negative plastin expression in normal colonic epithelia within CRC tissue

Four μm thick, formalin-fixed paraffin embedded tissue sections were deparaffinised using xylene, followed by 100% ethanol and endogenous peroxidase activity was blocked in 0.3% hydrogen peroxide. Antigen retrieval was performed by microwave with Tris-EDTA buffer pH 8.0. Sections were incubated with Dann1a primary antibody at 1:100, prior to detection with DAB and photography at x10/20 magnification. B = blood vessel, C = colonic crypts, L = lymphocytes, M = muscle of arterial wall, MP = *Muscularis propria*, R = red blood cells, S = stromal cells. (A & B) Plastin is strongly expressed in red blood cells, weakly in surrounding stromal tissue and is absent from leukocytes and normal colonic crypts. (C and D) Plastin is expressed in muscle cells. Blue (hematoxylin) staining represents the nuclear staining and brown (DAB) staining represents the antibody (Dann1a). Each image is from a different patient. (A & D: x10 magnification; scale bar = 200 μm ; B & C: x20 magnification; scale bar = 50 μm).

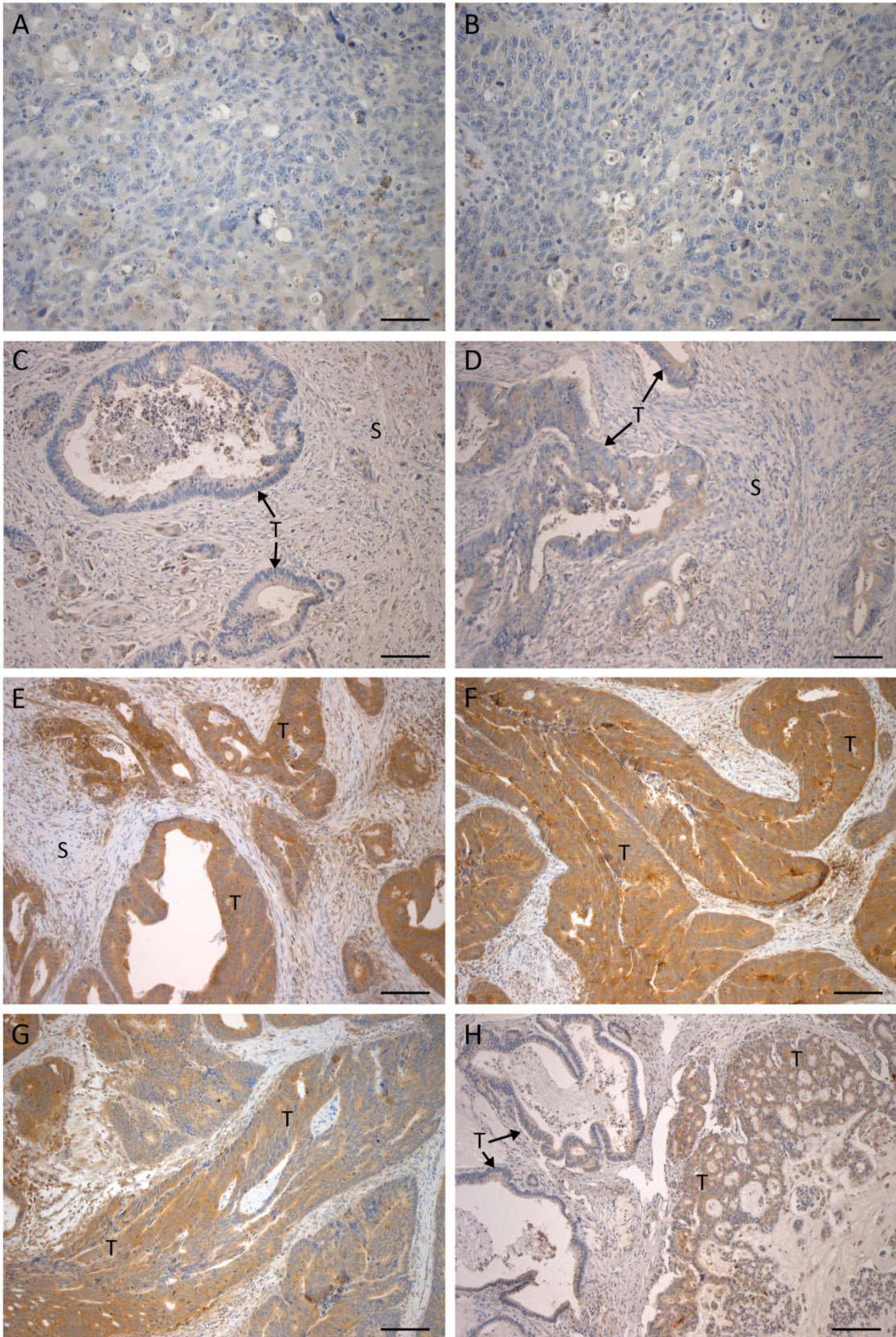


Figure 5.5: T/L-plastin expression in CRC

Four μm thick, formalin-fixed paraffin embedded tissue sections were deparaffinised using xylene, followed by 100% ethanol and endogenous peroxidase activity was blocked in 0.3% hydrogen peroxide. Antigen retrieval was performed by microwave with Tris-EDTA buffer pH 8.0. Sections were incubated with Dann1a primary antibody at 1:100, prior to detection with DAB and photography at x5/10/20 magnification. (A-B) Negative: plastin expression is absent in the tumour and surrounding stromal cells. (C-D) Weak: plastin expression is weak in the tumour and surrounding stromal tissue and (E-G) Positive: plastin is strongly expressed in the adenocarcinoma (D) Heterogeneous: plastin expression is strong in some tumour cells, and weaker in others within the same tissue. T = tumour cells, S = stromal cells. Blue (hematoxylin) staining represents the nuclear staining and brown (DAB) staining represents the antibody (Dann1a). Each image is from a different patient. A-B: x20 magnification; scale bar = 50 μm ; C-G: x10 magnification; scale bar = 200 μm ; H: x5 magnification; scale bar = 400 μm).

5.2.3 T/L-plastin is strongly expressed at the invasive front of colorectal tumours

Having demonstrated that 81% of colon cancers were positive for plastin (including weak, positive and heterogeneous), we went on to examine more closely the expression pattern of plastin in the tumours. Strikingly, we observed in a number of samples that plastin was strongly expressed at the invasive front and comparatively weak at the luminal side of the tumour (Figures 5.6 and 5.7). These observations suggest that plastin expression might play a role in invasiveness or metastasis, since the leading edge of the tumour is the most motile.

5.2.4 T/L-plastin expression in signet ring carcinoma

During our immunohistochemical analysis, we examined one case of signet ring carcinoma (SCC) (Figure 5.8). This is a very rare type of epithelial malignancy that accounts for less than 1% of all CRC cases. SCC is characterised by the histological appearance of individual neoplastic cells containing intracytoplasmic vacuoles with pleomorphic nuclei (Verhulst et al., 2012). Although SCC is rare, data from immunohistochemical studies may provide important information that can aid in the development of better prognostic biomarkers and therapeutic interventions. In the one sample analysed, it was observed that T/L-plastin expression was elevated in this type of cancer, suggesting that plastin could be investigated further as a biomarker for SCC (Figure 5.8). Interestingly, SCCs have mutations in the E-cadherin gene suggesting that there may be a relationship between T/L-plastin and E-cadherin function (Darwanto et al., 2003).

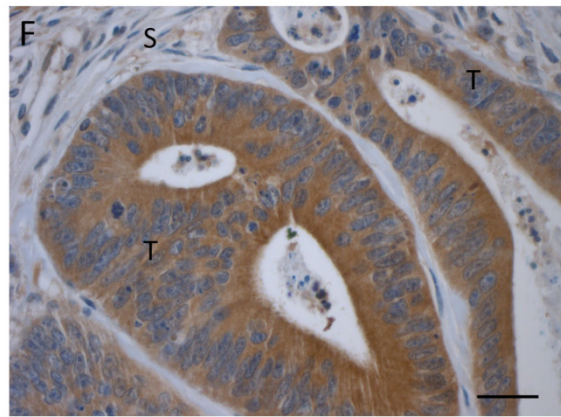
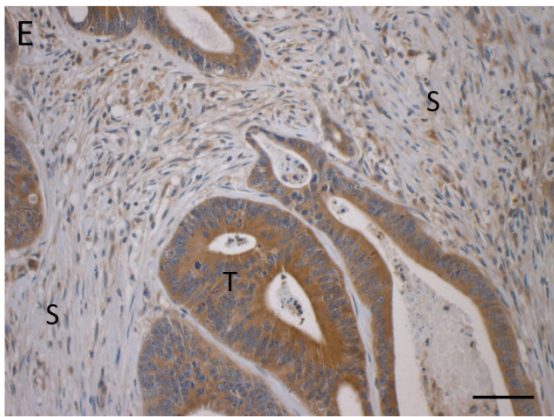
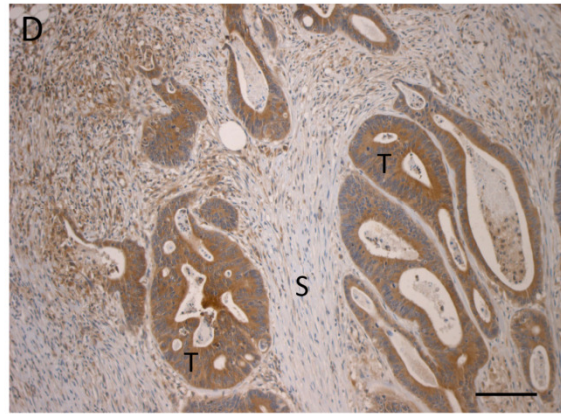
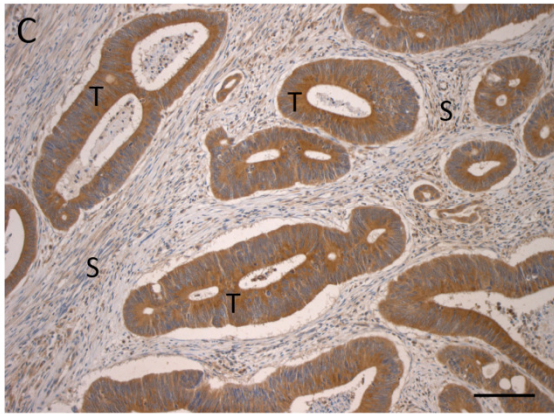
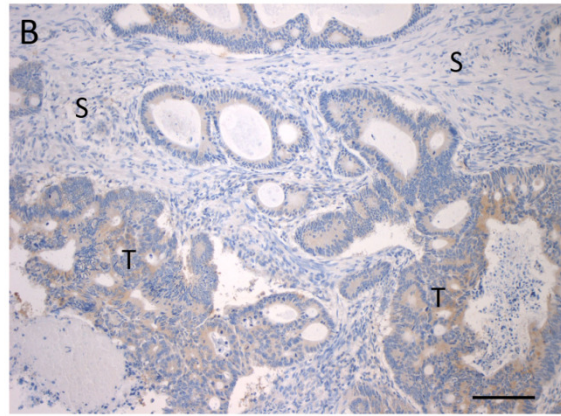
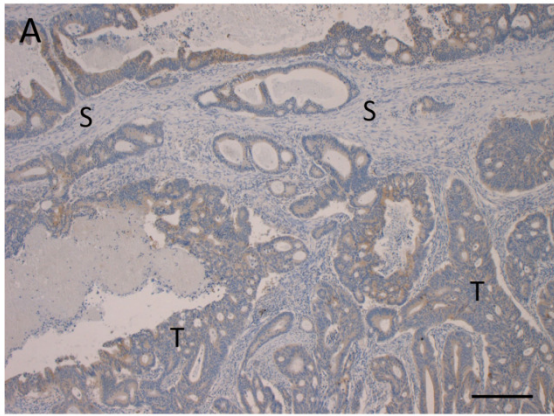


Figure 5.6: T/L-plastin expression at the invasive front of a tumour (patient 1)

Four μm thick, formalin-fixed paraffin embedded tissue sections were deparaffinised using xylene, followed by 100% ethanol and endogenous peroxidase activity was blocked in 0.3% hydrogen peroxide. Antigen retrieval was performed by microwave with Tris-EDTA buffer pH 8.0. Sections were incubated with Dann1a primary antibody, prior to detection with DAB and photography at x5/10/20/40 magnification. All images were taken from the same patient. (A) weak plastin expression at the luminal side of the tissue (x5 magnification) and (B) at x10 magnification. (C) Strong plastin expression at the invasive front of the tumour (x10 magnification) (D) at x10 magnification (E) at x20 magnification and (F) at x40 magnification. Data shows that plastin was strongly expressed at the leading edge of the tumour compared to the luminal counterpart. T = tumour cells, S = stromal cells. Blue (haematoxylin) staining represents the nuclear staining and brown (DAB) staining represents the antibody (Dann1a). Scale bar = 400 μm (x5 magnification); 200 μm (x10 magnification); 50 μm (x20 magnification); 25 μm (x40 magnification).

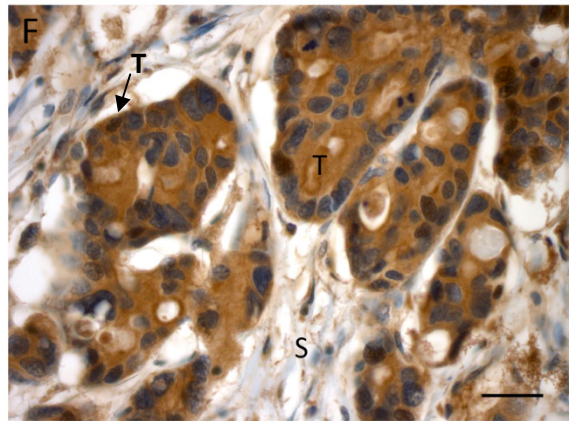
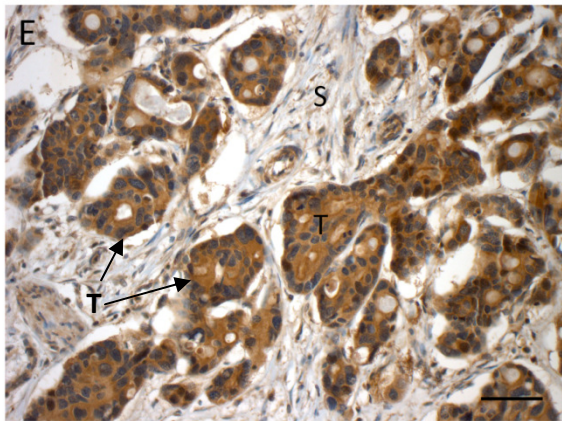
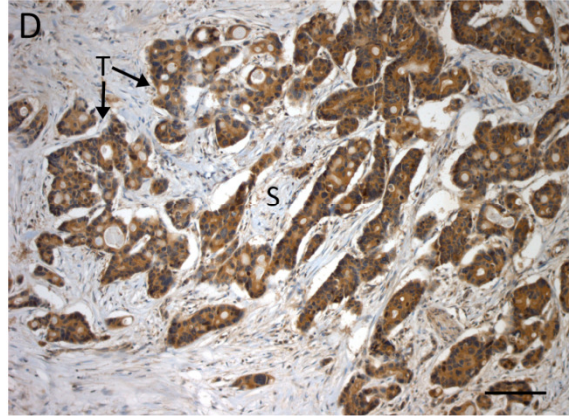
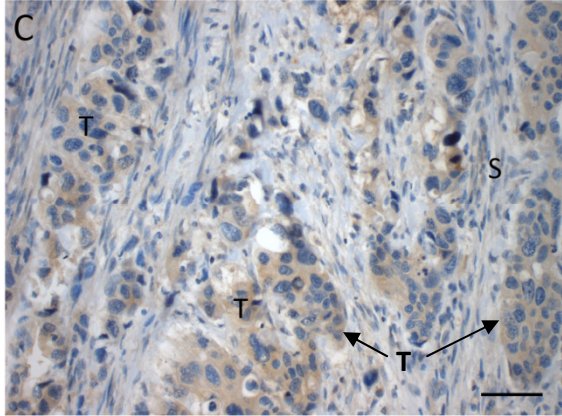
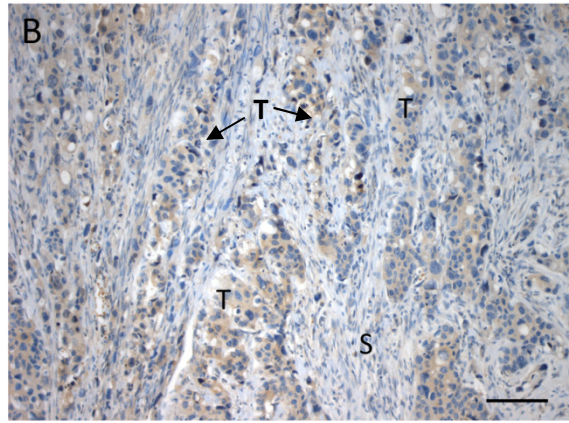
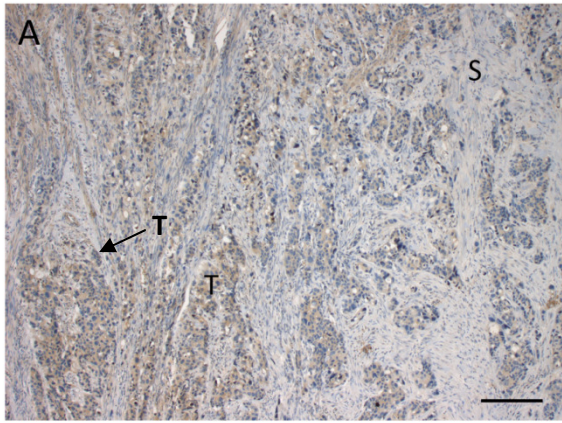


Figure 5.7: T/L-plastin expression at the invasive front of a tumour (patient 2)

Four μm thick, formalin-fixed paraffin embedded tissue sections were deparaffinised using xylene, followed by 100% ethanol and endogenous peroxidase activity was blocked in 0.3% hydrogen peroxide. Antigen retrieval was performed by microwave with Tris-EDTA buffer pH 8.0. Sections were incubated with Dann1a primary antibody, prior to detection with DAB and photography at x5/10/20/40 magnification. All images are taken from the same patient. (A) weak plastin expression at the luminal side of the tissue (x5 magnification) (B) at x10 magnification (C) at x20 magnification. (D) Strong plastin expression at the leading edge of the tumour (x10 magnification) (E) at x20 magnification (F) at x40 magnification. Data shows that plastin was strongly expressed at the leading edge of the tumour compared to the luminal counterpart. T = tumour cells, S = stromal cells. Blue (hematoxylin) staining represents the nuclear staining and brown (DAB) staining represents the antibody (Dann1a). Scale bar = 400 μm (x5 magnification); 200 μm (x10 magnification); 50 μm (x20 magnification); 25 μm (x40 magnification).

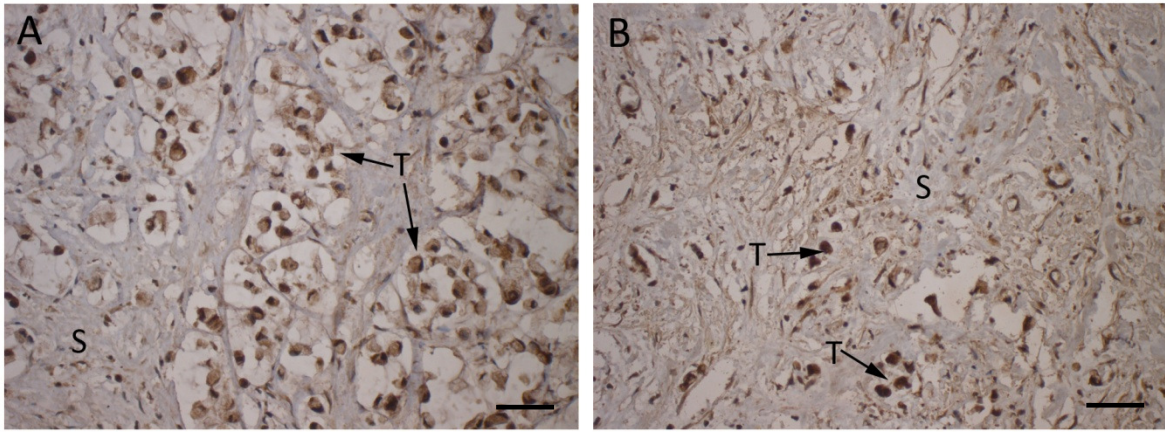


Figure 5.8: T/L-plastin expression in signet cell carcinoma

Four μm thick, formalin-fixed paraffin embedded tissue sections were deparaffinised using xylene, followed by 100% ethanol and endogenous peroxidase activity was blocked in 0.3% hydrogen peroxide. Antigen retrieval was performed by microwave with Tris-EDTA buffer pH 8.0. Sections were incubated with Dann1a primary antibody, prior to detection with DAB and photography at x20 magnification. (A-B) Elevated plastin expression in signet cell carcinomas. T = tumour cells, S = stromal cells. Blue (hematoxylin) staining represents the nuclear staining and brown (DAB) staining represents the antibody (Dann1a). Scale bar = $50\mu\text{m}$.

5.2.5 Patient analysis

The patients included in this study developed cancer between 1989 and 1994. Information on mortality from 1st January 1989 until 1996 (7 years) was retrieved through linkage with the Central Bureau for Statistics. CRC related death was concluded if CRC was determined to be either the primary cause of death or as a primary, secondary or tertiary complication, using the ICD system. Differences in patient, tumour and follow-up characteristics were analysed using the Chi-square (χ^2) test. Kaplan-Meier analysis was selected to investigate survival. Hazard ratios (HR) (an estimate of the relative effect of a variable [e.g. platin expression status] on an event [e.g. CRC mortality]) and corresponding 95% confidence intervals (CI) for CRC-related mortality according to platin status were estimated using Cox regression analysis. All analysis was performed using SPSS. This work was carried out in collaboration with senior epidemiologist Dr Kim Smits (University Hospital, Maastricht).

5.2.5.1 Platin expression versus tumour progression and location

Initial baseline analysis was performed on all patient and tumour characteristics in relation to CRC related mortality (outlined in Table 5.1). The study population characteristics appeared to be normal with 50% (n = 29) of patients being male and 50% (n = 29) of patients being female. There was no statistically significant difference between CRC-related mortality and sex ($p = 0.311$). There was no difference in age at diagnosis and CRC-related mortality ($p = 0.323$). Classification using Dukes' staging system were as follows: Dukes' A, 24% (n = 14), Dukes' B, 24% (n = 14), Dukes' C, 36% (n = 21) and Dukes' D, 16% (n = 9). Furthermore, there was no association between platin expression status and Dukes stage ($p = 0.658$) (Figure 5.9 A). Thus platin expression is present throughout the Dukes stages, indicating that the platin gene must be activated early on during cancer initiation. Although no statistical significance could be attributed to the level of platin expression versus Dukes' stage, there was a trend towards a higher proportion of negatively staining tumours at Dukes' stage B, when the cancer cells are penetrating through the muscle layer. The explanation for this is not known. It would be necessary to follow individual cancers from Dukes' stage A through to Dukes' stage B to establish whether platin can become downregulated upon contact with the muscle cells. The percentage of 'positive' platin expressing tumours does rise from ~70% in Dukes' C to ~90% in Dukes' D, indicating that the more advanced the cancer is, the more likely it is that platin will be expressed. This observation also suggests that platin

expression is not switched off once the tumour cell has acquired the necessary changes to invade and metastasize. Similarly, no association was found between plastin expression and tumour location within the colon ($p= 0.372$) (Figure 5.9 B). However, examination of rectosigmoid tumours showed that the ratio between positive and absent expression was lower than that found in proximal distal and rectal cancers. Further analysis of more rectosigmoid tumour samples will be required to investigate this trend further.

Table 5.1: Follow-up analysis

	Plastin absent	Plastin weak	Plastin positive	Plastin heterogeneous	<i>p</i> -value
Total population, N	11	4	38	5	
Dukes' A, N	2	1	9	2	
Dukes' B, N	5	1	6	2	
Dukes' C, N	3	2	15	1	
Dukes' D, N	1	0	8	0	0.658
Proximal	2	1	12	3	
Distal	4	1	13	0	
Rectosigmoid	3	0	5	2	
Rectum	2	2	8	0	0.372
Male patients, N	8	1	18	2	
Female patients, N	3	3	20	3	0.311
Age at diagnosis, mean (SD)	69.7 (4.41)	70.8 (5.50)	67.6 (3.83)	68.8 (6.14)	0.323

5.2.5.2 T/L-plastin expression versus lamin A/C expression

We previously reported that lamin A/C is a prognostic biomarker for CRC, and that ectopic expression of lamin A/C in CRC cell line SW480 increases the level of T-plastin (Willis et al., 2008). Moreover, it has been shown that L-plastin is elevated in its metastatic counterpart in SW620 (Foran et al., 2005). Here, we have asked whether there was an association between lamin A/C expression (staining previously carried out on the NLCS by Willis et al. 2008) and T/L-plastin expression by χ^2 analysis. This statistical analysis shows that although plastin is expressed in CRC, there is no association between T/L-plastin expression and lamin A/C expression in the samples analysed (Figure 5.10).

5.2.5.3 T/L-plastin expression and patient survival analysis

In order to investigate whether plastin expression was linked to patient survival, two statistical analyses were carried out. Firstly, Kaplan-Meier curves were produced to estimate survival probability (Figure 5.11). Secondly, Cox regression analysis using the Breslow method for ties was performed to estimate the cumulative hazard. The cumulative hazard refers to death as a result of CRC. Co-efficients or hazard ratios > 1 indicate a worse prognosis and a coefficient of < 1 indicates a protective effect. Analysis suggests that plastin expression may be an indicator of worse prognosis (HR = 2.27). However, this observation is not statistically significant in a population in which lamin A/C shows a positive correlation with poor survival (Figure 5.11 A). Moreover, stratified analysis of expression status also confirms that there is no association between plastin and lamin A/C expression (Willis et al., 2008). There does appear to be a trend for patients exhibiting heterogeneous expression to have poor survival, but given that $n = 5$, no reliable conclusions can be drawn.

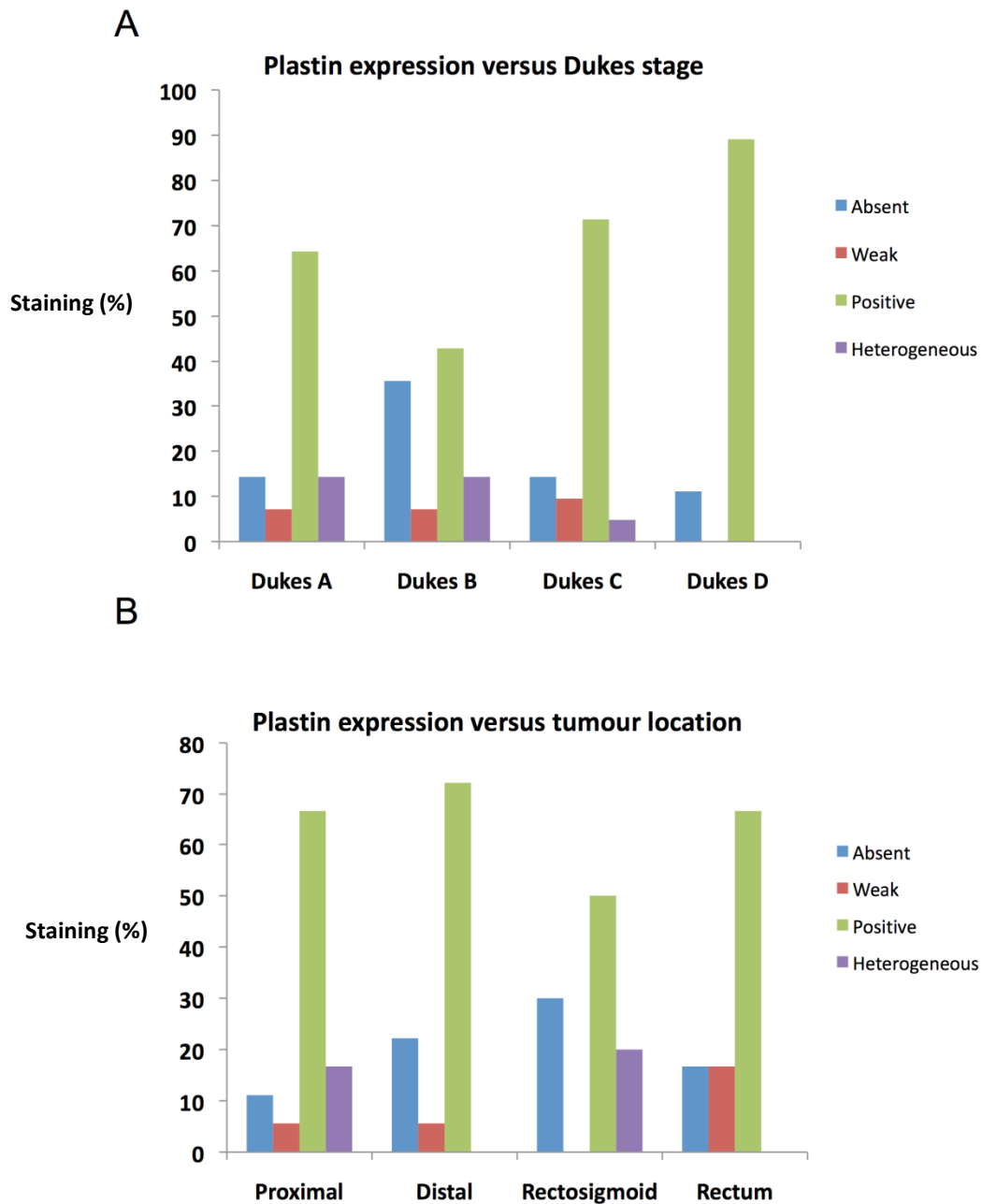


Figure 5.9: T/ L-plastin expression in relation to Dukes' stage and tumour location

(A) Histogram of T/L-plastin expression by stage assessed using 58 tumour samples. Plastin is expressed in all Dukes stages, with highest expression in Dukes' D. There is no association between T/L-plastin expression status and tumour progression ($p = 0.658$). (B) Histogram of T/L-plastin expression by tumour location. There is no association between the frequency of plastin expression and tumour location ($p = 0.372$). Statistical analysis was performed using the Chi (χ^2) test. All p values are two-sided.

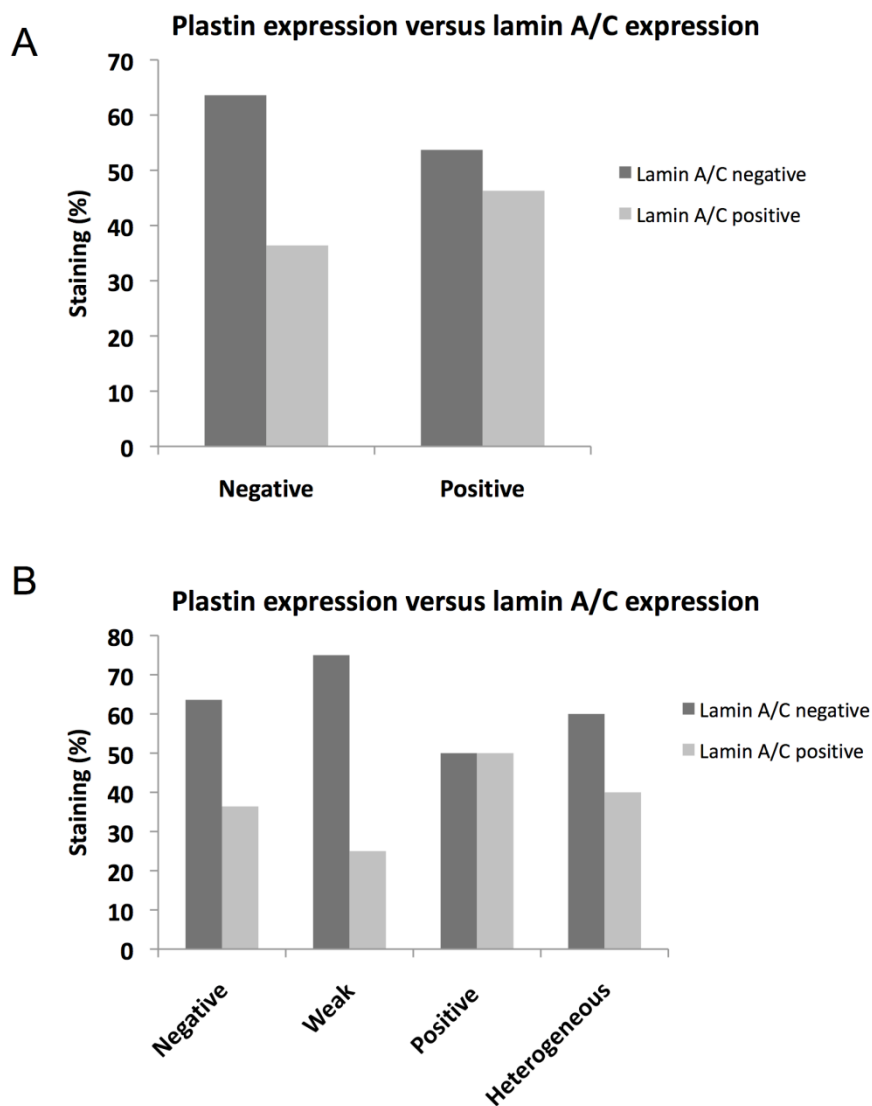


Figure 5.10: T/L-plastin expression versus lamin A/C expression in NLCS tumours

Histograms of T/L-plastin expression status by lamin A/C expression (staining previously carried out by Willis et al. 2008) assessed using 58 tumour samples. (A) There is no association between the presence or absence of T/L-plastin and lamin A/C expression ($p= 0.531$). (B) There is no association between the frequency of T/L-plastin expression and lamin A/C expression in either absent, weak, positive or heterogeneous categories ($p = 0.703$). Statistical analysis was performed using the Chi (χ^2) test. All p values are two-sided.

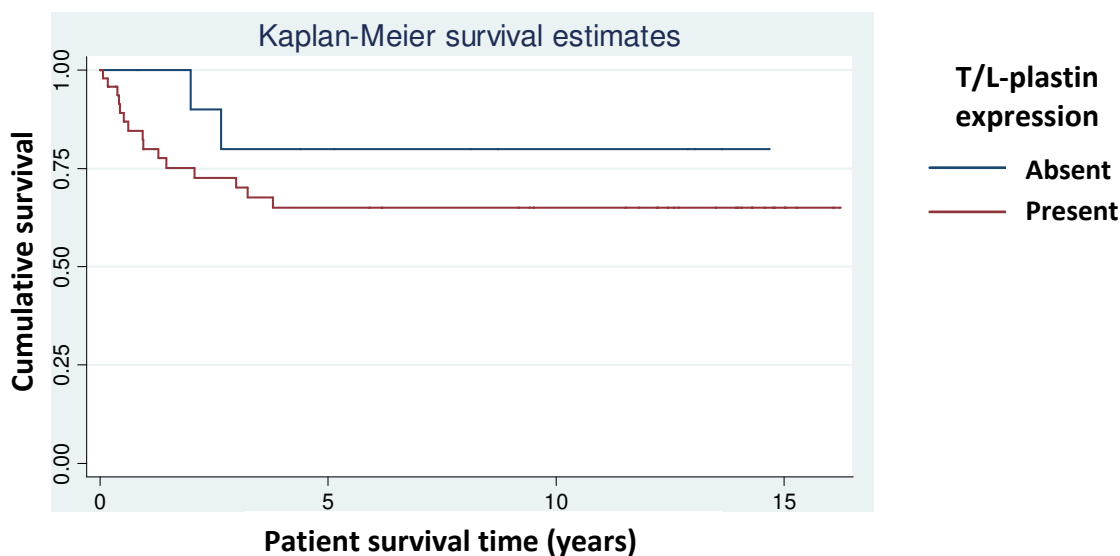
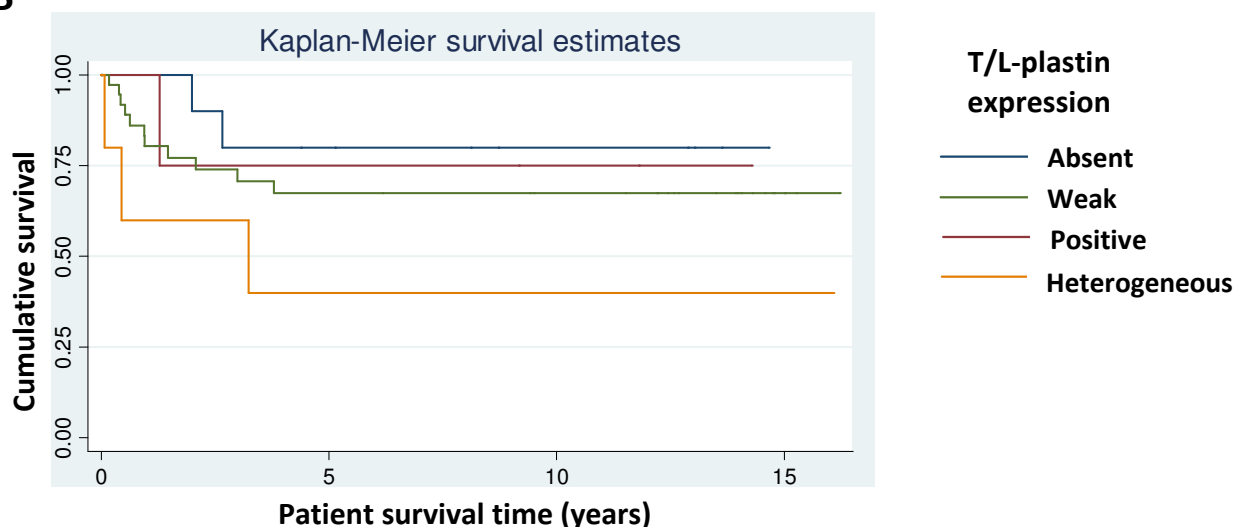
A**B**

Figure 5.11: T/L-plastin expression in CRC and survival

(A) Kaplan-Meier plots of cumulative survival for CRC patients in relation to T/L-plastin expression. Data shows that there is no statistically significant correlation between presence or absence of T/L-plastin expression and survival. Relative hazard ratio (HR) = 2.27 (95% C.I. = 0.50 – 10.18), $p = 0.31$ (adjusted for gender and age at diagnosis). (B) Kaplan-Meier plot of cumulative survival for CRC patients in relation to differential plastin expression. Data shows that there is no statistically significant correlation between expression pattern and survival. Relative hazard ratio (HR) = 1.65 (95% C.I. = 0.87 – 3.15), $p = 0.32$ (adjusted for gender and age at diagnosis).

5.3 Discussion

The availability of the NLCS archive material (University Hospital Maastricht, Netherlands) allowed the expression pattern of T/L-plastin to be investigated in a population in which positive lamin A/C expression is predictive of poor prognosis in CRC. Following successful optimisation of previously established protocols, this study showed that plastin protein epitopes can be successfully re-exposed in formalin-fixed paraffin-embedded tissue specimens and immunohistochemically stained using the Dann1a antibody. This technical approach was both reliable and reproducible (Figure 5.2-5.4).

Plastin expression has previously been implicated in cancer (Lin et al., 1993; Park et al., 1994; Delanote et al., 2005; Ikeda et al., 2005; Sasaki et al., 2002). However, the relationship between its expression and tumourigenesis and prognosis is unknown. Here, we attempted to link T/L-plastin expression to CRC progression and patient survival. Analysis of clinicopathological features in relation to T/L-plastin did not reveal any dramatic findings. In the 58 patient samples analysed, T/L-plastin expression was not associated with gender, age, tumour location or tumour stage (Table 5.1. and Figure 5.9). Moreover, T/L-plastin expression is not associated with the expression of lamin A/C (Figure 5.10), nor was it associated with patient survival (Figure 5.11). In short, T/L-plastin is not a prognostic biomarker for CRC. However, despite this, some interesting observations were made.

Firstly, we demonstrated that T/L-plastin is absent in histologically normal colonic mucosa (Figures 5.3 and 5.4). This is in support of the literature, which states that human plastin isoforms are mutually exclusive and exhibit a tightly controlled tissue-specific expression pattern. I-plastin is the only isoform usually present in the colon (Lin et al., 1993b; Delanote, et al. 2005). Given the absence of T/L-plastin in normal colon, finding that at least one of these plastin isoforms is switched on in CRC is quite remarkable (Figure 5.5). Over 80% of the tumour samples that were analysed exhibited weak, positive or heterogeneous expression. Thus it is clear that the onset of T/L-plastin expression must be associated with a switch from a normal cell type to a dysregulated cancer cell type. During the preparation of this thesis, a recent publication reported that L-plastin is expressed in 82.5% of CRC, independently validating our results. These investigators also showed that L-plastin is associated with tumour stage, size and lymph node metastasis (Li and Zhao, 2011). Given that our study

showed highest expression of plastin in Dukes' stage D, it would be interesting to examine the expression of plastin in the lymph nodes and other organs of Dukes' D patients, to assess whether plastin levels remain high in cells that have metastasized. One limitation of our study was that the Dann1a antibody used could not differentiate between T/L-plastin. Thus it is possible that either T or L-plastin may have independent prognostic value and may become correlated with lamin A/C expression. To explore this further, it would be useful to have specific antibodies, preferably of monoclonal origin, to differentially detect the plastin isoforms.

Within our cohort of 58 tumour samples, one was classified as a signet ring carcinoma (Figure 5.8). Although this type of cancer is less prevalent than adenocarcinomas, it was interesting to observe that this specimen showed elevated levels of T/L-plastin. Signet ring tumours are characterised by loss of E-cadherin, a hallmark of metastasis (Gopalan et al., 2011). E-cadherin plays a crucial role in epithelial cell-cell adhesion and in the maintenance of tissue architecture. It has been extensively documented that downregulation of E-cadherin correlates with a loss of cell adhesion and a strong invasive potential (Tsanou et al., 2008). Moreover, Foran and co-workers have shown that ectopic expression of L-plastin in the SW480 CRC cell line caused a downregulation of E-cadherin and increased invasiveness of the cells (Foran et al., 2006). Taken together, this suggests that E-cadherin and T/L-plastin are dysregulated as part of the cytoskeletal signalling network that leads to changes in a cells capacity to migrate. The effect of A-type lamin expression on E-cadherin levels will be explored in Chapter 6.

Another interesting observation was the presence of strong plastin expression at the invasive front of the tumour compared to the luminal counterpart (Figure 5.6 and 5.7). What this represents functionally within the tumour remains unclear. However, two potential scenarios can be imagined. In the first scenario, upregulation of plastin could promote invasion and metastasis through the increased formation of actin-rich protrusions. In cancer, cytoskeletal remodelling is essential for a cell to acquire invasive and metastatic abilities (Stevenson et al., 2012). Metastatic cancer cells use specialised cell structures such as filopodium and invadopodium which allow the cancerous cell to escape from the primary tumour and pervade the surrounding tissue (Mattila and Lappalainen, 2008; Stevenson et al., 2012; Weaver, 2006). Upon reaching the vasculature or lymphatic system, the cancer cell

can establish a new niche and seed a new tumour (Hanahan and Weinberg, 2011). Since recent evidence shows that that T-plastin may be involved in filopodia formation, it is conceivable that plastin(s) help to increase force generation and mechanical stiffness through the generation of these specialized cell structures. For example, Xue et al. have used mouse melanoma cells transfected with mCherry-T-plastin and shown that T-plastin is enriched in filopodia (Xue et al., 2010). When cell movement was studied using time-lapse confocal microscopy, the lateral motion of these structures was related to the direction in which cancer cells migrate. Interestingly, the lateral filopodia decorated with T-plastin appeared at the 'leading edge' of the cell and moved in the opposite direction to that of the cell with time, implying that a force generating system was at work.

Increased mechanical stiffness is frequently observed in cancer and is often associated with metastasis and poor prognosis (Evans et al., 2012; Fung et al., 2011; Narumiya et al., 2009). So in a second scenario, aberrant expression of plastin may lead may alter the mechanical stiffness of a cell and disrupt its normal contextual behaviour. Cells sense mechanical cues from the ECM using an interconnected mechanochemical system that links adhesion receptors to the cytoskeletal network (Butcher et al., 2009; Erler and Weaver, 2009). Alterations in this mechanical interaction between the cell and the environment may compromise tissue integrity, potentially contributing to cancer formation. For example, numerous members of the cell survival MAPK/ERK signalling pathway are increased/activated when osteoblasts are subjected to a mechanical stress of 0.5 Hz for one hour per day (Yan et al., 2012) and notably a similar set of genes are also associated with a lamin A related cancer gene network which will be discussed in Chapter 6. Increased 'stiffness' and increased matrix remodelling is frequently observed at the tumour invasive front where we found T-plastin to be highly expressed. To test the hypothesis that T-plastin contribute to mechanical stiffness, mechanical stress experiments could be performed (perhaps in association with scratch-wound migration studies) in colon cancer cells that either overexpress T-plastin, or are downregulated for T-plastin using optical tweezers positioned at filopodial locations (Bordeleau et al., 2011). This approach could also be used to establish whether direct binding of T-plastin to F-actin resulted in the acquisition of stiffness through combined confocal, co-immunoprecipitation and co-localisation studies. Experiments could also be performed to compare the mechanical response of T-plastin

expressing cells grown in conventional culture conditions with those grown in 3D in gels or on a support matrix (Gjorevski and Nelson, 2012).

In conclusion, further study of plastin is merited because its role in microfilament organisation may help us to understand neoplastic transformation events in cancer. T/L-plastin is not a prognostic biomarker for CRC. However, T/L-plastin is strongly expressed in CRC and most strikingly, at the leading edge of tumours. Although these results are encouraging, the mechanism that determines its expression pattern is unknown, and molecular data is required to explain how increased or ectopic plastin expression contributes to tumour formation. These approaches may help resolve whether individual plastins could indeed serve as part of a multi-panel cancer biomarker, or whether plastins could be valuable targets for cancer drug development.

Chapter 6: Identification and validation of a candidate colorectal cancer gene network

6.1 Introduction

CRCs arise from benign neoplasms and evolve into adenocarcinomas through a stepwise histological progression sequence, characterised by the sequential accumulation of both genetic and epigenetic alterations (Fearon, 2011; van Engeland et al., 2011). CRC is a truly heterogeneous disease, encompassing several histological and clinical behaviours. Current histopathological classification systems are based on descriptive entries such as tumour location and size (Compton and Greene, 2004). In the UK, the implementation of the Dukes' staging system has made an enormous contribution to the diagnosis, prognosis and treatment of CRC (Graziano and Cascinu, 2003). However, tumours with similar histological features may display disparate clinical behaviours due to the innate biological and genetic variability of CRC (Draht et al., 2012; Newton et al., 2010). The quest for robust and reliable immunohistochemical biomarkers that can predict patient prognosis or treatment response has gone some way to addressing this problem. Nevertheless, the information gained from a subjective antibody assessment cannot reveal the underlying molecular mechanisms involved in carcinogenesis.

The development of innovative high-throughput molecular technologies has revolutionized our understanding of the cancer genome, of which microarray-based gene expression has received most attention (Nannini et al., 2009). In comparison with traditional methods such as Northern blotting and Southern blotting, microarray technologies have a higher density of probes that enable the precise quantification of hundreds to thousands of gene transcripts in a single sample, providing a measurement of gene expression patterns (Duftner et al., 2008; Jung et al., 2011; Nannini et al., 2009). Briefly, microarrays are slides dotted with a panel of gene probes used to quantify the relative amount of RNA transcripts present in a cell or tissue. A fluorescent signal is produced when labelled cDNA is bound to the complementary sequence on the microarray. Changes in gene expression can be compared between samples by using two different fluorescent probe colours.

By enabling simultaneous expression analysis of thousands of genes, microarray technology has shed light on the molecular changes associated with tumour progression, and enabled the subsequent discovery of novel prognostic biomarkers and therapeutic targets (Colombo et al., 2011). Breast cancer has been the most studied with respect to gene expression profiling and clinical outcomes. One group were able to find a distinct gene expression signature that was indicative of poor prognosis (van 't Veer et al., 2002).

The data in Chapter 5 shows that T/L-plastin expression status cannot be used a prognostic biomarker in a population where lamin A/C can predict CRC patient prognosis. Nevertheless, we demonstrated that T/L-plastin is elevated in tumour tissue compared to normal colonic mucosa and thus plastin may be downstream of key genes that do have prognostic potential. A comprehensive knowledge of plastin signalling networks with respect to lamin A may assist in the discovery of novel biomarkers and the development of new drugs.

It has been shown that increased expression of lamin A causes the SW480 cells to adopt a more motile phenotype, as determined by wound-healing assays (Willis et al., 2008). In an attempt to elucidate the potential mechanisms responsible for this observation, our lab carried out quantitative genome-wide DNA pair wise screening on the SW480/lamin A and SW480/control CRC cell lines using the Human Genome U133 Plus 2.0 high density oligonucleotide Affymetrix GeneChip® Array. The overarching aim of this work was to identify candidate genes for future analysis using a bioinformatics approach. Here, we describe the generation of a cancer gene network, and validation of the microarray data by quantitative real-time PCR (qPCR) and immunoblotting.

6.2 Results

6.2.1 Generation of interaction network

Genome-wide DNA microarray analysis was previously carried out on SW480/lamA and SW480/cntl CRC cell lines by Dr N. Willis (Durham University) and Dr H. Peters (Newcastle University). A two-fold change or more between genes from the SW480/cntl cells and the SW480/lamA cells was considered to be indicative of differential expression. Changes in gene expression were observed in a total of 1,211 genes when expression patterns were compared between the two cell lines. In order to extract the most relevant biological information from the microarray data and to identify a network based on known interactions, we used Ingenuity Pathway Analysis (IPA®). The microarray dataset analysis was performed in collaboration with Dr Dan Swan (Newcastle University) and Dr Clare Foster (Durham University). IPA® is a professionally curated, web-based application containing an extensive database of biological interactions between genes, proteins, cells, drugs and diseases based on information from over 200,000 peer-reviewed publications (Calvano et al., 2005). Functional analysis of probesets showing greater than 2.5-fold differential expression between genes from SW480/lamA and SW480/cntl cells was performed by IPA®. The outputs that met this criterion were integrated into a molecular network or 'interactome' based on the connectivity of the inputted genes. IPA® was run using standard settings to check for significance against biological functions and disease and canonical pathways (significance indicated by Fischer Exact Test $p < 0.05$).

The interaction networks that were obtained represent biological processes that are over-represented in the microarray data and identify candidate genes for further analysis. The algorithm that creates the networks ensures that as many genes from the dataset are included as possible. The program also identifies genes that are likely to be part of a network but were not part of the experimental dataset. These genes were added to the networks obtained by IPA®. Approximately 35 molecules were represented in each network, with the most highly significant network clustering together proteins linked to cancer, cellular movement, cellular growth and proliferation. Genes within the network that were up- or downregulated in the SW480/lamA cells compared to SW480/cntl cells are shown in Table 6.1. The Cancer, Cellular Movement, Cellular Growth and Proliferation Network is shown in

Figure 6.1. The nodes represent the molecules or genes within the network and the lines between the nodes indicate a functional relationship. The genes that were upregulated in the SW480/lamA cells are circled in blue and genes downregulated in the SW840/lamA cells compared to SW480/cntl cells are circled in red. Interestingly, *PLS3* was not identified in this network analysis, even though the microarray analysis revealed that *PLS3* was upregulated 13-fold in the SW480/lamA compared to the SW480/cntl. This observation indicates that *in silico* analysis has some limitations in identifying novel interactions, for example between intracellular compartments, previously unrelated pathways or novel protein products.

Table 6.1: List of genes identified in a cancer network by Ingenuity Pathway Analysis

Gene ID	Gene name	Fold Change	Gene Function(s)
<i>EMP1</i>	epithelial membrane protein 1	6.40 up	Cell growth/cell proliferation
<i>DKK1</i>	dickkopf homolog 1 (<i>Xenopus laevis</i>)	6.30 up	Antagonises canonical Wnt signalling
<i>EREG</i>	Epiregulin	5.73 up	Mediator of cell proliferation/angiogenesis
<i>AREG</i>	Amphiregulin	5.22 up	Carcinoma growth inhibitor
<i>SNAI2</i>	snail homolog 2 (<i>Drosophila</i>)	4.05 up	Transcriptional repressor
<i>FOSL1</i>	FOS-like antigen 1	4.04 up	Positive regulator of cell proliferation
<i>IL6R</i>	interleukin 6 receptor	3.97 up	Receptor for Interleukin 6/immune response
<i>SERPINE1</i>	serpin peptidase inhibitor (plasminogen activator inhibitor type 1)	3.81 up	Regulator of mRNA stability
<i>ETS1</i>	erythroblastosis virus E26 oncogene homolog 1 (avian)	3.61 up	Transcription factor/regulation
<i>MSX1</i>	msh homeobox 1	3.54 up	Acts as a transcriptional repressor
<i>CDC42EP5</i>	CDC42 effector protein (Rho GTPase binding) 5	3.43 up	Organisation of actin cytoskeleton
<i>FN1</i>	fibronectin 1	3.31 up	Cell adhesion/cell motility/cell shape
<i>AKAP11</i>	A kinase (PRKA) anchor protein 11	3.18 up	Protein kinase A regulator
<i>EIF4E</i>	eukaryotic translation initiation factor 4E	3.15 up	Facilitates ribosome binding
<i>EGFR</i>	epidermal growth factor receptor	2.99 up	Cell surface receptor/ tyrosine kinase signalling
<i>BRCA2</i>	breast cancer 2, early onset	2.93 up	DNA repair/homologous recombination
<i>CKAP2</i>	cytoskeleton associated protein 2	2.78 up	Microtubule stabilizing properties/cell cycle
<i>NRP1</i>	neuropilin 1	2.75 up	Receptor involved in development/angiogenesis
<i>IGF2BP1</i>	insulin-like growth factor 2 mRNA binding protein 1	2.68 up	RNA-binding protein/regulates RNA stability
<i>IGF2BP3</i>	insulin-like growth factor 2 mRNA binding protein 3	2.37 up	RNA-binding protein/regulates RNA translation
<i>IGF2</i>	insulin-like growth factor 2	8.61 down	Growth-promoting activities
<i>BMP4</i>	bone morphogenetic protein 4	7.19 down	Inducer of bone/cartilage formation
<i>CHGA</i>	chromogranin A (parathyroid secretory protein 1)	4.80 down	Inhibits glucose-induced insulin
<i>CDH1</i>	cadherin 1, type 1, E-cadherin (epithelial)	3.43 down	Cell adhesion molecule/motility
<i>MSX2</i>	msh homeobox 2	2.89 down	Transcriptional regulator in bone development
<i>COL18A1</i>	collagen, type XVIII, alpha 1	2.70 down	Inhibits proliferation and angiogenesis
<i>INSIG1</i>	insulin induced gene 1	2.41 down	Mediates control of cholesterol synthesis

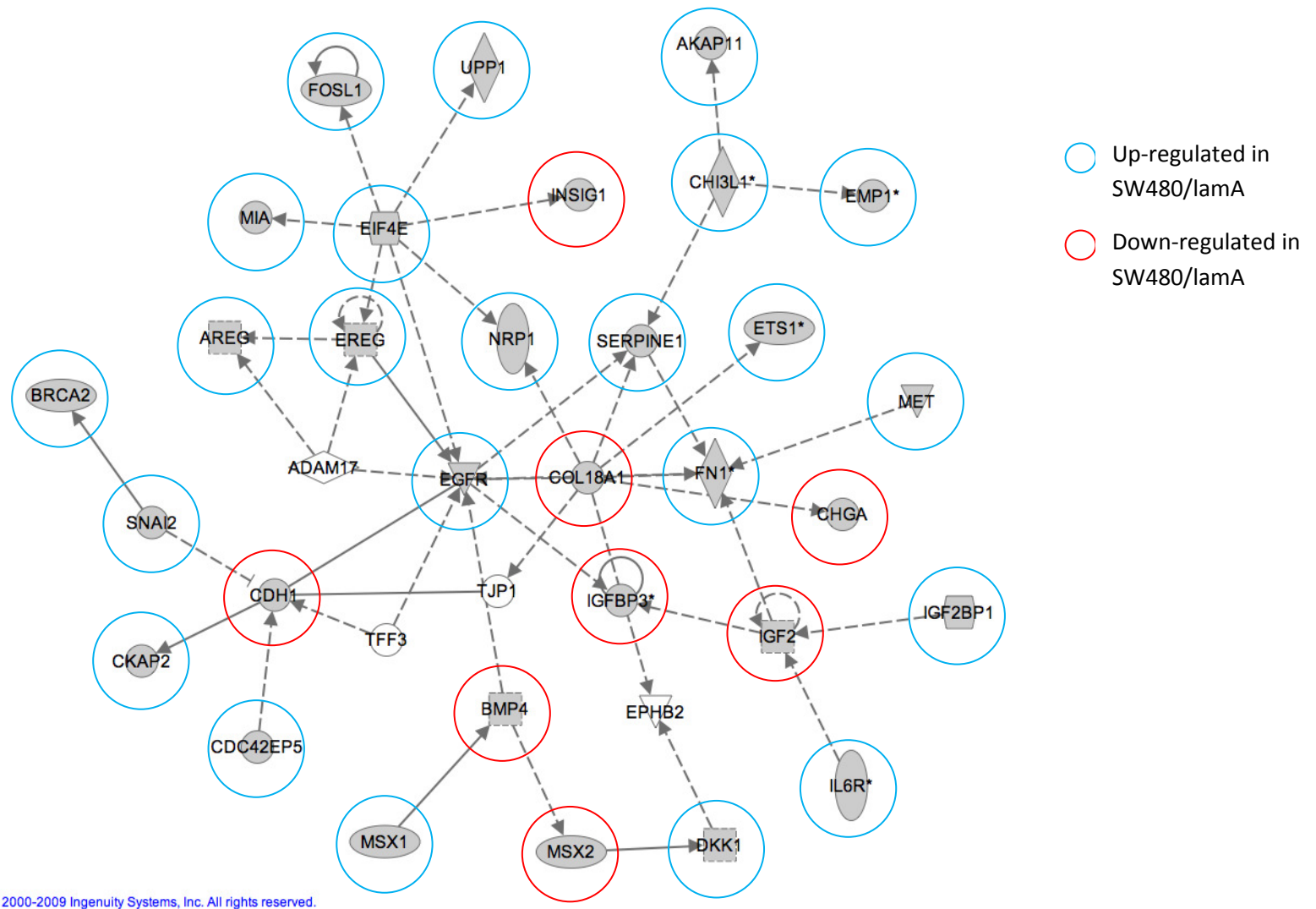


Figure 6.1: Biological network linked to Cancer, Cellular movement, Cellular growth and Proliferation

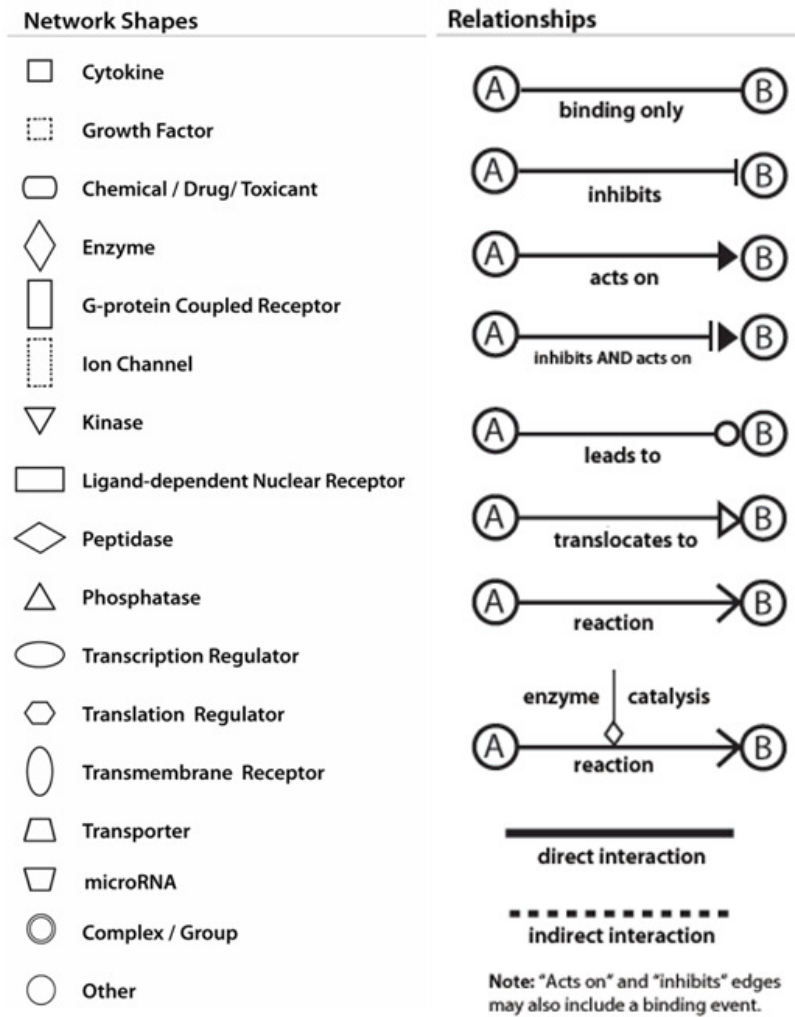
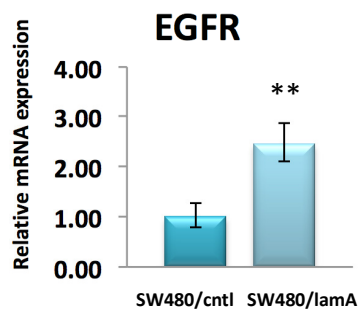
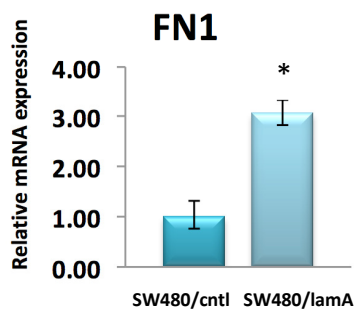
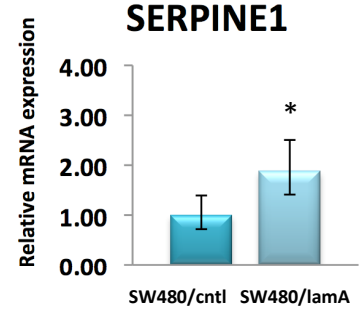
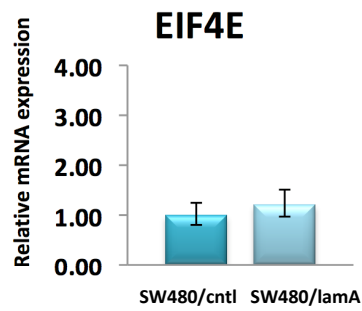
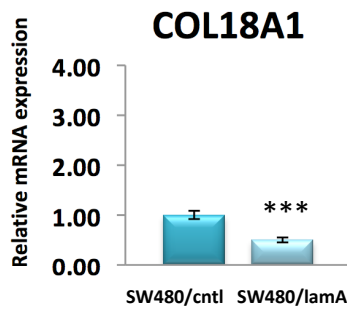
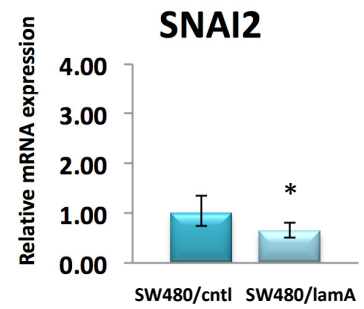
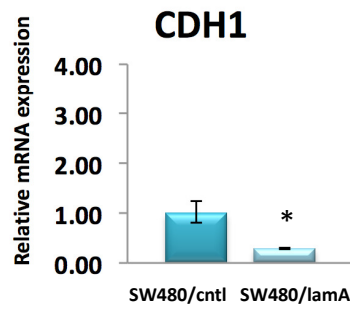
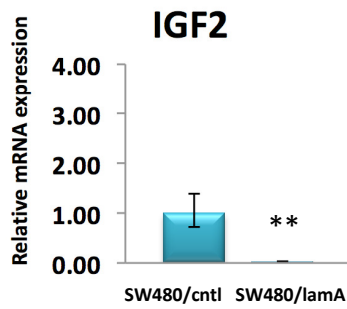
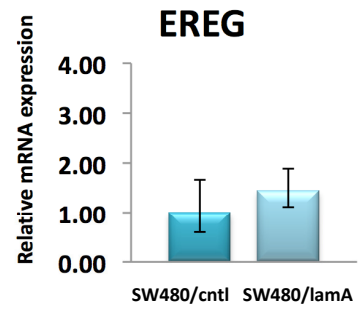
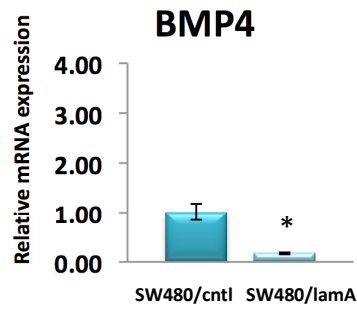
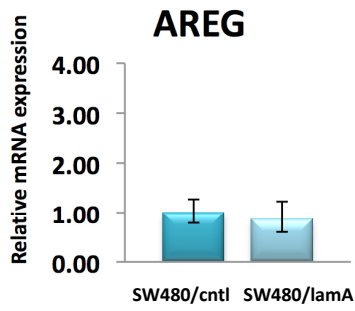


Figure 6.2: Interactions and molecules used in Ingenuity Pathway Analysis network

The shape surrounding the gene name represents the type of molecule encoded by the gene. The lines that link the genes together refer to known interactions dotted lines represents an indirect interaction. The arrowheads indicate directionality. Curved arrows designate self-regulation. Lines without an arrowhead refer to a binding interaction.

6.2.2 Confirmation of microarray data by real-time PCR

Once an interaction network has been generated from the microarray data, the gene expression profiles and linkages must be validated using a biological assay. Quantitative real-time PCR (qPCR) is the gold standard for the precise quantification of mRNA expression and is predominantly used to validate microarray data. Before confirming the data by qPCR, primers for the genes of interest were optimised as described in (Chapter 2, Section 2.6). From the cancer network, 11 nodes were chosen for analysis by qPCR. The selection was based on genes that were connected to at least two other genes in the network shown in Figure 6.1. Q-PCR was performed for *AREG*, *BMP4*, *CDH1*, *COL18A1*, *EGFR*, *EIF4E*, *EREG*, *FN1*, *IGF2*, *SERPINE1* and *SNAI2* in the SW480/lamA and SW480/cntl cells. The mRNA expression between SW480/cntl and SW480/lamA was calculated using the $2^{-\Delta\Delta CT}$ method (Livak and Schmittgen, 2001b). The $2^{-\Delta\Delta CT}$ method was chosen as it is a convenient way to perform relative quantification of mRNA expression between two samples. Normalisation was against housekeeping gene GAPDH. Statistical significance was determined by student t-tests (two-sided). Of the eleven genes analysed, eight genes showed statistically significant changes in gene expression between the two cell types; *BMP4*, *CDH1*, *COL18A1*, *EGFR*, *EIF4E*, *FN1*, *IGF2*, and *SERPINE1* (Figure 6.3). *AREG* and *EREG* were identified as differentially expressed by microarray analysis (Table 6.1), but this was not confirmed by qPCR (Figure 6.4). Moreover, *SNAIL*, which was shown to be upregulated ~4-fold in the SW480/lamA cells compared to the SW480/cntl cells by microarray analysis was actually statistically significantly down regulated in the SW480/lamA cells as determined by qPCR (Figure 6.4). However, since ~70% of the genes investigated by qPCR were consistent with the microarray analysis, the microarray as a whole was considered to be valid.



* $p < 0.05$, ** $p < 0.01$, *** $p < 0.005$

Figure 6.3: Confirmation of microarray data by quantitative real-time PCR

Gene mRNA levels measured by real-time PCR in CRC cell lines SW480/lamA and SW480/cntl. Normalisation was against the housekeeping gene GAPDH. For each gene, the level of mRNA expression in SW480/cntl was set to equal 1. Data are presented as the relative changes in gene expression using the $2^{-\Delta\Delta CT}$ method, from three to five biological replicates. The upper error bar corresponds to $2^{-(\text{mean } \Delta\Delta CT - SE)}$ and the lower error bar corresponds to $2^{-(\text{mean } \Delta\Delta CT + SE)}$. Statistical analysis was performed using the student t-test (two-sided) to compare the changes in gene expression between SW480/lamA and SW480/cntl. * = statistical significance. *BMP4*: $p = 0.02$, *CDH1*: $p = 0.03$, *COL18A1*: $p = <0.01$, *EGFR*: $p = <0.01$, *FN1*: $p = 0.04$, *IGF2*: $p = <0.01$, *SERPINE1*: $p = 0.01$, *SNAI2*: $p = 0.04$.

Microarray vs realtime PCR: fold change in gene expression

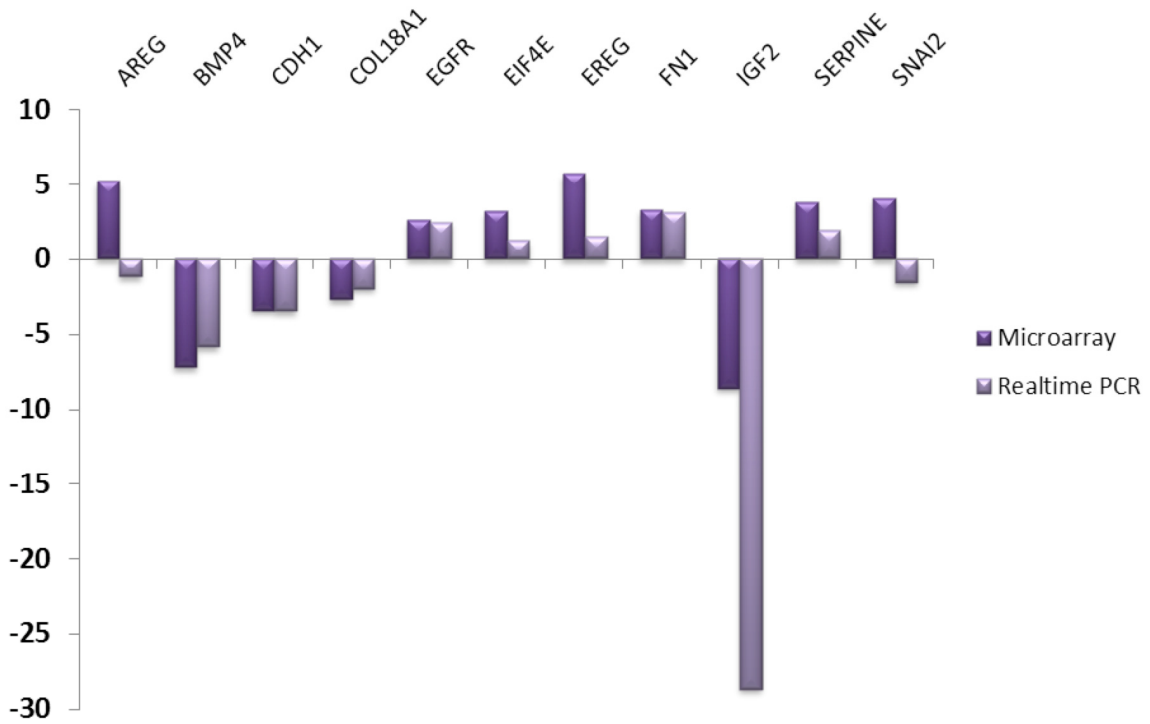


Figure 6.4: Microarray versus quantitative real-time PCR: fold change in gene expression

The relative fold change in gene expression in SW480/lamA cells compared to SW480/cntl cells is shown for the real time qPCR data (light purple bars), and the microarray data (dark purple bars). Of the eleven genes investigated, eight showed a similar trend, whereas AREG and SNAI2 were slightly downregulated in the qPCR and EREG was not significantly upregulated.

6.2.3 Confirmation of microarray data by Western blotting

Although the microarray data were mostly confirmed at the mRNA level by qPCR this did not necessarily mean that there was a difference in the level of protein expression. This is because proteins may have long half-lives, may be highly abundant, could be subject to post-translational regulatory mechanisms or there may be compensatory mechanisms that counter changes at the transcript level. To investigate whether changes in gene expression in the SW480/lamA cells were reflected at the protein level, immunoblotting was performed (Figure 6.5). Lysates from the SW480/lamA cells were compared with those from SW480/cntl cells. A Bradford assay was used to calculate the protein levels in the lysates and SDS-PAGE followed by Coomassie staining was used to verify protein loading (Chapter 2, Section 2.9.4). GFP-lamin A was clearly expressed in the SW480/lamA cells only. The calcium dependent cell adhesion protein E-cadherin was downregulated in the SW480/lamA cell line as expected from the microarray data and from previous studies (Willis et al., 2008). The tyrosine kinase growth receptor EGFR was upregulated in the SW480/lamA cells, consistent with the microarray results. In addition, plasminogen activator inhibitor 1 (PAI-1) is a serine proteinase inhibitor protein encoded by the *SERPINE1* gene. Predominantly synthesised by the vascular endothelial cells, it functions as fibrinolytic inhibitor by controlling the urokinase-type plasminogen activity (Sakakibara et al., 2005). Importantly, PAI-1 has been linked to tumour metastasis and has been associated with poor prognosis in several cancers (Cantero et al., 1997; Chambers et al., 1998; Konecny et al., 2001). In the Western blotting analysis shown, the level PAI-1 looked very similar between the two cell lines, suggesting that a two-fold change in the level of mRNA was not sufficient to make a difference to the steady-state level of this protein (Figure 6.5).

Examination of *SNAI2* (which encodes a zinc finger transcriptional repressor protein also known as Slug), gave conflicting results. In the microarray experiment *SNAI2* levels were elevated in the SW480/lamA cells, whereas in the qPCR and Western blot there was a decrease in *SNAI2* expression. In addition to these proteins, the expression of cofilin and MHC class I molecules was examined. Given that plastins are involved in binding and regulating the actin cytoskeleton, cofilin was chosen because it binds to both monomeric actin and F-actin. Cofilin is a small ~19 kDa protein that plays an important role in severing actin filament assembly and is upregulated in many cancers including renal cell carcinoma and ovarian cancer (Unwin et al., 2003; Martoglio et al., 2000). Moreover, cofilin has been

implicated with tumour invasion and metastasis (Wang et al., 2007). MHC class I levels were examined because MHC class I molecules are key determinants of the adaptive immune system and present viral and tumour peptides to cytotoxic CD8+ T cells. Expression of MHC class I molecules is thus required for tumour surveillance by cytotoxic T cells and for recognition of altered self by NK cells (Bubenik, 2003). Interestingly, MHC class I expression was strongly decreased in the SW480/lamA cells (Figure 6.5), suggesting that this may be a mechanism to allow the cancer cell to escape from immune surveillance. Unlike the result for MHC class 1, the actin binding protein cofilin was unchanged in the SW480/lamA cells, suggesting that lamin A expression does not effect cofilin expression (Chapter 4, Section 4.2.3.6).

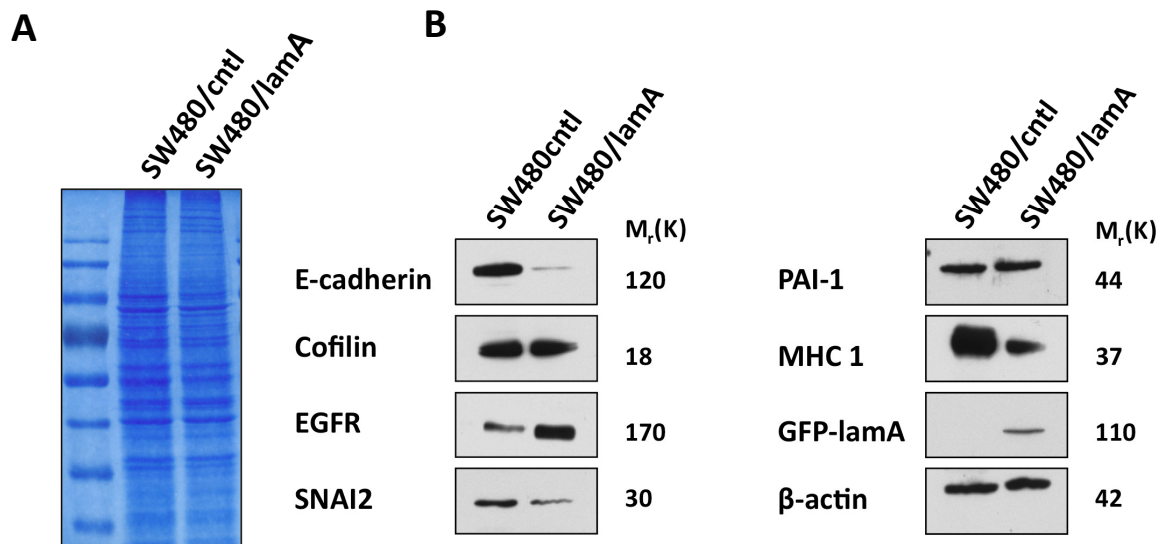


Figure 6.5: Coomassie and immunoblotting of selected proteins identified by microarray

Lysates from SW480/lamA and SW480/cntl cells were analysed by SDS-PAGE, and stained with (A) colloidal Coomassie or (B) probed with a panel of antibodies. Molecular weight markers are given in kDa. β -actin was used a loading control. Data shows that E-cadherin, MHC 1 and Snail are downregulated in the SW480/lamA cells compared to SW480/cntl cells. EGFR was upregulated in the SW480/lamA cells compared to SW480/cntl cells. There was no change in protein expression between the cell lines for cofilin and plasminogen activator inhibitor 1 (PAI-1).

6.3 Discussion

By sampling the expression of thousands of genes, microarray technology has revolutionised how we assess the molecular changes associated with tumour progression and biological responses in general. In this thesis, we have shown that T/L-plastin may be important in colorectal tumour formation, using diverse experimental approaches ranging from epigenetic studies to immunohistochemistry and western blotting. Having established that T-plastin is elevated when lamin A is overexpressed in CRC cell lines, we extended the analysis to seek other genes that responded to changes in lamin A expression in CRC and that might be linked to a functional network. A quantitative genome-wide DNA pair wise screening on the SW480/lamA and SW480/cntl cell lines was previously carried out. In order to identify other candidate genes that could be investigated for prognostic value (to be used in combination with lamin A/C), and to shed light on the molecular mechanisms involved in the lamin cancer pathway, we took a bioinformatic stance. IPA[®] analysis generated a highly significant cancer network (Figures 6.1 and 6.2), drawing on literature-curated interactions that allowed us to focus on the most promising genes from the microarray experiment (Figure 6.3). The most statistically significant network to arise out of this work was linked to cancer, cell motility, cellular growth and proliferation.

It was important to confirm the microarray data by other biological assays. This was achieved by performing qPCR (Figure 6.4). Results revealed that eight out of the eleven genes investigated showed a statistically significant change in gene expression in SW480/lamA compared to SW480/cntl cells. However, *AREG* and *EREG* were identified as differentially expressed by microarray analysis, but this was not confirmed by qPCR. Moreover, *SNAI2* was down regulated in the SW480/lamA cells according to the qPCR analysis (Figure 6.4). How can these discrepancies be explained?

Firstly, it is possible that there are biological differences in the cells, as the RNA samples for the microarray and the RNA for the PCR experiments were isolated years apart, albeit from the same cell line. The SW480 cell line is genetically unstable (Camps et al., 2005; Lengauer et al., 1997; Ribas et al., 2003) and it is also possible that the expression of GFP-lamin A varies with time, or that passage number, confluency, stress or even batch to batch

variations in the composition of fetal calf serum influence the expression of a fraction of the lamin A target genes.

Alternatively, differences in expression of *SNAI2* may be due to changes in the way that transcription factors are expressed during cancer progression. Interestingly, gene expression can change during transition from one stage of the EMT to the next (Savagner et al., 1997; Vetter et al., 2009). Thus it is possible that *SNAI2* is switched on and then off once the expression of its target genes has been initiated. Snail may initiate the repression of epithelial genes (Guaita et al., 2002; Peinado et al., 2007) and loss of E-cadherin, which occurs on expression of lamin A in the experiments shown in this chapter, could stabilise the mesenchymal state (Onder et al., 2008). This idea is backed up by data from the immunoblotting analysis, which showed that *SNAI2* is downregulated at the protein level in the GFP-lamin A cells (Figure 6.5), with E-cadherin protein expression being markedly reduced.

Another possible explanation for the differences observed between the microarray and qPCR data is the nature of the experimental setup. Some genes have more than one corresponding probeset on the microarray chip, including *AREG* and *EREG*. For these genes, only one of the two probesets showed up-regulation of the gene. For *SNAI2* only one probeset was present on the microarray. It is possible that the results for these three genes were not reproducible because of variation in hybridisation efficiency, or in the amplification/detection steps of the microarray experiment. Comparison of the microarray and qPCR data shows why it is important to use different assays and approaches to reproduce and understand complex biological phenomena.

Furthermore, the data in this chapter showed that a number of genes were downregulated in the SW480/lamA cells, as determined by qPCR analysis. One of the most striking genes that was downregulated was *BMP4* which encodes BMP4, a protein usually involved in bone and cartilage formation but also involved in mesoderm induction and the inhibition of hair follicle induction (Wozney et al., 1988). BMP4 has been shown to be a downstream target of Ras in SW480, Hela, and 293 cells (Duerr et al., 2012). In this work, oncogenic KRAS downregulated RNA levels of BMP4 through the ERK pathway, fitting with the enhanced level of EGFR expression seen in our study.

An example of a gene that was upregulated in the SW480/lamA cells compared to the SW480/cntl cells was the fibronectin gene *FN1*. Fibronectin is a secreted protein that is well established as protein that can bind collagens and actin, and is important for cell adhesion, motility and the maintenance of cell shape. Studies in ovarian cancer cells suggest that fibronectin cleavage by matrix metalloprotease-2 (MMP2) is a key step in the initial stages of metastasis and allows the cell to break away from the tumour cell mass. Mutations in *FN1* have also been noted from DNA sequencing of breast and colon cancer tissue (Sjoebloom et al., 2006). Since a number of *FN1* isoforms exist and fibronectin is subject to extensive post-translational modification, it would be interesting to study the relationship between fibronectin and MMPs in the lamin A expressing cell line in future studies.

The consequences of changes in transcript levels on the corresponding proteins were assessed by immunoblotting (Figure 6.5) and were largely in agreement with the qPCR data, with the exception of PAI-1. A possible explanation for this observation is that western blotting is not fully quantitative so that small differences in PAI-1 protein expression are not picked up. To address this, pulse chase experiments or semi-quantitative blotting using fluorescent probes could be used. Alternatively, changes in the transcript levels of *SERPINE1* could be buffered by post-translational feedback and regulatory mechanisms that maintain steady state levels of the protein. Although the influence of lamin A expression on *SERPINE1* remains unclear from our analysis, it has recently been shown that PAI-1 is expressed more strongly in SW480 cells than in CaCo-2 cells and that PAI-1 levels are increased in more aggressive colorectal tumors, from an analysis of 50 CRC specimens (Mazzoccoli et al., 2012).

Notably, microarray, qPCR and immunoblotting analysis all confirmed that *EGFR* was upregulated in the SW480/lamA compared to SW480/cntl cells. *EGFR* is frequently expressed in solid tumors including CRC, and promotes cancer cell growth and cell division (Harris and McCormick, 2010). In this chapter, it was noted that downregulation of E-cadherin was inversely correlated with the upregulation of *EGFR* in the lamin A overexpressing cells. It has recently been published that the same inverse correlation has been seen in head and neck squamous cancer cells (Wang et al., 2011) and *EGFR* has been reported to directly downregulate E-cadherin transcription. This suggests that the effect of lamin A on E-cadherin could be an indirect one in colon cancer cells and may proceed via *EGFR*. Further studies will be required to test this hypothesis, for example, by using an inducible lamin A construct to

evaluate the timing of E-cadherin downregulation and EGFR upregulation through pulse-chase experiments. Two anti-EGFR monoclonal antibody therapies are currently prescribed for patients with metastatic colon cancer, namely Erbitux (cetuximab) and Vectibix (panitumumab), but these drugs are only prescribed to patients with wild-type KRAS genes, as ‘activating’ mutations in KRAS make patients unresponsive to anti-EGFR treatment (Sheridan, 2008). Therefore, lamin A, or a downstream target of lamin A, might be worth exploring as a drug target for CRC patients who are unresponsive to EGFR therapy. It would be interesting to revisit the NLCS tissue archive to examine the expression of EGFR and lamin A, and check the history of drug responsiveness in these patients. Given that an inverse relationship between EGFR and E-cadherin is also seen in head and neck cancer (Wang et al., 2011), it would also be interesting to examine the expression of lamin A and T-plastin in this solid tumour type. It would also be important to explore whether EGFR signaling is activated in the SW480/lamA cell lines by using phosphorylation-specific antibodies and checking for activation through the ERK or JAK/STAT pathways, since EGFR signalling can lead to activation of genes involved in cell survival (through Ras/ERK or JAK/STAT), or the induction of protein synthesis (through the AKT pathway) (Figure 6.6).

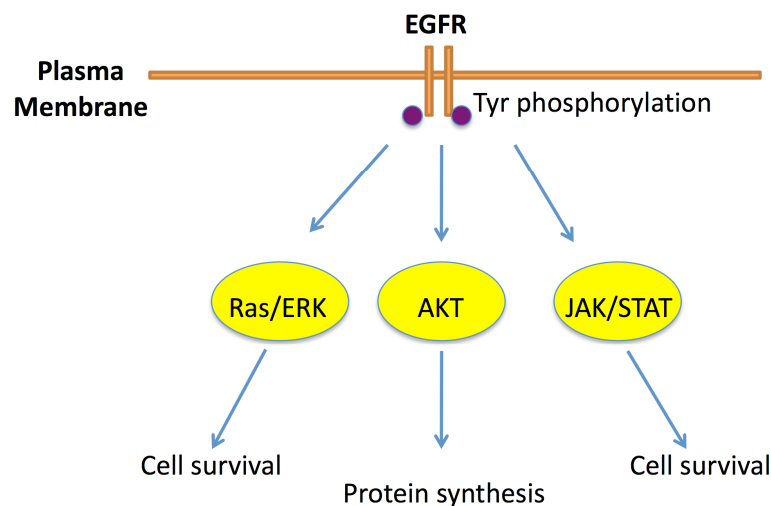


Figure 6.6: Overview of the EGF signaling pathway

Activation of the EGF receptor results in tyrosine autophosphorylation. Phosphorylated EGFR binds proteins through the Src homology 2 (SH2) domain. Downstream signalling occurs through the RAS/extracellular signal regulated kinase (ERK) pathway, the phosphatidylinositol 3-kinase (PI3) AKT3 pathway and the Janus kinase/Signal transducer and activator of transcription (JAK/ STAT) pathway. Together, these pathways co-ordinate cell survival.

A notable feature of the SW480/lamA cell line was the marked downregulation of MHC class I expression. MHC class I molecules are present on all nucleated cells (but not red blood cells), and have a central role in the immune system. They are chiefly involved in presenting antigenic peptides from intracellular sources, such as viruses, to CD8⁺ T cells. The CD8⁺ T cells are usually cytotoxic T cells that destroy an infected cell. However, MHC class I molecules are also involved in tumour surveillance. This is because mutations in the coding regions of genes can lead to a change in the amino acid sequence of the protein. This change can be detected by cytotoxic T cells in the context of the MHC class I molecule, enabling the killer T cells to destroy the tumour cell. There is a strong selection pressure on some tumours to escape detection by cytotoxic T cells, and hence MHC class I is downregulated in a number of cancer types, including CRC cell lines (Browning et al., 1996). Interestingly, a recent publication reported that positive MHC 1 expression is a biomarker of good prognosis in CRC patients (Simpson et al., 2010). However, the exact mechanisms underlying this aspect of tumour immunology are not well understood. It is therefore very exciting that simply overexpressing the lamin A gene has such a dramatic effect on MHC class I levels. The effect is not likely to be direct, given that lamin A is a nuclear protein and MHC class I molecules are trafficked to the cell surface through the ER-Golgi secretory pathway. However, lamins has been implicated in the global control of gene expression by influencing chromosome positioning and the organisation of heterochromatin close the nuclear periphery (Dechat et al., 2008). Therefore, one possibility is that lamin A may bring areas of Chromosome 6 to the nuclear periphery and shut down gene expression. Chromosome painting experiments in the SW480/lamA cells could be conducted to test this idea directly. Another possibility is that lamin A directly influences an intermediary protein, such as an MHC class I transcription factor, or a protease that increases the turnover of MHC class I molecules. This could be tested by performing pulse chase labelling studies and with cell surface biotinylation experiments to compare the synthesis and turnover of the MHC class I molecules in SW480/lamA and SW480/cntl cells.

In summary, the work in this chapter has identified a candidate cancer network, with lamin A at the heart, influencing a number of genes involved in signalling and tumour metastasis. As a first step towards understanding the biological relationship with the genes identified in the microarray screen, qPCR and Western blotting were performed to confirm that EGFR was upregulated and that E-cadherin was downregulated. Taken together, the results suggest

that there is functional relationship between EGFR and lamin A, and how T-plastin fits in to this network merits further exploration as a biologically important hub and a clinically important therapeutic target.

Chapter 7: Discussion and future perspectives

7.1 Background and aims of thesis

CRC is the third most common form of malignancy in the Western world (Ferlay et al. 2010). Intimately linked with environment and lifestyle, the disease represents a huge challenge to global health organisations (Kolonel et al., 2004; Smits et al., 2008; Jemal et al., 2011). CRC starts as a benign polyp, which develops into an invasive carcinoma through a step-wise histological progression sequence spanning 10-15 years (Fearon et al., 2011). Current methods of clinicopathological staging used to predict patient prognosis are based on the Dukes'/TNM system (Compton and Greene, 2004). However, survival rates vary between 90% - 10% with tumour progression (Fretwell et al, 2010). Since the discovery of the first oncogene in 1989, the central tenet has been that mutations in our genetic make-up drive the initiation and progression of carcinogenesis (Brower, 2011; Dawson and Kouzarides, 2012). Whilst this theory remains irrefutable, we still lack a robust and reliable genetic biomarker that can accurately predict patient prognosis. This can be explained, at least in part, by two phenomena; firstly, the fact that CRC is a truly heterogeneous disease with thousands of abnormalities in the cancer genome and secondly, that 'genetic' events are not the sole contributors to neoplastic formation. Since 1994, when Baylin and Herman showed that the tumour suppressor gene von-Hippel Lindau (VHL) was silenced in renal cell carcinoma by DNA methylation, the appreciation that epigenetics plays a significant role in cancer formation has dawned on the scientific community (Herman et al., 1994). Until recently, epigenetic modifications have been thought of as a proxy for genetic changes in cancer. The argument for causality is confounded by a lack of mutations in epigenetic machinery (Feinberg, 2007; Dawson and Kouzarides, 2012). However, the idea that aberrations in the epigenome are a cause rather than a consequence of cancer has been strengthened by the finding that DNA methyltransferase *DNMT3a* is mutated in patients with acute myeloid leukemia (Ley et al., 2010).

Understanding the molecular basis of this disease is crucial to help develop accurate biomarkers and treatments for CRC patients (Smits et al., 2008). As a step towards this aim, *PLS3* promoter methylation and expression of the actin-bundling protein plastin has been studied in this thesis. This work arose from a study in our laboratory which identified lamin

A/C as a prognostic biomarker in CRC (Willis et al., 2008). When lamin A was overexpressed in the CRC cell line SW480, this caused the cancer cells to adopt a more motile phenotype. Strikingly, T-plastin expression was upregulated by GFP-lamin A expressing cells when compared with the GFP control counterparts (Willis et al., 2008). This finding stimulated the further study of plastins in CRC, in the hope that plastins may have some prognostic influence, perhaps together with lamin A as part of a biomarker panel. The overall objectives of this thesis were: to investigate *PLS3* promoter methylation in CRC by N-MSP and explore whether there was an association between *PLS3* methylation and clinicopathological characteristics; produce and characterise polyclonal plastin antibodies by immunoblotting; investigate the expression of plastin in CRC tissue archive by immunohistochemistry and determine the utility of plastin expression as a prognostic biomarker for CRC. The final objective of this thesis was to look at the global changes based on the expression on GFP-lamin A in CRC SW480, generate a candidate gene network and validate this network by qPCR and immunoblotting.

7.2 *PLS3* promoter CpG island methylation is a mechanism for controlling T-plastin expression

We began our investigation by assessing the methylation status of the *PLS3* promoter in both CRC cell lines and DNA taken from the NLCS tissue archive. Whilst our data showed that *PLS3* promoter methylation cannot be used as an independent prognostic biomarker, some interesting observations were made that warrant further research. Firstly, we found that the *PLS3* promoter was unmethylated in SW620, SW480, LS and CaCo-2 cells and methylated in SW948 and HT29 CRC cell lines, as determined by N-MSP (Figure 3.3). The SW620 and SW948 cell lines were selected for bisulphite sequence analysis. Results confirmed that SW620 and SW948 are indeed unmethylated and methylated, respectively (Figure 3.5). In order to establish whether there was a relationship between *PLS3* promoter methylation and T-plastin expression, we subjected the female methylated cell lines SW948 and HT29 to epigenetic drug treatment. We observed that upon DAC treatment, T-plastin mRNA expression was restored in a dose-dependent manner, suggesting that methylation at the *PLS3* promoter regulates the T-plastin gene. This is supported by the current literature (Ikeda et al., 2005; Sasaki et al., 2002). However, the regulation of T-plastin expression is likely to involve additional factors (e.g. transcription factors and repressors) given that the T-plastin

protein is detected in 'unmethylated' SW620 cells but not in 'unmethylated' SW480 cells (Figure 4.1). This hypothesis is also based on the mixed results that were obtained from the methylation studies of normal and CRC colon tissue. In normal colon tissue, where T-plastin is never expressed, the frequency of methylation at the *PLS3* promoter was only 65%, whereas in CRC patients, although the degree of methylation fell, ~50% of primary colorectal tumours analysed remained methylated. If methylation at the *PLS3* promoter were the only mechanism that suppressed T-plastin expression, then 100% of normal colonic mucosa samples should be methylated. This idea is backed up by a growing body of literature that suggests that DNA methylation status does not always correlate with transcriptional activity (Suzuki and Bird, 2008). Future experiments to understand the consequences of *PLS3* methylation with respect to T-plastin protein expression could be conducted to clarify this issue. For example, it would be informative to know whether methylation at specific sites in the *PLS3* promoter influences gene expression through the recruitment of transcription factors, and how lysine methylation of histone proteins relates to *PLS3* gene expression. Very little is known about the control of plastin expression by transcriptional regulators, and perhaps ChIP experiments to compare *PLS3* promoter occupancy from 'methylated' and 'unmethylated' CRC cell lines would be informative in this regard.

7.3 Does *PLS3* promoter hypomethylation play a pivotal role in switching on T-plastin in CRC?

Significantly, in the patient's samples analysed (from frozen tissue), we noted a switch in the methylation status between normal colonic mucosa and corresponding tumour tissue. Quantitative real-time PCR analysis showed that T-plastin expression was suppressed in the 'methylated' normal colonic tissue and upregulated in the 'unmethylated' tumour tissue. However, one limitation of this study is the small number of patients examined. In addition, we did not assess the same samples for T-plastin protein expression. Nevertheless, the increase of T-plastin mRNA observed in the patient colorectal tumor tissue, compared with their corresponding normal colonic mucosa (Figure 3.11), suggests that hypomethylation or demethylation of the *PLS3* promoter may play a critical role in switching on T-plastin expression during neoplastic transformation. In the support of this theory, it has been recently reported by Jones and colleagues that the *PLS3* promoter is hypomethylated causing an upregulation of T-plastin in Sezary syndrome patients (Jones et al., 2012). The

exact mechanisms involved and consequences of promoter methylation and demethylation in CRC are not fully understood. In general, it is well established that *de novo* methylation is initiated during embryogenesis by the DNMT3 family of methyltransferases and maintained by DNMT1 during DNA replication (Law and Jacobsen, 2010). DNMT1 is recruited to a position just downstream of the replication complex and associates with PCNA and UHRF1, a protein that specifically targets hemimethylated DNA in the post-replication phase. DNMT1 can then restore the hemimethylated DNA to its fully methylated state (Bostick et al., 2007; Sharif et al., 2007). UHRF1 is only detectable in actively proliferating cells and its expression level is elevated in various cancers, including prostate, lung, breast, pancreatic, bladder and cervical cancer but not, until recently, CRC (Unoki et al., 2009). A difficulty in interpreting complex methylation patterns and predicting their effects in CRC is that proteins such as UHRF1 can both positively and negatively regulate gene expression. Therefore, further research is required to establish whether and how mutations in the DNMT1-associated methylation machinery contribute to CRC.

7.4 Is there a role for active demethylation in CRC?

In contrast to the active methylation of CpG dinucleotides, demethylation is usually thought of as a passive process in which the methylated cytosine is lost during replication in the absence of DNMT1 activity. However, evidence has accumulated to support a role for an active demethylation pathway, and although some findings remain controversial (Ooi and Bestor, 2008) investigating the dysregulation of demethylation in CRC and other cancers is likely to be an area of intensive research in the future. Active demethylation in plants is orchestrated by the DME1/ROS1 family of glycosylases, but orthologues of these proteins have not been identified in animals (Zhu, 2009). Instead it is thought that in animals, deamination of the methylated cytosine is catalysed by AID/APOBEC, resulting in a thymine base (mismatched to guanine). The mismatched A/T pair is probably recognized by the glycosidases Tdg and Mbd4, which cleave the N-glycosidic bond to leave an abasic site that is removed by an as yet unidentified apyrimidic lyase. The single nucleotide gap in the DNA sequence must then be repaired by as yet unknown DNA polymerase/ligase activities. Evidence for this pathway mainly comes from work in zebrafish embryos in which over-expression of Aid, Apobec2a and Apobec2b resulted in loss of methylation in an Mbd4 dependent manner (Rai et al., 2008). Knocking out Aid in mice also results in a genome-wide

reduction of demethylation in primordial germ cells (Popp et al., 2010). Given these recent discoveries, it would be very interesting to examine the expression and activities of Aid/Apobec and Tdg/Mbd4 in the CRC cell lines and patients that we have presented in this study, and to determine whether there is any relationship with T-plastin expression.

T-plastin is expressed in the embryonic development of the intestinal system and then switched off, but is re-expressed during the initiation of colon cancer (Chapter 3). Of relevance to this finding is that loss of the APC tumour suppressor gene in zebrafish results in upregulation of the DNA demethylase machinery (Rai et al., 2010). The model proposed by Rai et al, in which APC controls intestinal cell fate by downregulating demethylation and promoting differentiation is consistent with the finding that T-plastin is expressed early during embryonic gut development, is switched off in adults and is re-expressed in CRC (Chapters 3 and 5). Since loss of APC is a key step in the initiation of CRC, one would predict that DNA demethylase activity is also enhanced in CRC patients. Demethylase activity is indirectly repressed by retinoic acid (Zhu, 2009), so it would be interesting to see whether treating T-plastin positive CRC cells with retinoids results in the re-establishment of *PLS3* promoter methylation and subsequent repression of T-plastin protein expression.

An alternative mechanism to demethylation by AID/APOBEC is the conversion of 5-methylcytosine (5-mc) to 5-hydroxymethylcytosine (5-hmc) by hydroxylation, which can be catalysed, at least *in vitro*, by TET1 (Tahiliani et al., 2009). The DNMT1 machinery has a low affinity for 5-hmc, and thus may not be recruited to replication complexes if 5-hmc is present. The 5-hmc modification has been found mainly in brain tissue and ES cells (Kriaucionis and Heintz, 2009) but is also present in aged tissues (Song et al., 2011). The bisulfite sequencing technique described in Chapters 2 and 3 cannot distinguish between 5-mc and 5-hmc (Huang et al., 2010). Thus whether 5-hmc modifications play a role in demethylation of the *PLS3* promoter in CRC remains to be established. Recently developed 5-hmc-specific antibodies and a newly established 5hmC-qPCR technique (Nestor et al., 2012) could be used to revisit the *PLS3* locus (Chapter 3) and to reanalyze bowel tissue sections (Chapter 5) for 5hmc expression.

7.5 *PLS3* methylation is strongly associated with sex and tumour location

In Chapter 3, we observed that there was a remarkable difference in *PLS3* promoter methylation and the sexes ($p = <0.0001$) (Figure 3.14). Over 85% of the female samples analysed were methylated for *PLS3* and over 85% of male samples were unmethylated for *PLS3*. DNA methylation helps maintain the inactivation of one of the X chromosomes in females, where *PLS3* is located. Promoters on the inactive, but not the active, X chromosome are often methylated (Lock et al., 1987), so one possibility is that X chromosome-specific regulatory factors could modulate T-plastin expression in the female CRC patients examined in our study. However, it has been shown that DNMT1-deficient mice embryos can maintain imprinted X inactivation in non-embryonic cell lineages, despite extensive CpG demethylation (Sado et al., 2000). Although this paper implies that demethylation of X chromosomal genes (such as *PLS3*) would not necessarily lead to their activation, further detailed methylation studies of both X-chromosomes in the T-plastin expressing female cohort would be required to investigate this further.

The extent to which LOH affects the sex chromosomes is not clear. For example, Cheng and colleagues showed that the inactivated X-chromosome had the ability to influence the development of ovarian epithelial cancers (Cheng et al., 1996), suggesting that some genes on the silenced X-chromosome may escape inactivation and may subsequently be subject to transforming mutations, epigenetic dysregulation, or chromosomal gene rearrangements that influence cancer onset. Interestingly, a number of leukaemias and lymphomas are associated with X-chromosome rearrangements (Shaknovich et al., 2011). Notably, Sezary syndrome is also a rare type of cutaneous lymphoma (discussed above). It is tempting to speculate that *PLS3* could therefore be associated with sex linked lymphoma as well as sex linked CRC. Sezary syndrome has a male: female incidence ratio of 2.5:1, so it would be interesting to determine the epigenetic regulation of *PLS3* expression in male and female Sezary patients and to determine whether there was any correlation with *PLS3* expression levels and metastasis from the primary lymphoma in this type of cancer.

In this thesis, we have also demonstrated that there is a statistically significant relationship between *PLS3* promoter methylation and tumour location ($p = 0.044$) (Figure 3.15). The

frequency of *PLS3* methylation was higher in the proximal (right-sided) colon compared to the distal (left-sided) colon. As previously discussed, there is a large body of evidence which suggests that there are sex-specific differences between left-sided and right-sided CRC (Benedix et al., 2010). More men than women have LCCs and the survival of cancer patients with LCCs tends to be higher than those with RCCs. According to the work in this thesis, the *PLS3* promoter is more likely to be methylated in both RCC and in females, consistent with the literature. A study of differential gene expression in CRC that compared the caecum and sigmoid/rectosigmoid bowel is informative in this regard. They showed that keratins 8, 19, 20 and carbonic anhydrases II, IV and VII were downregulated in left sided cancers whereas other genes such as COX2 were upregulated in left sided adenocarcinomas. T-plastin was identified by this study as one of 30 genes differentially expressed more than 3-fold in at least one Dukes' stage compared to normal mucosa, with T-plastin expression being highest on the left side (Birkenkamp-Demtroder et al. 2005). This would support the assertion in this thesis that methylation controls T-plastin expression in colon cancer. This could be followed up by examining more patients from the NLCS and improving the recovery of methylated DNA from fixed tissues so that historical samples from RCCs and LCCs can be studied for the methylation of *PLS3* in these patients.

7.6 T/L-plastin expression is switched on in CRC and frequently observed at the invasive front of the tumour

After investigating *PLS3* promoter methylation in Chapter 3, we went on to examine plastin protein expression. Six polyclonal antibodies were raised and tested for their specificity and suitability using immunoblotting. The Dann1a antibody was taken forward for immunohistochemical staining of patient tissue (Chapter 5), based on its relative specificity and ability to detect T- and L-plastins using a range of techniques. In support of the literature, no T/L-plastin expression was observed in histologically normal colonic mucosa by immunohistochemical analysis (Delanote et al., 2005). Remarkably, when we turned to the tumour tissue from the NLCS archive, we found that ~80% of samples were positive for plastin expression (Chapter 5, Figure 5.5). A recent investigation reported the expression of L-plastin in ~82% of CRCs (Li and Zhao, 2011). This group also observed a correlation between L-plastin and tumour stage, size and lymph node metastasis. Conversely, we found no association between plastin expression and clinicopathological features or survival.

However, the interpretation of our results is limited because Dann1a detects both T- and L-plastin. To overcome this limitation, T- and L-plastin monoclonal antibodies could be developed, northern blotting could be used, or laser capture microdissection (LCM) could be employed to firmly establish which plastin is expressed in a cohort of CRC patients. Furthermore, it would be useful to assess plastin expression using other tissue archives such as the Western Australia tissue bank. It would also be appealing to see whether T/L-plastin and lamin A is switched on in other epithelial cancers.

Having discussed how epigenetics might control gene expression in CRC, it is of interest to consider how those changes in gene expression might influence cellular function and confer a growth advantage to the transformed cell. As an actin bundling protein, plastin is involved in controlling actin dynamics. We noted in our study that T/L-plastin expression was significantly increased at the invasive front of tumours (Chapter 5, Figures 5.6-5.7). One possible explanation for this observation is that plastin expression at the leading edge increases cellular movement and hence encourages cells to break away from the tissue mass and metastasise (Figure 7.1).

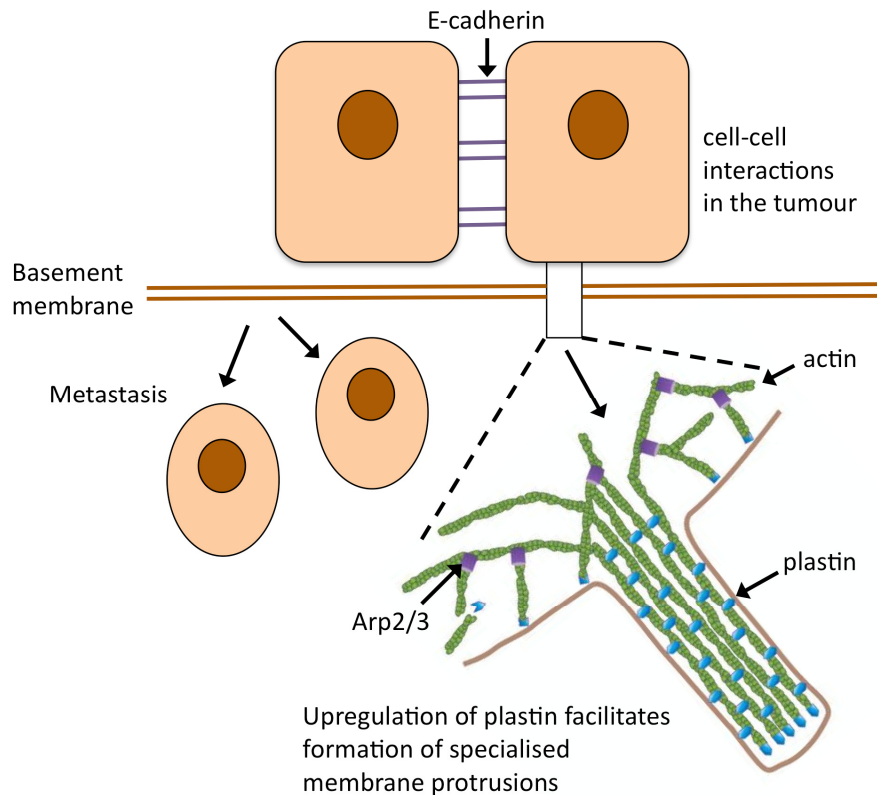


Figure 7.1: Upregulation of platin at the invasive front may lead to increased formation of specialised membrane protrusions and hence metastasis

This hypothesis is supported by the observations of Giganti et al. (2005) who showed that T-platin increased the rate of movement of beads coated with actin (and actin nucleating proteins) and stabilized the actin comets. In future, immunofluorescence studies will be required to determine whether T-platin is preferentially co-localised with actin in cells at the leading edge, or in transformed CRC cells in culture. If so, studies could be performed to test whether over-expression of platin (by transfection) is sufficient to induce a migratory phenotype in CRC cell lines. An alternative explanation for the role of T/L-platin at the leading edge is that platin plays a role in modulating the mechanical stiffness of cells, possibly together with lamin A. An interesting study from Leight et al. has shown that culturing epithelial cells on gels with varying rigidity induces changes in signalling through the PI3K/AKT pathway (Leight et al., 2012). EGFR is upregulated in the lamin-A responsive network described in Chapter 6, and also signals through the PI3K/AKT pathway; therefore, platin may be one of a number of proteins that helps modify cell stiffness and hence

modulates signal transduction as transformed cells 'prepare' for EMT (Swaminathan et al., 2011).

Moreover, there is evidence to suggest that there is a direct mechanical link between chromatin and the cytoskeleton, via nuclear lamins, and that the application of force can be sensed by adhesion molecules and transmitted to DNA to induce remodeling events. Thus platin could be an important player in the 'tensegrity' network model (which achieves complex architecture through tensional integrity) developed by Donald Ingber (Ingber, 1993).

Although platin expression was observed at the leading edge, it was expressed at all Dukes' stages of CRC. Thus, another possible explanation for the elevated expression of platin in CRC is that platin may cause aberrant signalling processes to occur that pave the way for EMT. In this scenario, platin overexpression may prevent transmembrane receptors from being clustered appropriately, may prevent signalling complexes from being disassembled in a timely fashion, or may prevent regulatory molecules from being recruited to the signalling node (Stephenson et al., 2012). The hypothesis that aberrant signalling caused by platin overexpression results in cancer progression could be tested in a number of ways. For example, one could analyse global signalling patterns in cells expressing platin by probing the phosphoproteome e.g. using anti-phosphotyrosine antibodies in a proteomic experiment. Changes in the phosphorylation pattern (compared with non-platin expressing cells) could be determined by mass spectrometry, and signalling through candidate receptors could be confirmed using receptor specific antibodies in a western blotting or radiolabeling experiment. Alternatively, tagged platin could be used as bait to immunoprecipitate cross-linked associated proteins, and any candidate signalling receptors or signal transduction regulators identified by mass spectrometry could be confirmed by follow up blotting studies. Another possibility is that aberrant platin expression perturbs cell polarity, which is essential for normal tissue homeostasis and is known to be disrupted in tumorigenesis (Royer and Lu, 2011). Actin bundling is important in the polarity of and positioning of epithelial cells, so inappropriate expression of platin could lead to perturbations in the normal cytoskeletal architecture thus promoting neoplastic transformation (Stevenson et al, 2012).

Although T-plastin is predominantly found in the cytoskeleton, there are reports that actin and other actin binding proteins can be functionally active in the nucleus, for example in muscle cells, where actin may regulate transcription factor complexes (Zheng et al., 2009). The staining observed in Chapter 5 of skin epithelial cells also suggested that T/L-plastin was found in the nucleus. However, the staining of potentially nuclear-localised T/L-plastin was harder to observe in CRC because of the stronger co-staining with haematoxylin. A potential role for nuclear localised plastins in the control of gene expression cannot be ruled out and further work is required to confirm immunohistochemically whether plastin expression occurs in the nucleus of CRC tissue, preferably using T- and L-plastin specific antibodies.

7.7 Identification of a candidate gene network based on the expression of GFP-lamin A in CRC cell line SW480

Finally, in order to address the mechanism by which lamin A causes CRC cells to adopt a more motile phenotype, and to identify candidate genes for biomarker/drug development, we performed IPA on a microarray dataset from a model cell line overexpressing GFP-lamin A. The IPA analysis identified a candidate gene network linked to cancer, cellular movement, cellular growth and proliferation ($p < 0.05$). The validity of this network was confirmed using a qPCR and Western blotting approach. Upon the expression of GFP-lamin A in CRC cell line SW480, we observed a significant increase in EGFR and decrease in E-cadherin both at the mRNA and protein level. Interestingly, both EGFR and E-cadherin are involved in the EMT pathway, whereby stationary polarised epithelial cells, communicating by cell-cell junctions, break up their junctions and switch to a non-polarised, mobile and invasive mesenchymal cell state. EGFR signalling has been shown to induce the down regulation of E-cadherin and induce EMT in ovarian cancer cells (Cheng et al., 2012). Given the data presented in this thesis, lamin A may have an important role in the transition of epithelial cells to a more mesenchymal state, and thus metastasis (Figure 7.2).

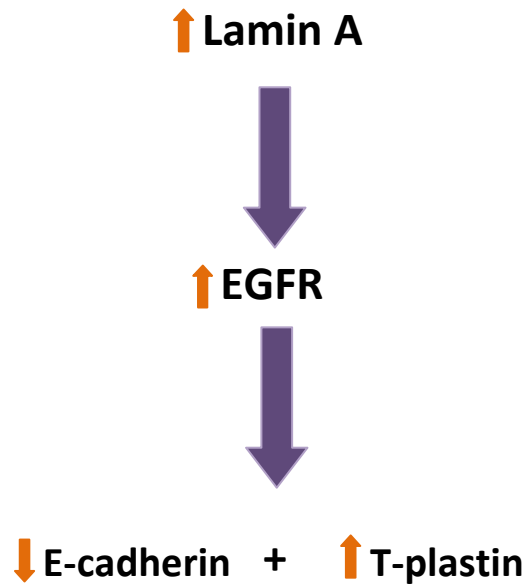


Figure 7.2: Increased expression of lamin A in SW480 cells may induce EMT through the upregulation of EGFR, down regulation of E-cadherin and upregulation of T-plastin

T-plastin was not identified as part of this network, despite being upregulated 13-fold in the SW480/lamA cells compared to the SW480/cntl cells. This highlights the limitations of this type of computational analysis, as this IPA is based on literature-curated interactions. Experiments will now be required to establish whether T-plastin is upstream, downstream or acting in parallel with other members of this network. This could be tested by transfecting T-plastin into T-plastin negative CRC cells and analyzing whether EGFR is upregulated, E-cadherin is downregulated, and whether other lamin A responsive genes are influenced by T-plastin expression. The findings from Chapter 6 provide a framework to revisit the NLCS tissue archive and examine the expression of key genes such as EGFR and E-cadherin, in combination with lamin A and T-plastin in a multi-factorial biomarker study.

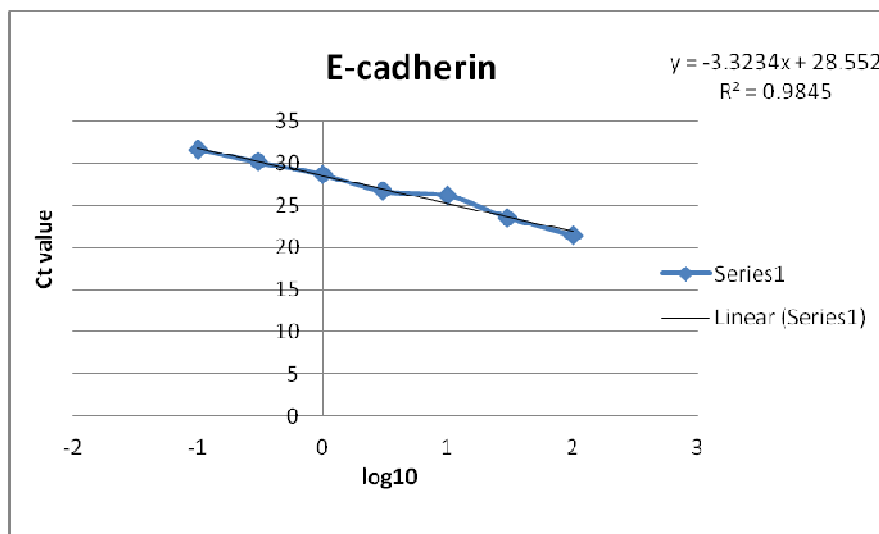
7.8 Conclusion

In conclusion, the data described in this thesis suggests that *PLS3* promoter methylation is an important mechanism of controlling T-plastin expression. Strikingly, T/L-plastin was aberrantly expressed in CRC suggesting that plastin has a potential role in neoplastic transformation. Finally, we identified a novel gene network based on the overexpression of lamin A in CRC cells. The data suggests that lamin A is potentially a master regulator of a pathway that co-ordinates the cytoskeletal changes required for cell motility and tumour

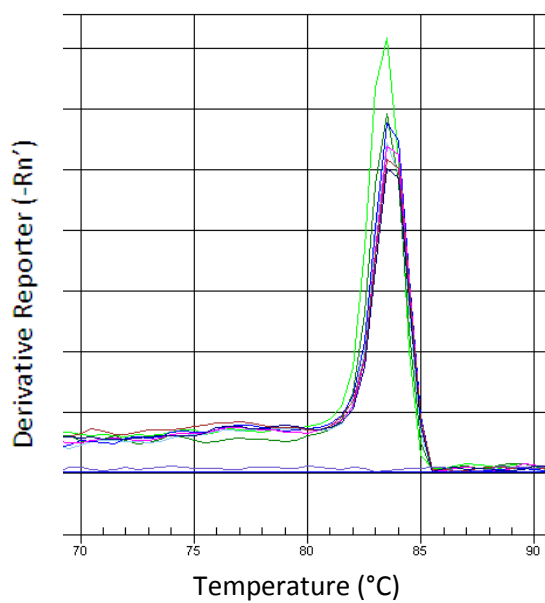
invasiveness. Overall, *PLS3* methylation status will not be a stand-alone biomarker for CRC and combining a promoter methylation approach (e.g. for *PLS3*) together with an immunohistochemical approach (e.g. for lamin A) may prove to be too complex for routine diagnostic/prognostic use. However, improvements in the technology used to detect methylation may be required before combined methylation/protein biomarker panels can be taken forward into the clinic. Advances in our technological capacity to perform microarrays on large datasets, and to sequence individual cancer genomes in a time and cost-effective manner, will help us to understand how these multiple and complex factors are related in cancer biology and will pave the way for the development of personalised medicine.

Appendix: supplementary figures

A



B



C

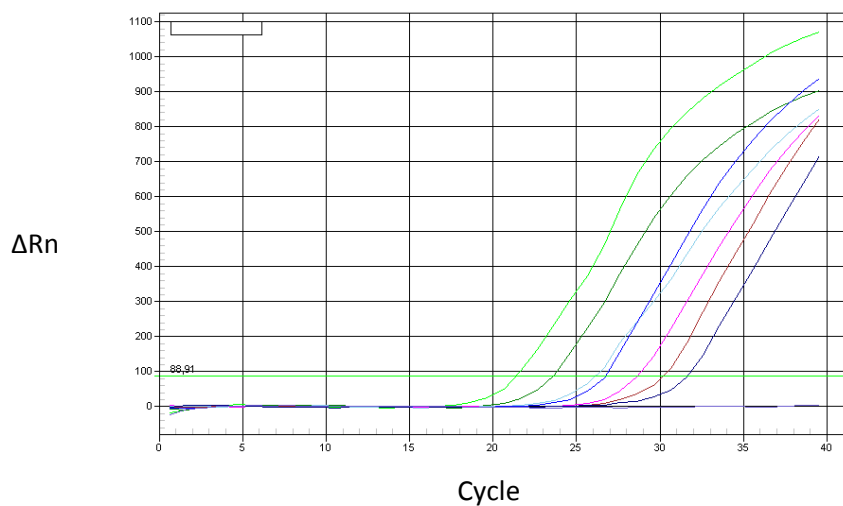
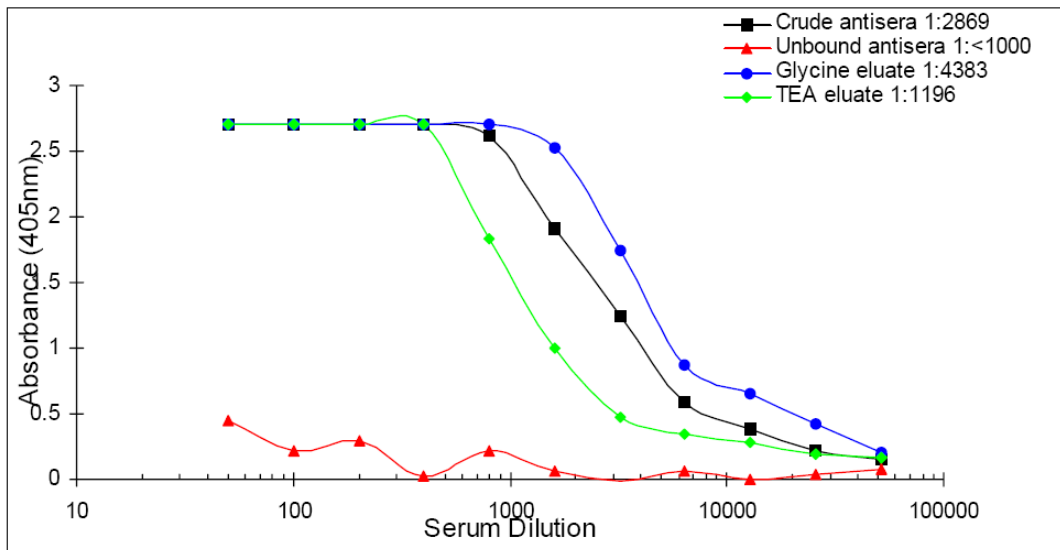
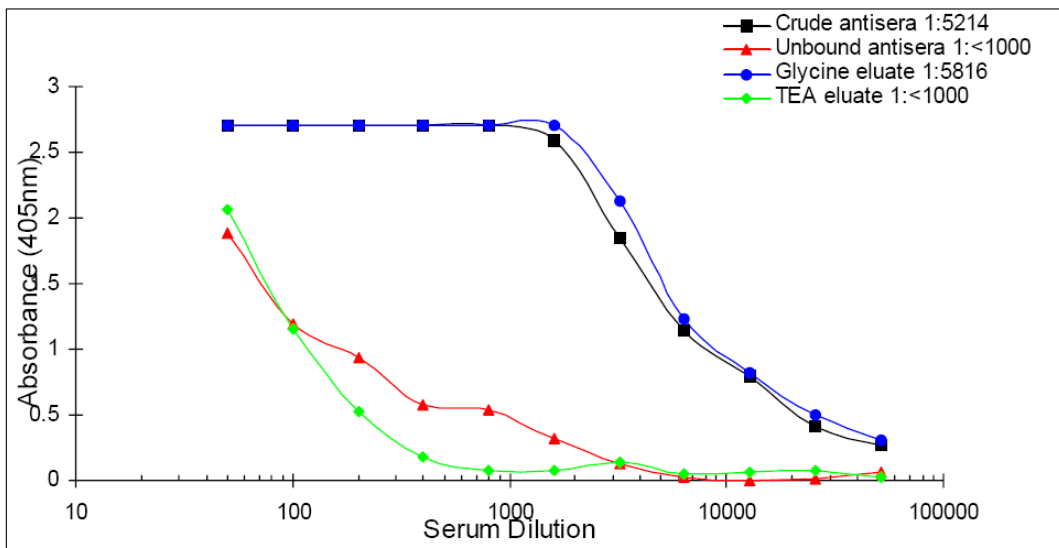
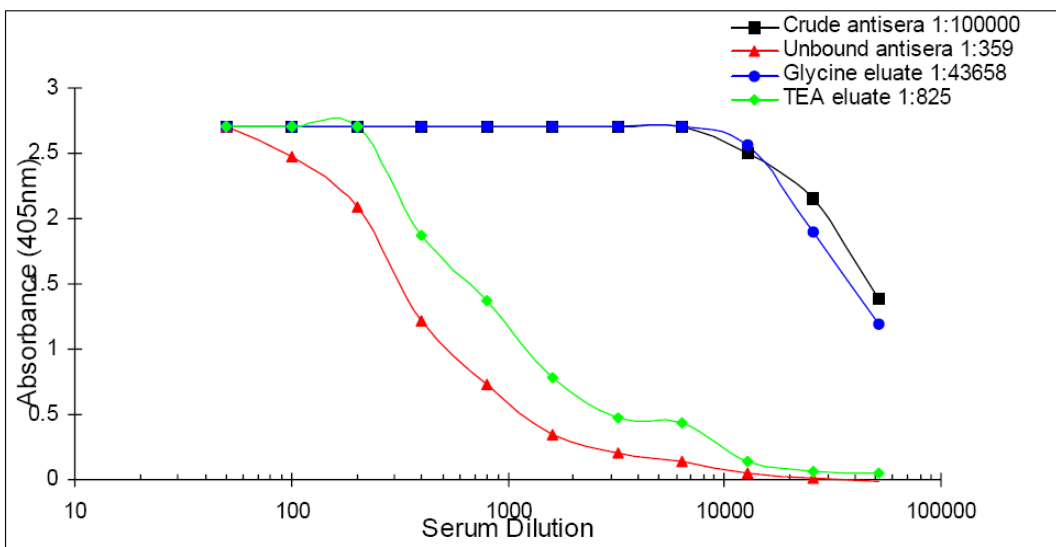


Figure S1: Representative graphs generated from qPCR experiments

In this case, all graphs were generated using CDH1 primers and performing qPCR on cDNA from CRC cell line SW480 (A) qPCR was performed on a cDNA dilution series. Standard curve (where X axis = \log_{10} and Y axis = C_T value) shows that that CDH1 primers are specific as the gradient of the graph is between -3.3 ± 0.3 . (B) Melt curve analysis was performed to confirm the integrity of the PCR product. A single peak corresponds to the decreased fluorescence at the melting point of the PCR product. (C) Amplification plot indicating the changes in SYBR green fluorescence during the reaction.

A**B****C**

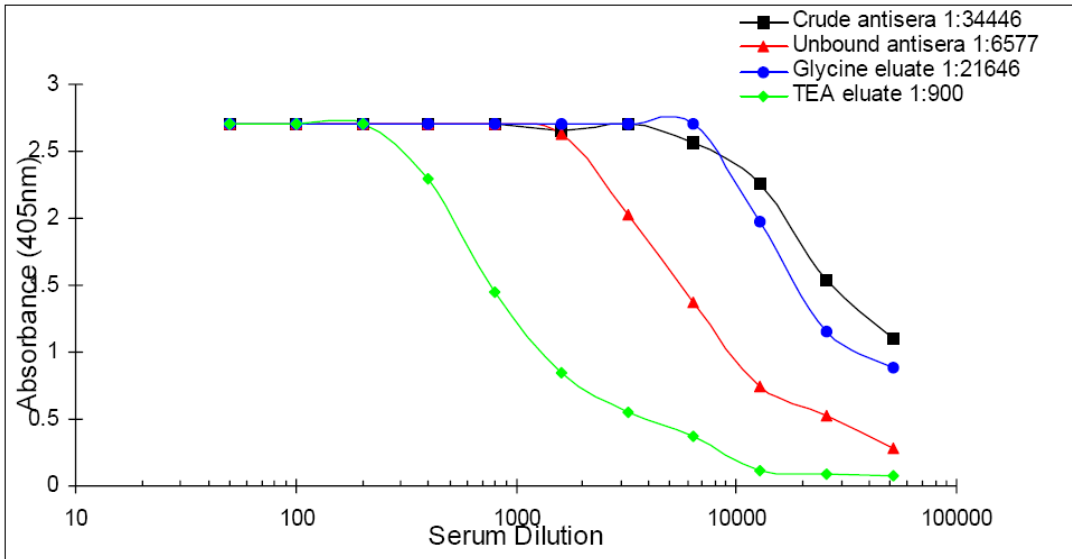
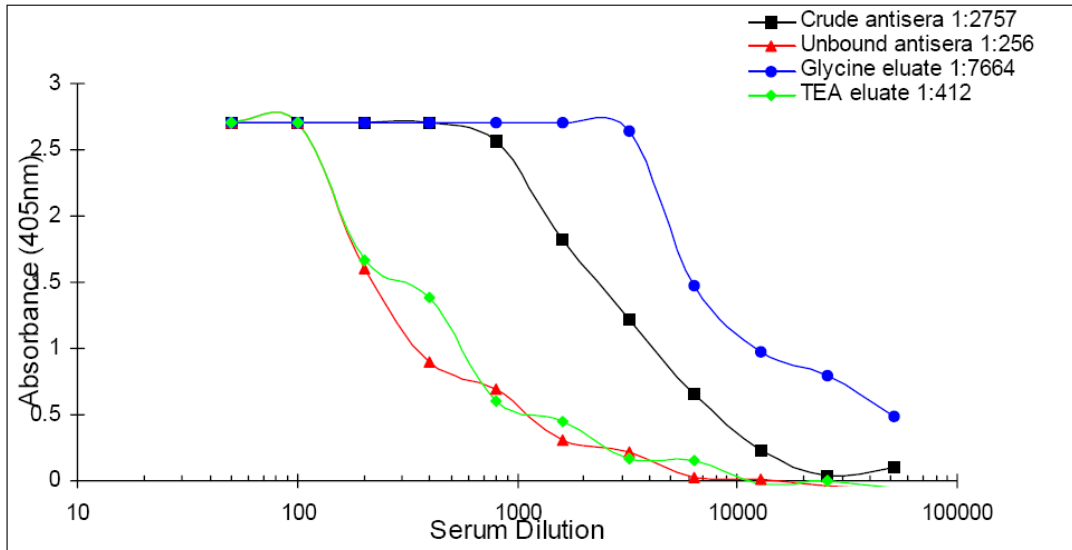
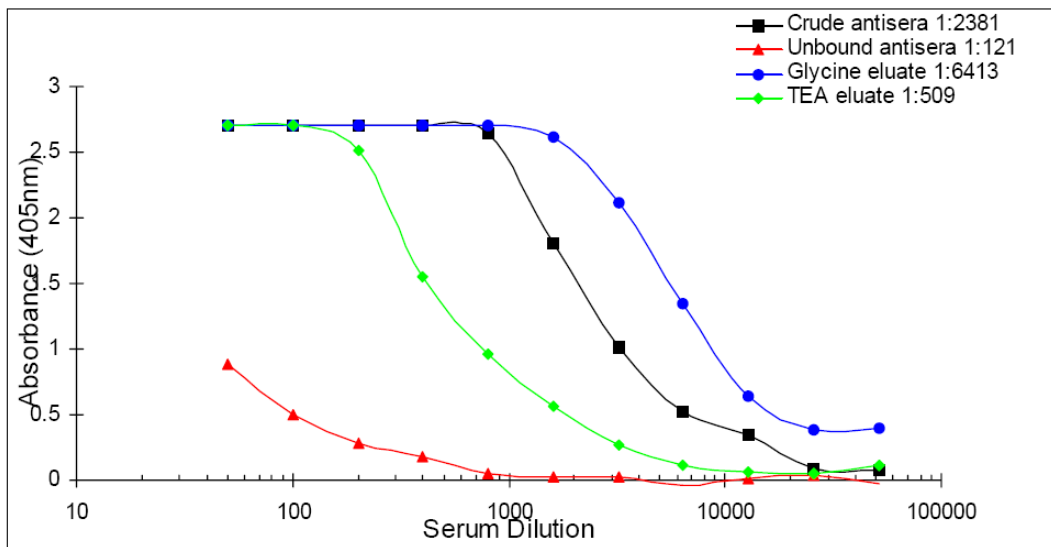
D**E****F**

Figure S2: ELISA analysis for Dann antibodies

Affinity purified rabbit polyclonal anti-plastin antibodies characterised by ELISA against the immunising peptides over a range of dilutions up to 1/100000 and compared with the crude antisera. From this the antibody titre (antibody dilution at half maximum response) can be determined. The antibody concentration is determined from the UV absorbance at 405 nm. Antisera obtained from each animal displayed varying titres of anti-peptide antibody (A) 1:4383 (Dann1a antibody) (B) 1:5816 (Dann1b antibody) (C) 1:43658 (Dann2a antibody) (D) 1:21646 (Dann2b antibody) (E) 1:7664 (Dann3a antibody) (F) 1:6413 (Dann3b antibody). Dann2a has the highest titre of antibody (1:43658) compared with Dann1a, which has the lowest (1:4283).

atttcctcaacaaaaatggttaCGactggaaacaggaaagggccttagactttttcttctacagctatcccacaagtcagtc
 ctcttgacctgacctgcaaaatccctcaaacctctggctctctgagttgattttggatataCGatgaaacctaggttt
 ggaatgcagataacctccaCGtgtatataagaaagggtcagctatgaCGtggaagccatctcctgggagagaga
 gaagaaatggcagctctggggagtagtaacatgtctccaaatcttctctgggtgaaaggagactgatgagaattgatacc
 cattedCGgtcaaaagagtggaaaccaatgtacttccaaaccctctctcaacccctctcCGcatggacaacaatacc
 agacaggtgatgtgggctaacaatttacttggcatgaggccaaaggcttgagggccctgcccgcccatattcttctc
 ccttgacttcttaaggaaaggaatgatgtctgatgtttcccctctgacccctttggcacctggactgattgttgcagat
 gtaattaggaatgttccccacaatgCGttattcttctcaCGattctgggagaaactgtacccccccccatagactt
 atataggtggcattcaaatcttgttcccaactttttcatctgtttattaatcccacaagattgtgtgaatgtgtact
 cCGagccaggcaCGttggacttctaacttctcttagcccaagtaggaaggggagactcaggCGctggggaccattct
 cctctcccctgcagcagagttgcagtccttatacccctctgggtgcccatacccCGtgcttatttcttgatccccacc
 agttgatgtgacaggctCGtgcccaatcccccttctgggttcccaggcCGactgctagcaccaccCGagccaatggCG
 gCGcCGaggggCGgagggggctggcaggaggggagggagCGctggcttttagagccacagctgcaagattcCGaggt
 gcagaagttgtctgagtgCGttggtCGgCGcagtCGggccagaccaggactctgCGactttaCGtaagtgtttgt
 aggCGcCGCGggccactaggggagCGggttctctgggCGtgggagagagtggtccCGgggagagcatctCGttaag
 ctcagcaggaaCGtgCGgCGcaCGtggggCGggggttgggggagagggaggtCGgagaaatttcagttggagccctC
 GggCGccCGgCGatCGgtCGcaacCGaaatgggtgtgagtgCGgggagtttccctactagcatcCGcCGcagacaC
 Gttttctgcacttcaactgtattaagtgtgtttcttactagttgctcttaactgttgcagctcttgggctggagtc
 ctagaCGccagcccttgccctgattccccctCGCGctgCGcccCGaagtggaaagggagCGcacaacttcccctctg
 tCGtcttctccagctactgccatcccccttctcccctccCGccCGgactcaggaaatccCGgagccagcagccctgctac
 tccctccagccccacaCGccCGcctCGggtgacctggctggcttaagcCGaccctggggctctggagagggggggcCG
 tggcCGagggaaaggcaCGaggtttgggttgcctgcttctgcttcttcccctccccttgccttagCGagggCGtCGCG
 aaCGcaccctagcttcccctatgagtaagcaacttttttcttctcagtaggagaacatctctgggctagtaggacagtac
 ctttcCGttctccccctggccccacccccctgtctttttctcagctcttcttgaacttgcgcccCGggCGCGCGgtCG
 gggCGgCGgcagtcCGgacctctccCGactcttgagagagagaggcaaggggCGaCGggaggggagtaatagctc
 accccccCGcccttcccCGcacagctgcaacttgcctgtgtttacttttct

Figure S3: PLS3 promoter sequence: location of the CpG island

The CpG island is 431 bp (highlighted in yellow). CG dinucleotides are highlighted in red. The transcription initiation start site (TSS) is indicated in purple. Note that the PLS3 promoter sequence displayed is post sodium-bisulphite modification.

atTTTTtaataaaatggttaCGattggaataggaaagggttttagattTTTTTTTTtatagtttatTTTataagttagt
TTTTgatttgatttTgtaaaatTTTTaaattttggTTTTtgagttgattttggatataCGatgaattataggttt
ggaatgtagataaTTTTaCGtgtattaatgaaagggttagttatgaCGtggaagttatTTTTgggttagagaagga
gaagaaatggttagttgggggagtagtaatatgtTTTTaaatTTTTtggtgaaaggagattgatgagaattgatatt
tattttCGgttaaagagtggaattaatgtatTTTTaaTTTTTTTTtaTTTTTTtCGtatggataaataatatt
agataggtgatgtgggttaataaatttatTTggatgaggTTaaaggTTtgagggtttgTTTTgTTTatTTTTTTT
TTTTgattTTTTtaaggaaaggaatgatgttgatgtTTTTTTTTgtTTTTTTggTatttggattgattgtttagat
gtaattaggaatgtTTTTaatagtCGttatTTTTTTaCGatttgggagaaattgtatTTTTTTTTatagattt
atataggtggTattttaaTTTTgtTTTTaaTTTTTTtatttgtttattaatTTTataagattgtgtgaatgtgtatt
tCGagttaggtaCGttggattTTTTaaTTTTTTtagTTTaaagtaggaaggggagatttaggCGttggggattTTTT
TTTTTTTTgttagtagagtttagtTTTTatTTTTTTgggtgTTTTatttCGgtttatTTTTTTggattTTTTattt
agttgatgtgataggttCGtggTTTTaaTTTTTTTTggTTTTtaggtCGattgtagtattattCGagttaatggCG
gCGgtCGaggggCGgagggggttggtaggaggggagggagCGttggttttagagttatagttgtaaaagatttCGaggt
gtagaagttgtttgagtgCGttggtCGgCGtagtCGggttagatttaggattttgCGattttaCGtaagtgTTTTgt
aggCGtCGCGggtatttaggggagCGggtTTTTgggCGtggttaggagtggtttCGgggagagtatttCGgttaag
tttagtaggaaCGtCGCGtCGtCGtgggCGggggtgggggagaggaggtCGgagaaTTTTtagttggagTTTTC
GggCGttCGggCGatCGtCGtaatCGaaatgggtgtgagtgaCGgggagTTTTTTtatttagtatCGtCGtagataC
GTTTTgtatTTTTattgtattaagtgtgtTTTTtattagttgTTTTaaTTTgttttagttttgggttggagtt
ttagaCGttagttttgttttgattTTTTtCGCGgttgCGgtttCGaagtggaaagggagCGtataaTTTTTTTTg
tCGTTTTTTTTtagttattgtttTTTTTTTTTTTTCGttCGgatttaggaaatttCGgagttagtagtttgttat
TTTTtagTTTTtaCGttCGtttCGggtgatttggttggtTTTaaagTCGatttggggTTTTggagagggggggtCG
tggtCGagggaaaggttaCGaggtttgggttgtttgTTTTTgtttgTTTTTTTTTTTgtTTTTtagCGagggCGtCGCG
aaCGatttttagTTTTtatgagtaagtattTTTTTTTTTTTTtagtaggagaatattttgggttagtaggatagtat
TTTTCGTTTTTTTTggTTTTatTTTTTgtTTTTTTTTtagTTTTTTgattttgCGgtttCGggCGCGCGgtCG
gggCGCGgttagtttCGgattTTTTtCGatttttgagagagagaggttaaaggggCGaCGggagggaggtaatagttt
atTTTTCGTTTTTTTTCGtatagttgtattgtttgtgtttatTTTTTT

Primer set 1

Outside	<u>165bp</u>		
Flank up	GAGAGTATTTYGGTTAAGTTTAGTAGG	55.7-57.6°C	27 bp
Flank down	ACRAATACTAATAAAAAAACTCCC	56.1-58.0°C	25 bp
Inside	<u>115 bp</u> – <u>123 bp</u>		
US	GGTTAAGTTTAGTAGGAATGTGTGGT	58.1°C	26 bp
MS	AGTTTAGTAGGAACGTGCGGC	58.5°C	21bp
UAS	CACACCCATTTCAATTACAACCA	59.5°C	23 bp
MAS	ACCATTTTCGATTACGACCG	59.1°C	20 bp

Primer set 2

Outside	<u>166bp</u>		
Flank up	GATTGTTAGTATTATTYAGTTAATGG	54.3-56.7°C	27 bp
Flank down	TCRCAAATCCTAAATCTAACCC	55.2-59.9°C	23 bp
Inside	<u>144 bp</u> - <u>155 bp</u>		
US	TTGTTAGTATTATTTGAGTTAATGGTGGT	60.1°C	29 bp
MS	GTATTATTCGAGTTAATGGCGGC	60.3°C	23 bp
UAS	CCTAAATCTAACCAACTACCACCA	61.2°C	25 bp
MAS	ATCTAACCCGACTACCGCCG	60.9°C	20 bp

Figure S4: *PLS3* promoter sequence: location of N-MSP primer sets 1 and 2

The 'outside' primer sets are underlined. The blue (primer pair 1) and purple (primer pair 2) regions highlight methylated primers. The green (primer pair 1) and yellow (primer pair 2) regions highlight the unmethylated primers. The TSS is highlighted in pink. CG dinucleotides are highlighted in red. Note that the *PLS3* promoter sequence displayed is post sodium-bisulfite modification. US = unmethylated sense, MS = methylated sense, UAS = unmethylated antisense, MAS = methylated sense.

atTTTTtaataaaatggttaCGattggaataggaaagggttttagatTTTTTTTTtatagttattTTtaagttagt
TTTTgatttgatttTgtaaaatTTTTtaaatTTTggTTTTtgagttgattttggatataCGatgaaTTatagttt
ggaatgtagataaTTTTaCGtgtattaatgaaagggttagttatgaCGtggaagttatTTTTgggtagagaagga
gaagaaatgtagttTggggagtagtaatatgtTTTTaaatTTTTTgggtgaaaggagattgatgagaattgatatt
tattttCGgttaaaagagtggaattaatgtatTTTTtaattTTTTTTTTtaattTTTTtCGtatggataaataatatt
agataggtgatgtgggttaataaatttatTTTggatgaggTTaaaggTTTgagggtTTTgTTTgTTTatattTTTTT
TTTTgatTTTTtaaggaaaggaatgatTgtgatgtTTTTTTTTgtattTTTTTggTattTggattgattgtTtagat
gtaattaggaatgTTTTtaataTgtCGttatTTTTTTaCGattTgggagaaatTgtatTTTTTTTTatagattt
atataggtggTattTaaatTTTTgtTTTTaaTTTTTTtatTTgtttattaatTTTataagattgtgtgaatgtgtatt
tCGagttaggtaCGttggattTTTTaatTTTTTTtagTTTaaagtaggaaggggagatttaggCGttggggattTTTT
TTTTTTTTgttagtagagttTtagttTTTatTTTTTTgggtgTTTTatTTTtCGgtttatTTTTTggattTTTTattt
agttgatgtgataggttCGtggtTTTaaTTTTTTTTggTTTTtaggtCGattgttagtattattCGagTTaatggCG
gCGtCGaggggCGgagggggtTggtaggaggggagggagCGttggTTTTtagagTTatagttgtTaaagatttCGaggt
gtagaagttgtTtgagtgCGttggTgCGCGtagtCGggttagaTTtaggattTgCGattTTaCGtaagtgTTTTgt
aggCGtCGCGggtatttaggggagCGggtTTTTgggCGtggttaggagtggtttCGgggagagtatttCGgttaag
TTtagtaggaaCGtgCGCGTatCGtggggCGggggtTgggggagagggaggtCGgagaaTTTTtagTggagTTTTC
GggCGttCGggCGatCGgtCGtaattCGaaatgggtgtgagtgaCGgggagTTTTTTatttagtatCGtCGtagataC
GTTTTgtattTTattgtattaagTgggtTTTTtatttagttgTTTTtaattTgtTtagttTgggtTggagtt
ttagaCGttagTTTTgtTTTTgattTTTTTTCGCGgtTgCGgtttCGaaagtggaaagggagCGtataaTTTTTTTTg
tCGTTTTTTTTtagttattgttattTTTTTTTTTTTTCGttCGgatttaggaaatttCGgagtttagtagtttTttat
TTTTtagTTTTtaCGttCGtttCGggtgattTggTggTTTTaaagTCGattTTggggTTTTggagagggggggtCG
tggtCGagggaaaggttaCGaggtTgggtTgtTgtTTTTTgtTgtTTTTTTTTTgtTTTTtagCGagggCGtCGCG
aaCGatttttagTTTTtatgagtaagtattTTTTTTTTTTTTtagtaggagaatattTTTTgggttagtaggatagtat
TTTTCGTTTTTTTTggTTTTatTTTTTgtTTTTTTTTtagTTTTTTgattTgCGgtttCGggCGCGCGgtCG
gggCGCGgttagtttCGgattTTTTTTCGattTTTggagagagagaggtTaaaggggCGaCGggagggaggtaatagtt
atTTTTCGTTTTTTTTCGtatagttgtattTgtTgtTttatTTTTT

Primer set 3

Outside	<u>131 bp</u>		
Flank up	YGGAGAAATTTTAGTTGGAGTTTT	57.0-58.9°C	24 bp
Flank down	CCACTTAATACAATAAAATACAAAAAAC	57.0°C	28 bp
Inside	<u>104 bp</u> – <u>113 bp</u>		
US	TGGAGTTTTTGGGTGTTTGGGT	62.6°C	22 bp
MS	TTTCGGGCGTTCGGGC	61.7°C	16 bp
UAS	CTTAATACAATAAAATACAAAAACATATCTACA	60.9°C	34 bp
MAS	AATACAATAAAATACAAAAACGTATCTACG	61.4°C	31 bp

Figure S5: PLS3 promoter sequence: location of N-MSP primer set 3

The ‘outside’ primer set is underlined. The methylated primer pair is highlighted in blue. The unmethylated primer pair is highlighted in green. The TSS is highlighted in pink. CG dinucleotides are highlighted in red. Note that the *PLS3* promoter sequence displayed is post sodium-bisulfite modification. US = unmethylated sense, MS = methylated sense, UAS = unmethylated antisense, MAS = methylated sense.

attttttaataaaaatgggta**CG**attggaataggaaagggttttagatTTTTTTTTTatagttatTTTataagttagt
 TTTtgatttgattttgtaaaatTTTTaaatTTTggTTTTtgagttgattttggatata**CG**atgaaTTataggttt
 ggaatgtagataaTTTT**CG**gtatTaatgaaagaggttagttatga**CG**tggaagttatTTTTgggtagagaagga
 gaagaaatggtagtttggggagtagtaatatgtTTTTaaatTTTTTTTgggtgaaaggagattgatgagaattgatatt
 TTTTT**CG**gtTaaaagagtggaaTTaatgtatTTTTaaTTTTTTTTTaaTTTTTTT**CG**tatggataaaatataatt
 agataggtgatgtgggtTaaTaatTTatTTTggTatgaggTTaaaggTTTgagggtTTTgTTTgTTTatTTTTTTT
 TTTTgatTTTTtaaggaaaggaatgatTgtgatgtTTTTTTTgtTTTTTTTggTattTggattgattgtTtagat
 gTaattaggaatgtTTTTTaaatgt**CG**TatTTTTTTT**CG**atTTTgggagaaatTgtTTTTTTTTTatagattt
 atataggtggTatTTTaaatTTTgtTTTTTaaTTTTTTTatTTTgtTTTattaatTTTataagattgtgtgaatgtgtatt
T**CG**agTTaggT**CG**ttggatTTTTaaTTTTTTTtagTTTaaagtaggaaggggagatttag**CG**ttggggattTTTT
 TTTTTTTTgtagtagagtttagttTTTatTTTTTTTgggtgTTTTTTTT**CG**gtTTTatTTTTTTggattTTTTTTTT
 agttgatgtgataggt**CG**tggtTaaTTTTTTTTTggTTTTTTtaggt**CG**attgttagtattTT**CG**agTTaatgg**CG**
 g**CG**gt**CG**agggg**CG**gagggggtTggtaggaggggagggag**CG**ttggTTTTtagagTTatagTTgtTaaagattTT**CG**aggt
 gtagaagttgtTtgagTg**CG**ttggt**CG**g**CG**gt**CG**ggttagatttaggattTT**CG**attTTa**CG**taagtgtTTTgt
 agg**CG**t**CG**g**CG**ggtatttaggggag**CG**ggtTTTTTggg**CG**tggttaggagtggtTT**CG**gggagagtatt**CG**gttaag
 TTTtagtaggaa**CG**Tg**CG**g**CG**Tat**CG**Tggg**CG**ggggtTgggggagagggaggt**CG**gagaaTTTTtagttggagTTTT**C**
Ggg**CG**tt**CG**gg**CG**at**CG**Tat**CG**Taat**CG**aaatgggtgtgagtga**CG**gggagTTTTTTTattagTat**CG**t**CG**tagata**C**
GTTTTTgTatTTTTattTgTattaagTggtgtTTTTTatttagTtgTTTTTaaTTTgtTgTtagTttTgggTtgagTt
 Ttaga**CG**TTtagTTTTTgTTTTgattTTTTTT**CGCG**gtTg**CG**gtTT**CG**aaTggaaagggag**CG**TataaTTTTTTTTTg
 T**CG**TTTTTTTTtagTtattgTtTTTTTTTTTTTT**CG**tt**CG**gatttaggaaatTT**CG**gagTTtagtagTTTgTtatt
 TTTTTtagTTTTTata**CG**tt**CG**tt**CG**ggtgattTggTtggtTaaT**CG**attTTggggTTTTTggagaggggggT**CG**
 TggT**CG**agggaaaggt**CG**aggtTgggtTgtTgTTTTTgTtTTTTTTTTTgTTTTTTtag**CG**aggg**CG**t**CGCG**
 aa**CG**attTTtagTTTTTatgagTaaTatTTTTTTTTTTTTtagtaggagaatTTTTTgggTtagtaggatagTat
 TTTTT**CG**TTTTTTTTTggTTTTTatTTTTTgTTTTTTTTTtagTTTTTTgattTg**CG**gtTT**CG**gg**CGCGCG**gt**CG**
 ggg**CG**g**CG**gtagTT**CG**gattTTTTTT**CG**attTTTggagagagagaggtTaaagggg**CG**a**CG**ggagggaggtaatagTt
 atTTTT**CG**TTTTTTTT**CG**TatagTgtattTgTtTgTtTTTTTTTT

Outside	<u>131 bp</u>		
Forward	YGGAGAAATTTAGTTGGAGTTTT	57.0-58.9°C	24 bp
Reverse	CCACTTAATACAATAAAATACAAAAAAC	57.0°C	28 bp

Figure S6: PLS3 promoter sequence: location of bisulfite sequencing primers

The bisulfite sequencing primers were designed to amplify sodium bisulfite-modified DNA and are highlighted in purple. The TSS is highlighted in pink. CG dinucleotides are highlighted in red. The size of the amplicon is 309 bp and this region encompasses the N-MSP primers shown in Supplementary Figure S5.

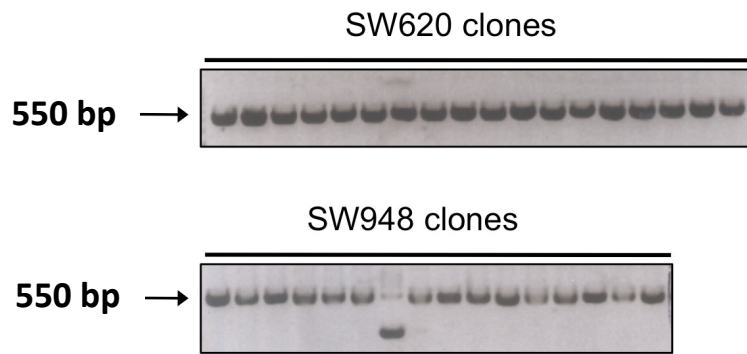
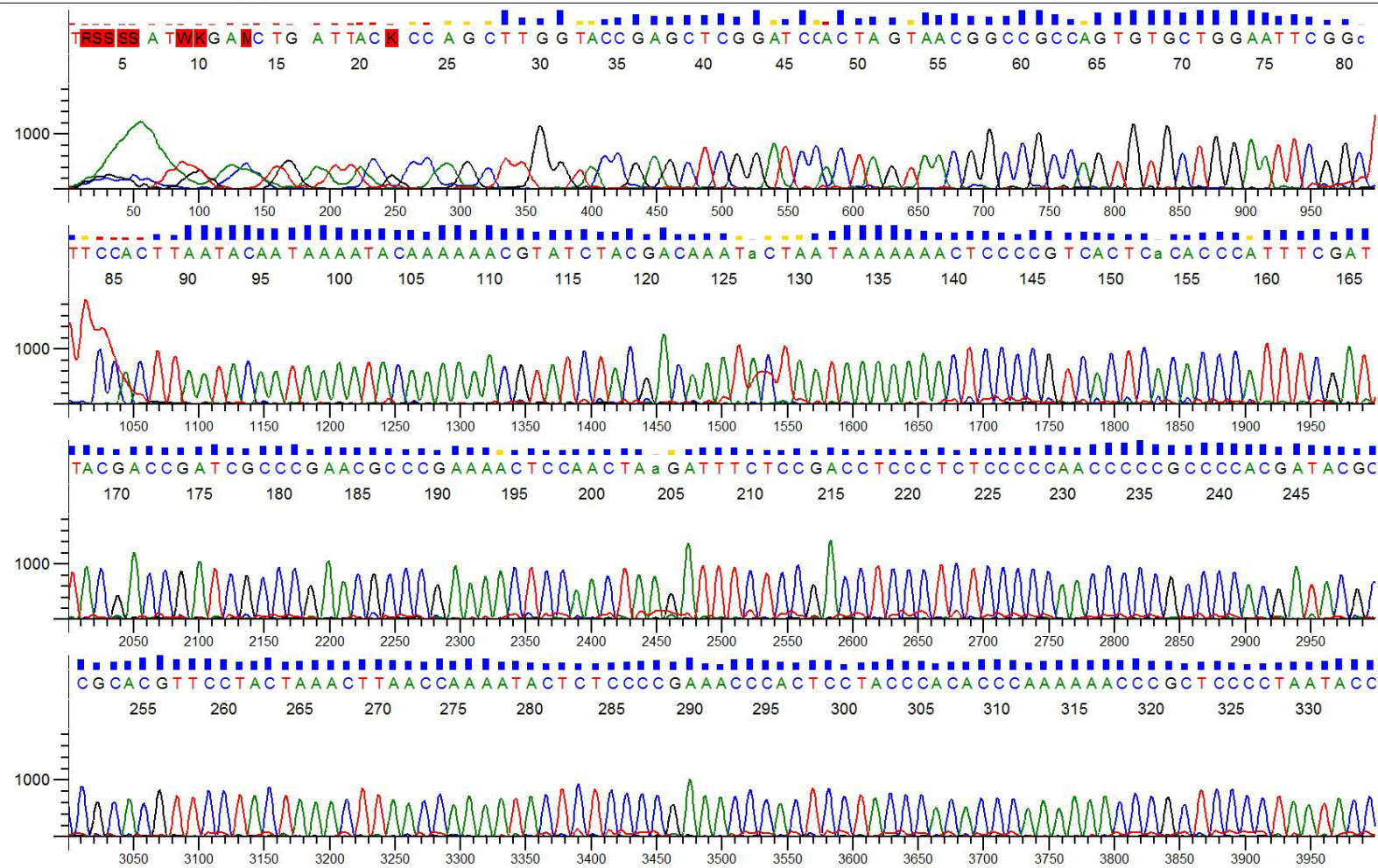


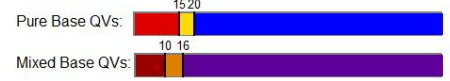
Figure S7: Colony PCR: CRC cells

Colony PCR was performed to check the validity of the recombinants. The PCR products were analysed on a 2% agarose gel and compared with empty vector (245 bp). PCR products containing the correct insert (~550 bp) were selected for DNA sequencing.



Inst Model/Name:3730/3730Sequencer-17119-014

Sequence Scanner v1.0



Printed on: Sep 16, 2011 21:23:40 GMT

Electropherogram Data Page 1 of 5

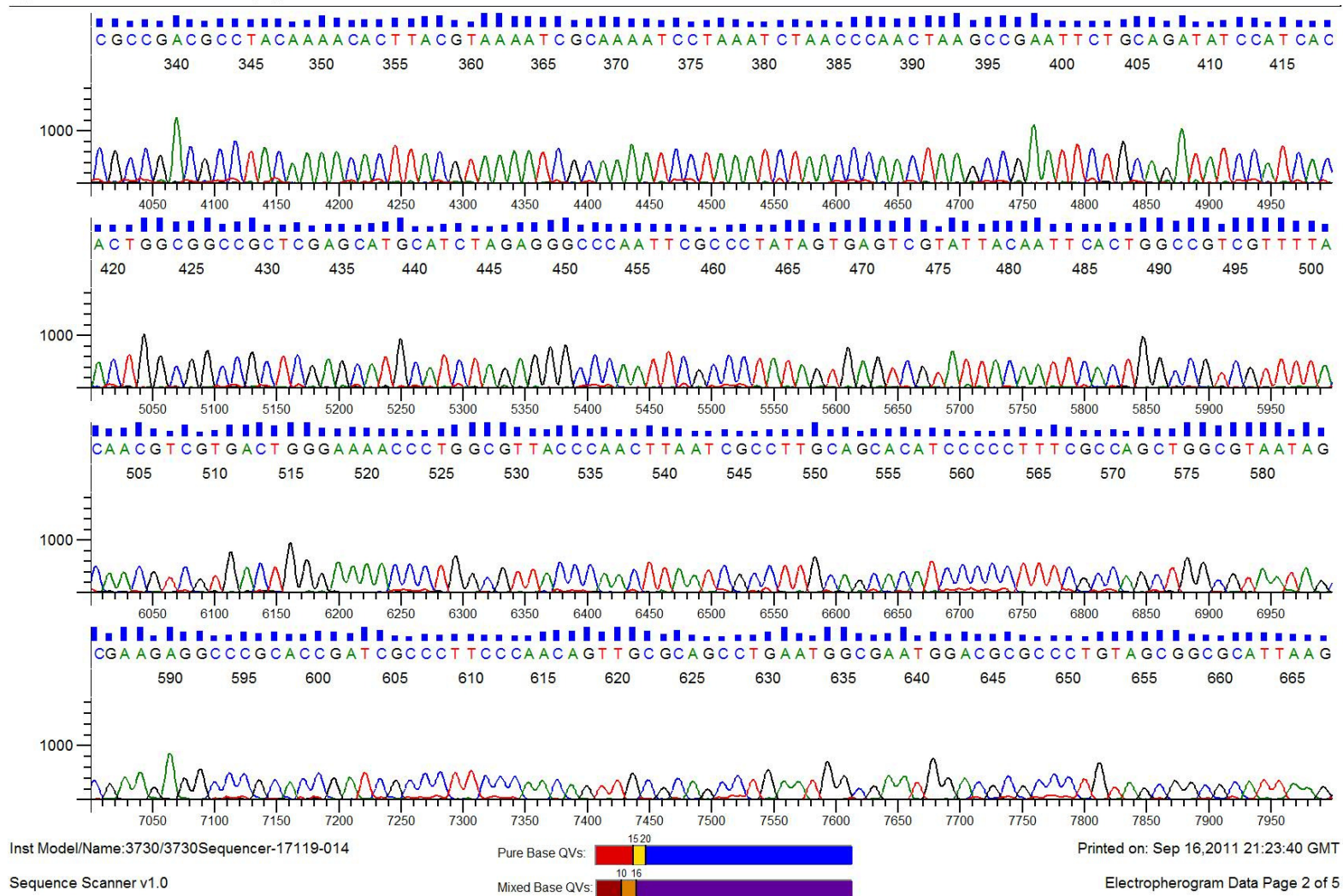
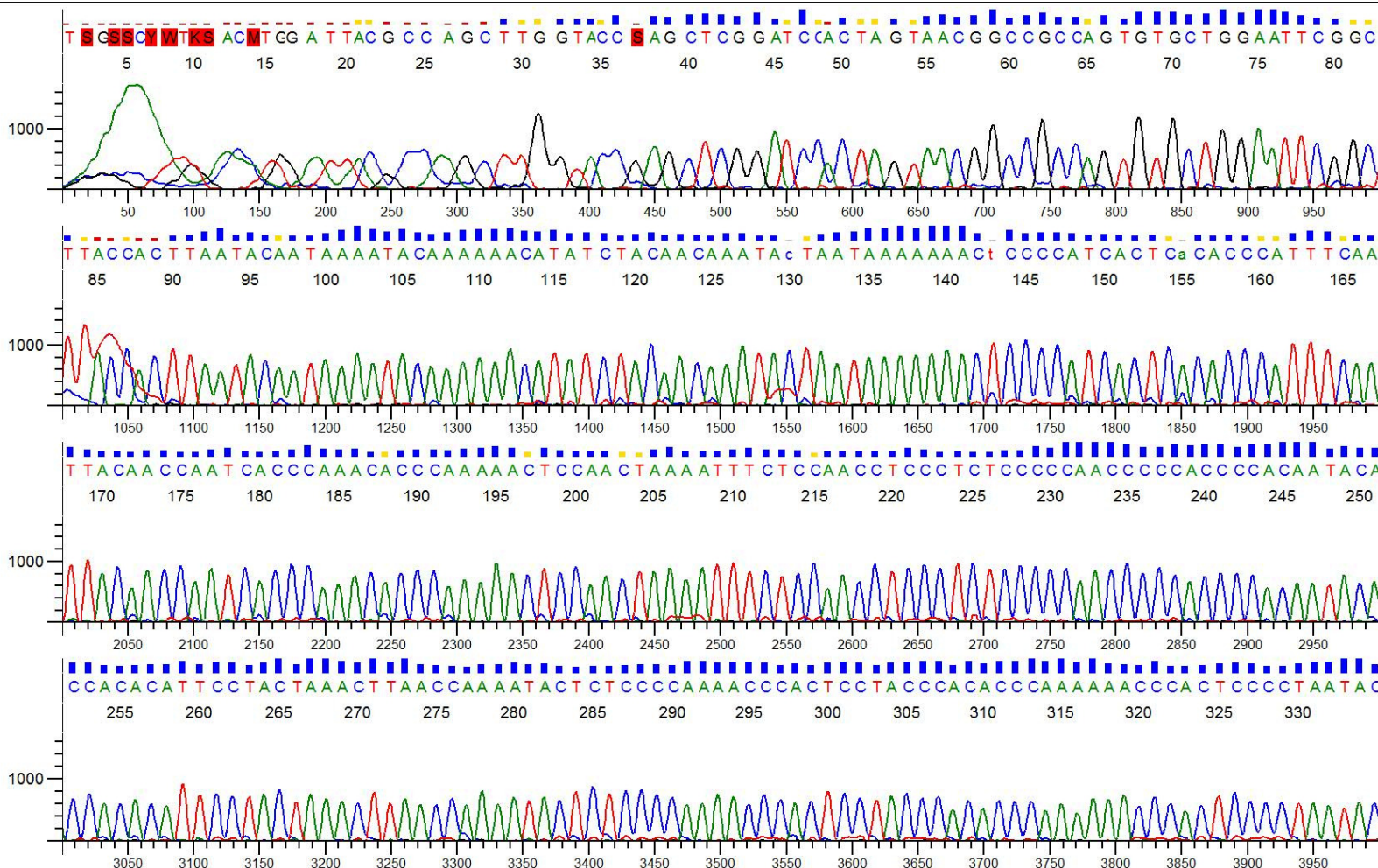
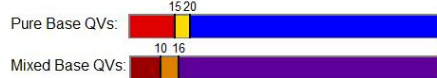


Figure S8: Bisulfite sequencing analysis of *PLS3* CpG island in SW948 CRC cell line



Inst Model/Name:3730/3730Sequencer-171119-014

Sequence Scanner v1.0



Printed on: Sep 16, 2011 21:37:26 GMT

Electropherogram Data Page 1 of 5

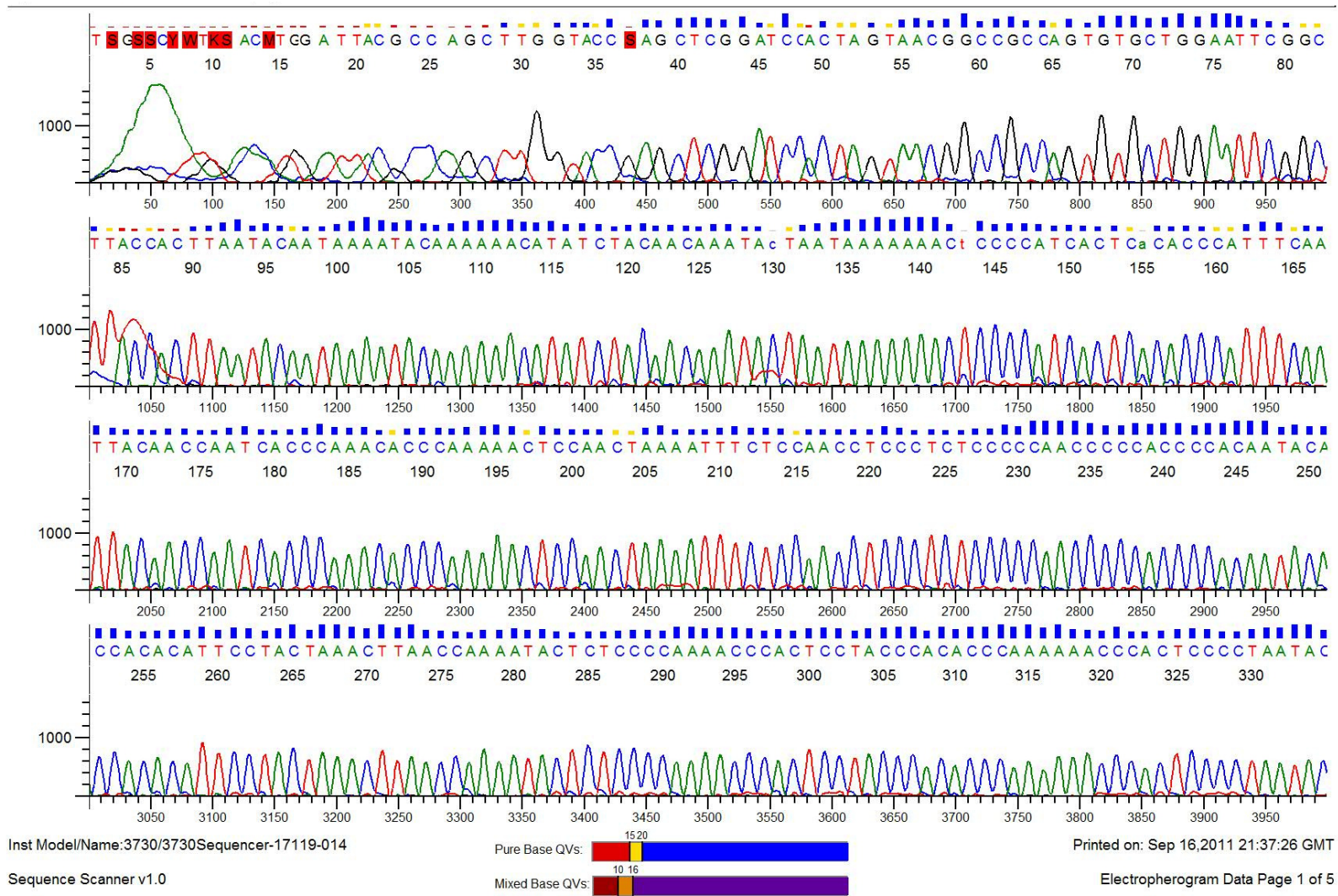


Figure S9: Bisulfite sequencing analysis of *PLS3* CpG island in SW620 CRC cell line

A

MAGTCGGGTTAGATTTAGGATTTTCGATTTTACGT 35
UAGTTGGGTTAGATTTAGGATTTTGTGATTTTATGT 35
C GGCTTAGTTGGGTTAGATTTAGGATTTTCGATTTTACGT 40
 agt ggggttagatattaggattttg gatttta gt

AAGTGTTTTGTAGCCGTCCGGCGGGTATTAGGGGAGCGGGT 75
 AAGTGTTTTGTAGCGTTCGGTGGGTATTAGGGGAGTCGGT 75
 AAGTGTTTTGTAGCCGTCCGGCGGGTATTAGGGGAGCGGGT 80
 aagtgtttttagg gt gg ggggtattaggggag gggT

TTTTGGGCGTGGGTAGGAGTGGGTTCCGGGAGAGTATT 115
 TTTTGGGCGTGGGTAGGAGTGGGTTCCGGGAGAGTATT 115
 TTTTGGGCGTGGGTAGGAGTGGGTTCCGGGAGAGTATT 120
 tttttggg gtgggttaggagtgggttt ggggagagtatt

TCGGTTAAGTTTAGTAGGAACTCGGCCGATCCGTGGGC 155
 TCGGTTAAGTTTAGTAGGAACTCGGGTATTCGTGGGGT 155
 TCGGTTAAGTTTAGTAGGAACTCGGCCGATCCGTGGGC 160
 t ggTTaagtttagtaggaa gtg gg gTat gtgggg

GGGGTTGGGGAGAGGGAGGTCGGAGAAATTTAGTTGG 195
 GGGGTTGGGGAGAGGGAGGTCGGAGAAATTTAGTTGG 195
 GGGGTTGGGGAGAGGGAGGTCGGAGAAATTTAGTTGG 200
 ggggTtgggggagaggaggt ggagaaat ttagttgg

AGTTTTGGGCGTTCGGCCGATCCGTCGTAATCGAAATGG 235
 AGTTTTGGGCGTTCGGCCGATCCGTCGTAATCGAAATGG 235
 AGTTTTGGGCGTTCGGCCGATCCGTCGTAATCGAAATGG 240
 agtttt ggg gtt ggg gat ggt gTaat gaaatgg

GTGTGAGTGAACGGGAGTTTTTTTATTAGTATTCGTCCGTA 275
 GTGTGAGTGAACGGGAGTTTTTTTATTAGTATTCGTCCGTA 275
 GTGTGAGTGAACGGGAGTTTTTTTATTAGTATTCGTCCGTA 280
 gtgtgagtga ggggagttttttattagTatt gt gta

GATACGTTTTTGTATTTTATTGTATTAAGTGGT... 309
 GATACGTTTTTGTATTTTATTGTATTAAGTGGT... 309
 GATACGTTTTTGTATTTTATTGTATTAAGTGGTAAGC 317
 gata gttttttgtattttattgtattaagtgg

B

...AGTCGGGTTAGATTTAGGATTTTCGATTTTACGTA 36
 ...AGTTGGGTTAGATTTAGGATTTTGTGATTTTATGTA 36
 GCTTAGTTGGGTTAGATTTAGGATTTTCGATTTTATGTA 40
 agt ggggttagatattaggattttg gatttta gta

AGTGTTTTGTAGCCGTCCGGCGGGTATTAGGGGAGCGGGT 76
 AGTGTTTTGTAGCGTTCGGTGGGTATTAGGGGAGTCGGT 76
 AGTGTTTTGTAGCCGTCCGGCGGGTATTAGGGGAGTCGGT 80
 agtgtttttagg gt gg ggggtattaggggag gggTt

TTTTGGGCGTGGGTAGGAGTGGGTTCCGGGAGAGTATT 116
 TTTTGGGCGTGGGTAGGAGTGGGTTCCGGGAGAGTATT 116
 TTTTGGGCGTGGGTAGGAGTGGGTTCCGGGAGAGTATT 120
 tttttggg gtgggttaggagtgggttt ggggagagtattt

CCGTTAAGTTTAGTAGGAACTCGGCCGATCCGTGGGGC 156
 CCGTTAAGTTTAGTAGGAACTCGGGTATTCGTGGGGT 156
 CCGTTAAGTTTAGTAGGAACTCGGGTATTCGTGGGGT 160
 ggTTaagtttagtaggaa gtg gg gTat gtgggg g

GGGGTTGGGGAGAGGGAGGTCGGAGAAATTTAGTTGGA 196
 GGGGTTGGGGAGAGGGAGGTCGGAGAAATTTAGTTGGA 196
 GGGGTTGGGGAGAGGGAGGTCGGAGAAATTTAGTTGGA 200
 ggggTtgggggagaggaggt ggagaaatTTtagttgga

GTTTTGGGCGTTCGGCCGATCCGTCGTAATCGAAATGGG 236
 GTTTTGGGCGTTCGGCCGATCCGTCGTAATCGAAATGGG 236
 GTTTTGGGCGTTCGGCCGATCCGTCGTAATCGAAATGGG 240
 gtttt ggg gtt ggg gat ggt gTaat gaaatggg

TGTGAGTGAACGGGAGTTTTTTTATTAGTATTCGTCCGTA 276
 TGTGAGTGAACGGGAGTTTTTTTATTAGTATTCGTCCGTA 276
 TGTGAGTGAACGGGAGTTTTTTTATTAGTATTCGTCCGTA 280
 tgtgagtga ggggagttttttattagTatt gt gtag

ATACGTTTTTGTATTTTATTGTATTAAGTGGT... 309
 ATACGTTTTTGTATTTTATTGTATTAAGTGGT... 309
 ATACGTTTTTGTATTTTATTGTATTAAGTGGTAAGC 317
 ata gttttttgtattttattgtattaagtggT

Figure S10: Bisulphite sequence alignment of methylated T-plastin (M), unmethylated T-plastin (U) and consensus sequence (C) for **(A)** SW948 CRC cell line **(B)** SW620 CRC cell line.

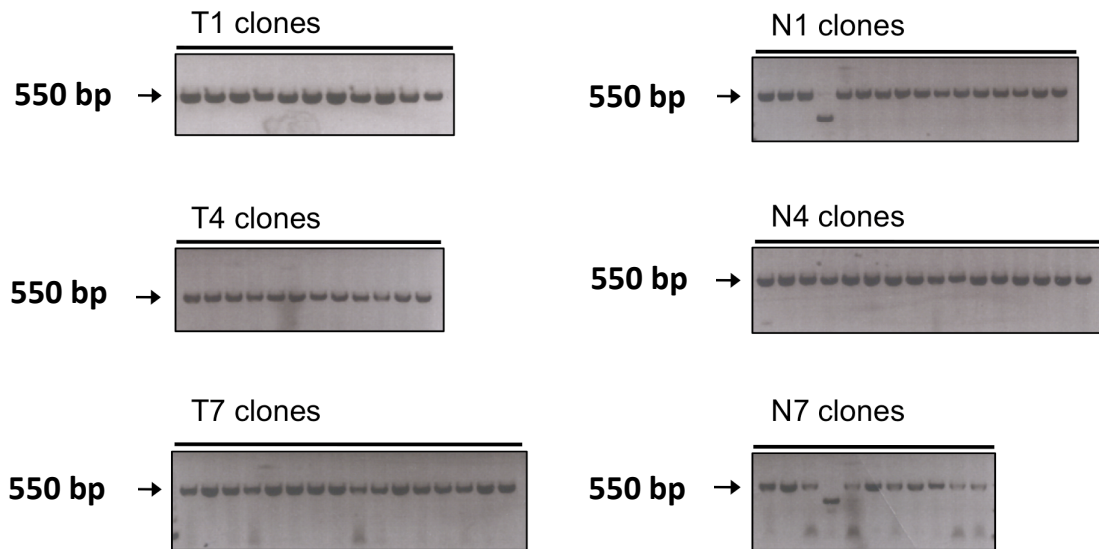
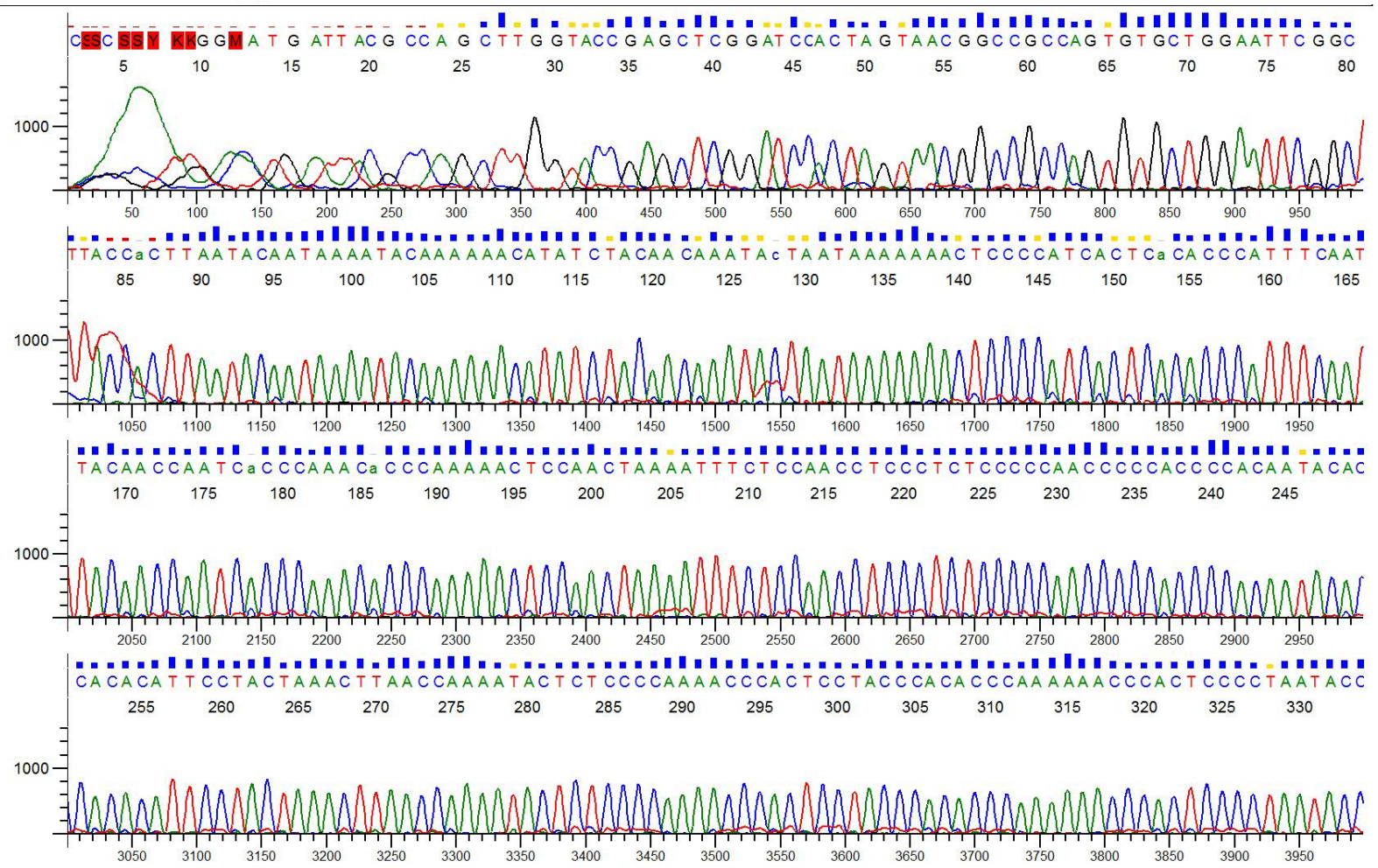


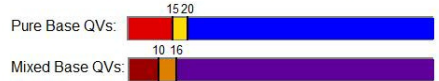
Figure S11: Colony PCR: patient DNA

Colony PCR was performed to check the validity of the recombinants. The PCR products were analysed on a 2% agarose gel and compared with empty vector (245 bp). PCR products containing the correct insert (~550 bp) were selected for DNA sequencing.



Inst Model/Name:3730/3730Sequencer-17119-014

Sequence Scanner v1.0



Printed on: Sep 16, 2011 21:54:31 GMT

Electropherogram Data Page 1 of 5

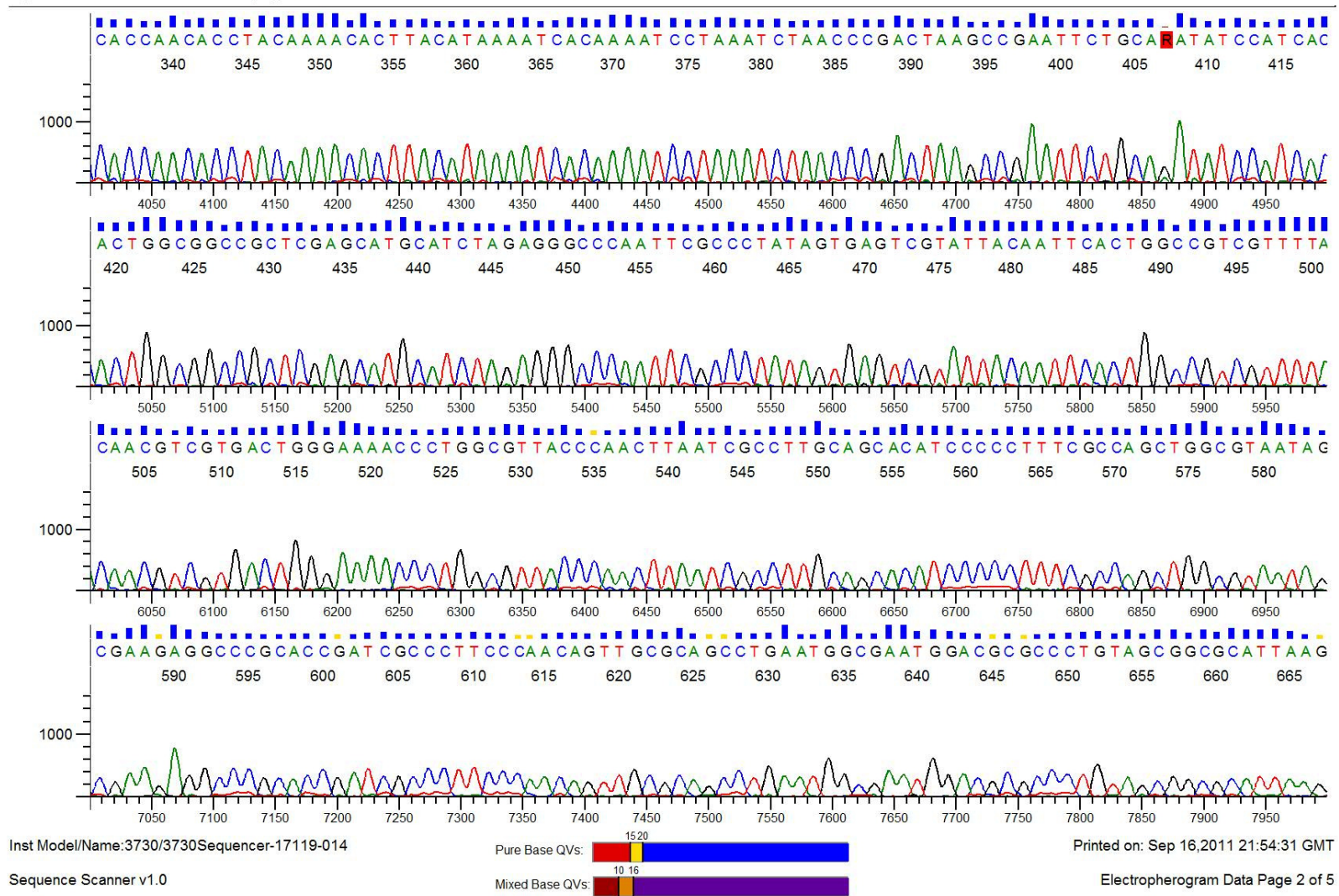


Figure S12: Bisulfite sequencing analysis of *PLS3* CpG island in normal colonic mucosa (Patient 1)

A

MAGTGGGTTAGATTTAGGATTTTCCGATTTTACGT 35
UAGTGGGTTAGATTTAGGATTTTCTGATTTTATGT 35
C GGCTTAGTGGGTTAGATTTAGGATTTTCTGATTTTATGT 40
 agt gggttagatttaggattttg gattttta gt

AAGTGTTTTGTAGCCGTCGGCGGGTATTAGGGGAGCGGT 75
 AAGTGTTTTGTAGCTGTGGCGGGTATTAGGGGAGCGGT 75
 AAGTGTTTTGTAGCTGTGGCGGGTATTAGGGGAGCGGT 80
 aagtgtttttagg gt gg gggatttagggag ggg

TTTTGGCCGTGGTAGGAGTGGGTTCCGGGAGAGTATT 115
 TTTTGGCTGTGGTAGGAGTGGGTTCCGGGAGAGTATT 115
 TTTTGGCTGTGGTAGGAGTGGGTTCCGGGAGAGTATT 120
 tttttggg gtggtaggagtggtttt ggggagagtatt

TCGGTTAAGTTTAGTAGGAACTGCGGCATCGTGGGCC 155
 TTGGTTAAGTTTAGTAGGAACTGCGGCATCGTGGGCC 155
 TTGGTTAAGTTTAGTAGGAACTGCGGCATCGTGGGCC 160
 t ggттаagtttagtaggaa gtg gg gtat gtggg

GGGGTTGGGGAGAGGAGGTCGGAGAAATTTAGTTGG 195
 GGGGTTGGGGAGAGGAGGTCGGAGAAATTTAGTTGG 195
 GGGGTTGGGGAGAGGAGGTCGGAGAAATTTAGTTGG 200
 gggggttggggagaggaggt ggagaatttttagttg

AGTTTTGGCCGTTCCGGCCGATCGGTCGTAATCGAAATGG 235
 AGTTTTGGCTGTTTGGGTGATCGGTCGTAATCGAAATGG 235
 AGTTTTGGCTGTTTGGGTGATCGGTCGTAATCGAAATGG 240
 agtttt ggg gtt ggg gat ggt gtaat gaaatgg

GTGTGAGTGAAGGGGAGTTTTTTTATTAGTATTCTCGTA 275
 GTGTGAGTGAAGGGGAGTTTTTTTATTAGTATTCTCGTA 275
 GTGTGAGTGAAGGGGAGTTTTTTTATTAGTATTCTCGTA 280
 gtgtgagtga ggggagtttttttattagattt gt gta

GATACGTTTTTTGTATTTTATTGTATTAAGTGGT.... 309
 GATACGTTTTTTGTATTTTATTGTATTAAGTGGT.... 309
 GATACGTTTTTTGTATTTTATTGTATTAAGTGGTAAGC 318
 gata gttttttgtattttattgtattaagtgg

B

.....AGTGGGTTAGATTTAGGATTTTCCGATTTTACGT 35
AGTGGGTTAGATTTAGGATTTTCTGATTTTATGT 35
 GGCTTAGTGGGTTAGATTTAGGATTTTCTGATTTTATGT 40
 agt gggttagatttaggattttg gattttta gt

AAGTGTTTTGTAGCCGTCGGCGGGTATTAGGGGAGCGGT 75
 AAGTGTTTTGTAGCTGTGGCGGGTATTAGGGGAGCGGT 75
 AAGTGTTTTGTAGCTGTGGCGGGTATTAGGGGAGCGGT 80
 aagtgtttttagg gt gg gggatttagggag ggg

TTTTGGCCGTGGTAGGAGTGGGTTCCGGGAGAGTATT 115
 TTTTGGCTGTGGTAGGAGTGGGTTCCGGGAGAGTATT 115
 TTTTGGCTGTGGTAGGAGTGGGTTCCGGGAGAGTATT 120
 tttttggg gtggtaggagtggtttt ggggagagtatt

TCGGTTAAGTTTAGTAGGAACTGCGGCATCGTGGGCC 155
 TTGGTTAAGTTTAGTAGGAACTGCGGCATCGTGGGCC 155
 TTGGTTAAGTTTAGTAGGAACTGCGGCATCGTGGGCC 160
 t ggттаagtttagtaggaa gtg gg gtat gtggg

GGGGTTGGGGAGAGGAGGTCGGAGAAATTTAGTTGG 195
 GGGGTTGGGGAGAGGAGGTCGGAGAAATTTAGTTGG 195
 GGGGTTGGGGAGAGGAGGTCGGAGAAATTTAGTTGG 200
 gggggttggggagaggaggt ggagaatttttagttg

AGTTTTGGCCGTTCCGGCCGATCGGTCGTAATCGAAATGG 235
 AGTTTTGGCTGTTTGGGTGATCGGTCGTAATCGAAATGG 235
 AGTTTTGGCTGTTTGGGTGATCGGTCGTAATCGAAATGG 240
 agtttt ggg gtt ggg gat ggt gtaat gaaatgg

GTGTGAGTGAAGGGGAGTTTTTTTATTAGTATTCTCGTA 275
 GTGTGAGTGAAGGGGAGTTTTTTTATTAGTATTCTCGTA 275
 GTGTGAGTGAAGGGGAGTTTTTTTATTAGTATTCTCGTA 280
 gtgtgagtga ggggagtttttttattagattt gt gta

GATACGTTTTTTGTATTTTATTGTATTAAGTGGT... 309
 GATACGTTTTTTGTATTTTATTGTATTAAGTGGT... 309
 GATACGTTTTTTGTATTTTATTGTATTAAGTGGTAAG 317
 gata gttttttgtattttattgtattaagtgg

Figure S13: Bisulphite sequence alignment of methylated T-plastin (M), unmethylated T-plastin (U) and consensus sequence (C) for (A) normal colonic mucosa and (B) corresponding tumour tissue from patient 1.

Bibliography

Adams, A.E., Botstein, D., and Drubin, D.G. (1991). Requirement of yeast fimbrin for actin organization and morphogenesis in vivo. *Nature* 354, 404-408.

Adams, A.E., Shen, W., Lin, C.S., Leavitt, J., and Matsudaira, P. (1995). Isoform-specific complementation of the yeast *sac6* null mutation by human fimbrin. *Mol Cell Biol* 15, 69-75.

Agrelo, R., Setien, F., Espada, J., Artiga, M.J., Rodriguez, M., Pérez-Rosado, A., Sanchez-Aguilera, A., Fraga, M.F., Piris, M.A., and Esteller, M. (2005). Inactivation of the Lamin A/C Gene by CpG Island Promoter Hypermethylation in Hematologic Malignancies, and Its Association With Poor Survival in Nodal Diffuse Large B-Cell Lymphoma. *Journal of Clinical Oncology* 23, 3940-3947.

Ahlquist, D.A., McGill, D.B., Schwartz, S., Taylor, W.F., and Owen, R.A. (1985). Fecal blood levels in health and disease. *N Engl J Med* 312, 1422-1428.

Al Tanoury, Z., Schaffner-Reckinger, E., Halavaty, A., Hoffmann, C., Moes, M., Hadzic, E., Catillon, M., Yatskou, M., and Friederich, E. (2010). Quantitative kinetic study of the actin-bundling protein L-plastin and of its impact on actin turn-over. *PLoS One* 5, e9210.

Alrawi, S.J., Schiff, M., Carroll, R.E., Dayton, M., Gibbs, J.F., Kulavlat, M., Tan, D., Berman, K., Stoler, D.L., and Anderson, G.R. (2006). Aberrant crypt foci. *Anticancer Res* 26, 107-119.

Amagase, H., Petesch, B.L., Matsuura, H., Kasuga, S., and Itakura, Y. (2001). Intake of Garlic and Its Bioactive Components. *The Journal of Nutrition* 131, 955S-962S.

Andre, T., Boni, C., Navarro, M., Tabernero, J., Hickish, T., Topham, C., Bonetti, A., Clingan, P., Bridgewater, J., Rivera, F., *et al.* (2009). Improved overall survival with oxaliplatin, fluorouracil, and leucovorin as adjuvant treatment in stage II or III colon cancer in the MOSAIC trial. *J Clin Oncol* 27, 3109-3116.

Anwar, S., Frayling, I.M., Scott, N.A., and Carlson, G.L. (2004). Systematic review of genetic influences on the prognosis of colorectal cancer. *Br J Surg* 91, 1275-1291.

Arpin, M., Friederich, E., Algrain, M., Vernel, F., and Louvard, D. (1994). Functional differences between L- and T-plastin isoforms. *J Cell Biol* 127, 1995-2008.

Astler, V.B., and Collier, F.A. (1954). The prognostic significance of direct extension of carcinoma of the colon and rectum. *Ann Surg* 139, 846-852.

Atkin, W.S., Edwards, R., Kralj-Hans, I., Wooldrage, K., Hart, A.R., Northover, J.M., Parkin, D.M., Wardle, J., Duffy, S.W., and Cuzick, J. (2010). Once-only flexible sigmoidoscopy screening in prevention of colorectal cancer: a multicentre randomised controlled trial. *Lancet* 375, 1624-1633.

Avivi-Green, C., Polak-Charcon, S., Madar, Z., and Schwartz, B. (2000). Apoptosis cascade proteins are regulated in vivo by high intracolonic butyrate concentration: correlation with colon cancer inhibition. *Oncol Res* 12, 83-95.

Baird, C.L., Fischer, C.J., Pefaur, N.B., Miller, K.D., Kagan, J., Srivastava, S., and Rodland, K.D. (2009). Developing recombinant antibodies for biomarker detection. *Cancer Biomarkers* 6, 271-279.

- Baker, S., Fearon, E., Nigro, J., Hamilton, Preisinger, A., Jessup, J., vanTuinen, P., Ledbetter, D., Barker, D., Nakamura, Y., *et al.* (1989). Chromosome 17 deletions and p53 gene mutations in colorectal carcinomas. *Science* *244*, 217-221.
- Baker, S., Markowitz, S., Fearon, E., Willson, J., and Vogelstein, B. (1990). Suppression of human colorectal carcinoma cell growth by wild-type p53. *Science* *249*, 912-915.
- Barault, L. (2008). Hypermethylator phenotype in sporadic colon cancer: study on a population-based series of 582 cases. *Cancer Res* *68*, 8541-8546.
- Barker, N. (2007). Identification of stem cells in small intestine and colon by marker gene Lgr5. *Nature* *449*, 1003-1007.
- Baron, J.A., Cole, B.F., Sandler, R.S., Haile, R.W., Ahnen, D., Bresalier, R., McKeown-Eyssen, G., Summers, R.W., Rothstein, R., Burke, C.A., *et al.* (2003). A Randomized Trial of Aspirin to Prevent Colorectal Adenomas. *New England Journal of Medicine* *348*, 891-899.
- Batlle, E. (2002). [beta]-catenin and TCF mediate cell positioning in the intestinal epithelium by controlling the expression of EphB/ephrinB. *Cell* *111*, 251-263.
- Baylin, S.B., Herman, J.G., Graff, J.R., Vertino, P.M., and Issa, J.P. (1998). Alterations in DNA methylation: a fundamental aspect of neoplasia. *Adv Cancer Res* *72*, 141-196.
- Benedetti, S., and Merlini, L. (2004). Laminopathies: from the heart of the cell to the clinics. *Current Opinion in Neurology* *17*, 553-560.
- Benedix, F., Kube, R., Meyer, F., Schmidt, U., Gastinger, I., and Lippert, H. (2010). Comparison of 17,641 patients with right- and left-sided colon cancer: differences in epidemiology, perioperative course, histology, and survival. *Dis Colon Rectum* *53*, 57-64.
- Birkenkamp-Demtroder K., Olesen S.H., Sørensen, F.B., Laurbergm S., Laiho, P., Aaltonen, L.A. and Orntoft, T.F. (2005). Differential gene expression in colon cancer of the caecum versus the sigmoid and rectosigmoid. *Gut* *54*(3), 374-384.
- Bernstein, H., Bernstein, C., Payne, C.M., Dvorakova, K., and Garewal, H. (2005). Bile acids as carcinogens in human gastrointestinal cancers. *Mutat Res* *589*, 47-65.
- Beroud, C., and Soussié, T. (1996). APC gene: database of germline and somatic mutations in human tumors and cell lines. *Nucleic Acids Res* *24*, 121-124.
- Bertario, L., Russo, A., Sala, P., Varesco, L., Giarola, M., Mondini, P., Pierotti, M., Spinelli, P., Radice, P., and Registry, f.t.H.C.T. (2003). Multiple Approach to the Exploration of Genotype-Phenotype Correlations in Familial Adenomatous Polyposis. *Journal of Clinical Oncology* *21*, 1698-1707.
- Bestor, T.H. (2000). The DNA methyltransferases of mammals. *Hum Mol Genet* *9*, 2395-2402.
- Bhangu, A., Wood, G., Mirnezami, A., Darzi, A., Tekkis, P., and Goldin, R. (2012). Epithelial mesenchymal transition in colorectal cancer: Seminal role in promoting disease progression and resistance to neoadjuvant therapy. *Surgical Oncology* *21*, 316-323.
- Biasco, G., Pantaleo, M.A., Di Febo, G., Calabrese, C., and Brandi, G. (2004). Risk of duodenal cancer in patients with familial adenomatous polyposis. *Gut* *53*, 1547.
- Bienz, M., and Clevers, H. (2000). Linking colorectal cancer to Wnt signaling. *Cell* *103*, 311-320.

- Bingham, S.A., Norat, T., Moskal, A., Ferrari, P., Slimani, N., Clavel-Chapelon, F., Kesse, E., Nieters, A., Boeing, H., Tjonneland, A., *et al.* (2005). Is the association with fiber from foods in colorectal cancer confounded by folate intake? *Cancer Epidemiol Biomarkers Prev* *14*, 1552-1556.
- Bird, A. (2002). DNA methylation patterns and epigenetic memory. *Genes Dev* *16*, 6-21.
- Bisgaard, M.L., and Bulow, S. (2006). Familial adenomatous polyposis (FAP): genotype correlation to FAP phenotype with osteomas and sebaceous cysts. *Am J Med Genet A* *140*, 200-204.
- Booth, C., and Potten, C.S. (2000). Gut instincts: thoughts on intestinal epithelial stem cells. *The Journal of Clinical Investigation* *105*, 1493-1499.
- Bordeleau, F., Bessard, J., Marceau, N., and Sheng, Y. (2011). Measuring integrated cellular mechanical stress response at focal adhesions by optical tweezers. *Journal of Biomedical Optics* *16*, 095005-095005.
- Bork, P., Sander, C., and Valencia, A. (1992). An ATPase domain common to prokaryotic cell cycle proteins, sugar kinases, actin, and hsp70 heat shock proteins. *Proceedings of the National Academy of Sciences* *89*, 7290-7294.
- Bos, J.L. (1989). ras Oncogenes in Human Cancer: A Review. *Cancer Research* *49*, 4682-4689.
- Bos, J.L., Fearon, E.R., Hamilton, S.R., Vries, M.V.-d., van Boom, J.H., van der Eb, A.J., and Vogelstein, B. (1987). Prevalence of ras gene mutations in human colorectal cancers. *Nature* *327*, 293-297.
- Bostick, M., Kim, J.K., Estève, P.-O., Clark, A., Pradhan, S., and Jacobsen, S.E. (2007). UHRF1 Plays a Role in Maintaining DNA Methylation in Mammalian Cells. *Science* *317*, 1760-1764.
- Bray, F., Sankila, R., Ferlay, J., and Parkin, D.M. (2002). Estimates of cancer incidence and mortality in Europe in 1995. *European Journal of Cancer* *38*, 99-166.
- Brazao, T.F., Demmers, J., van Ijcken, W., Strouboulis, J., Fornerod, M., Romao, L., and Grosveld, F.G. (2012). A new function of ROD1 in nonsense-mediated mRNA decay. *FEBS Lett* *586*, 1101-1110.
- Brehm-Stecher, B.F., and Johnson, E.A. (2004). Single-Cell Microbiology: Tools, Technologies, and Applications. *Microbiol Mol Biol Rev* *68*, 538-559.
- Bressler, B., Lo, C., Amar, J., Whittaker, S., Chaun, H., Halparin, L., and Enns, R. (2004). Prospective evaluation of screening colonoscopy: who is being screened? *Gastrointest Endosc* *60*, 921-926.
- Bretscher, A. (1981). Fimbrin is a cytoskeletal protein that crosslinks F-actin in vitro. *Proc Natl Acad Sci U S A* *78*, 6849-6853.
- Bretscher, A., and Weber, K. (1978). Purification of microvilli and an analysis of the protein components of the microfilament core bundle. *Exp Cell Res* *116*, 397-407.
- Broers, J.L., Raymond, Y., Rot, M.K., Kuijpers, H., Wagenaar, S.S., and Ramaekers, F.C. (1993). Nuclear A-type lamins are differentially expressed in human lung cancer subtypes. *Am J Pathol* *143*, 211-220.
- Broers, J.L.V., Ramaekers, F.C.S., Bonne, G., Yaou, R.B., and Hutchison, C.J. (2006). Nuclear Lamins: Laminopathies and Their Role in Premature Ageing. *Physiological Reviews* *86*, 967-1008.
- Brower, V. (2011). Epigenetics: Unravelling the cancer code. *Nature* *471*, S12-S13.

- Browning, M., Petronzelli, F., Bicknell, D., Krausa, P., Rowan, A., Tonks, S., Murray, N., Bodmer, J., and Bodmer, W. (1996). Mechanisms of loss of HLA class I expression on colorectal tumor cells. *Tissue Antigens* 47, 364-371.
- Bufill, J.A. (1990). Colorectal cancer: evidence for distinct genetic categories based on proximal or distal tumor location. *Ann Intern Med* 113, 779-788.
- Burgess, A.W., Faux, M.C., Layton, M.J., and Ramsay, R.G. (2011). Wnt signaling and colon tumorigenesis — A view from the periphery. *Experimental Cell Research* 317, 2748-2758.
- Burke, B., and Roux, K.J. (2009). Nuclei Take a Position: Managing Nuclear Location. *Developmental cell* 17, 587-597.
- Burt, R.W., Leppert, M.F., Slattery, M.L., Samowitz, W.S., Spirio, L.N., Kerber, R.A., Kuwada, S.K., Neklason, D.W., Disario, J.A., Lyon, E., *et al.* (2004). Genetic testing and phenotype in a large kindred with attenuated familial adenomatous polyposis. *Gastroenterology* 127, 444-451.
- Butcher, D.T., Alliston, T., and Weaver, V.M. (2009). A tense situation: forcing tumour progression. *Nature Rev Cancer* 9, 108-122.
- Cai, S.R., Zhu, H.H., Li, Q.R., Ma, X.Y., Yao, K.Y., Zhang, S.Z., and Zheng, S. (2012). Gender disparities in dietary status and its risk factors in underserved populations. *Public Health* 126, 324-331.
- Calvano, S.E., Xiao, W., Richards, D.R., Felciano, R.M., Baker, H.V., Cho, R.J., Chen, R.O., Brownstein, B.H., Cobb, J.P., Tschoeke, S.K., *et al.* (2005). A network-based analysis of systemic inflammation in humans. *Nature* 437, 1032-1037.
- Camps, J., Ponsa, I., Ribas, M., Prat, E., Egozcue, J., Peinado, M.A., and Miro, R. (2005). Comprehensive measurement of chromosomal instability in cancer cells: combination of fluorescence in situ hybridization and cytokinesis-block micronucleus assay. *FASEB J* 19, 828-830.
- Cantero, D., Friess, H., Deflorin, J., Zimmermann, A., Brundler, M.A., Riesle, E., Korc, M., and Buchler, M.W. (1997). Enhanced expression of urokinase plasminogen activator and its receptor in pancreatic carcinoma. *Br J Cancer* 75, 388–395.
- Castagnola, P., and Giaretti, W. (2005). Mutant KRAS, chromosomal instability and prognosis in colorectal cancer. *Biochim Biophys Acta* 1756, 115-125.
- Chafel, M.M., Shen, W., and Matsudaira, P. (1995). Sequential expression and differential localization of I-, L-, and T-fimbrin during differentiation of the mouse intestine and yolk sac. *Dev Dyn* 203, 141-151.
- Chambers, S.K., Ivins, C.M., and Carcangiu, M.L. (1998). Plasminogen activator inhibitor-1 is an independent poor prognostic factor for survival in advanced stage epithelial ovarian cancer patients. *Int J Cancer* 79, 449–454.
- Chapuis, P.H., Chan, C., and Dent, O.F. (2011). Clinicopathological staging of colorectal cancer: Evolution and consensus-an Australian perspective. *J Gastroenterol Hepatol* 26 Suppl 1, 58-64.
- Chau, I., Allen, M.J., Cunningham, D., Norman, A.R., Brown, G., Ford, H.E.R., Tebbutt, N., Tait, D., Hill, M., Ross, P.J., *et al.* (2004). The Value of Routine Serum Carcino-Embryonic Antigen Measurement and Computed Tomography in the Surveillance of Patients After Adjuvant Chemotherapy for Colorectal Cancer. *Journal of Clinical Oncology* 22, 1420-1429.

- Chen, T.R., Drabkowski, D., Hay, R.J., Macy, M., and Peterson Jr, W. (1987). WiDr is a derivative of another colon adenocarcinoma cell line, HT-29. *Cancer Genetics and Cytogenetics* 27, 125-134.
- Cheng, J.C., Auersperg, N., and Leung*, P.C. EGF-Induced EMT and Invasiveness in Serous Borderline Ovarian Tumor Cells: A Possible Step in the Transition to Low-Grade Serous Carcinoma Cells? *PLoS ONE* 7(3).
- Cheng, P.C., Gosewehr, J.A., Kim, T.M., Velicescu, M., Wan, M., Zheng, J., Felix, J.C., Cofer, K.F., Luo, P., Biela, B.H., Godorov, G., and Dubeau, L. J. Potential role of the inactivated X chromosome in ovarian epithelial tumor development. *Natl Cancer Inst.* 88(8).
- Colombo, P.-E., Milanezi, F., Weigelt, B., and Reis-Filho, J. (2011). Microarrays in the 2010s: the contribution of microarray-based gene expression profiling to breast cancer classification, prognostication and prediction. *Breast Cancer Research* 13, 212.
- Comb, M., and Goodman, H.M. (1990). CpG methylation inhibits proenkephalin gene expression and binding of the transcription factor AP-2. *Nucleic Acids Res* 18, 3975-3982.
- Compton, C.C., and Greene, F.L. (2004). The staging of colorectal cancer: 2004 and beyond. *CA Cancer J Clin* 54, 295-308.
- Crockett, S.D., Long, M.D., Dellon, E.S., Martin, C.F., Galanko, J.A., and Sandler, R.S. (2011). Inverse relationship between moderate alcohol intake and rectal cancer: analysis of the north Carolina colon cancer study. *Dis Colon Rectum* 54, 887-894.
- Cross, A.J., Pollock, J.R., and Bingham, S.A. (2003). Haem, not protein or inorganic iron, is responsible for endogenous intestinal N-nitrosation arising from red meat. *Cancer Res* 63, 2358-2360.
- Cui, H. (2002). Loss of imprinting in colorectal cancer linked to hypomethylation of H19 and IGF2. *Cancer Res* 62, 6442-6446.
- Cui, W., Fowles, D.J., Bryson, S., Duffie, E., Ireland, H., Balmain, A., and Akhurst, R.J. (1996). TGFbeta1 inhibits the formation of benign skin tumors, but enhances progression to invasive spindle carcinomas in transgenic mice. *Cell* 86, 531-542.
- Dahl, K.N., and Kalinowski, A. (2011). Nucleoskeleton mechanics at a glance. *Journal of Cell Science* 124, 675-678.
- Daudet, N., and Lebart, M.C. (2002). Transient expression of the t-isoform of plastins/fimbrin in the stereocilia of developing auditory hair cells. *Cell Motil Cytoskeleton* 53, 326-336.
- Davies, R.J., Miller, R., and Coleman, N. (2005). Colorectal cancer screening: prospects for molecular stool analysis. *Nat Rev Cancer* 5, 199-209.
- Dawson, Mark A., and Kouzarides, T. (2012). Cancer Epigenetics: From Mechanism to Therapy. *Cell* 150, 12-27.
- De Nardo, D., and Latz, E. (2011). NLRP3 inflammasomes link inflammation and metabolic disease. *Trends in Immunology* 32, 373-379.
- Dechat, T., Pflieger, K., Sengupta, K., Shimi, T., Shumaker, D.K., Solimando, L., and Goldman, R.D. (2008). Nuclear lamins: major factors in the structural organization and function of the nucleus and chromatin. *Genes & Development* 22, 832-853.

- Delanote, V., Vandekerckhove, J., and Gettemans, J. (2005). Plastins: versatile modulators of actin organization in (patho)physiological cellular processes. *Acta Pharmacol Sin* 26, 769-779.
- Denlinger, C.S., and Engstrom, P.F. (2011). Colorectal cancer survivorship: movement matters. *Cancer Prev Res (Phila)* 4, 502-511.
- Derks, S., Lentjes, M.F.M., Hellebrekers, D.M.E.I., de Bruïne, A.P., Herman, J.G., and van Engeland, M. (2004). Methylation-specific PCR unraveled. *Analytical Cellular Pathology* 26, 291-299.
- Deschoolmeester, V., Baay, M., Specenier, P., Lardon, F., and Vermorken, J.B. (2010). A review of the most promising biomarkers in colorectal cancer: one step closer to targeted therapy. *Oncologist* 15, 699-731.
- Dietrich, C.G., Vehr, A.K., Martin, I.V., Gassler, N., Rath, T., Roeb, E., Schmitt, J., Trautwein, C., and Geier, A. (2011). Downregulation of breast cancer resistance protein in colon adenomas reduces cellular xenobiotic resistance and leads to accumulation of a food-derived carcinogen. *Int J Cancer* 129, 546-552.
- Doherty, G.J., and McMahon, H.T. (2008). Mediation, Modulation, and Consequences of Membrane-Cytoskeleton Interactions. *Annual Review of Biophysics* 37, 65-95.
- Dos Remedios, C.G., Chhabra, D., Kekic, M., Dedova, I.V., Tsubakihara, M., Berry, D.A., and Nosworthy, N.J. (2003). Actin Binding Proteins: Regulation of Cytoskeletal Microfilaments. *Physiological Reviews* 83, 433-473.
- Draht, M.X.G., Riedl, R.R., Niessen, H., Carvalho, B., Meijer, G.A., Herman, J.G., van Engeland, M., Melotte, V., and Smits, K.M. (2012). Promoter CpG island methylation markers in colorectal cancer: the road ahead. *Epigenomics* 4, 179-194.
- Drubin, D.G., Miller, K.G., and Botstein, D. (1988). Yeast actin-binding proteins: evidence for a role in morphogenesis. *J Cell Biol* 107, 2551-2561.
- Duerr, E.M., Mizukami, Y., Moriichi, K., Gala, M., Jo, W.S., Kikuchi, H., Xavier, R.J., Chung, D.C. (2012). Oncogenic KRAS regulates BMP4 expression in colon cancer cell lines. *Am J Physiol Gastrointest Liver Physiol*. 302(10)
- Duftner, N., Larkins-Ford, J., Legendre, M., and Hofmann, H.A. (2008). Efficacy of RNA amplification is dependent on sequence characteristics: Implications for gene expression profiling using a cDNA microarray. *Genomics* 91, 108-117.
- Dunlop, M.G., Dobbins, S.E., Farrington, S.M., Jones, A.M., Palles, C., Whiffin, N., Tenesa, A., Spain, S., Broderick, P., Ooi, L.-Y., *et al.* (2012). Common variation near CDKN1A, POLD3 and SHROOM2 influences colorectal cancer risk. *Nat Genet* 44, 770-776.
- Eads, C.A., Nickel, A.E., and Laird, P.W. (2002). Complete Genetic Suppression of Polyp Formation and Reduction of CpG-Island Hypermethylation in ApcMin/+ Dnmt1-Hypomorphic Mice. *Cancer Research* 62, 1296-1299.
- Eheman, C., Henley, S.J., Ballard-Barbash, R., Jacobs, E.J., Schymura, M.J., Noone, A.-M., Pan, L., Anderson, R.N., Fulton, J.E., Kohler, B.A., *et al.* (2012). Annual Report to the Nation on the status of cancer, 1975-2008, featuring cancers associated with excess weight and lack of sufficient physical activity. *Cancer* 118, 2338-2366.

- Erler, J., and Weaver, V. (2009). Three-dimensional context regulation of metastasis. *Clinical and Experimental Metastasis* 26, 35-49.
- Etienne-Manneville, S., and Hall, A. (2003). Cdc42 regulates GSK-3[β] and adenomatous polyposis coli to control cell polarity. *Nature* 421, 753-756.
- Etournay, R., Zwaenepoel, I., Perfettini, I., Legrain, P., Petit, C., and El-Amraoui, A. (2007). Shroom2, a myosin-VIIa- and actin-binding protein, directly interacts with ZO-1 at tight junctions. *Journal of Cell Science* 120, 2838-2850.
- Evans, A., Whelehan, P., Thomson, K., McLean, D., Brauer, K., Purdie, C., Baker, L., Jordan, L., Rauchhaus, P., and Thompson, A. (2012). Invasive Breast Cancer: Relationship between Shear-wave Elastographic Findings and Histologic Prognostic Factors. *Radiology* 263, 673-677.
- Farber, M.J., Rizaldy, R., and Hildebrand, J.D. (2011). Shroom2 regulates contractility to control endothelial morphogenesis. *Molecular Biology of the Cell* 22, 795-805.
- Fearon, E.R. (2011). Molecular genetics of colorectal cancer. *Annu Rev Pathol* 6, 479-507.
- Fearon, E.R., and Vogelstein, B. (1990). A genetic model for colorectal tumorigenesis. *Cell* 61, 759-767.
- Fedirko, V., Tramacere, I., Bagnardi, V., Rota, M., Scotti, L., Islami, F., Negri, E., Straif, K., Romieu, I., La Vecchia, C., *et al.* (2011). Alcohol drinking and colorectal cancer risk: an overall and dose-response meta-analysis of published studies. *Ann Oncol*.
- Feinberg, A., and Vogelstein, B. (1983). Hypomethylation distinguishes genes of some human cancers from their normal counterparts, pp. 89-92.
- Feinberg, A.P. (2007). Phenotypic plasticity and the epigenetics of human disease. *Nature* 447, 433-440.
- Feinberg, A.P., and Tycko, B. (2004). The history of cancer epigenetics. *Nat Rev Cancer* 4, 143-153.
- Ferlay, J., Shin, H.R., Bray, F., Forman, D., Mathers, C., and Parkin, D.M. (2010). Estimates of worldwide burden of cancer in 2008: GLOBOCAN 2008. *Int J Cancer* 127, 2893-2917.
- Fernandez, A.F., Assenov, Y., Martin-Subero, J., Balint, B., Siebert, R., Taniguchi, H., Yamamoto, H., Hidalgo, M., Tan, A.-C., Galm, O., *et al.* (2011). A DNA methylation fingerprint of 1,628 human samples. *Genome Research*.
- Figueredo, A., Coombes, M.E., and Mukherjee, S. (2008). Adjuvant therapy for completely resected stage II colon cancer. *Cochrane Database Syst Rev*, CD005390.
- Fink, D. (1996). The role of DNA mismatch repair in platinum drug resistance. *Cancer Res* 56, 4881-4886.
- Finlan, L.E., Sproul, D., Thomson, I., Boyle, S., Kerr, E., Perry, P., Ylstra, B., Chubb, J.R., and Bickmore, W.A. (2008). Recruitment to the Nuclear Periphery Can Alter Expression of Genes in Human Cells. *PLoS Genet* 4, e1000039.
- Fogh, J., Fogh, J.M., and Orfeo, T. (1977). One hundred and twenty-seven cultured human tumor cell lines producing tumors in nude mice. *J Natl Cancer Inst* 59(1), 221-226.

- Foran, E., McWilliam, P., Kelleher, D., Croke, D.T., and Long, A. (2006). The leukocyte protein L-plastin induces proliferation, invasion and loss of E-cadherin expression in colon cancer cells. *Int J Cancer* *118*, 2098-2104.
- Fretwell, V.L., Ang, C.W., Tweedle, E.M., and Rooney, P.S. (2010). The impact of lymph node yield on Duke's B and C colorectal cancer survival. *Colorectal Dis* *12*, 995-1000.
- Fung, J., Lai, C.L., Seto, W.K., Wong, D.K.H., and Yuen, M.F. (2011). Prognostic significance of liver stiffness for hepatocellular carcinoma and mortality in HBeAg-negative chronic hepatitis B. *Journal of Viral Hepatitis* *18*, 738-744.
- Galiatsatos, P., and Foulkes, W.D. (2006). Familial adenomatous polyposis. *Am J Gastroenterol* *101*, 385-398.
- Galkin, V.E., Orlova, A., Cherepanova, O., Lebart, M.C., and Egelman, E.H. (2008). High-resolution cryo-EM structure of the F-actin-fimbrin/plastin ABD2 complex. *Proc Natl Acad Sci U S A* *105*, 1494-1498.
- Gammon, A., Jasperson, K., Kohlmann, W., and Burt, R.W. (2009). Hamartomatous polyposis syndromes. *Best Practice & Research Clinical Gastroenterology* *23*, 219-231.
- Gardiner-Garden, M., and Frommer, M. (1987). CpG islands in vertebrate genomes. *J Mol Biol* *196*, 261-282.
- George, B., and Kopetz, S. (2011). Predictive and prognostic markers in colorectal cancer. *Curr Oncol Rep* *13*, 206-215.
- Giganti, A., Plastino, J., Janji, B., Van Troys, M., Lentz, D., Ampe, C., Sykes, C., and Friederich, E. (2005). Actin-filament cross-linking protein T-plastin increases Arp2/3-mediated actin-based movement. *J Cell Sci* *118*, 1255-1265.
- Giovannucci, E., and Ogino, S. (2005). DNA methylation, field effects, and colorectal cancer. *J Natl Cancer Inst* *97*, 1317-1319.
- Gjorevski, N., and Nelson, Celeste M. (2012). Mapping of Mechanical Strains and Stresses around Quiescent Engineered Three-Dimensional Epithelial Tissues. *Biophysical journal* *103*, 152-162.
- Glenney, J.R., Jr., Bretscher, A., and Weber, K. (1980). Calcium control of the intestinal microvillus cytoskeleton: its implications for the regulation of microfilament organizations. *Proc Natl Acad Sci U S A* *77*, 6458-6462.
- Glenney, J.R., Jr., Kaulfus, P., Matsudaira, P., and Weber, K. (1981). F-actin binding and bundling properties of fimbrin, a major cytoskeletal protein of microvillus core filaments. *J Biol Chem* *256*, 9283-9288.
- Goldsmith, S.C., Pokala, N., Matsudaira, P., and Almo, S.C. (1997). Crystallization and preliminary crystallographic analysis of the N-terminal actin binding domain of human fimbrin. *Proteins* *28*, 452-453.
- Goldstein, D., Djeu, J., Latter, G., Burbeck, S., and Leavitt, J. (1985). Abundant synthesis of the transformation-induced protein of neoplastic human fibroblasts, plastin, in normal lymphocytes. *Cancer Res* *45*, 5643-5647.

- Gonzalez-Suarez, I., and Gonzalo, S. (2010). Nurturing the genome: A-type lamins preserve genomic stability. *Nucleus* *1*, 129-135.
- Gopalan, V., Smith, R., Ho, Y.-H., and Lam, A. (2011). Signet-ring cell carcinoma of colorectum—current perspectives and molecular biology. *International Journal of Colorectal Disease* *26*, 127-133.
- Goss, K.H., and Groden, J. (2000). Biology of the Adenomatous Polyposis Coli Tumor Suppressor. *Journal of Clinical Oncology* *18*, 1967-1979.
- Grady, W.M. (2005). Molecular basis for subdividing hereditary colon cancer? *Gut* *54*, 1676-1678.
- Graziano, F., and Cascinu, S. (2003). Prognostic molecular markers for planning adjuvant chemotherapy trials in Dukes' B colorectal cancer patients: how much evidence is enough? *Annals of Oncology* *14*, 1026-1038.
- Grimm-Gunter, E.M., Revenu, C., Ramos, S., Hurbain, I., Smyth, N., Ferrary, E., Louvard, D., Robine, S., and Rivero, F. (2009). Plastin 1 binds to keratin and is required for terminal web assembly in the intestinal epithelium. *Mol Biol Cell* *20*, 2549-2562.
- Groden, J., Thliveris, A., Samowitz, W., Carlson, M., Gelbert, L., Albertsen, H., Joslyn, G., Stevens, J., Spirio, L., Robertson, M., *et al.* (1991). Identification and characterization of the familial adenomatous polyposis coli gene. *Cell* *66*, 589-600.
- Guaita, S., Puig, I., Franci, C., Garrido, M., Dominguez, D., Batlle, E., Sancho, E., Dedhar, S., De Herreros, A.G., and Baulida, J. (2002). Snail induction of epithelial to mesenchymal transition in tumor cells is accompanied by MUC1 repression and ZEB1 expression. *J Biol Chem* *277*, 39209-39216.
- Hague, A., Manning, A.M., Hanlon, K.A., Huschtscha, L.I., Hart, D., and Paraskeva, C. (1993). Sodium butyrate induces apoptosis in human colonic tumour cell lines in a p53-independent pathway: implications for the possible role of dietary fibre in the prevention of large-bowel cancer. *Int J Cancer* *55*, 498-505.
- Half, E., Bercovich, D., and Rozen, P. (2009). Familial adenomatous polyposis. *Orphanet Journal of Rare Diseases* *4*(22).
- Hall, A. (2009). The cytoskeleton and cancer. *Cancer and Metastasis Reviews* *28*, 5-14.
- Hampel, H., Frankel, W., Panescu, J., Lockman, J., Sotamaa, K., Fix, D., Comeras, I., La Jeunesse, J., Nakagawa, H., Westman, J.A., *et al.* (2006). Screening for Lynch syndrome (hereditary nonpolyposis colorectal cancer) among endometrial cancer patients. *Cancer Res* *66*, 7810-7817.
- Hanahan, D., and Weinberg, R.A. (2000). The hallmarks of cancer. *Cell* *100*, 57-70.
- Hanahan, D., and Weinberg, Robert A. (2011). Hallmarks of Cancer: The Next Generation. *Cell* *144*, 646-674.
- Hanein, D., Volkmann, N., Goldsmith, S., Michon, A.M., Lehman, W., Craig, R., DeRosier, D., Almo, S., and Matsudaira, P. (1998). An atomic model of fimbrin binding to F-actin and its implications for filament crosslinking and regulation. *Nat Struct Biol* *5*, 787-792.
- Hanson, J., Lowy, J., and Reedy, M.K. (1964). The Structure of Actin Filaments and the Origin of the Axial Periodicity in the I-Substance of Vertebrate Striated Muscle [and Discussion]. *Proceedings of the Royal Society of London Series B, Biological Sciences* *160*, 449-460.

- Hao, L.T., Wolman, M., Granato, M., and Beattie, C.E. (2012). Survival Motor Neuron Affects Plastin 3 Protein Levels Leading to Motor Defects. *The Journal of Neuroscience* 32, 5074-5084.
- Harris, T.J.R., and McCormick, F. (2010). The molecular pathology of cancer. *Nat Rev Clin Oncol* 7, 251-265.
- Hawkes, E.A., and Cunningham, D. (2010). Flexible sigmoidoscopy--valuable in colorectal cancer. *Nat Rev Clin Oncol* 7, 488-490.
- Herman, J.G., and Baylin, S.B. (2003). Gene Silencing in Cancer in Association with Promoter Hypermethylation. *New England Journal of Medicine* 349, 2042-2054.
- Herman, J.G., Graff, J.R., Myöhänen, S., Nelkin, B.D., and Baylin, S.B. (1996). Methylation-specific PCR: a novel PCR assay for methylation status of CpG islands. *Proceedings of the National Academy of Sciences* 93, 9821-9826.
- Hermesen, M., Postma, C., Baak, J., Weiss, M., Rapallo, A., Sciotto, A., Roemen, G., Arends, J.W., Williams, R., Giaretti, W., *et al.* (2002). Colorectal adenoma to carcinoma progression follows multiple pathways of chromosomal instability. *Gastroenterology* 123, 1109-1119.
- Herrera, L., Kakati, S., Gibas, L., Pietrzak, E., Sandberg, A.A., and Reynolds, J.F. (1986). Gardner syndrome in a man with an interstitial deletion of 5q. *American Journal of Medical Genetics* 25, 473-476.
- Hisano, T., Ono, M., Nakayama, M., Naito, S., Kuwano, M., and Wada, M. (1996). Increased expression of T-plastin gene in cisplatin-resistant human cancer cells: identification by mRNA differential display. *FEBS Lett* 397, 101-107.
- Hodzic, D.M., Yeater, D.B., Bengtsson, L., Otto, H., and Stahl, P.D. (2004). Sun2 Is a Novel Mammalian Inner Nuclear Membrane Protein. *Journal of Biological Chemistry* 279, 25805-25812.
- Holaska, J.M., Lee, K.K., Kowalski, A.K., and Wilson, K.L. (2003). Transcriptional repressor germ cell-less (GCL) and barrier to autointegration factor (BAF) compete for binding to emerin in vitro. *J Biol Chem* 278, 6969-6975.
- Hornbeck, P. (2001). Enzyme-Linked Immunosorbent Assays. In *Current Protocols in Immunology* (John Wiley & Sons, Inc.).
- Howe, C.L., Mooseker, M.S., and Graves, T.A. (1980). Brush-border calmodulin. A major component of the isolated microvillus core. *J Cell Biol* 85, 916-923.
- Huang, Y., Pastor, W.A., Shen, Y., Tahiliani, M., Liu, D.R., and Rao, A. (2010). The Behaviour of 5-Hydroxymethylcytosine in Bisulfite Sequencing. *PLoS One* 5, e8888.
- Huber, M.A., Kraut, N., and Beug, H. (2005). Molecular requirements for epithelial-mesenchymal transition during tumor progression. *Curr Opin Cell Biol* 17, 548-558.
- Hutchison, C.J. (2002). Lamins: building blocks or regulators of gene expression? *Nature Rev Mol Cell Biol* 3, 848-858.
- Hutchison, C.J., Alvarez-Reyes, M., and Vaughan, O.A. (2001). Lamins in disease: why do ubiquitously expressed nuclear envelope proteins give rise to tissue specific disease phenotypes? *J Cell Sci* 114, 9-19.

- Hutchison, C.J., and Worman, H.J. (2004). A-type lamins: Guardians of the soma? *Nat Cell Biol* 6, 1062-1067.
- Ikeda, H., Sasaki, Y., Kobayashi, T., Suzuki, H., Mita, H., Toyota, M., Itoh, F., Shinomura, Y., Tokino, T., and Imai, K. (2005). The role of T-fimbrin in the response to DNA damage: silencing of T-fimbrin by small interfering RNA sensitizes human liver cancer cells to DNA-damaging agents. *Int J Oncol* 27, 933-940.
- Issa, J.-P.J., Shen, L., and Toyota, M. (2005). CIMP, at Last. *Gastroenterology* 129, 1121-1124.
- Issa, J.P. (1994). Methylation of the oestrogen receptor CpG island links ageing and neoplasia in human colon. *Nat Genet* 7, 536-540.
- Issa, J.P. (2004). CpG island methylator phenotype in cancer. *Nature Rev Cancer* 4, 988-993.
- Janji, B., Vallar, L., Al Tanoury, Z., Bernardin, F., Vetter, G., Schaffner-Reckinger, E., Berchem, G., Friederich, E., and Chouaib, S. (2010). The actin filament cross-linker L-plastin confers resistance to TNF-alpha in MCF-7 breast cancer cells in a phosphorylation-dependent manner. *J Cell Mol Med* 14, 1264-1275.
- Jasperson, K.W., Tuohy, T.M., Neklason, D.W., and Burt, R.W. (2010). Hereditary and familial colon cancer. *Gastroenterology* 138, 2044-2058.
- Jass, J.R. (1991). Subsite distribution and incidence of colorectal cancer in New Zealand, 1974-1983. *Dis Colon Rectum* 34, 56-59.
- Jass, J.R. (2006). Colorectal cancer: a multipathway disease. *Crit Rev Oncog* 12, 273-287.
- Jemal, A., Bray, F., Center, M.M., Ferlay, J., Ward, E., and Forman, D. (2011). Global cancer statistics. *CA: A Cancer Journal for Clinicians* 61, 69-90.
- Jemal, A., Siegel, R., Xu, J., and Ward, E. (2010). Cancer statistics, 2010. *CA Cancer J Clin* 60, 277-300.
- Jones, C.L., Ferreira, S., McKenzie, R.C., Tosi, I., Caesar, J.A., Bagot, M., Whittaker, S.J., and Mitchell, T.J. (2012). Regulation of T-Plastin Expression by Promoter Hypomethylation in Primary Cutaneous T-Cell Lymphoma. *J Invest Dermatol*.
- Jones, P.A., and Baylin, S.B. (2002). The fundamental role of epigenetic events in cancer. *Nat Rev Genet* 3, 415-428.
- Jones, S.L., Wang, J., Turck, C.W., and Brown, E.J. (1998). A role for the actin-bundling protein L-plastin in the regulation of leukocyte integrin function. *Proc Natl Acad Sci U S A* 95, 9331-9336.
- Jung, S.-R., Seo, J.B., Shim, D., Hille, B., and Koh, D.-S. (2012). Actin cytoskeleton controls movement of intracellular organelles in pancreatic duct epithelial cells. *Cell Calcium* 51, 459-469.
- Jung, Y., Lee, S., Choi, H.S., Kim, S.N., Lee, E., Shin, Y., Seo, J., Kim, B., Kim, W.K., Chun, H.K., *et al.* (2011). Clinical validation of colorectal cancer biomarkers identified from bioinformatics analysis of public expression data. *Clin Cancer Res* 17, 700-709.
- Kalluri R., and Weinberg R.A. (2009). The basics of epithelial-mesenchymal transition. *J Clin Invest* 119, 1420-1428.

- Kane, M.A., Folias, A.E., Wang, C., and Napoli, J.L. (2010). Ethanol elevates physiological all-trans-retinoic acid levels in select loci through altering retinoid metabolism in multiple loci: a potential mechanism of ethanol toxicity. *The FASEB Journal* 24, 823-832.
- Kaneda, A., and Feinberg, A.P. (2005). Loss of imprinting of IGF2: a common epigenetic modifier of intestinal tumor risk. *Cancer Res* 65, 11236-11240.
- Kari, L., Loboda, A., Nebozhyn, M., Rook, A.H., Vonderheid, E.C., Nichols, C., Virok, D., Chang, C., Horng, W.H., Johnston, J., *et al.* (2003). Classification and prediction of survival in patients with the leukemic phase of cutaneous T cell lymphoma. *J Exp Med* 197, 1477-1488.
- Kastrinos, F., Mukherjee, B., Tayob, N., Wang, F., Sparr, J., Raymond, V.M., Bandipalliam, P., Stoffel, E.M., Gruber, S.B., and Syngal, S. (2009). Risk of pancreatic cancer in families with Lynch syndrome. *JAMA* 302, 1790-1795.
- Key, T.J. (2011). Fruit and vegetables and cancer risk. *Br J Cancer* 104, 6-11.
- Kim, K., Lu, Z., and Hay, E.D. (2002). Direct evidence for a role of beta-catenin/LEF-1 signaling pathway in induction of EMT. *Cell Biol Int* 26, 463-476.
- Kind, J., and van Steensel, B. (2010). Genome–nuclear lamina interactions and gene regulation. *Current Opinion in Cell Biology* 22, 320-325.
- Kinzler, K.W., and Vogelstein, B. (1996). Lessons from hereditary colorectal cancer. *Cell* 87, 159-170.
- Kiss, T. (2002). Small Nucleolar RNAs: An Abundant Group of Noncoding RNAs with Diverse Cellular Functions. *Cell* 109, 145-148.
- Klein, M.G., Shi, W., Ramagopal, U., Tseng, Y., Wirtz, D., Kovar, D.R., Staiger, C.J., and Almo, S.C. (2004). Structure of the actin crosslinking core of fimbrin. *Structure* 12, 999-1013.
- Kolonel, L.N., Altshuler, D., and Henderson, B.E. (2004). The multiethnic cohort study: exploring genes, lifestyle and cancer risk. *Nat Rev Cancer* 4, 519-527.
- Kondo, Y., and Issa, J.-P.J. (2004). Epigenetic changes in colorectal cancer. *Cancer and Metastasis Reviews* 23, 29-39.
- Konecny, G., Untch, M., Pihan, A., Kimmig, R., Gropp, M., Stieber, P., Hepp, S., Slamon, D., and Pegram, M. (2001). Association of urokinase-type plasminogen activator and its inhibitor with disease progression and prognosis in ovarian cancer. *Clin Cancer Res* 7, 1743–1749.
- Korenbaum, E., and Rivero, F. (2002). Calponin homology domains at a glance. *J Cell Sci* 115, 3543-3545.
- Korinek, V., Barker, N., Morin, P.J., van Wichen, D., de Weger, R., Kinzler, K.W., Vogelstein, B., and Clevers, H. (1997). Constitutive Transcriptional Activation by a β -Catenin-Tcf Complex in APC–/– Colon Carcinoma. *Science* 275, 1784-1787.
- Kouzarides, T. (2007). Chromatin Modifications and Their Function. *Cell* 128, 693-705.
- Kozuka, S., Nogaki, M., Ozeki, T., and Masumori, S. (1975). Premalignancy of the mucosal polyp in the large intestine: II. Estimation of the periods required for malignant transformation of mucosal polyps. *Dis Colon Rectum* 18, 494-500.

- Kriaucionis, S., and Heintz, N. (2009). The Nuclear DNA Base 5-Hydroxymethylcytosine Is Present in Purkinje Neurons and the Brain. *Science* *324*, 929-930.
- Krimm, I. (2002). The Ig-like structure of the C-terminal domain of lamin A/C, mutated in muscular dystrophies, cardiomyopathy, and partial lipodystrophy. *Structure* *10*, 811-823.
- Kritchovsky, D. (1993). Colorectal cancer: the role of dietary fat and caloric restriction. *Mutation Research/Fundamental and Molecular Mechanisms of Mutagenesis* *290*, 63-70.
- Kroboth, K., Newton, I.P., Kita, K., Dikovskaya, D., Zumbunn, J., Waterman-Storer, C.M., and Nathke, I.S. (2007). Lack of adenomatous polyposis coli protein correlates with a decrease in cell migration and overall changes in microtubule stability. *Mol Biol Cell* *18*, 910-918.
- Kubler, E., and Riezman, H. (1993). Actin and fimbrin are required for the internalization step of endocytosis in yeast. *EMBO J* *12*, 2855-2862.
- Lammerding, J., Schulze, P.C., Takahashi, T., Kozlov, S., Sullivan, T., Kamm, R.D., Stewart, C.L., and Lee, R.T. (2004). Lamin A/C deficiency causes defective nuclear mechanics and mechanotransduction. *The Journal of Clinical Investigation* *113*, 370-378.
- Lamond, A.I., and Earnshaw, W.C. (1998). Structure and Function in the Nucleus. *Science* *280*, 547-553.
- Lao, V.V., and Grady, W.M. (2011). Epigenetics and colorectal cancer. *Nat Rev Gastroenterol Hepatol* *advance online publication*.
- Law, J.A., and Jacobsen, S.E. (2010). Establishing, maintaining and modifying DNA methylation patterns in plants and animals. *Nat Rev Genet* *11*, 204-220.
- Leavitt, J. (1994). Discovery and characterization of two novel human cancer-related proteins using two-dimensional gel electrophoresis. *Electrophoresis* *15*, 345-357.
- Lee, J.K., and Chan, A.T. (2011). Molecular Prognostic and Predictive Markers in Colorectal Cancer: Current Status. *Curr Colorectal Cancer Rep* *7*, 136-144.
- Lee, S., and Dominguez, R. (2010). Regulation of actin cytoskeleton dynamics in cells. *Molecules and Cells* *29*, 311-325.
- Leibovitz, A., Stinson, J.C., McCombs, W.B., McCoy, C.E., Mazur, K.C., and Mabry, N.D. (1976). Classification of Human Colorectal Adenocarcinoma Cell Lines. *Cancer Research* *36*, 4562-4569.
- Leight, J.L., Wozniak, M.A., Chen, S., Lynch, M.L., and Chen, C.S. (2012). Matrix rigidity regulates a switch between TGF- β 1-induced apoptosis and epithelial-mesenchymal transition. *Molecular Biology of the Cell* *23*, 781-791.
- Lengauer, C., Kinzler, K.W., and Vogelstein, B. (1997). Genetic instability in colorectal cancers. *Nature* *386*, 623-627.
- Levi, F., Randimbison, L., and La Vecchia, C. (1993). Trends in subsite distribution of colorectal cancers and polyps from the Vaud Cancer Registry. *Cancer* *72*, 46-50.
- Levine, A.J. (1997). p53, the Cellular Gatekeeper for Growth and Division. *Cell* *88*, 323-331.

- Ley, T.J., Ding, L., Walter, M.J., McLellan, M.D., Lamprecht, T., Larson, D.E., Kandoth, C., Payton, J.E., Baty, J., Welch, J., *et al.* (2010). DNMT3A Mutations in Acute Myeloid Leukemia. *New England Journal of Medicine* *363*, 2424-2433.
- Li, E., Bestor, T.H., and Jaenisch, R. (1992). Targeted mutation of the DNA methyltransferase gene results in embryonic lethality. *Cell* *69*, 915-926.
- Li, G.-M. (2008). Mechanisms and functions of DNA mismatch repair. *Cell Res* *18*, 85-98.
- Li, J., and Zhao, R. (2011). Expression and Clinical Significance L-plastin in colorectal carcinoma. *Journal of Gastrointestinal Surgery* *15*, 1982-1988.
- Li, W., Yeo, L.S., Vidal, C., McCorquodale, T., Herrmann, M., Fatkin, D., and Duque, G. (2011). Decreased Bone Formation and Osteopenia in Lamin A/C-Deficient Mice. *PLoS One* *6*, e19313.
- Liang, P.S., Chen, T.Y., and Giovannucci, E. (2009). Cigarette smoking and colorectal cancer incidence and mortality: systematic review and meta-analysis. *Int J Cancer* *124*, 2406-2415.
- Lim, R.Y.H., and Fahrenkrog, B. (2006). The nuclear pore complex up close. *Current Opinion in Cell Biology* *18*, 342-347.
- Lin, C.S., Chen, Z.P., Park, T., Ghosh, K., and Leavitt, J. (1993a). Characterization of the human L-plastin gene promoter in normal and neoplastic cells. *J Biol Chem* *268*, 2793-2801.
- Lin, C.S., Lau, A., Huynh, T., and Lue, T.F. (1999). Differential regulation of human T-plastin gene in leukocytes and non-leukocytes: identification of the promoter, enhancer, and CpG island. *DNA Cell Biol* *18*, 27-37.
- Lin, C.S., Park, T., Chen, Z.P., and Leavitt, J. (1993b). Human plastin genes. Comparative gene structure, chromosome location, and differential expression in normal and neoplastic cells. *J Biol Chem* *268*, 2781-2792.
- Lin, C.S., Shen, W., Chen, Z.P., Tu, Y.H., and Matsudaira, P. (1994). Identification of I-plastin, a human fimbrin isoform expressed in intestine and kidney. *Mol Cell Biol* *14*, 2457-2467.
- Liu, B., Wang, J., Chan, K.M., Tjia, W.M., Deng, W., Guan, X., Huang, J.-d., Li, K.M., Chau, P.Y., Chen, D.J., *et al.* (2005). Genomic instability in laminopathy-based premature aging. *Nat Med* *11*, 780-785.
- Liu, J., Ben-Shahar, T.R., Riemer, D., Treinin, M., Spann, P., Weber, K., Fire, A., and Gruenbaum, Y. (2000). Essential Roles for *Caenorhabditis elegans* Lamin Gene in Nuclear Organization, Cell Cycle Progression, and Spatial Organization of Nuclear Pore Complexes. *Molecular Biology of the Cell* *11*, 3937-3947.
- Liu, Y., Balaraman, Y., Wang, G., Nephew, K.P., and Zhou, F.C. (2009). Alcohol exposure alters DNA methylation profiles in mouse embryos at early neurulation. *Epigenetics* *4*, 500-511.
- Livak, K.J., and Schmittgen, T.D. (2001a). Analysis of Relative Gene Expression Data Using Real-Time Quantitative PCR and the $2^{-\Delta\Delta CT}$ Method. *Methods* *25*, 402-408.
- Livak, K.J., and Schmittgen, T.D. (2001b). Analysis of relative gene expression data using real-time quantitative PCR and the $2^{-(\Delta\Delta C(T))}$ Method. *Methods* *25*, 402-408.
- Lock, L.F., Takagi, N., and Martin, G.R. (1987). Methylation of the Hprt gene on the inactive X occurs after chromosome inactivation. *Cell* *48*, 39-46.

- Loupakis, F., Masi, G., Vasile, E., and Falcone, A. (2008). First-line chemotherapy in metastatic colorectal cancer: new approaches and therapeutic algorithms. Always hit hard first? *Curr Opin Oncol* 20, 459-465.
- Ludérus, M.E., den Blaauwen, J.L., de Smit, O.J., Compton, D.A., and van Driel, R. (1994). Binding of matrix attachment regions to lamin polymers involves single-stranded regions and the minor groove. *Molecular and Cellular Biology* 14, 6297-6305.
- Lupton, J.R., Steinbach, G., Chang, W.C., O'Brien, B.C., Wiese, S., Stoltzfus, C.L., Glober, G.A., Wargovich, M.J., McPherson, R.S., and Winn, R.J. (1996). Calcium supplementation modifies the relative amounts of bile acids in bile and affects key aspects of human colon physiology. *J Nutr* 126, 1421-1428.
- Lynch, H.T., and Lynch, J.F. (2004). Lynch syndrome: history and current status. *Dis Markers* 20, 181-198.
- Lynch, H.T., Lynch, P.M., Lanspa, S.J., Snyder, C.L., Lynch, J.F., and Boland, C.R. (2009). Review of the Lynch syndrome: history, molecular genetics, screening, differential diagnosis, and medicolegal ramifications. *Clin Genet* 76, 1-18.
- Macdonald, J.S. (1999). Adjuvant therapy of colon cancer. *CA: A Cancer Journal for Clinicians* 49, 202-219.
- Manz, R.A., Hauser, A.E., Hiepe, F., and Radbruch, A. (2005). MAINTENANCE OF SERUM ANTIBODY LEVELS. *Annual Review of Immunology* 23, 367-386.
- Markowitz, S.D., and Bertagnolli, M.M. (2009). Molecular origins of cancer: Molecular basis of colorectal cancer. *N Engl J Med* 361, 2449-2460.
- Marshman, E., Booth, C., and Potten, C. (2002). The intestinal epithelial stem cell. *Bioessays* 24, 91-98.
- Matsudaira, P.T., and Burgess, D.R. (1979). Identification and organization of the components in the isolated microvillus cytoskeleton. *J Cell Biol* 83, 667-673.
- Mattila, P.K., and Lappalainen, P. (2008). Filopodia: molecular architecture and cellular functions. *Nat Rev Mol Cell Biol* 9, 446-454.
- Mayer, D.K., Terrin, N.C., Menon, U., Kreps, G.L., McCance, K., Parsons, S.K., and Mooney, K.H. (2007). Screening practices in cancer survivors. *J Cancer Surviv* 1, 17-26.
- Mayor, S. (2010). Cancer survival rates are improving but regional disparities remain across England. *BMJ* 341.
- Mazzocoli, G., Paziienza, V., Panza, A., Valvano, M., Benegiamo, G., Vinciguerra, M., Andriulli, A., and Piepoli, A. (2012). ARNTL2 and SERPINE1: potential biomarkers for tumor aggressiveness in colorectal cancer. *Journal of Cancer Research and Clinical Oncology* 138, 501-511.
- McCabe, M.T., Lee, E.K., and Vertino, P.M. (2009). A multifactorial signature of DNA sequence and polycomb binding predicts aberrant CpG island methylation. *Cancer Res* 69, 282-291.
- McKeon, F. (1991). Nuclear lamin proteins: domains required for nuclear targeting, assembly, and cell-cycle-regulated dynamics. *Current Opinion in Cell Biology* 3, 82-86.

- McLean, M.H., Murray, G.I., Stewart, K.N., Norrie, G., Mayer, C., Hold, G.L., Thomson, J., Fyfe, N., Hope, M., Mowat, N.A., *et al.* (2011). The inflammatory microenvironment in colorectal neoplasia. *PLoS One* *6*, e15366.
- McLeod, H.L., and Church, R.D. (2003). Molecular predictors of prognosis and response to therapy in colorectal cancer. *Cancer Chemother Biol Response Modif* *21*, 791-801.
- Meguid, R.A., Slidell, M.B., Wolfgang, C.L., Chang, D.C., and Ahuja, N. (2008). Is there a difference in survival between right- versus left-sided colon cancers? *Ann Surg Oncol* *15*, 2388-2394.
- Menendez, D., Inga, A., and Resnick, M.A. (2009). The expanding universe of p53 targets. *Nat Rev Cancer* *9*, 724-737.
- Mimori-Kiyosue, Y., Shiina, N., and Tsukita, S. (2000). Adenomatous polyposis coli (APC) protein moves along microtubules and concentrates at their growing ends in epithelial cells. *J Cell Biol* *148*, 505-517.
- Miranda, E., Destro, A., Malesci, A., Balladore, E., Bianchi, P., Baryshnikova, E., Franchi, G., Morengi, E., Laghi, L., Gennari, L., *et al.* (2006). Genetic and epigenetic changes in primary metastatic and nonmetastatic colorectal cancer. *Br J Cancer* *95*, 1101-1107.
- Miyakura, Y., Sugano, K., Konishi, F., Fukayama, N., Igarashi, S., Kotake, K., Matsui, T., Koyama, Y., Maekawa, M., and Nagai, H. (2003). Methylation profile of the MLH1 promoter region and their relationship to colorectal carcinogenesis. *Genes, Chromosomes and Cancer* *36*, 17-25.
- Momparler, R.L. (2003). Cancer epigenetics. *Oncogene* *22*, 6479-6483.
- Moss, S.F., Krivosheyev, V., de Souza, A., Chin, K., Gaetz, H.P., Chaudhary, N., Worman, H.J., and Holt, P.R. (1999). Decreased and aberrant nuclear lamin expression in gastrointestinal tract neoplasms. *Gut* *45*, 723-729.
- Munro, A.J., Lain, S., and Lane, D.P. (2005). P53 abnormalities and outcomes in colorectal cancer: a systematic review. *Br J Cancer* *92*, 434-444.
- Namba, Y., Ito, M., Zu, Y., Shigesada, K., and Maruyama, K. (1992). Human T cell L-plastin bundles actin filaments in a calcium-dependent manner. *J Biochem* *112*, 503-507.
- Nannini, M., Pantaleo, M.A., Maleddu, A., Astolfi, A., Formica, S., and Biasco, G. (2009). Gene expression profiling in colorectal cancer using microarray technologies: results and perspectives. *Cancer Treat Rev* *35*, 201-209.
- Narumiya, S., Tanji, M., and Ishizaki, T. (2009). Rho signaling, ROCK and mDia1, in transformation, metastasis and invasion. *Cancer Metastasis Rev* *28*, 65-76.
- Nathke, I. (2006). Cytoskeleton out of the cupboard: colon cancer and cytoskeletal changes induced by loss of APC. *Nat Rev Cancer* *6*, 967-974.
- Nathke, I.S., Adams, C.L., Polakis, P., Sellin, J.H., and Nelson, W.J. (1996). The adenomatous polyposis coli tumor suppressor protein localizes to plasma membrane sites involved in active cell migration. *J Cell Biol* *134*, 165-179.
- Nelson, H., Petrelli, N., Carlin, A., Couture, J., Fleshman, J., Guillem, J., Miedema, B., Ota, D., and Sargent, D. (2001). Guidelines 2000 for Colon and Rectal Cancer Surgery. *Journal of the National Cancer Institute* *93*, 583-596.

- Nelson, R.L. (2001). Iron and colorectal cancer risk: human studies. *Nutr Rev* 59, 140-148.
- Nestor, C.E., Ottaviano, R., Reddington, J., Sproul, D., Reinhardt, D., Dunican, D., Katz, E., Dixon, J.M., Harrison, D.J., and Meehan, R.R. (2012). Tissue type is a major modifier of the 5-hydroxymethylcytosine content of human genes. *Genome Research* 22, 467-477.
- Newton, K.F., Newman, W., and Hill, J. (2010). Review of Biomarkers in Colorectal Cancer. *Colorectal Dis.*
- Ngo, S.N., Williams, D.B., Cobiac, L., and Head, R.J. (2007). Does garlic reduce risk of colorectal cancer? A systematic review. *J Nutr* 137, 2264-2269.
- Nieuwenhuis, M.H., Mathus-Vliegen, L.M., Slors, F.J., Griffioen, G., Nagengast, F.M., Schouten, W.R., Kleibeuker, J.H., and Vasen, H.F. (2007). Genotype-phenotype correlations as a guide in the management of familial adenomatous polyposis. *Clin Gastroenterol Hepatol* 5, 374-378.
- Nieuwenhuis, M.H., and Vasen, H.F. (2007). Correlations between mutation site in APC and phenotype of familial adenomatous polyposis (FAP): a review of the literature. *Crit Rev Oncol Hematol* 61, 153-161.
- Nikolova, V. (2004). Defects in nuclear structure and function promote dilated cardiomyopathy in lamin A/C-deficient mice. *J Clin Invest* 113, 357-369.
- Nishisho, I., Nakamura, Y., Miyoshi, Y., Miki, Y., Ando, H., Horii, A., Koyama, K., Utsunomiya, J., Baba, S., and Hedge, P. (1991). Mutations of chromosome 5q21 genes in FAP and colorectal cancer patients. *Science* 253, 665-669.
- Norat, T., Bingham, S., Ferrari, P., Slimani, N., Jenab, M., Mazuir, M., Overvad, K., Olsen, A., Tjonneland, A., Clavel, F., *et al.* (2005). Meat, fish, and colorectal cancer risk: the European Prospective Investigation into cancer and nutrition. *J Natl Cancer Inst* 97, 906-916.
- Norat, T.C., D.; Lau, R.; Aune, D.; Vieira, R. (2010). WCRF/AICR Systematic Literature Review Continuous Update Project Report. The Associations between Food, Nutrition and Physical Activity and the Risk of Colorectal Cancer.
- Norman E, W. (1999). Chapter 23 Immunoprecipitation Procedures. In *Methods in Cell Biology*, J.A. David, and D.F. James, eds. (Academic Press), pp. 449-453.
- O'Byrne, K.J., Dalglish, A.G., Browning, M.J., Steward, W.P., and Harris, A.L. (2000). The relationship between angiogenesis and the immune response in carcinogenesis and the progression of malignant disease. *Eur J Cancer* 36, 151-169.
- Obrand, D.I., and Gordon, P.H. (1998). Continued change in the distribution of colorectal carcinoma. *Br J Surg* 85, 246-248.
- Ogino, S., and Goel, A. (2008). Molecular classification and correlates in colorectal cancer. *J Mol Diagn* 10, 13-27.
- Ogino, S., Kawasaki, T., Kirkner, G.J., Loda, M., and Fuchs, C.S. (2006). CpG Island Methylator Phenotype-Low (CIMP-Low) in Colorectal Cancer: Possible Associations with Male Sex and KRAS Mutations. *The Journal of Molecular Diagnostics* 8, 582-588.

- Onder, T.T., Gupta, P.B., Mani, S.A., Yang, J., Lander, E.S., and Weinberg, R.A. (2008). Loss of E-cadherin promotes metastasis via multiple downstream transcriptional pathways. *Cancer Res* 68, 3645-3654.
- Ooi, S.K.T., and Bestor, T.H. (2008). The Colorful History of Active DNA Demethylation. *Cell* 133, 1145-1148.
- Oprea, G.E., Krober, S., McWhorter, M.L., Rossoll, W., Muller, S., Krawczak, M., Bassell, G.J., Beattie, C.E., and Wirth, B. (2008). Plastin 3 is a protective modifier of autosomal recessive spinal muscular atrophy. *Science* 320, 524-527.
- Ortiz, A.P., Thompson, C.L., Chak, A., Berger, N.A., and Li, L. (2012). Insulin resistance, central obesity, and risk of colorectal adenomas. *Cancer* 118, 1774-1781.
- Otani, T., Iwasaki, M., Yamamoto, S., Sobue, T., Hanaoka, T., Inoue, M., and Tsugane, S. (2003). Alcohol Consumption, Smoking, and Subsequent Risk of Colorectal Cancer in Middle-Aged and Elderly Japanese Men and Women. *Cancer Epidemiology Biomarkers & Prevention* 12, 1492-1500.
- Otsuka, M., Kato, M., Yoshikawa, T., Chen, H., Brown, E.J., Masuho, Y., Omata, M., and Seki, N. (2001). Differential expression of the L-plastin gene in human colorectal cancer progression and metastasis. *Biochem Biophys Res Commun* 289, 876-881.
- Oussoultzoglou, E., Rosso, E., Fuchshuber, P., Stefanescu, V., Diop, B., Giraudo G., Pessaux, P., Bachellier, P., Jaeck, D. (2008). Perioperative carcinoembryonic antigen measurements to predict curability after liver resection for colorectal metastases: a prospective study. *Arch Surg* 143, 1150-1158.
- Park, T., Chen, Z.P., and Leavitt, J. (1994). Activation of the leukocyte plastin gene occurs in most human cancer cells. *Cancer Res* 54, 1775-1781.
- Parkin, D.M., Bray, F., Ferlay, J., and Pisani, P. (2005). Global cancer statistics, 2002. *CA Cancer J Clin* 55, 74-108.
- Peinado, H., Olmeda, D., and Cano, A. (2007). Snail, Zeb and bHLH factors in tumour progression: an alliance against the epithelial phenotype? *Nat Rev Cancer* 7, 415-428.
- Pino, M.S., and Chung, D.C. (2010). The chromosomal instability pathway in colon cancer. *Gastroenterology* 138, 2059-2072.
- Pinto, D., and Clevers, H. (2005). Wnt control of stem cells and differentiation in the intestinal epithelium. *Exp Cell Res* 306, 357-363.
- Pollard, T.D., Almo, S., Quirk, S., Vinson, V., and Lattman, E.E. (1994). Structure of Actin Binding Proteins: Insights about Function at Atomic Resolution. *Annual Review of Cell Biology* 10, 207-249.
- Pollard, T.D., and Borisy, G.G. (2003). Cellular motility driven by assembly and disassembly of actin filaments. *Cell* 112, 453-465.
- Pollard, T.D., and Cooper, J.A. (1986). ACTIN AND ACTIN-BINDING PROTEINS - A CRITICAL-EVALUATION OF MECHANISMS AND FUNCTIONS. *Annual Review of Biochemistry* 55, 987-1035.
- Pollard, T.D., and Cooper, J.A. (2009). Actin, a central player in cell shape and movement. *Science* 326, 1208-1212.

- Popat, S., and Houlston, R.S. (2005). A systematic review and meta-analysis of the relationship between chromosome 18q genotype, DCC status and colorectal cancer prognosis. *Eur J Cancer* *41*, 2060-2070.
- Popp, C., Dean, W., Feng, S., Cokus, S.J., Andrews, S., Pellegrini, M., Jacobsen, S.E., and Reik, W. (2010). Genome-wide erasure of DNA methylation in mouse primordial germ cells is affected by AID deficiency. *Nature* *463*, 1101-1105.
- Potten, C.S., and Hendry, J.H. (1995). *Radiation and Gut* (Nature Publishing Group, a division of Macmillan Publishers Limited. All Rights Reserved.), pp. 1-31.
- Potter, J.D. (1999). Colorectal cancer: molecules and populations. *J Natl Cancer Inst* *91*, 916-932.
- Powell, D.W. (1999). Myofibroblasts. II. Intestinal subepithelial myofibroblasts. *Am J Physiol* *277*, C183-C201.
- Powell, S.M. (1992). APC mutations occur early during colorectal tumorigenesis. *Nature* *359*, 235-237.
- Puppa, G., Sonzogni, A., Colombari, R., and Pelosi, G. (2010). TNM staging system of colorectal carcinoma: a critical appraisal of challenging issues. *Arch Pathol Lab Med* *134*, 837-852.
- Rabeneck, L., Davila, J.A., and El-Serag, H.B. (2003). Is there a true 'shift' to the right colon in the incidence of colorectal cancer? *Am J Gastroenterol* *98*, 1400-1409.
- Rach, E.A., Winter, D.R., Benjamin, A.M., Corcoran, D.L., Ni, T., Zhu, J., and Ohler, U. (2011). Transcription Initiation Patterns Indicate Divergent Strategies for Gene Regulation at the Chromatin Level. *PLoS Genet* *7*, e1001274.
- Rai, K., Huggins, I.J., James, S.R., Karpf, A.R., Jones, D.A., and Cairns, B.R. (2008). DNA Demethylation in Zebrafish Involves the Coupling of a Deaminase, a Glycosylase, and Gadd45. *Cell* *135*, 1201-1212.
- Rai, K., Sarkar, S., Broadbent, T.J., Voas, M., Grossmann, K.F., Nadauld, L.D., Dehghanizadeh, S., Hagos, F.T., Li, Y., Toth, R.K., *et al.* (2010). DNA Demethylase Activity Maintains Intestinal Cells in an Undifferentiated State Following Loss of APC. *Cell* *142*, 930-942.
- Rajagopalan, H., Bardelli, A., Lengauer, C., Kinzler, K.W., Vogelstein, B., and Velculescu, V.E. (2002). Tumorigenesis: RAF/RAS oncogenes and mismatch-repair status. *Nature* *418*, 934-934.
- Rana, T.M. (2007). Illuminating the silence: understanding the structure and function of small RNAs. *Nat Rev Mol Cell Biol* *8*, 23-36.
- Ranjana P, B. (1987). Observation and quantification of aberrant crypts in the murine colon treated with a colon carcinogen: Preliminary findings. *Cancer Letters* *37*, 147-151.
- Reddy, K.L., Zullo, J.M., Bertolino, E., and Singh, H. (2008). Transcriptional repression mediated by repositioning of genes to the nuclear lamina. *Nature* *452*, 243-247.
- Reik, W., and Lewis, A. (2005). Co-evolution of X-chromosome inactivation and imprinting in mammals. *Nat Rev Genet* *6*, 403-410.
- Ribas, M., Masramon, L., Aiza, G., Capella, G., Miro, R., and Peinado, M.A. (2003). The structural nature of chromosomal instability in colon cancer cells. *FASEB J* *17*, 289-291.

- Robinson, R.C., Turbedsky, K., Kaiser, D.A., Marchand, J.-B., Higgs, H.N., Choe, S., and Pollard, T.D. (2001). Crystal Structure of Arp2/3 Complex. *Science* 294, 1679-1684.
- Rodrigues, N.R., Rowan, A., Smith, M.E., Kerr, I.B., Bodmer, W.F., Gannon, J.V., and Lane, D.P. (1990). p53 mutations in colorectal cancer. *PNAS* 87(19), 7555-7559.
- Roncucci, L., Medline, A., and Bruce, W.R. (1991). Classification of aberrant crypt foci and microadenomas in human colon. *Cancer Epidemiol Biomarkers Prev* 1, 57-60.
- Roskoski Jr, R. (2007). Vascular endothelial growth factor (VEGF) signaling in tumor progression. *Critical Reviews in Oncology/Hematology* 62, 179-213.
- Rusiñol, A.E., and Sinensky, M.S. (2006). Farnesylated lamins, progeroid syndromes and farnesyl transferase inhibitors. *Journal of Cell Science* 119, 3265-3272.
- Russo, A., Bazan, V., Iacopetta, B., Kerr, D., Soussi, T., and Gebbia, N. (2005). The TP53 colorectal cancer international collaborative study on the prognostic and predictive significance of p53 mutation: influence of tumor site, type of mutation, and adjuvant treatment. *J Clin Oncol* 23, 7518-7528.
- Rustgi, A.K. (2007). The genetics of hereditary colon cancer. *Genes Dev* 21, 2525-2538.
- Sado, T., Fenner, M.H., Tan, S.-S., Tam, P., Shioda, T., and Li, E. (2000). X Inactivation in the Mouse Embryo Deficient for Dnmt1: Distinct Effect of Hypomethylation on Imprinted and Random X Inactivation. *Developmental Biology* 225, 294-303.
- Sakakibara, T., Hibi, K., Koike, M., Fujiwara, M., Kodera, Y., Ito, K., and Nakao, A. (2005). Plasminogen activator inhibitor-1 as a potential marker for the malignancy of colorectal cancer. *Br J Cancer* 93(7), 799-803.
- Sakatani, T. (2005). Loss of imprinting of Igf2 alters intestinal maturation and tumorigenesis in mice. *Science* 307, 1976-1978.
- Samowitz, W.S. (2007a). The CpG island methylator phenotype in colorectal cancer. *J Mol Diagn* 9, 281-283.
- Samowitz, W.S. (2007b). The CpG Island Methylator Phenotype in Colorectal Cancer. *The Journal of Molecular Diagnostics* 9, 281-283.
- Samowitz, W.S., Albertsen, H., Herrick, J., Levin, T.R., Sweeney, C., Murtaugh, M.A., Wolff, R.K., and Slattery, M.L. (2005). Evaluation of a Large, Population-Based Sample Supports a CpG Island Methylator Phenotype in Colon Cancer. *Gastroenterology* 129, 837-845.
- Sandler, R.S., Halabi, S., Baron, J.A., Budinger, S., Paskett, E., Keresztes, R., Petrelli, N., Pipas, J.M., Karp, D.D., Loprinzi, C.L., *et al.* (2003). A Randomized Trial of Aspirin to Prevent Colorectal Adenomas in Patients with Previous Colorectal Cancer. *New England Journal of Medicine* 348, 883-890.
- Sanjoaquin, M.A., Appleby, P.N., Thorogood, M., Mann, J.I., and Key, T.J. (2004). Nutrition, lifestyle and colorectal cancer incidence: a prospective investigation of 10,998 vegetarians and non-vegetarians in the United Kingdom. *Br J Cancer* 90, 118-121.
- Sansom, O.J. (2004). Loss of Apc in vivo immediately perturbs Wnt signaling, differentiation, and migration. *Genes Dev* 18, 1385-1390.

- Sansom, O.J., Berger, J., Bishop, S.M., Hendrich, B., Bird, A., and Clarke, A.R. (2003). Deficiency of Mbd2 suppresses intestinal tumorigenesis. *Nat Genet* *34*, 145-147.
- Santi, D.V., Garrett, C.E., and Barr, P.J. (1983). On the mechanism of inhibition of DNA-cytosine methyltransferases by cytosine analogs. *Cell* *33*, 9-10.
- Sasaki, Y., Itoh, F., Kobayashi, T., Kikuchi, T., Suzuki, H., Toyota, M., and Imai, K. (2002a). Increased expression of T-fimbrin gene after DNA damage in CHO cells and inactivation of T-fimbrin by CpG methylation in human colorectal cancer cells. *International Journal of Cancer* *97*, 211-216.
- Sasaki, Y., Itoh, F., Kobayashi, T., Kikuchi, T., Suzuki, H., Toyota, M., and Imai, K. (2002b). Increased expression of T-fimbrin gene after DNA damage in CHO cells and inactivation of T-fimbrin by CpG methylation in human colorectal cancer cells. *Int J Cancer* *97*, 211-216.
- Savagner, P., Yamada, K.M., and Thiery, J.P. (1997). The zinc-finger protein slug causes desmosome dissociation, an initial and necessary step for growth factor-induced epithelial-mesenchymal transition. *J Cell Biol* *137*, 1403-1419.
- Scaffidi, P., and Misteli, T. (2006). Lamin A-Dependent Nuclear Defects in Human Aging. *Science* *312*, 1059-1063.
- Schreibman, I.R. (2005). The hamartomatous polyposis syndromes: a clinical and molecular review. *Am J Gastroenterol* *100*, 476-490.
- Seeff, L.C., Richards, T.B., Shapiro, J.A., Nadel, M.R., Manninen, D.L., Given, L.S., Dong, F.B., Wings, L.D., and McKenna, M.T. (2004). How many endoscopies are performed for colorectal cancer screening? Results from CDC's survey of endoscopic capacity. *Gastroenterology* *127*, 1670-1677.
- Seitz, H.K., and Stickel, F. (2007). Molecular mechanisms of alcohol-mediated carcinogenesis. *Nat Rev Cancer* *7*, 599-612.
- Shaknovich, R., and Melnick, A.C. (2011). Epigenetics and B-cell lymphoma. *Curr Opin Hematol* *18*(4), 293-9.
- Sharif, J., Muto, M., Takebayashi, S.-i., Suetake, I., Iwamatsu, A., Endo, T.A., Shinga, J., Mizutani-Koseki, Y., Toyoda, T., Okamura, K., *et al.* (2007). The SRA protein Np95 mediates epigenetic inheritance by recruiting Dnmt1 to methylated DNA. *Nature* *450*, 908-912.
- Sharma, S., Kelly, T.K., and Jones, P.A. (2010). Epigenetics in cancer. *Carcinogenesis* *31*, 27-36.
- Sheahan, M.B., Staiger, C.J., Rose, R.J., and McCurdy, D.W. (2004). A green fluorescent protein fusion to actin-binding domain 2 of Arabidopsis fimbrin highlights new features of a dynamic actin cytoskeleton in live plant cells. *Plant Physiol* *136*, 3968-3978.
- Shen, L. (2007). Integrated genetic and epigenetic analysis identifies three different subclasses of colon cancer. *Proc Natl Acad Sci USA* *104*, 18654-18659.
- Shen, L., Kondo, Y., Rosner, G.L., Xiao, L., Hernandez, N.S., Vilaythong, J., Houlihan, P.S., Krouse, R.S., Prasad, A.R., Einspahr, J.G., *et al.* (2005). MGMT promoter methylation and field defect in sporadic colorectal cancer. *J Natl Cancer Inst* *97*, 1330-1338.
- Sheridan, C. (2008). EGFR inhibitors embrace KRAS. *Nat Biotechnol* *26*, 839-840.
- Shinomiya, H. (2012). Plastin family of actin-bundling proteins: its functions in leukocytes, neurons, intestines, and cancer. *Int J Cell Biol* *2012*, 213492.

- Shinomiya, H., Hirata, H., Saito, S., Yagisawa, H., and Nakano, M. (1994). Identification of the 65-kDa phosphoprotein in murine macrophages as a novel protein: homology with human L-plastin. *Biochem Biophys Res Commun* 202, 1631-1638.
- Simpson, J.A., Al-Attar, A., Watson, N.F., Scholefield, J.H., Ilyas, M., and Durrant, L.G. (2010). Intratumoral T cell infiltration, MHC class I and STAT1 as biomarkers of good prognosis in colorectal cancer. *Gut* 59, 926-933.
- Sjöblom, T., Jones, S., Wood, L.D., Parsons, D.W., Lin, J., Barber, T.D., Mandelker, D., Leary, R.J., Ptak, J., Silliman, N., Szabo, S., Buckhaults, P., Farrell, C., Meeh, P., Markowitz, S.D., Willis, J., Dawson, D., Willson, J.K., Gazdar, A.F., Hartigan, J., Wu, L., Liu, C., Parmigiani, G., Park, B.H., Bachman, K.E., Papadopoulos, N., Vogelstein, B., Kinzler, K.W., and Velculescu, V.E. (2006) The Consensus Coding Sequences of Human Breast and Colorectal Cancers. *Science* 314, 268-274.
- Skvortsov, S., Schäfer, G., Stasyk, T., Fuchsberger, C., Bonn, G.K., Bartsch, G., Klocker, H., and Huber, L.A. (2010). Proteomics Profiling of Microdissected Low- and High-Grade Prostate Tumors Identifies Lamin A as a Discriminatory Biomarker. *Journal of Proteome Research* 10, 259-268.
- Smits, K.M., Cleven, A.H., Weijnenberg, M.P., Hughes, L.A., Herman, J.G., de Bruine, A.P., and van Engeland, M. (2008). Pharmacoeigenomics in colorectal cancer: a step forward in predicting prognosis and treatment response. *Pharmacogenomics* 9, 1903-1916.
- Song, C.-X., Szulwach, K.E., Fu, Y., Dai, Q., Yi, C., Li, X., Li, Y., Chen, C.-H., Zhang, W., Jian, X., *et al.* (2011). Selective chemical labeling reveals the genome-wide distribution of 5-hydroxymethylcytosine. *Nat Biotech* 29, 68-72.
- Soreide, K., Nedrebo, B.S., Knapp, J.C., Glomsaker, T.B., Soreide, J.A., and Korner, H. (2009). Evolving molecular classification by genomic and proteomic biomarkers in colorectal cancer: potential implications for the surgical oncologist. *Surg Oncol* 18, 31-50.
- Sosa, Brian A., Rothballer, A., Kutay, U., and Schwartz, Thomas U. (2012). LINC Complexes Form by Binding of Three KASH Peptides to Domain Interfaces of Trimeric SUN Proteins. *Cell* 149, 1035-1047.
- Spann, T.P., Moir, R.D., Goldman, A.E., Stick, R., and Goldman, R.D. (1997). Disruption of nuclear lamin organization alters the distribution of replication factors and inhibits DNA synthesis. *J Cell Biol* 136, 1201-1212.
- Speake, D., Evans, D.G., Laloo, F., Scott, N.A., and Hill, J. (2007). Desmoid tumours in patients with familial adenomatous polyposis and desmoid region adenomatous polyposis coli mutations. *Br J Surg* 94, 1009-1013.
- Stevenson, R.P., Veltman, D., and Machesky, L.M. (2012). Actin-bundling proteins in cancer progression at a glance. *Journal of Cell Science* 125, 1073-1079.
- Stoffel, E., Mukherjee, B., Raymond, V.M., Tayob, N., Kastrinos, F., Sparr, J., Wang, F., Bandipalliam, P., Syngal, S., and Gruber, S.B. (2009). Calculation of risk of colorectal and endometrial cancer among patients with Lynch syndrome. *Gastroenterology* 137, 1621-1627.
- Su, L.J., and Arab, L. (2004). Report: Alcohol Consumption and Risk of Colon Cancer: Evidence From the National Health and Nutrition Examination Survey I Epidemiologic Follow-Up Study. *Nutrition and Cancer* 50, 111-119.
- Su, M.W., Dorocicz, I., Dragowska, W.H., Ho, V., Li, G., Voss, N., Gascoyne, R., and Zhou, Y. (2003). Aberrant expression of T-plastin in Sezary cells. *Cancer Res* 63, 7122-7127.

- Sumiyoshi, H., and Wargovich, M.J. (1990). Chemoprevention of 1,2-Dimethylhydrazine-induced Colon Cancer in Mice by Naturally Occurring Organosulfur Compounds. *Cancer Research* *50*, 5084-5087.
- Sun, X.-F., Rütten, S., Zhang, H., and Nordenskjöld, B. (1999). Expression of the Deleted in Colorectal Cancer Gene Is Related to Prognosis in DNA Diploid and Low Proliferative Colorectal Adenocarcinoma. *Journal of Clinical Oncology* *17*, 1745.
- Sung, M.-K., Yeon, J.-Y., Park, S.-Y., Park, J.H.Y., and Choi, M.-S. (2011). Obesity-induced metabolic stresses in breast and colon cancer. *Annals of the New York Academy of Sciences* *1229*, 61-68.
- Suzuki, M.M., and Bird, A. (2008). DNA methylation landscapes: provocative insights from epigenomics. *Nat Rev Genet* *9*, 465-476.
- Swaminathan, V., Mythreye, K., O'Brien, E.T., Berchuck, A., Globe, G.C., and Superfine, R. (2011). Mechanical Stiffness Grades Metastatic Potential in Patient Tumor Cells and in Cancer Cell Lines. *Cancer Research* *71*, 5075-5080.
- Tahiliani, M., Koh, K.P., Shen, Y., Pastor, W.A., Bandukwala, H., Brudno, Y., Agarwal, S., Iyer, L.M., Liu, D.R., Aravind, L., *et al.* (2009). Conversion of 5-Methylcytosine to 5-Hydroxymethylcytosine in Mammalian DNA by MLL Partner TET1. *Science* *324*, 930-935.
- Takagi, Y., Kohmura, H., Futamura, M., Kida, H., Tanemura, H., Shimokawa, K., and Saji, S. (1996). Somatic alterations of the DPC4 gene in human colorectal cancers in vivo. *Gastroenterology* *111*, 1369-1372.
- Takagi, Y., Koumura, H., Futamura, M., Aoki, S., Ymaguchi, K., Kida, H., Tanemura, H., Shimokawa, K., and Saji, S. (1998). Somatic alterations of the SMAD-2 gene in human colorectal cancers. *Br J Cancer* *78*, 1152-1155.
- Takayama, T., Katsuki, S., Takahashi, Y., Ohi, M., Nojiri, S., Sakamaki, S., Kato, J., Kogawa, K., Miyake, H., and Niitsu, Y. (1998). Aberrant Crypt Foci of the Colon as Precursors of Adenoma and Cancer. *New England Journal of Medicine* *339*, 1277-1284.
- Tammariello, A.E., and Milner, J.A. (2010). Mouse models for unraveling the importance of diet in colon cancer prevention. *J Nutr Biochem* *21*, 77-88.
- Tan, E., Gouvas, N., Nicholls, R.J., Ziprin, P., Xynos, E., and Tekkis, P.P. (2009). Diagnostic precision of carcinoembryonic antigen in the detection of recurrence of colorectal cancer. *Surg Oncol* *18*, 15-24.
- Tan, F.-L., Moravec, C.S., Li, J., Apperson-Hansen, C., McCarthy, P.M., Young, J.B., and Bond, M. (2002). The gene expression fingerprint of human heart failure. *Proceedings of the National Academy of Sciences* *99*, 11387-11392.
- Tanaka, M., Chang, P., Li, Y., Li, D., Overman, M., Maru, D.M., Sethi, S., Phillips, J., Bland, G.L., Abbruzzese, J.L., *et al.* (2011). Association of CHFR Promoter Methylation with Disease Recurrence in Locally Advanced Colon Cancer. *Clinical Cancer Research* *17*, 4531-4540.
- Tang, C.W., Maya-Mendoza, A., Martin, C., Zeng, K., Chen, S., Feret, D., Wilson, S.A., and Jackson, D.A. (2008). The integrity of a lamin-B1-dependent nucleoskeleton is a fundamental determinant of RNA synthesis in human cells. *Journal of Cell Science* *121*, 1014-1024.
- Taniura, H., Glass, C., and Gerace, L. (1995). A chromatin binding site in the tail domain of nuclear lamins that interacts with core histones. *The Journal of Cell Biology* *131*, 33-44.

- Taranum, S. (2012). Cytoskeletal Interactions at the Nuclear Envelope Mediated by Nesprins. *International Journal of Cell Biology* 2012.
- Thibodeau, S., Bren, G., and Schaid, D. (1993). Microsatellite instability in cancer of the proximal colon. *Science* 260, 816-819.
- Thiery, J.P., and Sleeman, J.P. (2006). Complex networks orchestrate epithelial-mesenchymal transitions. *Nat Rev Mol Cell* 7(2) 131-42.
- Thun, M.J., Jacobs, E.J., and Patrono, C. (2012). The role of aspirin in cancer prevention. *Nat Rev Clin Oncol* 9, 259-267.
- Tiwari, V.K., McGarvey, K.M., Licchesi, J.D.F., Ohm, J.E., Herman, J.G., Schübeler, D., and Baylin, S.B. (2008). PcG Proteins, DNA Methylation, and Gene Repression by Chromatin Looping. *PLoS Biol* 6, e306.
- Todd, E.M., Deady, L.E., and Morley, S.C. (2011). The Actin-Bundling Protein L-Plastin Is Essential for Marginal Zone B Cell Development. *The Journal of Immunology* 187, 3015-3025.
- Toyooka, K., Liu, F., Ishii, M., Saito, S., Kirikae, T., Asano, Y., and Shinomiya, H. (2006). Generation and characterization of monoclonal antibodies that specifically recognize p65/L-plastin isoform but not T-plastin isoform. *Biosci Biotechnol Biochem* 70, 1402-1407.
- Toyota, M., and Issa, J.P. (1999). CpG island methylator phenotypes in aging and cancer. *Semin Cancer Biol* 9, 349-357.
- Tsai, H.C., and Baylin, S.B. (2011). Cancer epigenetics: linking basic biology to clinical medicine. *Cell Res* 21, 502-517.
- Tsanou, E., Peschos, D., Batistatou, A., Charalabopoulos, A., and Charalabopoulos, K. (2008). The E-cadherin adhesion molecule and colorectal cancer. A global literature approach. *Anticancer Res* 28, 3815-3826.
- Umetani, N., Takeuchi, H., Fujimoto, A., Shinozaki, M., Bilchik, A.J., and Hoon, D.S. (2004). Epigenetic inactivation of ID4 in colorectal carcinomas correlates with poor differentiation and unfavorable prognosis. *Clin Cancer Res* 10, 7475-7483.
- Unoki, M., Kelly, J.D., Neal, D.E., Ponder, B.A.J., Nakamura, Y., and Hamamoto, R. (2009). UHRF1 is a novel molecular marker for diagnosis and the prognosis of bladder cancer. *Br J Cancer* 101, 98-105.
- van 't Veer, L.J., Dai, H., van de Vijver, M.J., He, Y.D., Hart, A.A.M., Mao, M., Peterse, H.L., van der Kooy, K., Marton, M.J., Witteveen, A.T., *et al.* (2002). Gene expression profiling predicts clinical outcome of breast cancer. *Nature* 415, 530-536.
- van de Wetering, M., Sancho, E., Verweij, C., de Lau, W., Oving, I., Hurlstone, A., van der Horn, K., Batlle, E., Coudreuse, D., Haramis, A.-P., *et al.* (2002). The β -Catenin/TCF-4 Complex Imposes a Crypt Progenitor Phenotype on Colorectal Cancer Cells. *Cell* 111, 241-250.
- van den Brandt, P.A., Goldbohm, R.A., Van 't Veer, P., Volovics, A., Hermus, R.J.J., and Sturmans, F. (1990). A large-scale prospective cohort study on diet and cancer in the Netherlands. *Journal of Clinical Epidemiology* 43, 285-295.
- van den Ent, F., Amos, L., and Löwe, J. (2001a). Bacterial ancestry of actin and tubulin. *Current Opinion in Microbiology* 4, 634-638.

- van den Ent, F., Amos, L.A., and Lowe, J. (2001b). Prokaryotic origin of the actin cytoskeleton. *Nature* **413**, 39-44.
- van den Ent, F., Møller-Jensen, J., Amos, L.A., Gerdes, K., and Löwe, J. (2002). F-actin-like filaments formed by plasmid segregation protein ParM. *EMBO J* **21**, 6935-6943.
- van Engeland, M., Derks, S., Smits, K.M., Meijer, G.A., and Herman, J.G. (2011). Colorectal cancer epigenetics: complex simplicity. *J Clin Oncol* **29**, 1382-1391.
- Vane, J.R., and Botting, R.M. (2003). The mechanism of action of aspirin. *Thrombosis Research* **110**, 255-258.
- Varela, I., Cadinanos, J., Pendas, A.M., Gutierrez-Fernandez, A., Folgueras, A.R., Sanchez, L.M., Zhou, Z., Rodriguez, F.J., Stewart, C.L., Vega, J.A., *et al.* (2005). Accelerated ageing in mice deficient in Zmpste24 protease is linked to p53 signalling activation. *Nature* **437**, 564-568.
- Vatner, D.E., and Vatner, S.F. (1998). Physiological and biochemical adrenergic regulation of the stunned myocardium. *Molecular and Cellular Biochemistry* **186**, 131-137.
- Verhulst, J., Ferdinande, L., Demetter, P., and Ceelan, W. (2012) Muscinous subtype as prognostic factor in CRC: a systematic review and meta-analysis. *J Clin Pathol* **65**, 381-388.
- Vergnes, L., Péterfy, M., Bergo, M.O., Young, S.G., and Reue, K. (2004). Lamin B1 is required for mouse development and nuclear integrity. *Proceedings of the National Academy of Sciences of the United States of America* **101**, 10428-10433.
- Vetter, G., Le Behec, A., Muller, J., Muller, A., Moes, M., Yatskou, M., Al Tanoury, Z., Poch, O., Vallar, L., and Friederich, E. (2009). Time-resolved analysis of transcriptional events during SNAIL1-triggered epithelial to mesenchymal transition. *Biochem Biophys Res Commun* **385**, 485-491.
- Vogelstein, B. (1988). Genetic alterations during colorectal-tumor development. *N Engl J Med* **319**, 525-532.
- Voigt, B., Timmers, A.C., Samaj, J., Muller, J., Baluska, F., and Menzel, D. (2005). GFP-FABD2 fusion construct allows in vivo visualization of the dynamic actin cytoskeleton in all cells of Arabidopsis seedlings. *Eur J Cell Biol* **84**, 595-608.
- Wang, D., Su, L., Huang, D., Zhang, H., Shin, D., and Chen, Z. (2011). Downregulation of E-Cadherin enhances proliferation of head and neck cancer through transcriptional regulation of EGFR. *Molecular Cancer* **10**, 116.
- Wang, J., and Brown, E.J. (1999). Immune complex-induced integrin activation and L-plastin phosphorylation require protein kinase A. *J Biol Chem* **274**, 24349-24356.
- Wargovich, M.J. (1987). Diallyl sulfide, a flavor component of garlic (*Allium sativum*), inhibits dimethylhydrazine-induced colon cancer. *Carcinogenesis* **8**, 487-489.
- Weaver, A. (2006). Invadopodia: Specialized Cell Structures for Cancer Invasion. *Clinical and Experimental Metastasis* **23**, 97-105.
- Weisenberger, D.J. (2006). CpG island methylator phenotype underlies sporadic microsatellite instability and is tightly associated with BRAF mutation in colorectal cancer. *Nat Genet* **38**, 787-793.

- Whitfield, J.F., Bird, R.P., Chakravarthy, B.R., Isaacs, R.J., and Morley, P. (1995). Calcium-cell cycle regulator, differentiator, killer, chemopreventor, and maybe, tumor promoter. *J Cell Biochem Suppl* 22, 74-91.
- Whitney, D., Skoletsy, J., Moore, K., Boynton, K., Kann, L., Brand, R., Syngal, S., Lawson, M., and Shuber, A. (2004). Enhanced retrieval of DNA from human fecal samples results in improved performance of colorectal cancer screening test. *J Mol Diagn* 6, 386-395.
- Williams, C.D., Satia, J.A., Adair, L.S., Stevens, J., Galanko, J., Keku, T.O., and Sandler, R.S. (2010). Associations of Red Meat, Fat, and Protein Intake With Distal Colorectal Cancer Risk. *Nutrition and Cancer* 62, 701-709.
- Willis, N.D., Cox, T.R., Rahman-Casans, S.F., Smits, K., Przyborski, S.A., van den Brandt, P., van Engeland, M., Weijnenberg, M., Wilson, R.G., de Bruine, A., *et al.* (2008). Lamin A/C is a risk biomarker in colorectal cancer. *PLoS One* 3, e2988.
- Winawer, S., Fletcher, R., Rex, D., Bond, J., Burt, R., Ferrucci, J., Ganiats, T., Levin, T., Woolf, S., Johnson, D., *et al.* (2003). Colorectal cancer screening and surveillance: Clinical guidelines and rationale—Update based on new evidence. *Gastroenterology* 124, 544-560.
- Wong, H.K., Mishra, A., Hake, T., and Porcu, P. (2011). Evolving insights in the pathogenesis and therapy of cutaneous T-cell lymphoma (mycosis fungoides and Sezary syndrome). *Br J Haematol* 155, 150-166.
- Wood, L.D. (2007). The genomic landscapes of human breast and colorectal cancers. *Science* 318, 1108-1113.
- Wood, L.D., Parsons, D.W., Jones, S., Lin, J., Sjoblom, T., Leary, R.J., Shen, D., Boca, S.M., Barber, T., Ptak, J., *et al.* (2007). The genomic landscapes of human breast and colorectal cancers. *Science* 318, 1108-1113.
- Worman, H.J., and Courvalin, J.C. (2005). Nuclear Envelope, Nuclear Lamina, and Inherited Disease. In *International Review of Cytology*, W.J. Kwang, ed. (Academic Press), pp. 231-279.
- Worman, H.J., and Gundersen, G.G. (2006). Here come the SUNs: a nucleocytoskeletal missing link. *Trends in Cell Biology* 16, 67-69.
- Wozney J.M., Rosen V., Celeste A.J., Mitscock L.M., Whitters M.J., Kriz R.W., Hewick R.M., and Wang E.A. (1988). Novel regulators of bone formation: molecular clones and activities. *Science* 242, 1528-1534.
- Wu, Z., Wu, L., Weng, D., Xu, D., Geng, J., and Zhao, F. (2009). Reduced expression of lamin A/C correlates with poor histological differentiation and prognosis in primary gastric carcinoma. *Journal of Experimental & Clinical Cancer Research* 28, 8.
- Xue, F., Janzen, D.M., and Knecht, D.A. (2010). Contribution of Filopodia to Cell Migration: A Mechanical Link between Protrusion and Contraction. *Int J Cell Biol* 2010, 507821.
- Yan, Y.-x., Gong, Y.-w., Guo, Y., Lv, Q., Guo, C., Zhuang, Y., Zhang, Y., Li, R., and Zhang, X.-z. (2012). Mechanical Strain Regulates Osteoblast Proliferation through Integrin-Mediated ERK Activation. *PLoS One* 7, e35709.

Yi, J.M., Dhir, M., Van Neste, L., Downing, S.R., Jeschke, J., Glockner, S.C., de Freitas Calmon, M., Hooker, C.M., Funes, J.M., Boshoff, C., *et al.* (2011). Genomic and epigenomic integration identifies a prognostic signature in colon cancer. *Clin Cancer Res* 17, 1535-1545.

Yilmaz, M., and Christofori, G. (2009). EMT, the cytoskeleton, and cancer cell invasion. *Cancer Metastasis Rev* 28, 15-33.

Zavadil, J., and Bottinger, E.P. (2005). TGF-beta and epithelial-to-mesenchymal transitions. *Oncogene* 24, 5764-5774.

Zeki, S.S., Graham, T.A., and Wright, N.A. (2011). Stem cells and their implications for colorectal cancer. *Nat Rev Gastroenterol Hepatol* 8, 90-100.

Zheng, J., Rudra-Ganguly, N., Miller, G.J., Moffatt, K.A., Cote, R.J., and Roy-Burman, P. (1997). Steroid hormone induction and expression patterns of L-plastin in normal and carcinomatous prostate tissues. *Am J Pathol* 150, 2009-2018.

Zheng, B., Han, M., Bernier, M., and Wen, J.K. (2009). Nuclear actin and actin-binding proteins in the regulation of transcription and gene expression. *FEBS J* 276(10), 2669-2685.

Zheng, R., Ghirlando, R., Lee, M.S., Mizuuchi, K., Krause, M., and Craigie, R. (2000). Barrier-to-autointegration factor (BAF) bridges DNA in a discrete, higher-order nucleoprotein complex. *Proc Natl Acad Sci U S A* 97, 8997-9002.

Zhu, J.-K. (2009). Active DNA Demethylation Mediated by DNA Glycosylases. *Annual Review of Genetics* 43, 143-166.

Zinkin, L. (1983). A critical review of the classifications and staging of colorectal cancer. *Diseases of the Colon & Rectum* 26, 37-43.

Zlobec, I., and Lugli, A. (2008). Prognostic and predictive factors in colorectal cancer. *Postgrad Med J* 84, 403-411.

